

**Next Generation Shilov Catalysis: Ligand Design and Computational Analysis for
Improved Catalysis in C–H Activation and Functionalization Chemistry**

by

John Brannon Gary

**A dissertation submitted in partial fulfillment
of the requirements for the degree of
Doctor of Philosophy
(Chemistry)
in The University of Michigan
2012**

Doctoral Committee:

Professor Melanie S. Sanford, Chair
Professor Mark M. Banaszak Holl
Professor Levi T. Thompson Jr.
Assistant Professor Barry D. Dunietz

© John Brannon Gary
All rights reserved
2012

Dedication

To my parents, family, friends, and colleagues who have made this possible

Acknowledgements

I would first like to thank my parents who have always had unwavering support for my academic pursuits. Their belief, support, and encouragement have made all of my success possible and their contributions cannot be adequately stated. My family and friends have also been a wonderful resource and have allowed me to maintain what is important in life. While being away from Texas, my friends here in Ann Arbor in many ways have served as family. From the beginning, Anna, Corrine, and I survived classes and the various struggles of beginning and surviving the early years of graduate school. I am proud to say that Anna and I survived the process. Additions of Marisa, Deidra, Rick, and Rebecca have made my free time much more enjoyable while in Michigan. I also must thank my friend Ashley for all of her support and always enjoying the pretty pictures of my research.

I would like to thank my advisor Melanie Sanford for allowing me to join her group and give me a project and let me run. The strain of changing research groups was something that I would not like to go through again but turned out to be a very good transition. Her passion and drive for science have helped to shape me into a chemist in which I hope she would be proud. I would also like to thank Prof. Banaszak Holl for serving on my committee and always giving straight and honest career and chemistry advice. It has been invaluable in my growth as a chemist. I would also like to thank Prof. Dunietz for serving on my committee and giving me my first experience of computational chemistry through a rotation. Lastly, I would like to thank Prof.

Thompson for serving on my committee as a cognate and giving a different perspective to my research and pushing this project forward.

Many colleagues have been instrumental to my growth as a chemist. From the Johnson lab, I must thank Dr. Stephen Caskey, Dr. Andrea Geyer, Dr. Marisa Macnaughtan, Dr. Michael Stewart, and Dr. Eric Wiedner for their support, encouragement, and training through my first two years of graduate school. From the Sanford lab, I would like to specifically thank Dr. Janette Villalobos and Dr. Marion Emmert, two very talented postdoctoral associates I have had the pleasure to work with on this project. The chemistry discussions with them and their advice have allowed for the results that have been presented. I would also like to thank Dr. Matt Remy for his many discussion concerning computational studies which have helped to drive my research forward. I should also thank Dr. Nick Ball and Yingda Ye who I have collaborated with on the last project of the thesis, along with Amanda Cook for discussions of palladium chemistry, and Tyler Carter for assistance with rhodium chemistry. I would also like to thank fellow lab mates who have helped in the completion of this work: Dr. Rebecca Loy, Dr. Kevin Fortner, Dr. Andrew Higgs, Dr. Amanda Hickman, Dr. Kami Hull, Dr. Dipannita Kalyani, Kara Stowers, Joy Racowski, Asako Kubota, Sharon Neufeldt, Anna Wagner, Chelsea Huff, Kate Butler, Monica Lotz, and Ansis Maleckis. Specifically, I would also like to thank Rebecca, Amanda, Chelsea, and Sharon for helpful comments and proofreading of my thesis. The Michigan chemistry department staff have also been a wonderful aid in my time here and they deserve a significant acknowledgement: Tracy Stevenson, Laura Labut, Doug Cox,

Jennifer Rieger, Eugenio Alvarado, James Windak, Paul Lennon, Roy Wentz, and Rich Giszczak.

Lastly, I had the pleasure to work in a collaborative center during my time in the Sanford lab (CENTC – Center for Enabling New Technologies Through Catalysis). The contributions of various faculty, graduate students, and postdoctoral associates have been immeasurable. I would like to thank Prof. Karen Goldberg (University of Washington), Prof. Mike Heinekey (University of Washington), Prof. Bill Jones (University of Rochester), and Prof. Elon Ison (North Carolina State University) for their chemistry contributions to this project. I would also like to give a special thanks to Prof. Tom Cundari (University of North Texas) for his guidance in computational studies and “guru” consults. Lastly, I would also like to thank Roxanne Clément who I was able to go and work with for high-throughput catalysis at the University of Ottawa.

Finally, I would like to thank the National Science Foundation for a graduate research fellowship and funding through CENTC along with the Murrill Memorial Scholarship for funding.

Table of Contents

Dedication	ii
Acknowledgements.....	iii
List of Schemes.....	xi
List of Figures	xv
List of Tables	xvii
Abstract.....	xix
Chapter 1	1
Activation and Functionalization of C–H Bonds.....	1
1.1 Metal Mediated C–H Activation	2
1.2 Pioneering C–H Functionalization Chemistry: Shilov Chemistry.....	5
1.3 Selectivity in C–H Functionalization Chemistry: Directing Group Chemistry.....	7
1.4 Pioneering C–H Functionalization Chemistry: Catalytica System	8
1.5 Fundamental Project Strategy: Catalytica System Improvement	10
1.6 References.....	11
Chapter 2.....	14
Pt and Pd Catalyzed C–H Acetoxylation with Cationic Pyridine-Based Ligands.....	14
2.1 Background and Significance	14
2.2 Results and Discussions.....	18
2.2.1 Second Generation Cationic Ligands.....	18

2.2.2 Third Generation Cationic Ligands via High Throughput Screening.....	24
2.2.3 Validating High-Throughput Screening Results.....	33
2.2.4 Improving Catalysis Through Oxidant Modification	34
2.2.5 Catalysis with Lower Arene Equivalents.....	41
2.2.5 Arene Substrate Scope	43
2.3 Conclusions	45
2.4 Experimental Procedures	46
2.4.1 Instrumentation	46
2.4.2 Materials and Methods.....	46
2.4.3 Synthesis	48
2.4.3 Reaction Details	54
2.5 References.....	61
Chapter 3.....	65
Ir and Rh Cp* Complexes with Cationic Pyridine Ancillary Ligands for C–H Activation.....	65
3.1 Background and Significance	65
3.2 Results and Discussions.....	70
3.2.1 Complex Synthesis.....	70
3.2.2 Initial H/D Exchange Investigations.....	71
3.2.3 Expanding the Substrate Scope in H/D Exchange.....	74
3.2.4 H/D Exchange of Benzene.....	75
3.2.5 Solvent Effects in H/D Exchange of Benzene.....	77
3.2.6 Active Catalyst System	81

3.3 Conclusions.....	84
3.4 Experimental Procedures	85
3.4.1 Instrumentation	85
3.4.2 Materials and Methods.....	86
3.4.3 Synthesis	87
3.4.4 Reaction Details	89
3.5 References.....	93
Chapter 4.....	97
Rh ^I and Rh ^{III} Complexes with Pyridinium Substituted Bipyridine Ligands.....	97
4.1 Background and Significance	97
4.2 Results and Discussions.....	101
4.2.1 Computational Analysis – Competing Oxidative versus Electrophilic C–H Activation.....	101
4.2.2 Rh ^I Complexes for C-H Activation Studies.....	105
4.2.3 Rh ^{III} Complexes for C-H Activation Studies.....	107
4.2.4 Rh ^{III} Cyclometallated Complexes with 1 and dtbpy	111
4.2.5 Attempts at Functionalization of Rh ^{III} -Alkyl Bonds Through Reductive Elimination or Olefin/Alkyne Insertion	114
4.3 Conclusions.....	116
4.4 Experimental Procedures	117
4.4.1 Computational Methods.....	117
4.4.2 Instrumentation	117
4.4.3 Materials and Methods.....	118

4.4.4 Synthesis	119
4.4.5 Reaction Details	124
4.4.6 XYZ coordinates – Calculated Structures	126
4.5 References	134
Chapter 5	141
Computational Analysis on the Mechanism of Aryl–CF ₃ and Aryl–O ₂ CR Reductive Elimination.....	141
5.1 Background and Significance	141
5.1.1 Aryl–CF ₃ Bond Formation	141
5.1.2 Aryl–O ₂ CR Bond Formation	144
5.2 Results and Discussions	147
5.2.1 Experimental Rationale for Computational Studies	147
5.2.2 DFT calculations – Aryl–CF ₃ Coupling.....	150
5.2.3 Comparison of CF ₃ versus Cl and OAc Reductive Elimination	154
5.2.4 Aryl–O ₂ CR bond-forming reductive elimination with [(bpy)Pd(Ph)(CF ₃)(O ₂ CR)] ⁺	155
5.2.5 Examination of known C–OAc bond-forming reactions from Pd ^{IV} , Pd ^{III} , and Pd ^{II}	159
5.2.6 Comparison of C–OAc and C–OR bond-forming reductive elimination at Pd ^{II}	165
5.3 Conclusions.....	167
5.4 Experimental Procedures	169
5.4.1 Computational Methods.....	169

5.4.2 XYZ coordinates – Calculated Structures	169
5.5 References	173
Chapter 6.....	182
Conclusions and Future Prospects	182
6.1 Conclusions.....	182
6.2 Future Prospects.....	186
6.3 References.....	188

List of Schemes

Scheme 1.1 Traditional Organic Functional Group Conversion Chemistry	1
Scheme 1.2 Types of C–H Bonds in a Small Organic Molecule, Ethylbenzene	2
Scheme 1.3 Initial Observations of C–H Activation with AuCl ₃	3
Scheme 1.4 Stoichiometric Examples of Homogeneous C–H Activation	3
Scheme 1.5 Catalytic H/D Exchange with a Homogeneous Complex.....	4
Scheme 1.6 Shilov Catalytic Cycle	6
Scheme 1.7 Striking Terminal Selectivity in Shilov Systems	7
Scheme 1.8 Directed C–H Functionalization Chemistry	8
Scheme 1.9 Catalytic Methane Oxidation System	9
Scheme 1.10 Cationic Ligand Design Strategy	10
Scheme 2.1 Crabtree Benzene Acetoxylation	15
Scheme 2.2 Ebersson Benzene Acetoxylation	15
Scheme 2.3 Catalytic Methane Oxidation System	16
Scheme 2.4 pK _a of Substituted Aromatic Acids.....	16
Scheme 2.5 Cationic Ligand Design Strategy	18
Scheme 2.6 2nd Generation Ligand Synthesis	19
Scheme 2.7 Metal Complex Synthesis with 2nd Generation Ligands	19
Scheme 2.8 Catalyst Termination Step	22
Scheme 2.9 Possible Active Catalyst Systems	23
Scheme 2.10 Dual Catalyst Transmetalation Mechanism.....	23

Scheme 2.11 Pd(OAc) ₂ /Pyridine Catalyst System	24
Scheme 2.12 Yu's Oxidative Heck Reaction with Electron Deficient Arenes	24
Scheme 2.13 Ligand Dissociation Equilibrium.....	25
Scheme 2.14 General Cationic Pyridine Derivative Synthesis	26
Scheme 2.15 Ligand Library	26
Scheme 2.16 Pd(OAc) ₂ and Ligand Equilibrium	28
Scheme 2.17 Reaction Products	34
Scheme 2.18 Competing C–O versus C–C Bond Formation.....	40
Scheme 2.19 Charge Interactions Enhancing Oxidation Reactions	40
Scheme 2.20 Pd-catalyzed Acetoxylation versus Nitration	42
Scheme 3.1 Stoichiometric C–H Activation at IrCp* Complexes	66
Scheme 3.2 IrCp* C–X Bond Formation	69
Scheme 3.3 [MCp*LCl ₂] Synthesis with Rh and Ir	70
Scheme 3.4 Peris Synthesis of [IrCp*(NHC)Cl ₂].....	71
Scheme 3.5 Active Catalyst Isolation Attempts	82
Scheme 3.6 Observation of Putative Active Catalyst by ¹ H NMR Spectroscopy	83
Scheme 4.1 Shilov Catalytic Cycle	98
Scheme 4.2 C–H Activation of Pendant Carbon Fragments	99
Scheme 4.3 Catalytic C–H Functionalization Through Olefin Insertion	99
Scheme 4.4 Rh Catalyzed Arylation Reactions.....	100
Scheme 4.5 Rh-Catalyzed C–H Borylation.....	100
Scheme 4.6 Bipyridine Ligands Studied	101
Scheme 4.7 Oxidative versus Electrophilic C-H Activation	102

Scheme 4.8 Bipyridine Addition to $[\text{Rh}(\text{COE})_2\text{Cl}]_2$	105
Scheme 4.9 Rh^{III} -based Shilov Catalytic Cycle	108
Scheme 4.10 Rh^{III} Complex Synthesis	109
Scheme 4.11 Rh^{III} Cyclometallated Complex Synthesis	112
Scheme 4.12 Halide Abstraction Reactions with 7	113
Scheme 4.13 Halide Abstraction Reactions with 6	113
Scheme 4.14 Attempts at Oxidatively-Induced Reductive Elimination Studies with 7 .	115
Scheme 4.15 Attempts at Olefin or Alkyne into Rh–Aryl Bonds	116
Scheme 5.1 Stoichiometric Aryl– CF_3 Reductive Elimination	142
Scheme 5.2 General CF_3 Bond Forming Strategy	143
Scheme 5.3 Oxidative Aryl–X versus Aryl– CF_3 Bond Formation	147
Scheme 5.4 Pd^{IV} Intermediate Isolation	149
Scheme 5.5 Proposed Mechanisms for Aryl– CF_3 Reductive Elimination.....	149
Scheme 5.6 Proposed Mechanism for Aryl– CF_3 Reductive Elimination	150
Scheme 5.7 Calculated Reductive Elimination Pathway Calculated Energies	151
Scheme 5.8 Calculated Reductive Elimination Pathway for bpy versus tmeda.....	154
Scheme 5.9 Five-membered (17-1) and three-membered (17-2) transition states for reductive elimination from $[(\text{bpy})\text{Pd}(\text{Ph})(\text{CF}_3)(\text{OAc})]^+$ (17)	156
Scheme 5.10 Reductive Elimination Pathways from $[(\text{phpy})_2\text{Pd}^{\text{IV}}(\text{OAc})_2]$	161
Scheme 5.11 Reductive Elimination Pathways from $[(\text{phpy})\text{Pd}(\text{OAc})]_2(\mu\text{-OAc})_2$	163
Scheme 5.12 Reductive Elimination Transition states from $[\text{Pd}(\text{bq})(\text{allyl})(\text{OAc})]$	164
Scheme 5.13 Reductive Elimination Pathways from $(\text{PH}_3)_2\text{Pd}^{\text{II}}(\text{Ph})(\text{OAc})$ (24) and $(\text{PH}_3)\text{Pd}^{\text{II}}(\text{Ph})(\text{OAc})$ (25).....	165

Scheme 6.1 Benzene Acetoxylation Reaction.....	184
Scheme 6.2 sp^3 H/D Exchange.....	187
Scheme 6.3 Oxidatively Induced Reductive Elimination.....	187
Scheme 6.4 3rd Generation Ligands for Rh^{III} Complexes	188

List of Figures

Figure 2.1 Cationic Substituent Effects on Redox and Electronic Spectroscopy	17
Figure 2.2 H/D Exchange of Isolable Pt and Pd Complexes	20
Figure 2.3 Pd-Catalyzed Benzene Acetoxylation	22
Figure 2.4 Pd:Ligand Ratio Effect on Catalytic Activity.....	27
Figure 2.5 Pd(OAc) ₂ and Pyridine Equilibrium.....	30
Figure 2.6 Catalyst Inhibition at High Ligand Loadings	31
Figure 2.7 Ligand Effect on Catalysts Activity at Short Reaction Times.....	32
Figure 2.8 Lab Scale Reaction Yields.....	33
Figure 3.1 Benzene H/D Exchange with CD ₃ COOD	76
Figure 3.2 Silver Additive Effect on Catalytic Activity	77
Figure 3.3 Solvent Effects in H/D Exchange.....	78
Figure 3.4 Acetic Acid-D ₄ and D ₂ O Ratios in H/D Exchange.....	80
Figure 3.5 Potential H/D Exchange Catalytic Cycle.....	81
Figure 3.6 Catalyst Activity at Longer Reaction Times	84
Figure 4.1 Oxidative versus Electrophilic C–H Activation.....	103
Figure 4.2 Oxidative versus Electrophilic C–H Activation.....	104
Figure 5.1 Proposed Transition States for C–OR and C–O ₂ CR Bond-Forming Reductive Elimination from Pd.....	145
Figure 5.2 Proposed Transition States for O–H Bond-Forming Reductive Elimination from Ru-Hydride Complexes.....	146

Figure 5.3 Proposed Acetate Assisted Transition States for C–H Activation [M = Pd ^{II} , Ir ^{III}]	146
Figure 6.1. Shilov Catalytic Cycle	182
Figure 6.2. Catalytic Methane Oxidation System	183
Figure 6.3 Cationic Ligand Design Strategy	183

List of Tables

Table 2.1 Oxidant Screen for Benzene Acetoxylation.....	35
Table 2.2 Ligand and Counterion Effects in $K_2S_2O_8$ Oxidation	36
Table 2.3 Temperature Effects on Catalyst Yields and Reaction Times in Parenthesis ..	37
Table 2.4 Ligand Activity Comparison at Low Conversion	38
Table 2.5 Ligand and Temperature Effects on Selectivity.....	39
Table 2.6 Reaction Yields with Varying Benzene Equivalents	41
Table 2.7 Arene Substrate Scope with $K_2S_2O_8$	44
Table 2.8 Oxidant Screening.....	59
Table 2.9 Substrate Scope Quantities.....	61
Table 3.1 IrCp* Catalyzed H/D Exchange of Benzene.....	67
Table 3.2 H/D Exchange of Acetophenone with [IrCp*(L)Cl ₂] Complexes	72
Table 3.3 Solvent Affect in H/D Exchange of Acetophenone	73
Table 3.4 Mono-substituted Aromatic Substrates for H/D Exchange.....	74
Table 3.5 Substrate Volumes for H/D Exchange	91
Table 3.6 Solvent Volumes for H/D Exchange.....	93
Table 4.1 C–H Activation with Cyclometallating Reagents.....	107
Table 4.2 Benzene H/D Exchange in Various Solvents.....	109
Table 4.3 H/D Exchange of 2-Phenylpyridine.....	110
Table 4.4 Cyclometallated Complexes for 2-Phenylpyridine H/D Exchange	114
Table 5.1 Oxidative Aryl–X versus Aryl–CF ₃ Bond Formation	148

Table 5.2 Gas Phase Values of $\Delta H_{298}^{\ddagger}$ for C–CF ₃ Bond-Formation from [(bpy)Pd ^{IV} (<i>p</i> -XC ₆ H ₄)(CF ₃)(F)] ⁺	153
Table 5.3 Competing Aryl–CF ₃ versus Aryl–X Reductive Elimination	155
Table 5.4 Calculated energies for C–O bond-forming reductive elimination from complexes 17 and 18 via three-membered and five-membered transition states	157
Table 5.5 Selected bond distances (Å) for structures 17 , 17-1 , 17-2 and 18 , 18-1 , 18-2	158
Table 5.6 Calculated Energies for C–O Reductive Elimination from 19–23	160
Table 5.7 Calculated Energies for C–O Reductive Elimination from 24 and 25	167

Abstract

The activation and functionalization of C–H bonds has been a long standing goal in organometallic chemistry. The catalytic cycle involves three main catalytic steps: C–H activation, oxidation, and bond-forming reductive elimination. This work describes the combined use of computational analysis, ligand design, high-throughput screening, stoichiometric studies, and catalytic assays in an effort to achieve rational catalyst design. With recent advances in the field illustrating the use of *in situ* generated and decomposition susceptible cationic nitrogen based ligands, 2nd and 3rd generation stable and isolable bipyridine and pyridine-based ligands containing pyridinium substituents have been synthesized and fully characterized. With these ligands, catalysts based upon Pt, Pd, Rh, and Ir have been tested for C–H activation activity and compared against their neutral bipyridine and pyridine analogs. In all of these systems, the pyridinium substituent was found to have beneficial effects in catalyst activity for C–H activation through an H/D exchange assay with arene substrates. The Pd-based systems have also been utilized to achieve the catalytic C–H acetoxylation of aromatic substrates. The efficient use of potassium persulfate as a cheap stoichiometric oxidant has been achieved in these reactions (up to 73 turnovers), with the newly designed ligands key for achieving this reactivity. Computational studies have been employed to study the reductive elimination of coupling components which are traditionally difficult to achieve, Aryl–F

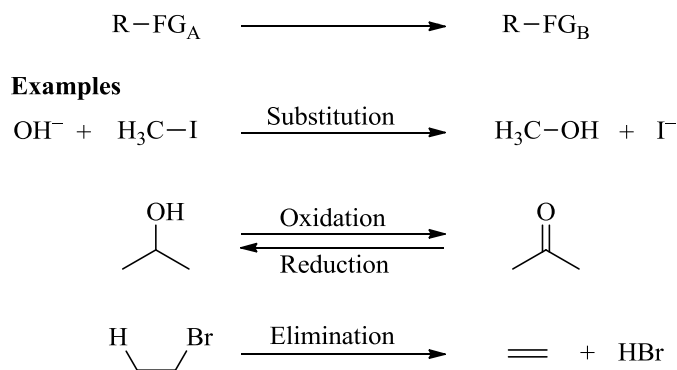
and Aryl-CF₃. Through these calculations, a novel mechanism for Aryl-carboxylate reductive elimination was discovered.

Chapter 1

Activation and Functionalization of C–H Bonds

The traditional approach for the introduction of desired functionality into organic molecules involves functional group transformations (Scheme 1.1). Thus, given this general scheme and the breadth of synthetic methodology, almost any functionality in organic molecules can be considered a starting material for organic synthesis.¹ In sharp contrast, while saturated hydrocarbons are ubiquitous in nature, they contain no chemical functionality, thus making them poor starting materials for traditional organic reactions.

Scheme 1.1 Traditional Organic Functional Group Conversion Chemistry.

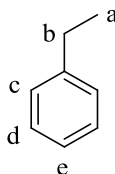


The activation and functionalization of C–H bonds has been often cited as a “Holy Grail” of organometallic chemistry.¹ The first major challenge involves the kinetic inertness of C–H bonds. The low reactivity is often attributed to the high bond dissociation energies and very low acidities. For example, benzene C–H bonds have bond dissociation energies of 111 kcal/mol,² while alkane C–H bonds range between 90-105 kcal/mol.^{1,3} Also, the low acidity of benzene C–H bonds ($\text{pK}_a=37$)² and alkyl C–H bonds ($\text{pK}_a=45-60$)¹ limits reactivity. While alkanes have

lower C–H bond strengths in comparison to aromatic compounds, Shilov explains the lower alkane reactivity with metals by the absence of both π or n-electrons.⁴ This lower reactivity is likely due to the fact that π or n-electrons allow substrate coordination prior to metal interaction with a C–H bond.

A second major challenge involves the issue of selectivity. Even in a relatively simple organic molecule such as ethyl benzene (Scheme 1.2), it quickly becomes apparent that the molecule possesses five types of unique C–H bonds (labeled a through e). Thus, when considering the use of C–H bonds as potential organic starting materials, one must consider the challenges associated with activating a strong chemical bond along with developing strategies to garner some degree of selectivity.

Scheme 1.2 Types of C–H Bonds in a Small Organic Molecule, Ethylbenzene.



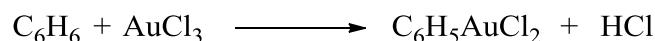
Many recent reviews have indicated the tremendous potential and scientific impact of the use of C–H bonds for useful chemical feedstocks and starting materials in the synthesis of more complex molecules.^{3,5-12}

1.1 Metal Mediated C–H Activation

Many reviews have detailed the field of C–H activation with both arenes and alkanes.^{1,3,13-20} Initial investigations concerning the activation of C–H bonds by transition metal compounds with organometallic intermediates began in the 1930's.⁴ The first observation of the interaction of C–H bonds with a transition metal was reported by Kharasch and Isbell in 1931.²¹

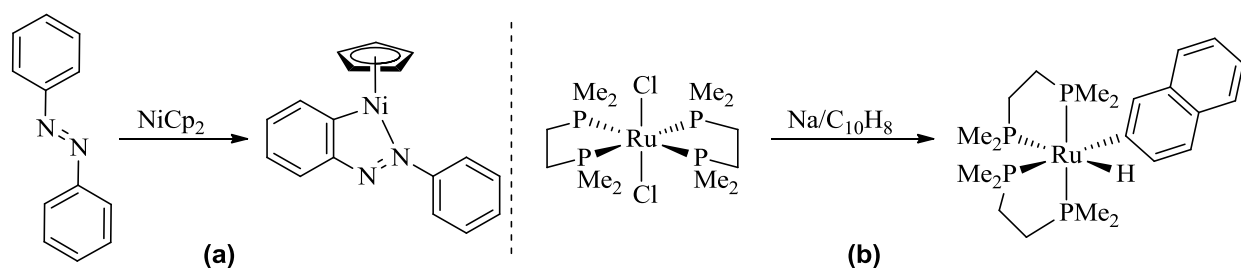
In this work, the authors reported the reaction of solid AuCl_3 with benzene to form phenyl chloride and a precipitate of auroous chloride (AuCl). Importantly, they were able to isolate an organometallic intermediate (Ph-AuCl_2) in this reaction by the addition of diethyl ether (Scheme 1.3).²¹

Scheme 1.3 Initial Observations of C–H Activation with AuCl_3 .



Following this report, Kleinman and Dubeck reported the stoichiometric C–H activation of azobenzene by Cp_2Ni (Cp =cyclopentadienyl) in 1963 (Scheme 1.4-a).²² Two years later, Chatt and Davidson reported the C–H activation of naphthalene through reduction of $[\text{RuCl}_2(\text{dmpe})_2]$ (dmpe =1,2-bis(dimethyl-phosphino)ethane) followed by oxidative C–H activation (Scheme 1.4-b).²³

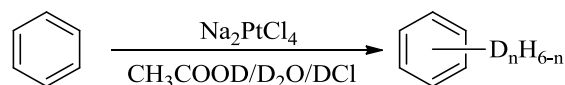
Scheme 1.4 Stoichiometric Examples of Homogeneous C–H Activation.



Following these observations of stoichiometric C–H activation by soluble metal complexes, Garnett and Hodges reported the catalytic deuteration of organic compounds using a homogeneous Pt complex (Scheme 1.5).²⁴ Acid is key to limit catalyst decomposition but strongly acidic conditions inhibit reactivity, which implicates a metal catalyzed process and not simply an electrophilic aromatic substitution mechanism. Interestingly, this report also included various substituted aromatic substrates such as fluorobenzene, toluene, and trifluorotoluene. A

key observation has subsequently been exploited in more recent chemistry today: the addition of acetic acid was required for catalytic activity.²⁵

Scheme 1.5 Catalytic H/D Exchange with a Homogeneous Complex.



Soon after this report of Pt^{II}-catalyzed C–H activation of arene substrates, Shilov achieved the deuteration of methane and ethane using D₂ as the deuterium source and H₃Co(PPh₃)₃ as a catalyst.²⁶ The deuterium incorporation was quite slow, with only about 2 % incorporation after 6 days. However, in the same report, they also illustrated that K₂PtCl₄ in CD₃COOD, hydrochloric acid, and D₂O could effectively deuterate methane and ethane (2-30 % incorporation depending on temperature in under 9 hours). Importantly, the authors note that metallic Pt is not responsible for the deuterium incorporation and that ethane reacts faster than methane under the published experimental conditions. Since these initial observations, the mechanism of Pt-mediated C–H activation has been heavily studied.^{18,27-35}

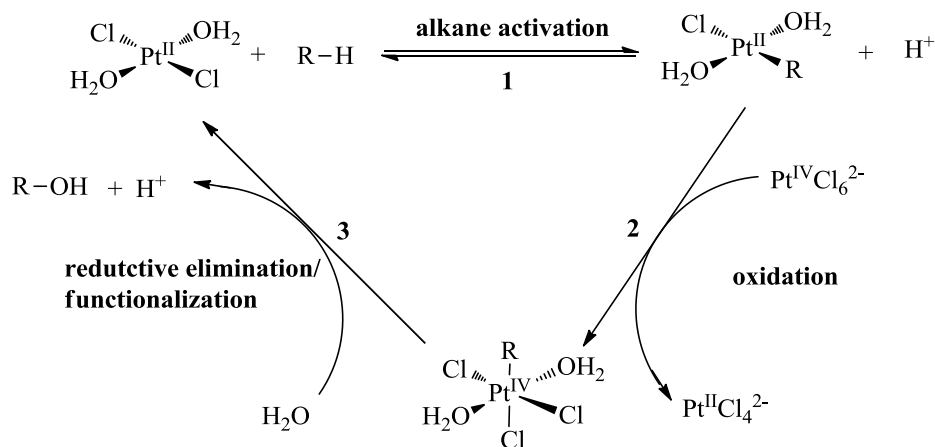
In comparison, aromatic substrates are at least twice as reactive as alkyl substrates in the Shilov system.⁴ In original examples of H/D exchange, sterics have a large effect on the selectivity observed. For example, terminal methyl groups undergo faster H/D exchange in normal and branched alkanes compared to methylene and methane groups.⁴ This trend is highlighted in the reactivity of pentane towards H/D exchange. Hodges showed that isotope exchange in the two terminal methyl positions of pentane is approximately five times faster than at the three internal methylene groups.³⁶ The steric effect can be seen in the alkyl reactivity trend of alkyl primary (1°), secondary (2°), and tertiary (3°) substituents, 1° > 2° > 3°.⁴ This trend is opposite to that typically observed in radical processes, thereby providing additional evidence for a metal catalyzed process with organometallic intermediates. Also, steric effects can clearly be

seen in the H/D exchange of monosubstituted aromatic substrates since exchange is only observed in the meta and para positions.⁴ Similar steric effects were reported by Garnett in which only the β -positions of naphthalene showed exchange.³⁷

1.2 Pioneering C–H Functionalization Chemistry: Shilov Chemistry

In 1968, Hodges and Garnett illustrated that heating a solution of benzene with H_2PtCl_6 resulted in the reduction of Pt.³⁸ Chlorobenzene, Pt^{II} , and small amounts of biphenyl were observed in these reactions. With the success of Pt^{II} complexes for activating alkane C–H bonds and the formation of Pt-alkyl intermediates,³⁶ Shilov next demonstrated the catalytic oxidative functionalization of C–H bonds in alkanes and aromatic substrates by the addition of H_2PtCl_6 in addition to Pt^{II} .³⁹ Two important observations provide key mechanistic evidence for this transformation. First, as seen with H/D exchange reactions, functionalization occurred predominantly at terminal methyl positions over tertiary or benzylic C–H bonds, which is in opposition to the selectivity typically seen for electrophiles and radicals.⁸ The second important observation concerns the reaction rates. It was observed that the rate of H/D exchange and subsequent functionalization were very similar.⁴ Given the $\text{Pt}^{\text{II}}/\text{Pt}^{\text{IV}}$ system, a mechanistic proposal for “Shilov” chemistry is summarized in Scheme 1.6.

Scheme 1.6 Shilov Catalytic Cycle.

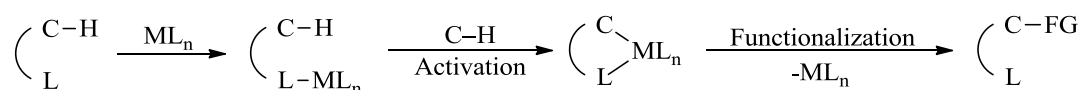


The Shilov cycle consists of three fundamental steps. The first step involves the reversible activation of an alkane C–H bond to form a Pt^{II}-alkyl intermediate.⁸ This reversible step is responsible for the H/D exchange reaction (*vide supra*). The second step involves a two electron oxidation of the Pt^{II}-alkyl intermediate to form a Pt^{IV}-alkyl species.⁴⁰ Importantly, this step was shown to occur by an electron transfer process rather than a transmetalation event.^{18,41,42} The third step involves reductive elimination. Two mechanistic routes could result in reductive elimination: external S_N2 attack or a concerted reaction via a three-center transition state. Zamashchikov and coworkers explored the mechanism of this step by kinetic analysis and concluded that an S_N2 pathway was operative.^{40,43,44} This step was subsequently studied through stereochemical analysis to clearly show that the reductive elimination step occurred through inversion of stereochemistry, thus clearly implicating an S_N2 mechanism.^{18,45}

While the Shilov system was a pioneering example showing the potential power of C–H functionalization chemistry, it has several severe limitations. First, the price of Pt^{IV} as a stoichiometric terminal oxidant is cost prohibitive (current price of H₂PtCl₆ from Pressure Chemicals on Oct. 12, 2011 : \$16,000/mol). Alkanes only react with the Pt^{II} catalyst, which complicates modification of the oxidant. The oxidant must selectively oxidize the Pt-alkyl

has been heavily studied and is often referred to as cyclometallation, given that the resulting product forms a ring of atoms containing a metal.⁴⁷ This strategy has also been utilized to achieve the selective catalytic functionalization of C–H bonds (Scheme 1.8). Tremendous efforts have been employed to use this approach with a variety of metals (*e.g.*, palladium, rhodium, and ruthenium) with great success.^{7,48,49} While the power of this strategy is significant, the substrate scope using this strategy is inherently limiting and often requires costly steps for both introduction and removal of the necessary directing group. Thus, achieving high reactivity and selectivity in non-directed systems remains a significant challenge.

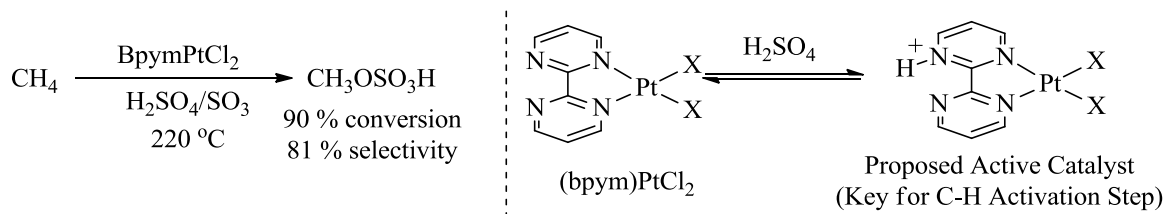
Scheme 1.8 Directed C–H Functionalization Chemistry.



1.4 Pioneering C–H Functionalization Chemistry: Catalytica System

In 1998, Periana *et al.*⁵⁰ published a novel system for the oxidation of methane. The goal of the work was to inhibit Pt^{II} decomposition, a problem in the Shilov system, by the addition of ligands. The authors found that (NH₃)₂PtCl₂ served as an active catalyst for the oxidation of methane in fuming sulfuric acid at 180 °C. However, the catalyst quickly decomposed (half-life ~15 minutes) under the reaction conditions through amine protonation. A significant improvement of this system occurred with the use of (bpym)PtCl₂ (bpym=2,2'-bipyrimidine) as a catalyst (Scheme 1.9). With this bpym-based catalyst, Periana observed ~90 % methane conversion and 81 % selectivity for CH₃OSO₃H in 2.5 hours.

Scheme 1.9 Catalytica Methane Oxidation System.



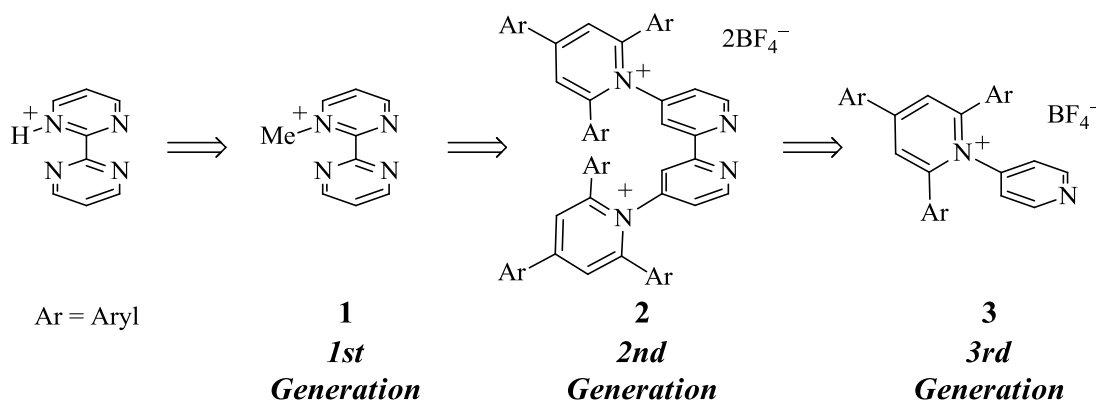
This catalytic system has been extensively studied by Periana and Goddard through computational analysis.⁵¹⁻⁵⁴ On the basis of these calculations, the authors propose that the catalyst is activated through protonation (Scheme 1.9). Thus, the highly acidic environment serves to generate the active catalyst, provide a solvent medium of weakly coordinating anions, and generate a methyl fragment (CH₃OSO₃H) with an electron withdrawing group to limit over-oxidation.

While the Catalytica system is a substantial improvement upon the use of Pt^{IV} as an oxidant, the system still has a large number of drawbacks. First, the reaction is performed with fuming sulfuric acid as the reaction medium. This harshly acidic and corrosive environment is not amenable to any acid sensitive functionality in complex molecules, which limits broad applicability. This highly corrosive environment would also require substantial capital investments for large-scale industrial processes. Second, the proposed active catalyst is not particularly modular and cannot be isolated due to the highly acidic proton of the active catalyst. The inability to isolate the catalyst has hindered catalyst optimization by limiting reaction medium and catalyst modifications. Finally, the reaction requires high temperatures and exhibits low reaction rates. All of these areas provide significant opportunities for improvement in the field.

1.5 Fundamental Project Strategy: Catalytica System Improvement

In an effort to improve upon the Catalytica system for alkane and aromatic oxidation, one would hope to develop isolable analogs of the proposed active catalyst (Scheme 1.10).

Scheme 1.10 Cationic Ligand Design Strategy.



Initial efforts in our group focused on the substitution of the acidic proton for a methyl group **1** (1st Generation).⁵⁵ It was hypothesized that this ligand would retain the desired activity and have the advantage of being isolable. While ligand **1** and bpym in LPtCl_2 complexes showed comparable activity for the activation of benzene C–H bonds, **1** was found to be slightly more active for the activation of methane.⁵⁵ Unfortunately, ligand **1** was prone to demethylation by attack of weak nucleophiles such as trifluoroacetate. Given this decomposition, more stable analogs were still required.

2nd and 3rd Generation ligands (**2** and **3**) (Scheme 1.10) have been developed and will serve as a basis for the chemistry in future chapters of this thesis. In subsequent chapters, studies to improve both fundamental steps and catalytic “Shilov-type” chemistry will be described. Chapter 2 focuses on ligands of type **2** and **3** for catalytic H/D exchange and catalytic C–H acetoxylation using Pt and Pd. Chapter 3 centers on the application of **3** in $\text{MCp}^*\text{Cl}_2\text{L}$ ($\text{M}=\text{Rh}, \text{Ir}$; $\text{Cp}^*=1,2,3,4,5\text{-pentamethylcyclopentadienyl}$) complexes for H/D exchange. Chapter

4 includes a fundamental discussion on the application of **2** in Rh^I and Rh^{III} C–H activation. Chapter 5 focuses on step 3 of the Shilov cycle (functionalization, Scheme 1.6) and discusses computational studies of the reductive elimination of aryl–CF₃ and aryl–acetate bonds from Pd complexes.

1.6 References

- (1) Arndtsen, B. A.; Bergman, R. G.; Mobley, T. A.; Peterson, T. H. *Acc. Chem. Res.* **1995**, *28*, 154.
- (2) Anslyn, E. V.; Dougherty, D. A. *Modern Physical Organic Chemistry*; University Science Books: Sausalito, California, 2006.
- (3) Labinger, J. A. *J. Mol. Catal. A-Chem.* **2004**, *220*, 27.
- (4) Shilov, A. E.; Shul'pin, G. B. *Activation and Catalytic Reactions of Saturated Hydrocarbons in the Presence of Metal Complexes*; Springer: Verlag, 2000.
- (5) Kakiuchi, F.; Chatani, N. *Adv. Synth. Catal.* **2003**, *345*, 1077.
- (6) Arakawa, H.; Aresta, M.; Armor, J. N.; Barteau, M. A.; Beckman, E. J.; Bell, A. T.; Bercaw, J. E.; Creutz, C.; Dinjus, E.; Dixon, D. A.; Domen, K.; DuBois, D. L.; Eckert, J.; Fujita, E.; Gibson, D. H.; Goddard, W. A.; Goodman, D. W.; Keller, J.; Kubas, G. J.; Kung, H. H.; Lyons, J. E.; Manzer, L. E.; Marks, T. J.; Morokuma, K.; Nicholas, K. M.; Periana, R.; Que, L.; Rostrup-Nielson, J.; Sachtler, W. M. H.; Schmidt, L. D.; Sen, A.; Somorjai, G. A.; Stair, P. C.; Stults, B. R.; Tumas, W. *Chem. Rev.* **2001**, *101*, 953.
- (7) Lyons, T. W.; Sanford, M. S. *Chem. Rev.* **2010**, *110*, 1147.
- (8) Crabtree, R. H. *J. Chem. Soc.-Dalton Trans.* **2001**, 2437.
- (9) Labinger, J. A.; Bercaw, J. E. *Nature* **2002**, *417*, 507.
- (10) Periana, R. A.; Bhalla, G.; Tenn, W. J.; Young, K. J. H.; Liu, X. Y.; Mironov, O.; Jones, C. J.; Ziatdinov, V. R. *J. Mol. Catal. A-Chem.* **2004**, *220*, 7.
- (11) Shilov, A. E.; Shulpin, G. B. *Uspekhi Khimii* **1987**, *56*, 754.
- (12) Conley, B. L.; Tenn, W. J.; Young, K. J. H.; Ganesh, S. K.; Meier, S. K.; Ziatdinov, V. R.; Mironov, O.; Oxgaard, J.; Gonzales, J.; Goddard, W. A.; Periana, R. A. *J. Mol. Catal. A* **2006**, *251*, 8.
- (13) Parshall, G. W. *Acc. Chem. Res.* **1975**, *8*, 113.

- (14) Lersch, M.; Tilset, M. *Chem. Rev.* **2005**, *105*, 2471.
- (15) Shilov, A. E.; Shul'pin, G. B. *Chem. Rev.* **1997**, *97*, 2879.
- (16) Shilov, A. E.; Shteinman, A. A. *Coord. Chem. Rev.* **1977**, *24*, 97.
- (17) Crabtree, R. H. *J. Organomet. Chem.* **2004**, *689*, 4083.
- (18) Luinstra, G. A.; Wang, L.; Stahl, S. S.; Labinger, J. A.; Bercaw, J. E. *J. Organomet. Chem.* **1995**, *504*, 75.
- (19) Shilov, A. E. *Activation of Saturated Hydrocarbons by Transition Metal Complexes*; D. Reidel Publishing Company: Dordrecht, Holland, 1984.
- (20) Atzrodt, J.; Derdau, V.; Fey, T.; Zimmermann, J. *Angew. Chem. Int. Ed.* **2007**, *46*, 7744.
- (21) Kharasch, M. S.; Isbell, H. S. *J. Am. Chem. Soc.* **1931**, *53*, 3053.
- (22) Kleiman, J. P.; Dubeck, M. *J. Am. Chem. Soc.* **1963**, *85*, 1544.
- (23) Chatt, J.; Davidson, J. M. *J. Chem. Soc.* **1965**, 843.
- (24) Garnett, J. L.; Hodges, R. J. *J. Am. Chem. Soc.* **1967**, *89*, 4546.
- (25) Lapointe, D.; Fagnou, K. *Chemistry Letters* **2010**, *39*, 1119.
- (26) Goldshleger, N. F.; Tyabin, M. B.; Shilov, A. E.; Shteinman, A. A. *Russ. J. Phys. Chem.* **1969**, *43*, 1222.
- (27) Heyduk, A. F.; Driver, T. G.; Labinger, J. A.; Bercaw, J. E. *J. Am. Chem. Soc.* **2004**, *126*, 15034.
- (28) Bercaw, J. E.; Chen, G. S.; Labinger, J. A.; Lin, B.-L. *Organometallics* **2010**, *29*, 4354.
- (29) Chen, G. S.; Labinger, J. A.; Bercaw, J. E. *Proc. Nat. Acad. Sci. USA* **2007**, *104*, 6915.
- (30) Iverson, C. N.; Carter, C. A. G.; Baker, R. T.; Scollard, J. D.; Labinger, J. A.; Bercaw, J. E. *J. Am. Chem. Soc.* **2003**, *125*, 12674.
- (31) Labinger, J. A.; Bercaw, J. E. In *Higher Oxidation State Organopalladium and Platinum Chemistry*; Canty, A. J., Ed.; Springer-Verlag Berlin: Berlin, 2011; Vol. 35, p 29.
- (32) Owen, J. S.; Labinger, J. A.; Bercaw, J. E. *J. Am. Chem. Soc.* **2006**, *128*, 2005.
- (33) Procelewska, J.; Zahl, A.; van Eldik, R.; Zhong, H. A.; Labinger, J. A.; Bercaw, J. E. *Inorg. Chem.* **2002**, *41*, 2808.
- (34) Wong-Foy, A. G.; Henling, L. M.; Day, M.; Labinger, J. A.; Bercaw, J. E. *J. Mol. Catal. A-Chem.* **2002**, *189*, 3.

- (35) Zhong, H. A.; Labinger, J. A.; Bercaw, J. E. *J. Am. Chem. Soc.* **2002**, *124*, 1378.
- (36) Hodges, R. J.; Webster, D. E.; Wells, P. B. *J. Chem. Soc. A* **1971**, 3230.
- (37) Garnett, J. L.; West, J. C. *Aust. J. Chem.* **1974**, *27*, 129.
- (38) Hodges, R. J.; Garnett, J. L. *J. Phys. Chem.* **1968**, *72*, 1673.
- (39) Goldshleger, N. F.; Eskova, V. V.; Shilov, A. E.; Shteinman, A. A. *Russ. J. Phys. Chem.* **1972**, *46*, 785.
- (40) Stahl, S. S.; Labinger, J. A.; Bercaw, J. E. *Angew. Chem. Int. Ed.* **1998**, *37*, 2180.
- (41) Wang, L.; Stahl, S. S.; Labinger, J. A.; Bercaw, J. E. *J. Mol. Catal. A* **1997**, *116*, 269.
- (42) Luinstra, G. A.; Wang, L.; Stahl, S. S.; Labinger, J. A.; Bercaw, J. E. *Organometallics* **1994**, *13*, 755.
- (43) Zamashchikov, V. V.; Kitaigorodskii, A. N.; Litvinenko, S. L.; Rudakov, E. S.; Uzhik, O. N.; Shilov, A. E. *Bulletin of the Academy of Sciences of the USSR Division of Chemical Science* **1985**, *34*, 1582.
- (44) Zamashchikov, V. V.; Rudakov, E. S.; Yaroshenko, A. P. *React. Kinet. Katal. Lett.* **1983**, *22*, 39.
- (45) Luinstra, G. A.; Labinger, J. A.; Bercaw, J. E. *J. Am. Chem. Soc.* **1993**, *115*, 3004.
- (46) Labinger, J. A.; Herring, A. M.; Bercaw, J. E. *J. Am. Chem. Soc.* **1990**, *112*, 5628.
- (47) Ryabov, A. D. *Chem. Rev.* **1990**, *90*, 403.
- (48) Kalyani, D.; Sanford, M.; Chatani, N., Ed.; Springer Berlin / Heidelberg: 2007; Vol. 24, p 85.
- (49) Ritleng, V.; Sirlin, C.; Pfeffer, M. *Chem. Rev.* **2002**, *102*, 1731.
- (50) Periana, R. A.; Taube, D. J.; Gamble, S.; Taube, H.; Satoh, T.; Fujii, H. *Science* **1998**, *280*, 560.
- (51) Xu, X.; Kua, J.; Periana, R. A.; Goddard, W. A. *Organometallics* **2003**, *22*, 2057.
- (52) Ahlquist, M.; Nielsen, R. J.; Periana, R. A.; Goddard Iii, W. A. *J. Am. Chem. Soc.* **2009**, *131*, 17110.
- (53) Ahlquist, M.; Periana, R. A.; Goddard Iii, W. A. *Chem. Commun.* **2009**, 2373.
- (54) Kua, J.; Xu, X.; Periana, R. A.; Goddard, W. A. *Organometallics* **2001**, *21*, 511.
- (55) Villalobos, J. M.; Hickman, A. J.; Sanford, M. S. *Organometallics* **2009**, *29*, 257.

Chapter 2

Pt and Pd Catalyzed C–H Acetoxylation with Cationic Pyridine-Based Ligands

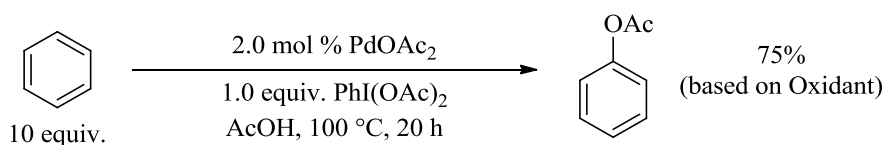
2.1 Background and Significance

The activation and functionalization of C–H bonds has long been considered a “Holy Grail” of organometallic chemistry.¹ In recent years, high-oxidation state palladium has been shown to serve as an effective catalyst for the oxidative functionalization of C–H bonds.^{2,3} Using a ligand directed approach to achieve high activity and site selectivity, arene and alkane C–H bonds have been converted to diverse C–X bonds (X = O, N, S, F, Cl, Br, C).⁴ In contrast, substrates that do not contain a directing group are plagued by slow reaction kinetics and poor selectivity.⁵⁻²⁷ Electron deficient aromatics have been especially challenging substrates for these transformations.^{10,21-24} Furthermore, in typical C–H functionalization reactions aimed at constructing C–X bonds, competing C–C coupling results in undesired biaryl side products.^{19,20} As such, catalyst improvement is required to enable practical undirected C–H functionalization reactions.

Often, catalyst modification through the use of ligands can improve metal based catalysis. However, most Pd-catalyzed processes to oxygenate aromatic C–H bonds are performed without added ligands and only use simple metal salts such as Pd(OAc)₂ or PdCl₂.⁷⁻²⁰ In an example by Crabtree,¹⁰ common ligands such as pyridine, 1,10-phenanthroline, triphenylphosphine oxide, and picolinic acid all suppressed the Pd-

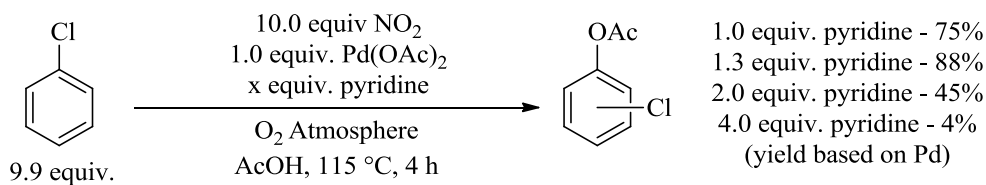
catalyzed oxidation of benzene (Scheme 2.1). For the acetoxylation of benzene, the addition of approximately 2.5 equivalents of pyridine to the reaction, resulted in suppressing catalytic activity by 60% when compared to Pd(OAc)₂ on its own.

Scheme 2.1 Crabtree Benzene Acetoxylation.¹⁰



However, an earlier account by Ebersson showed that sp²-nitrogen donor ligands such as pyridine and bipyridine can increase catalytic activity in this transformation.^{21,22} Most notably, Ebersson illustrated that the ratio of Pd to ligand (pyridine) had a substantial effect on reaction yields in the acetoxylation of chlorobenzene. The yield of the functionalized product varied between 88 and 4% based on Pd (less than one turnover) as the ratio of pyridine was modified (Scheme 2.2).²¹ Given the contrasting results of the Crabtree and Ebersson studies, we felt that the ligand effects in Pd-catalyzed C–H activation required a more systematic evaluation.

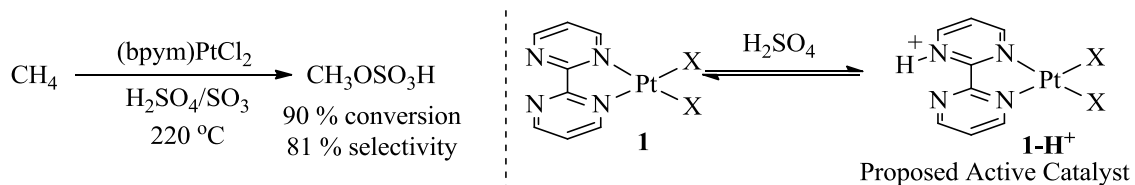
Scheme 2.2 Ebersson Benzene Acetoxylation.²¹



A pioneering example in the field of C–H oxidative functionalization occurred with Shilov's discovery of Pt^{II}-catalyzed functionalization of alkane C–H bonds using a Pt^{IV} oxidant.²⁸⁻³⁴ Following this work, subsequent research has focused on the use of more cost-effective oxidants and the identification of ligands that improve catalyst activity and selectivity in this reaction.^{12,35-37} Another revolutionary advancement in the

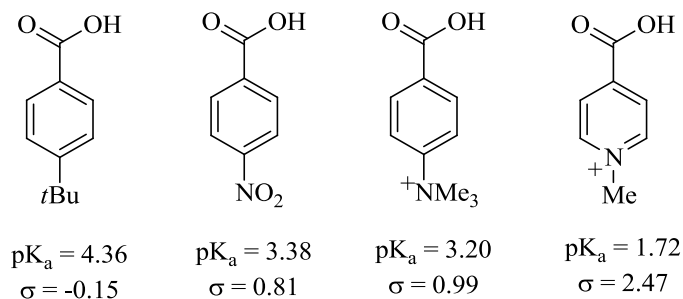
field occurred with the catalyst system disclosed by Periana in 1998, [(bpym)PtCl₂] (**1**) (bpym=2,2-bipyrimidine).³⁸ In this work, the authors illustrated the highly selective oxidation of methane to methyl bisulfate (Scheme 2.3). This system showed effective modification of the Shilov system by substituting the Pt^{IV} oxidant with SO₃.

Scheme 2.3 Catalytic Methane Oxidation System.



Subsequent computational investigations by Periana and Goddard suggested that the active catalyst is formed *in situ* through acid protonation of the ligand backbone (**1-H⁺**).³⁹⁻⁴⁴ The authors postulated that this catalyst modification generated an electrophilic metal center, resulting in high activity towards C–H bonds along with increasing the ligand stability towards oxidative decomposition. The increased electrophilic nature of the metal center can be rationalized by analogy to the effect of cationic substituents on the pK_a of substituted benzoic acid derivatives (Scheme 2.4).^{45,46}

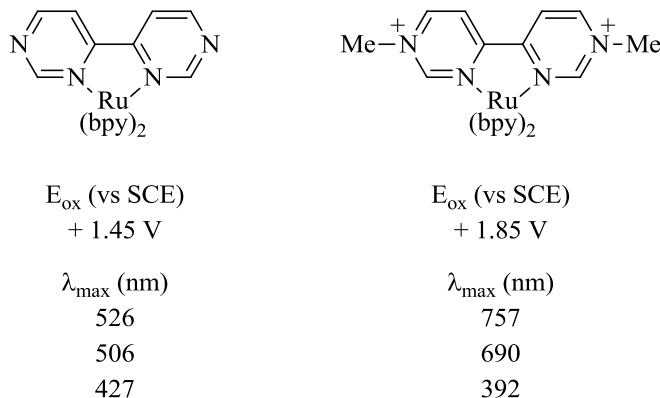
Scheme 2.4 pK_a of Substituted Aromatic Acids.



Given that the protonated ligand should be highly electron deficient through the electron withdrawing nature of the cationic group, we turned to the literature to examine other possible ligand systems containing related cationic substituents.⁴⁷⁻⁵⁵ These reports

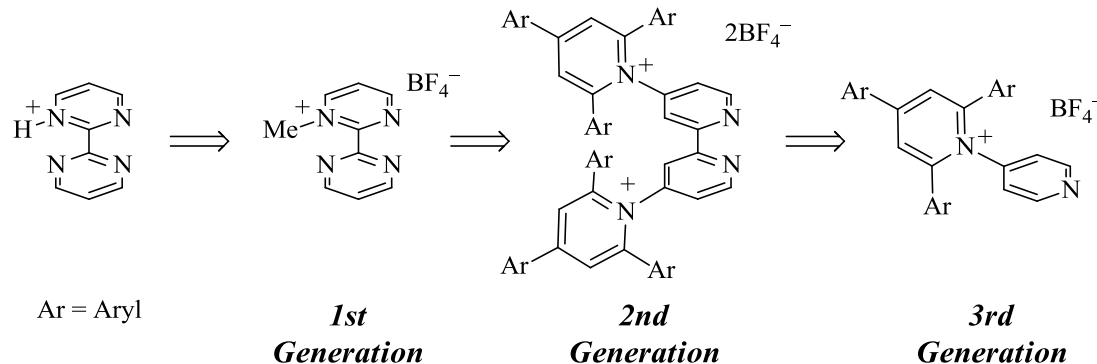
illustrate the fundamental electronic modifications that such ligand substituents impart on metal centers, which are observed through the changes to metal redox potentials and electronic spectra (Figure 2.1). However, these prior publications do not contain any information concerning the use of these substituents in catalysis of any kind.

Figure 2.1 Cationic Substituent Effects on Redox and Electronic Spectroscopy.⁴⁹



While the Periana system was a significant advance, the corrosive nature of the reaction medium and requirement for catalyst activation through protonation by solvent make systematic catalyst improvement difficult and also limit functional group tolerance. Given these limitations, our group has instead focused upon making isolable analogs of the Catalytica active catalyst (**1-H**⁺). Our first generation ligand (synthesized by Dr. Janette Villalobos, Scheme 2.5) was prone to decomposition through nucleophilic attack on the *N*-methyl substituent, which limited catalyst longevity.⁵⁶ This chapter describes our efforts to increase ligand stability and catalyst activity through the design of 2nd and 3rd generation (Scheme 2.5) ligand systems to improve Pd- and Pt-based catalytic C–H functionalization chemistry.

Scheme 2.5 Cationic Ligand Design Strategy.

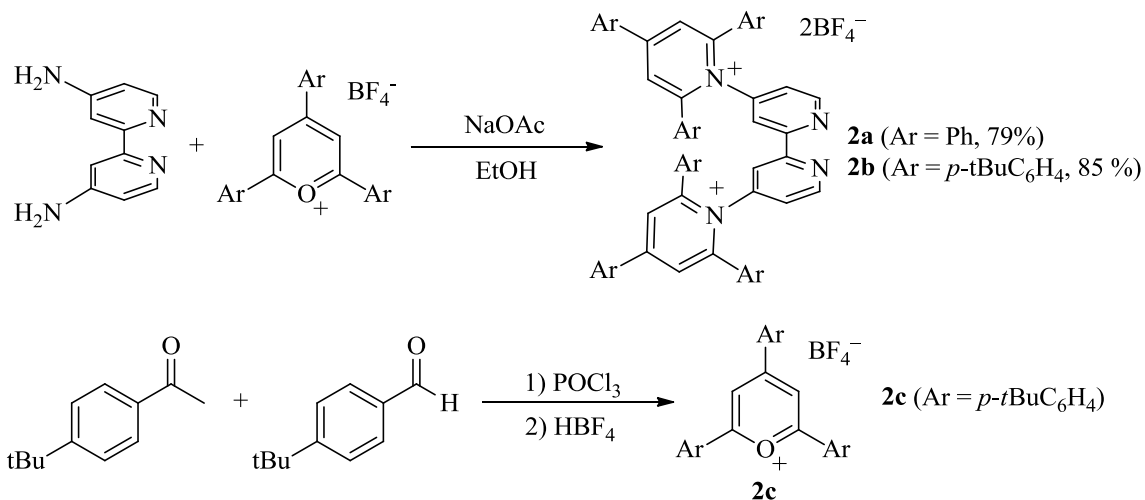


2.2 Results and Discussions

2.2.1 Second Generation Cationic Ligands

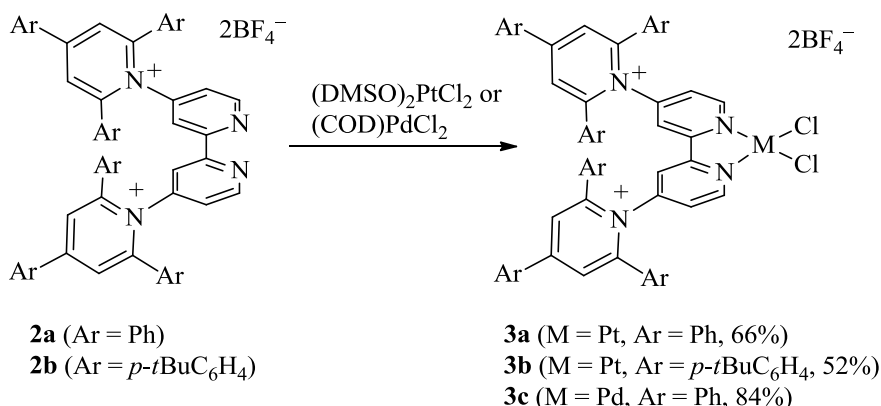
Given that the 1st generation ligand system (Scheme 2.5) was plagued by demethylation, we turned to the literature for other ligand scaffolds known to possess cationic pyridine substituents.⁴⁷⁻⁵⁵ In a report by Lainé and coworkers,⁵⁵ ruthenium bipyridine complexes were synthesized with the ligand **2a** (Scheme 2.6). The ligand can be prepared in high yield via the condensation of 4,4'-diamino-2,2'-bipyridine with the commercially available 2,4,6-triphenylpyrylium tetrafluoroborate (Scheme 2.6). While robust against decomposition under our reaction conditions, this ligand exhibited poor solubility (only appreciably soluble in acetonitrile, dimethylformamide, and dimethylsulfoxide). In an effort to improve solubility for these and future stoichiometric studies, we prepared an alternative *tert*-butyl-substituted pyrylium salt **2c**. The more soluble ligand **2b** was then prepared from **2c**⁵⁷ in 85% yield (Scheme 2.6).

Scheme 2.6 2nd Generation Ligand Synthesis.



With these ligands in hand, the related Pt-complexes (**3a** and **3b**) were synthesized along with the Pd analog (**3c**) according to Scheme 2.7. This work was conducted in collaboration with Dr. Marion Emmert.

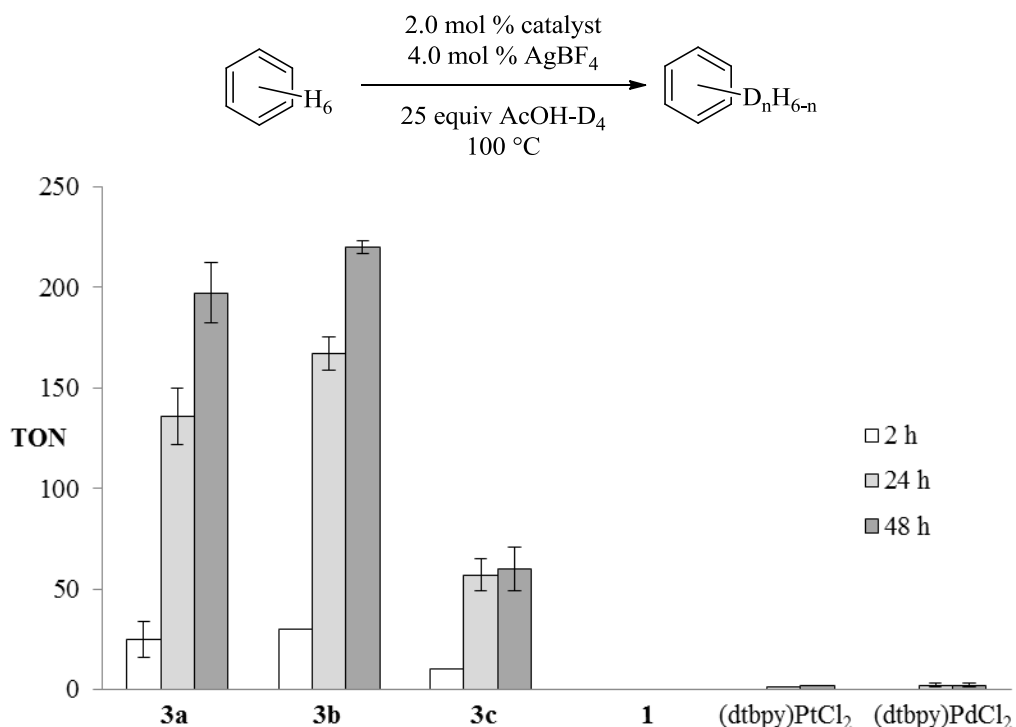
Scheme 2.7 Metal Complex Synthesis with 2nd Generation Ligands.⁵⁸



The catalytic activity of these complexes in C–H activation was studied using a standard assay for hydrogen/deuterium (H/D) exchange.⁵⁹ Under our standard H/D exchange conditions (2 mol % of [M], 4 mol % of AgBF₄, 1 equiv of C₆H₆, and 25 equiv of AcOH-D₄ at 150 °C), complexes containing the cationic ligands showed very high turnover frequencies (TOFs) (0.1 s⁻¹ for **3a** and **3b**; 0.05 s⁻¹ for **3c**) at 15 minute reaction

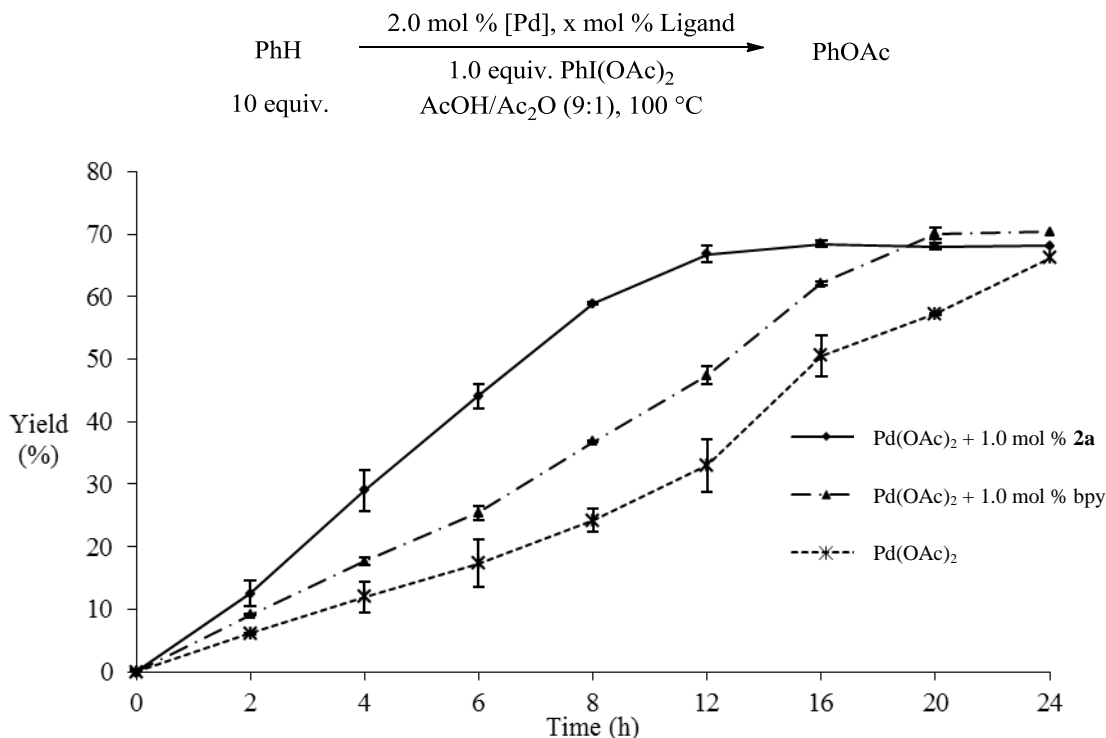
times. In contrast, [(dtbpy)PtCl₂] (dtbpy = 4,4'-di-*t*-butyl-2,2'-bipyridine), [(dtbpy)PdCl₂], and the Catalytica catalyst **1** showed TOFs of 0.0002, 0.002, and 0.003 s⁻¹ respectively. Given this high activity at 150 °C, we wanted to test the reactivity at lower reaction temperatures. As shown in Figure 2.2, complexes containing the 2nd generation cationic ligands exhibited impressive turnover numbers (TONs), even at 100 °C. The Catalytica catalyst **1** along with [(dtbpy)PtCl₂] and [(dtbpy)PdCl₂] showed effectively no catalytic activity at 2, 24, or 48 hours using acetic acid-D₄ as a deuterium source. In sharp contrast, complexes **3a**, **3b**, and **3c** show substantial activity even after 2 hours. Importantly, the more soluble complex **3b** showed measurably higher activity than **3a** at 24 and 48 hour time points.

Figure 2.2 H/D Exchange of Isolable Pt and Pd Complexes.⁵⁸



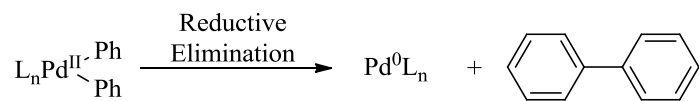
With the significant enhancement of C–H activation reactivity observed using these 2nd generation cationic ligands, we next turned to the oxidative functionalization of benzene to examine if enhanced H/D exchange was correlated with faster rates of C–H functionalization. In these studies, we focused on the Pd-catalyzed C–H acetoxylation of benzene with $\text{PhI}(\text{OAc})_2$ that was previously reported by Crabtree.¹⁰ With the success in H/D exchange of ligand **2a**, we initially used catalyst **3c** for the functionalization reactions. In comparison to $\text{Pd}(\text{OAc})_2$, catalyst **3c** was a worse catalyst in the reaction. With this result, we drew inspiration from earlier reports from Ebersson and considered 2 : 1 metal to ligand ratios.^{21,22} In Figure 2.3, the yield of phenyl acetate is plotted as a function of time for three catalyst systems. The bottom curve illustrates the time profile for the reaction using only $\text{Pd}(\text{OAc})_2$ as a catalyst. From the time profile, the reaction reached completion (~68% yield based upon oxidant) at 24 hours. Shown in the middle curve, the addition of 0.5 equiv of 2,2'-bipyridine (bpy) (Pd : bpy ratio = 2 : 1) resulted in a rate enhancement, and the reaction reached completion at approximately 20 hours. Gratifyingly, and consistent with the reactivity enhancement towards H/D exchange (*vide supra*), the addition of 0.5 equiv of **2a** (Pd : **2a** ratio = 2 : 1) led to a further rate enhancement, and the reaction reached completion in approximately 12 hours, half the time required by $\text{Pd}(\text{OAc})_2$ alone.

Figure 2.3 Pd-Catalyzed Benzene Acetoxylation.⁵⁸



It is important to note that reaction completion times are visually identifiable due to the precipitation of Pd⁰ via formation of biphenyl when complete consumption of the oxidant has occurred (Scheme 2.8).

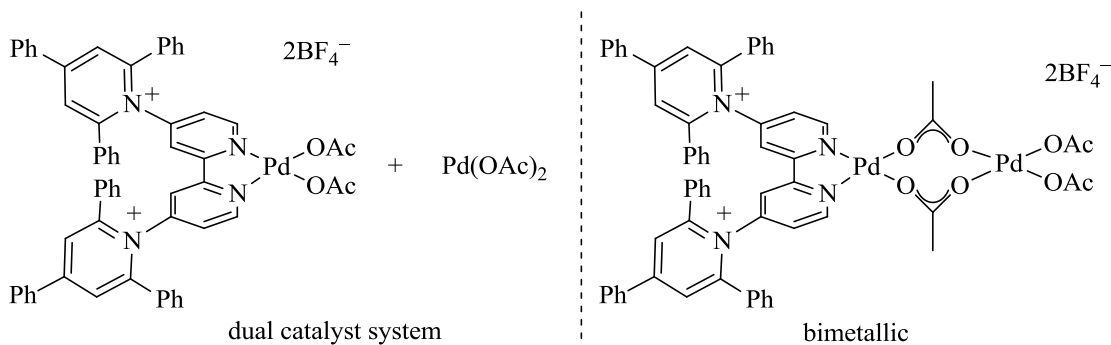
Scheme 2.8 Catalyst Termination Step.



The improved activity for H/D exchange and oxidative functionalization of benzene observed with the 2nd generation cationic ligand scaffold indicates that ligand modifications of Pd-based catalysts can improve catalytic activity. While the enhanced reactivity is exciting, the optimal Pd to ligand ratio (2:1) implicates a more complex catalyst system. At least two possible explanations could explain this enhanced activity:

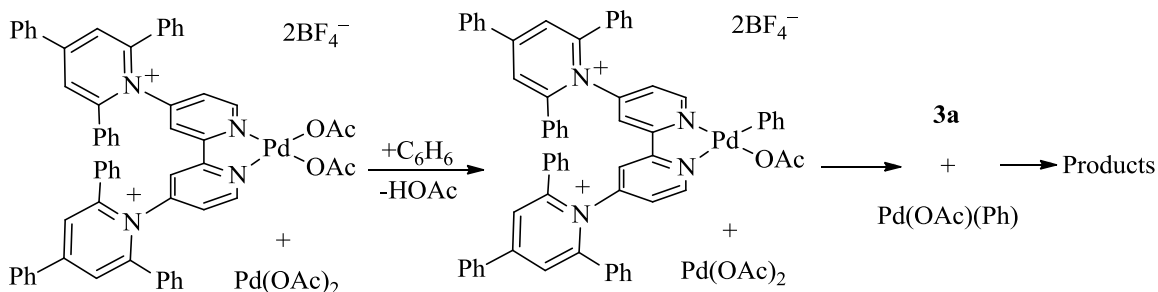
(1) a dual catalyst involving a transmetalation step or (2) a bimetallic catalyst system (Scheme 2.9).

Scheme 2.9 Possible Active Catalyst Systems.



For a dual catalyst system (Scheme 2.10), one could envision that each catalyst performs a specific role in the reaction. Given the rate enhancement associated with **3c** in both functionalization and H/D exchange, a possible mechanism could involve **3c** activating a benzene C–H bond followed by transmetalation to Pd(OAc)₂, which then effects the necessary functionalization step.

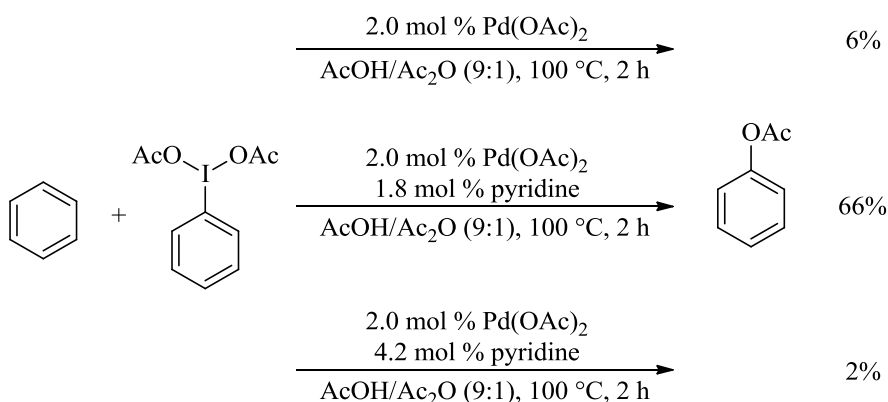
Scheme 2.10 Dual Catalyst Transmetalation Mechanism.



If transmetalation is key to catalytic activity, monodentate ligands might be expected to improve reactivity by increasing the rate of this step. Also, monodentate ligands could aid in generating an open coordination site necessary for C–H activation. Based on this hypothesis, several of my co-workers recently found that the addition of

pyridine as a supporting ligand promotes the Pd-catalyzed acetoxylation of benzene.⁶⁰ In this study, the Pd to pyridine ratio was key to achieving high activity. A 1:0.9 Pd to pyridine ratio resulted in a reaction completion time of approximately 2 hours as compared to 24 hours for Pd(OAc)₂ alone. Importantly, a 1:2.1 Pd to pyridine ratio greatly suppressed catalytic activity in this study (Scheme 2.11).

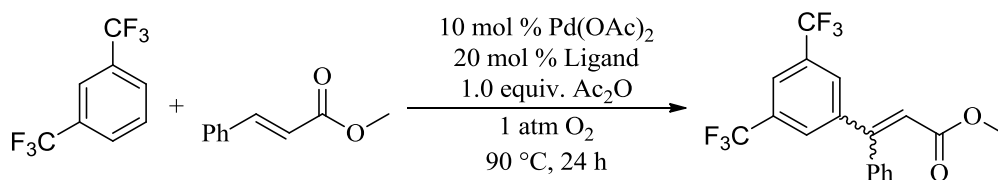
Scheme 2.11 Pd(OAc)₂/Pyridine Catalyst System.⁶⁰



2.2.2 Third Generation Cationic Ligands via High Throughput Screening

In trying to understand the dramatic ligand effects seen when varying the Pd to pyridine ratio, we turned to a recent report of Pd-catalyzed Fujiwara-Moritani reaction (oxidative Heck reaction) by Yu and co-workers (Scheme 2.12).⁶¹

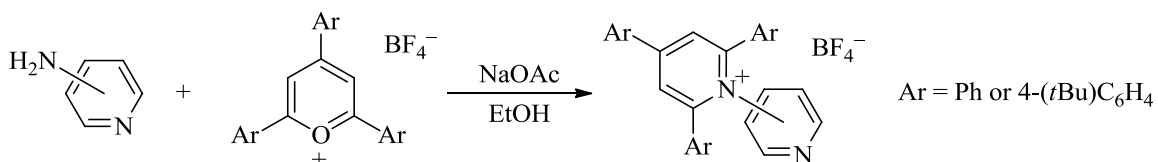
Scheme 2.12 Yu's Oxidative Heck Reaction with Electron Deficient Arenes.⁶¹



In this work, the authors described a key steric trend upon employing pyridine ligands with varied substitution patterns. With pyridine ligands such as pyridine, lutidine, 2,6-di-isopropylpyridine, less than 5% of the desired product was observed.

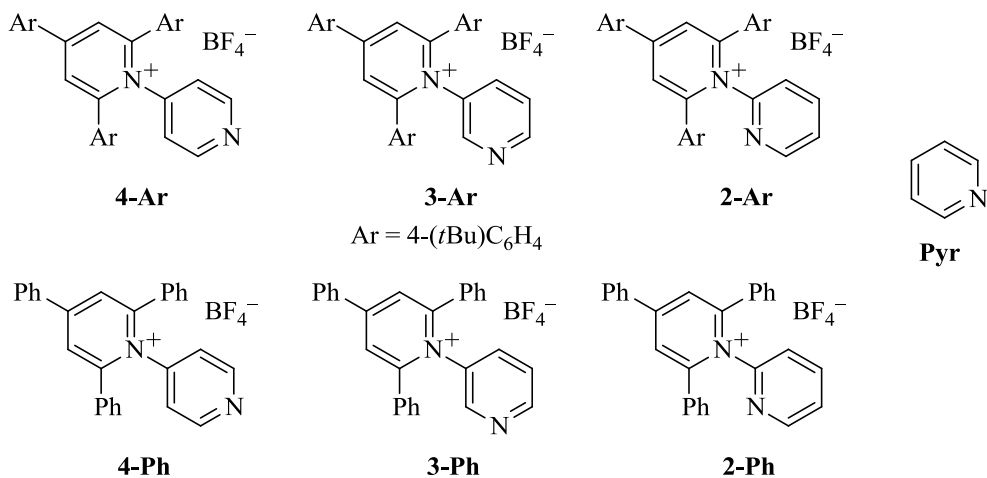
on monodentate pyridine ligands would increase catalytic activity. With this goal, we synthesized a library of cationic pyridine derivatives according to Scheme 2.14.

Scheme 2.14 General Cationic Pyridine Derivative Synthesis.



The ligand set contained six cationic pyridine derivatives in which the cationic group was positioned at the 2, 3, and 4 position of the pyridine ring and 4-*t*-butylphenyl and phenyl aryl groups were added on the pyridinium ring (Scheme 2.15).

Scheme 2.15 Ligand Library.

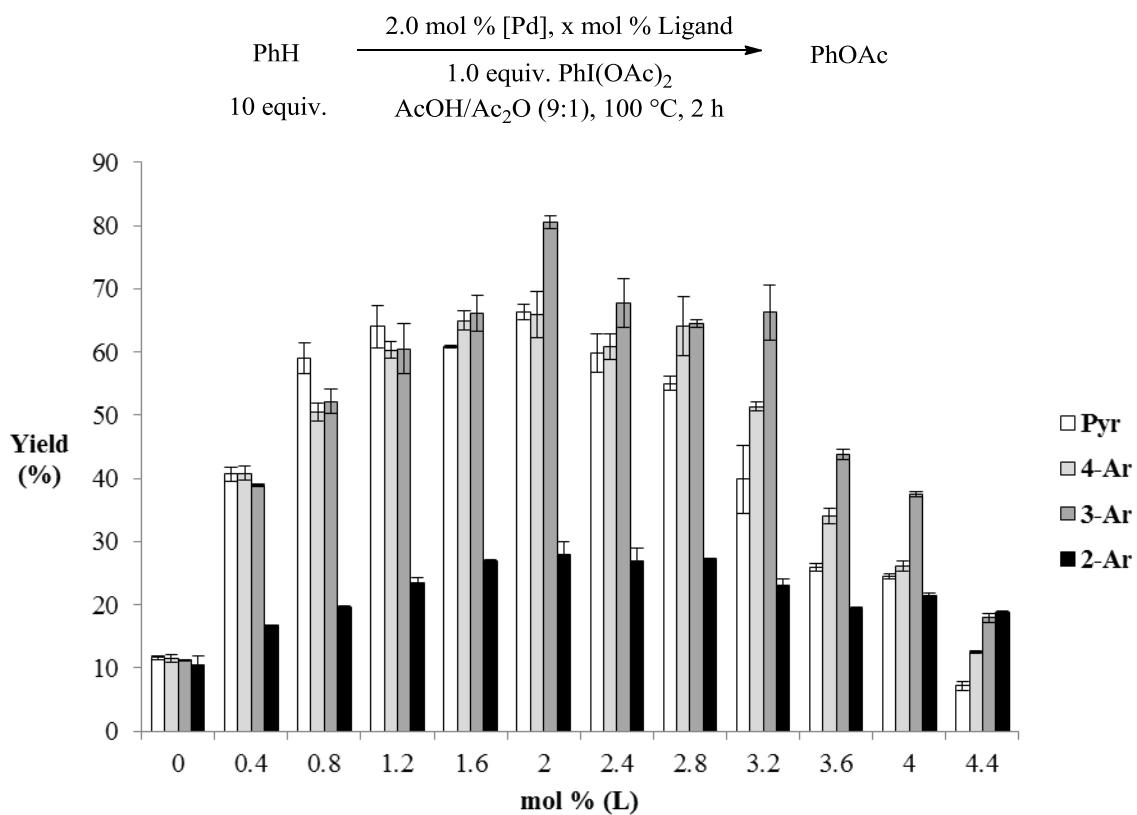


To quickly assess the ligand activity in the Pd-catalyzed benzene acetoxylation reaction, I traveled to the Centre for Catalysis Research and Innovation at the University of Ottawa and worked with Roxanne Clément (the high-throughput facilities manager). On the basis of our previous report on pyridine ligand effects,^{60,61} we hypothesized that these cationic ligand derivatives would exhibit similar palladium to ligand ratio effects. Given the competing factors of sterics, electronics, and charge, these ligands were expected to produce catalyst systems with varying activity. Notably, the standard

reaction conditions were altered slightly (one-quarter the reaction scale) to accommodate the high-throughput instrumentation requirements.

Our first catalyst screen involved variation of the Pd to ligand ratio using **4-Ar**, **3-Ar**, and **2-Ar**. Pyridine was also employed as a standard to serve as a reference to our previous data (Figure 2.4).⁶⁰

Figure 2.4 Pd:Ligand Ratio Effect on Catalytic Activity.

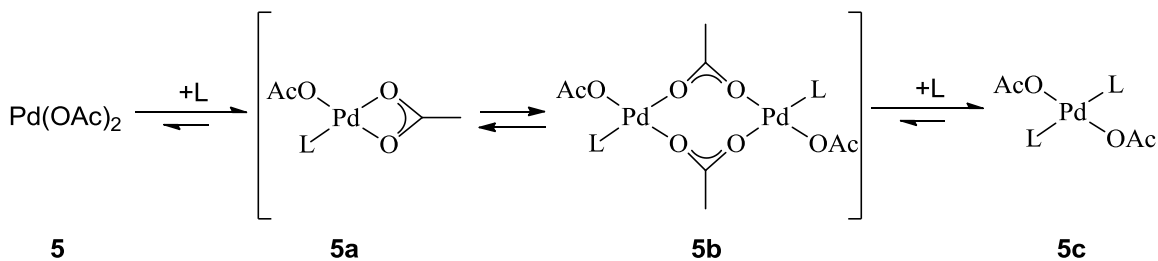


A series of important ligand effects can be observed from the data presented in Figure 2.4. As seen previously, Pd(OAc)_2 alone is not an effective catalyst and adding an excess [≥ 2 equiv/Pd (4 mol %)] of the monodentate pyridine ligand suppresses catalytic activity. Similar to the previous report with pyridine,⁶⁰ the cationic pyridine ligands show a continuum of reactivity in which the most active catalyst system consists of an ~1:1 ratio of Pd to ligand. At low ligand loadings (0.4-1.6 mol %), pyridine produces a

more effective catalyst system than the cationic pyridine analogs. In sharp contrast, higher ligand loadings (2.4-4.4 mol %) of **4-Ar** and **3-Ar** produce catalyst systems that are more active than with the addition of pyridine.

In light of the proposal by Yu for the high activity with sterically bulky 2,6-disubstituted pyridine ligands (Scheme 2.13),⁶¹ we hypothesize that Pd(OAc)₂ (**5**) is in equilibrium with a mono-ligated Pd-monomer (**5a**) or a mono-ligated acetate-bridged Pd dimer (**5b**) and PdL₂(OAc)₂ (**5c**) (Scheme 2.16). The activity curves shown in Figure 2.4, in which no ligand and excess ligand both suppress activity, suggest that **5** and **5c** are poor catalysts.

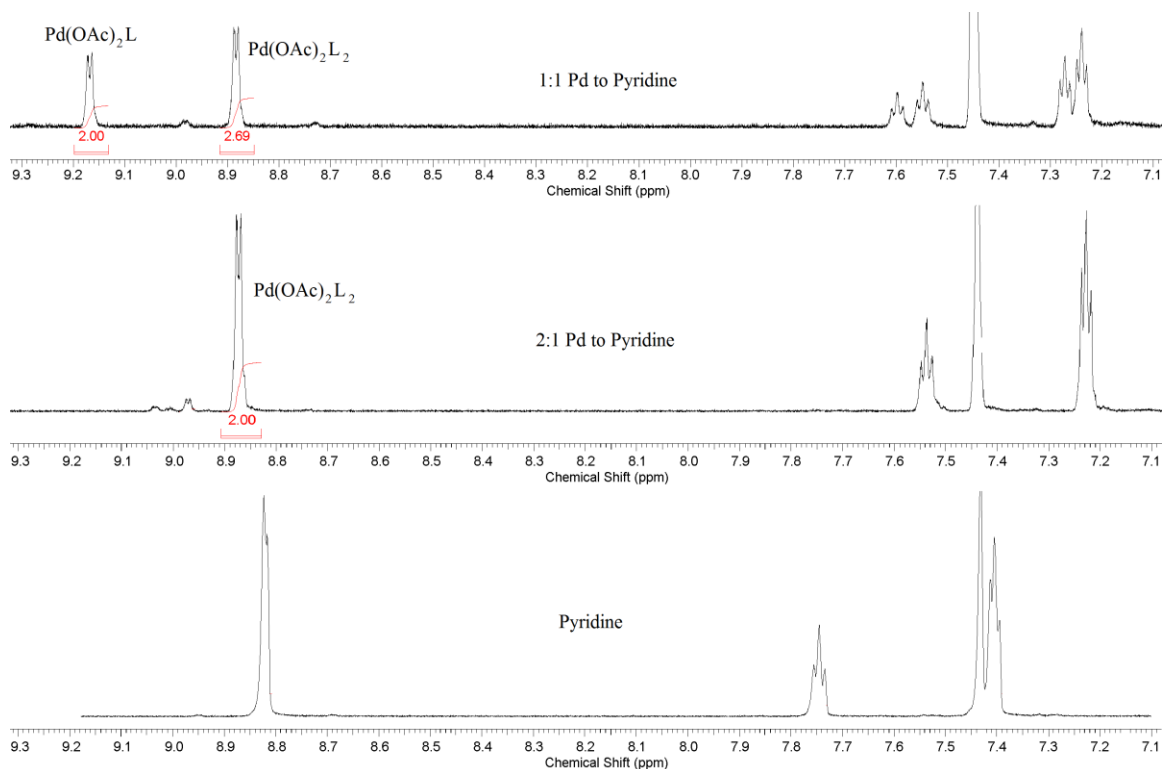
Scheme 2.16 Pd(OAc)₂ and Ligand Equilibrium.



Because pyridine serves as a relatively more effective ligand at low loadings (0.4-1.6 mol %), and **4-Ar** and **3-Ar** are more effective at high ligand loadings (2.4-4.4 mol %), we hypothesize that the identity of the ligand likely affects this equilibrium. If the change in activity was only related to changing activation energies, one would predict a consistent ligand activity ordering at each ligand loading, which is not observed. This indicates that ligand identity could affect the concentrations of Pd(OAc)₂ (**5**), Pd(L)(OAc)₂ (**5a** or **5b**), and Pd(L)₂(OAc)₂ (**5c**) in solution (Scheme 2.12). Given that maximum activity is achieved with a Pd to ligand ratio of 1:1, we hypothesize that the active species is either a mono-ligated Pd monomer (**5a**) or an acetate bridged dimer (**5b**).

In order to gain a better understanding of this equilibrium, ^1H NMR spectra were recorded of pyridine, $\text{Pd}(\text{OAc})_2$ plus one equivalent of pyridine, and $\text{Pd}(\text{OAc})_2$ plus two equivalents of pyridine in 500 μL of CD_3COOD plus 500 μL of C_6D_6 (an approximation of the catalytic reaction medium). While the metal acetate resonances quickly exchange with solvent (acetate- D_3), the *ortho*-pyridine hydrogens are distinct and allow for identification of all three species (pyridine, $\text{Pd}(\text{L})(\text{OAc})_2 = 9.17$ ppm, and $\text{Pd}(\text{L})_2(\text{OAc})_2 = 8.89$ ppm) (Figure 2.5). From these NMR spectra, it is clear that two equivalents of pyridine results in clean formation of a $\text{PdL}_2(\text{OAc})_2$ (**5c**). A spectrum of this mixture at the optimum ratio (1:1) was found to contain no free pyridine, 42% of a mono-pyridine species (**5a** or **5b**), and 58% of the bis-pyridine species (**5c**). Given that the bis-pyridine species would be formed along with an equal amount of $\text{Pd}(\text{OAc})_2$, the calculated ratio of the equilibrium mixture is 29% $\text{Pd}(\text{OAc})_2$, 42% $\text{PdL}(\text{OAc})_2$, and 29% $\text{PdL}_2(\text{OAc})_2$ (this calculation assumes that $\text{Pd}(\text{L})(\text{OAc})_2$ exists as the monomeric form **5a**).

Figure 2.5 Pd(OAc)₂ and Pyridine Equilibrium.

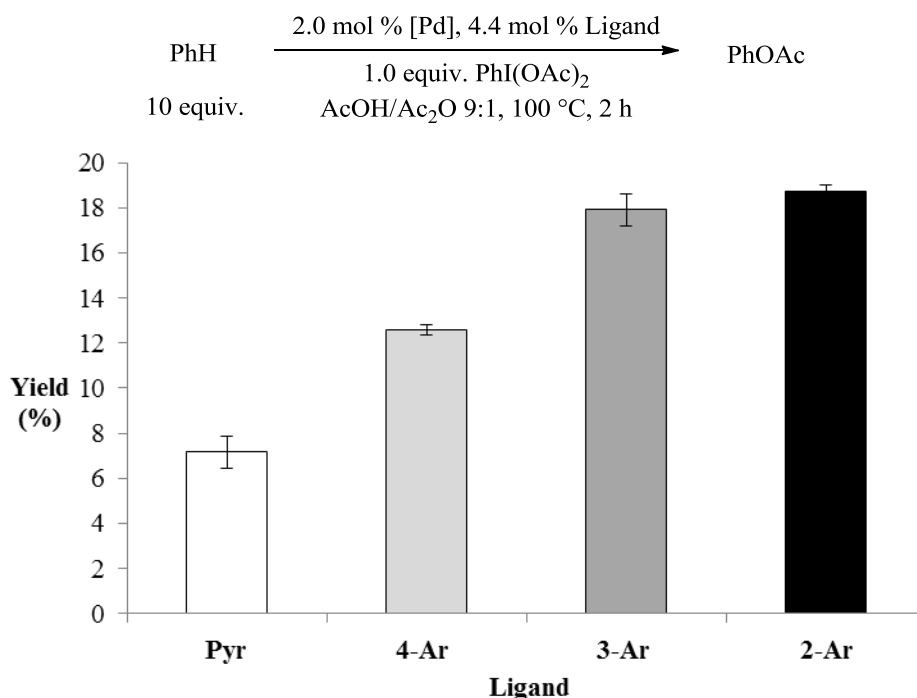


When analogous experiments were performed using **3-Ar**, two equivalents of ligand relative to Pd resulted in the precipitation of an off-white solid. An NMR of the solid precipitate showed a 2:1 ratio of **3-Ar** to Pd(OAc)₂ indicating the formation of Pd(**3-Ar**)₂(OAc)₂. When a 1:1 ratio of **3-Ar** : Pd(OAc)₂ was interrogated by ¹H NMR spectroscopy, two metal products were observed in a 10:3 ratio. Given the low solubility of the Pd(**3-Ar**)₂(OAc)₂ under these solvent conditions, it is unclear what the identity of these two complexes are. One possibility is that this mixture consists of a mixture of **5a** and **5b** or one is **5c**. Thus, when pyridine is used as a ligand for Pd in a 1:1 ratio, approximately 40% of the Pd appears to be in the catalytically active form (**5a** or **5b**) (29%, 42%, 29% ratio of products above). If 100% of the **3-Ar** system resulted in the form [Pd(L)(OAc)₂]_n, this would only account for a maximum of a 2.5 fold rate enhancement in the system if the ligands have no effect on the activation energy of the

reaction as long as both systems exist in the same form (monomeric **5a** or dimeric **5b**). Overall catalyst activity is compared below in Section 2.2.4.

The activity inhibition at high ligand loading supports the equilibrium modification hypothesis. When the ligand loading is high (4.4 mol%), the ligand charge and sterics appear to have a large effect on the inhibition of catalytic activity (Figure 2.6).

Figure 2.6 Catalyst Inhibition at High Ligand Loadings.

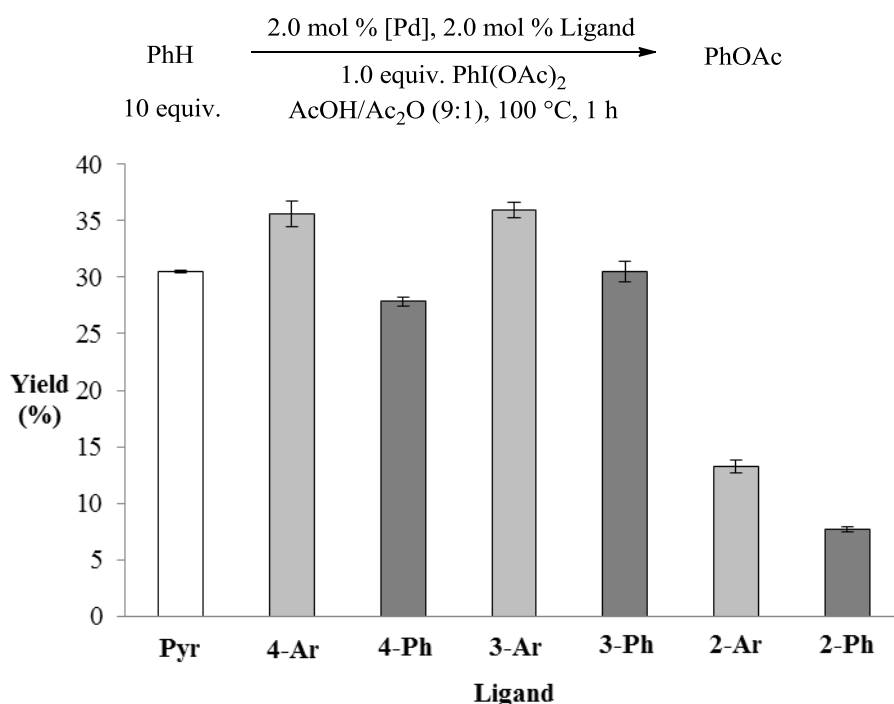


Pyridine shows the highest degree of inhibition at high ligand loadings, indicating that the equilibrium likely favors the bis-pyridine complex **5c** (Scheme 2.16). The cationic ligands show less inhibition, and the inhibition is directly related to the proximity of the steric bulk to the metal center. Thus, **2-Ar** and **3-Ar** show less inhibition, and **4-Ar** more closely resembles pyridine. The effect on catalyst inhibition could be a result of the electron withdrawing ability of the ligand or complex solubility affecting the equilibrium with the formation of $\text{Pd(L)}_2(\text{OAc})_2$ (**5c**), since cationic ligands would

produces a dicationic metal species. The formation of the dicationic species is not expected to be highly favorable under catalytic conditions given the reaction media of benzene and acetic acid given its observed low solubility (*vida supra*).

Within two hours, reactions at 1:1 Pd to ligand ratios are very close to reaching completion. To more accurately compare ligand activities, short reaction times (1 hour) at lower conversion were also performed with a 1:1 Pd to ligand ratio (Figure 2.7).

Figure 2.7 Ligand Effect on Catalysts Activity at Short Reaction Times.



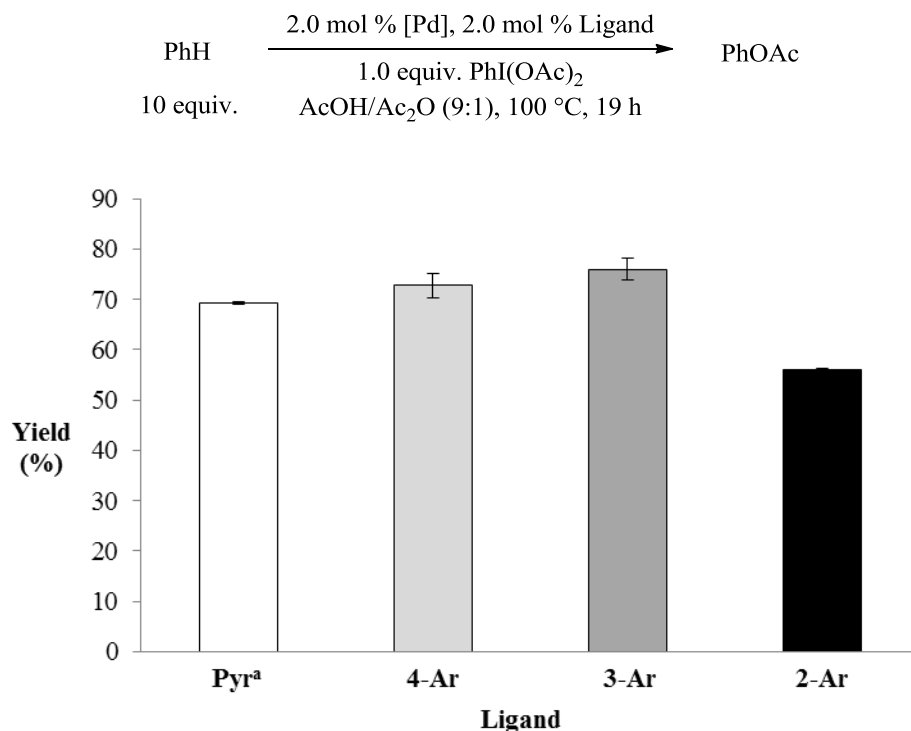
A few key comparisons can be made with the short reaction times. First, each 4-*t*-butylphenyl pyridinium-substituted derivative produced more active catalyst systems than the corresponding phenyl substituted derivative (e.g. **4-Ar** system is more active than **4-Ph**). Second, the 2-substituted ligands (**2-Ar** and **2-Ph**) produce catalysts systems that are significantly diminished in activity when compared to pyridine. Finally, and most

importantly, two of the 3rd generation ligands (**4-Ar** and **3-Ar**) form more active catalyst systems in comparison to pyridine.

2.2.3 Validating High-Throughput Screening Results

To ensure the validity of the high-throughput screening analysis, we repeated the ligand screen on the typical lab reaction scale. Using this scale, we confirmed the catalyst system activity order from the high-throughput screening (Figure 2.8): **3-Ar** > **4-Ar** > **Pyr** > **2-Ar**. The final reaction time point for this series was taken as the reaction completion time for the **2-Ar** ligand. Notably, the other systems reach completion at approximately two hours, but yields are not diminished under extended reaction times.

Figure 2.8 Lab Scale Reaction Yields.

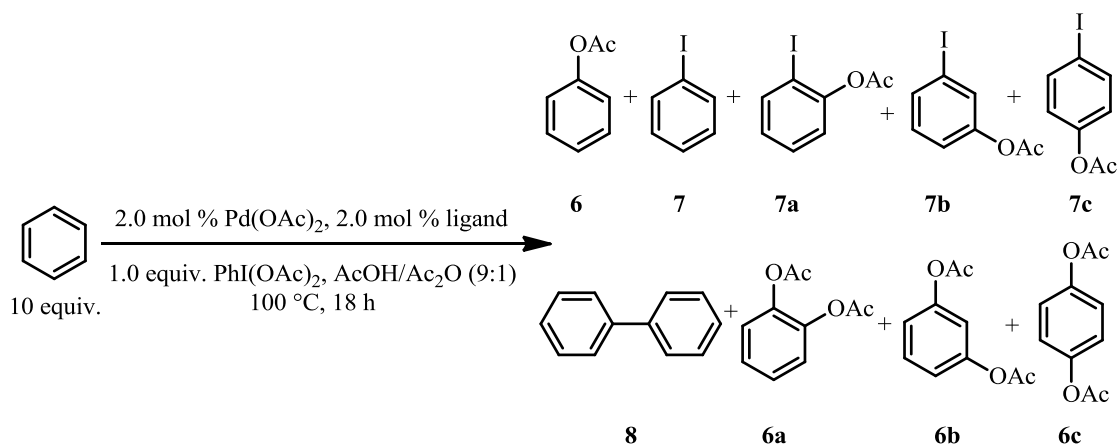


^a - 1.8 mol %

2.2.4 Improving Catalysis Through Oxidant Modification

Comparing the results from the original Pd/dicationic ligand system (Figure 2.3) to the Pd/cationic pyridine system (Figure 2.8), the maximum reaction yields for both systems are in the range of 70-76% yield. To identify the source of this maximum, one has to consider the total side products in this reaction.^{58,60} Previously in this chapter, the reaction shown is the conversion of benzene to phenyl acetate; however, this is only part of complex product distribution. With the use of iodobenzene diacetate, the byproduct from the oxidant is iodobenzene (**7**). Thus, the primary products from this reaction are phenyl acetate (**6**) and iodobenzene (**7**). However, both of these products can also undergo further oxidative functionalization reactions, forming acetoxyated iodobenzene (**7a-7c**) and diacetoxybenzene (**6a-6c**) derivatives. These secondary oxidation products can be formed as the *ortho*, *meta*, and *para* isomers (~ 1-2% of each product observed). Additionally, small amounts of biphenyl (**8**) are also observed in this reaction (~1-2%). The complete list of products from this reaction is shown below in Scheme 2.17.

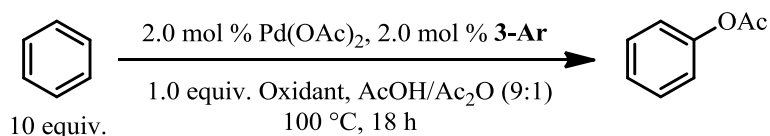
Scheme 2.17 Reaction Products.



In an effort to improve this reaction, we wanted to eliminate as much of the undesired secondary oxidation products as possible. As such, we chose to examine a

variety of other known oxidants that do not generate iodobenzene as a primary byproduct. Using our best ligand system from the high-throughput analysis (**3-Ar**), we screened a series of oxidants known to participate in Pd-catalyzed C–H oxygenation reactions (Table 2.1). In particular, these oxidants have been shown to be effective for the ligand directed oxidative functionalization of C–H bonds.^{4,62}

Table 2.1 Oxidant Screen for Benzene Acetoxylation.



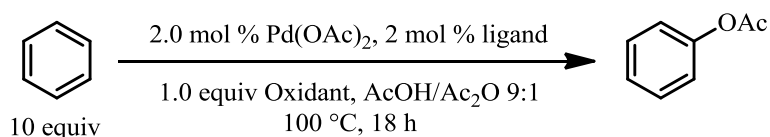
Oxidant	Yield (PhOAc)
PhI(OAc) ₂	76%
Oxone®	0%
NBu ₄ Oxone	0%
Cu(OAc) ₂ ·H ₂ O	2%
H ₄ PMo ₁₁ VO ₄₀ ^a	3%
K ₂ S ₂ O ₈	67%

^a-5 mol % polyoxometalate in air

As a benchmark from above, PhI(OAc)₂ results in a yield of 76%. Other common oxidants such as Oxone® (2KHSO₅·KHSO₄·K₂SO₄), NBu₄Oxone (potassium ions of Oxone have been substituted with tetrabutylammonium cations), copper(II) acetate, and a polyoxometalate resulted in negligible yields of the desired acetoxyated product. However, the use of potassium persulfate (K₂S₂O₈) resulted in a 67% yield. This is a significant improvement in the economics of this reaction, given that the price of PhI(OAc)₂ is approximately \$420 per mole while that of K₂S₂O₈ is approximately \$32 per mole (Sigma Aldrich Chemical Company). In addition, PhI is not formed as a by-

product with $\text{K}_2\text{S}_2\text{O}_8$. Previous reports had indicated that potassium persulfate could serve as an oxidant for the $\text{Pd}(\text{OAc})_2$ -catalyzed acetoxylation of aromatic substrates, but these reactions were plagued by low yields (<40%) and low catalyst turnovers (TON < 10).^{23,24} With this initial and promising result, we examined the ligand trends with $\text{K}_2\text{S}_2\text{O}_8$ as the oxidant (Table 2.2).

Table 2.2 Ligand and Counterion Effects in $\text{K}_2\text{S}_2\text{O}_8$ Oxidation.



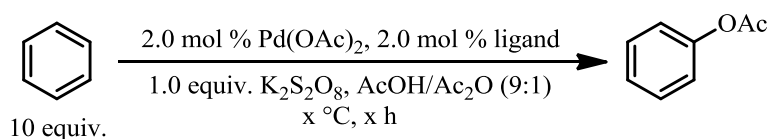
Oxidant	Ligand	Yield (PhOAc)
$\text{K}_2\text{S}_2\text{O}_8$	3-Ar	67%
$\text{K}_2\text{S}_2\text{O}_8$	4-Ar	64%
$\text{K}_2\text{S}_2\text{O}_8$	Pyr^a	55%
$\text{K}_2\text{S}_2\text{O}_8$	None	5%
$\text{Na}_2\text{S}_2\text{O}_8$	3-Ar	2%
$(\text{NH}_4)_2\text{S}_2\text{O}_8$	3-Ar	0%

^a-1.8 mol %

The reaction yields were consistent with previous results using $\text{PhI}(\text{OAc})_2$ as an oxidant (**3-Ar** > **4-Ar** > **Pyr**). Importantly and consistent with previous reports, $\text{Pd}(\text{OAc})_2$ as a catalyst with no ligand only produces a 5% yield of the product phenyl acetate.²¹⁻²⁴ The corresponding sodium and ammonium salts provided little of the desired product (< 2%). This may be due to the lower solubility of these salts as well as the physical properties of the compounds. The potassium salt is a fine powder, while the sodium and ammonium salts are crystalline in nature. This could affect surface area and thereby have dramatic effects on solubility of the reagents.

With this new oxidant system, we next wanted to ascertain the activity of this system at different temperatures. Thus, we compared reaction yields and times at 100, 80, and 60 °C using a 1:1 Pd to ligand ratio and monitored the reactions to completion.

Table 2.3 Temperature Effects on Catalyst Yields and Reaction Times in Parenthesis.



Ligand	Yield (Reaction Time)		
	100 °C	80 °C	60 °C
3-Ar	67% (18 h)	78% (19 h)	60% (42 h) ^b 74% (110 h)
3-Ar^a	64% (18 h)	73% (37 h)	N.D. ^c
Pyr^b	55% (18 h)	31% (19 h) ^b	17% (42 h) ^d

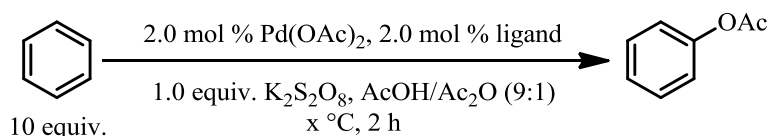
^a-Reaction with 1 mol % Pd(OAc)₂ and 1 mol % ligand. ^b-1.8 mol %. ^c-Not determined. ^d- Reaction not at completion.

Interestingly, with **3-Ar**, dropping the temperature from 100 to 80 °C resulted in a 10% improvement in yield, which is now actually higher than that observed with PhI(OAc)₂. Also, with the cationic ligand system **3-Ar**, the loading of Pd and ligand can be dropped to 1 mol % to achieve similar yields (within 5%). At 100 °C, the decreased catalyst loading had a negligible effect on the observed reaction completion time (as determined by the time at which Pd⁰ precipitation was observed). The reaction time at the lower catalyst loading approximately doubled when the reaction was performed at 80 °C. Lowering the temperature to 60 °C resulted in a much slower reaction, but this transformation still reached a yield of 74% at 110 hours. The activity at lower catalyst loading is important because this represents a doubling of the catalytic turnovers for the reaction. Previous examples have illustrated less than 10 turnovers using K₂S₂O₈ as the

oxidant for non-directed C–H functionalization to form C–O bonds.²²⁻²⁴ Using the **3-Ar** ligand, we have achieved turnover numbers greater than 70 at 80 °C.

Given the different yields obtained when using **3-Ar** and pyridine systems at long reaction times, we wanted to have a better comparison of catalyst system activity at an early stage of the reaction. Repeating the above reactions for two hours resulted in directly comparable data for catalyst activity. Given the temperature effects illustrated above, these studies were carried out at 80 °C, 100 °C, and 120 °C. The results are tabulated below in Table 2.4.

Table 2.4 Ligand Activity Comparison at Low Conversion.



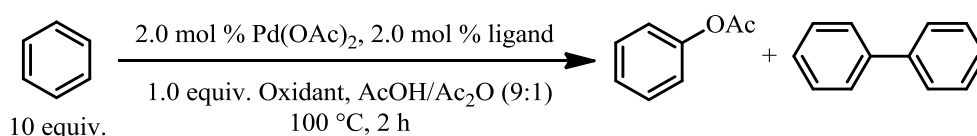
Temperature	Yield		Ratio of Yield (3-Ar / Pyr)
	3-Ar	Pyr ^a	
80 °C	10.3%	2.0%	5.2
100 °C	24.1%	5.3%	4.5
120 °C	32.5%	7.3%	4.5

^a-1.8 mol %

From this study we can see that with **3-Ar** as the ligand, approximately 5 times as much product is observed when compared to pyridine at two hours for all three temperatures. From the equilibrium discussion above, an equilibrium change should only account for a maximum of a 2.5-fold increase in activity. This indicates that **3-Ar** must have some effect on the activation energy of the system. Temperature also affects the rate of the reaction, as the yields differ by a factor of three between the lowest to highest temperature. Given that we had previously observed the formation of biphenyl in these

reactions with $\text{PhI}(\text{OAc})_2$, and $\text{K}_2\text{S}_2\text{O}_8$ has been used as an oxidant for the formation of biphenyl units in Pd-catalyzed reactions,⁶³ we hypothesized that phenyl acetate and biphenyl could be competing products in the reaction and that this competition might be altered by temperature and ligands. To test this hypothesis, we compared the ratio of phenyl acetate to biphenyl as a function of ligand at two hour reaction times. This data is compiled below in Table 2.5.

Table 2.5 Ligand and Temperature Effects on Selectivity.

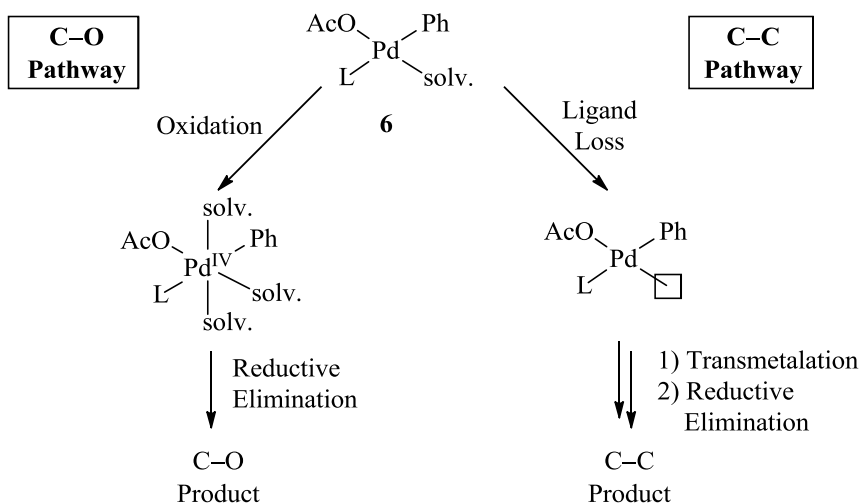


Temperature	Ratio (PhOAc : Ph-Ph)	
	3-Ar	Pyr ^a
80 °C	96 : 1	13 : 1
100 °C	47 : 1	8 : 1
120 °C	19 : 1	6 : 1

^a-1.8 mol %

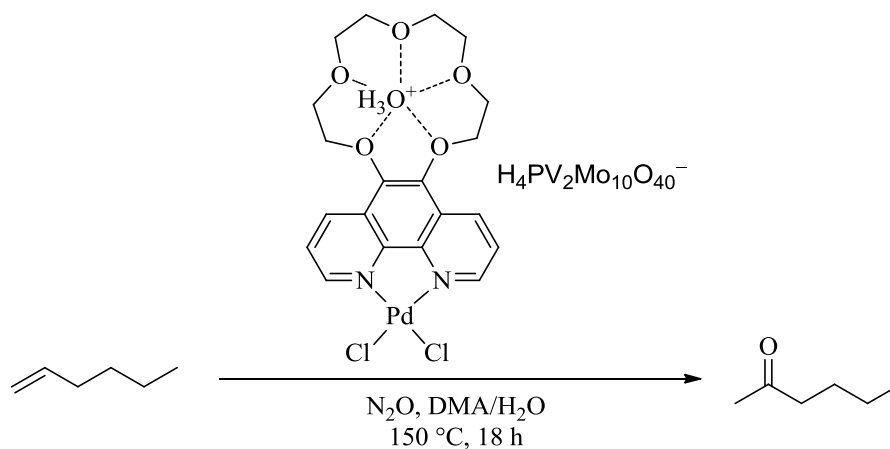
From this data, it is clear that the formation of biphenyl is competitive to acetoxylation over the course of the reaction. More importantly, this competitive process is affected by the temperature and ligand used in the reaction. This indicates a competing process in which an aryl complex (**6**) can either undergo a transmetallation or be oxidized leading to C–O bond formation (Scheme 2.18).

Scheme 2.18 Competing C–O versus C–C Bond Formation.



Given the cationic charge of **3-Ar**, ligand loss from **6** (with L = **3-Ar**) would likely be more difficult than if L is pyridine given the cationic nature of the complex with **3-Ar**. If ligand loss is slowed, one would expect a reduced rate for C–C bond formation. Ligand identity could also affect the rate of oxidation and C–O bond formation. Previous Pd-catalyzed oxidation reactions have been improved by the use of cationic catalysts. This report postulated that catalyst charge can be beneficial in oxidation reactions by anions through cation-anion charge interactions (Scheme 2.19).⁶⁴

Scheme 2.19 Charge Interactions Enhancing Oxidation Reactions.⁶⁴

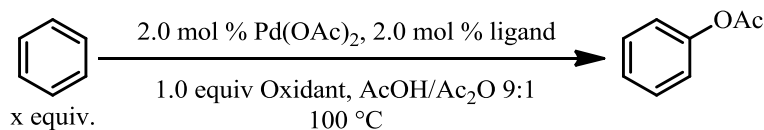


Similarly, **6** with L = **3-Ar** would have an overall cationic charge, which might increase the rate of oxidation by $S_2O_8^{2-}$. Thus, the improved chemoselectivity for the **3-Ar** system is likely a combination of increasing the rate of oxidation and suppressing ligand loss to prevent a second C–H activation.

2.2.5 Catalysis with Lower Arene Equivalents

Under typical reaction conditions, ten equivalents of arene are used in the reaction and the yield is based upon oxidant as the limiting reagent. The excess substrate is used to limit side reactions such as those shown in Scheme 2.17.^{58,60} In an effort to improve the synthetic utility of this reaction, we examined the effect the arene equivalents on the overall yield of C–H acetoxylation reactions with both $PhI(OAc)_2$ and $K_2S_2O_8$ (Table 2.6).

Table 2.6 Reaction Yields with Varying Benzene Equivalents.



Benzene	$PhI(OAc)_2$ (Yield) ^a		$K_2S_2O_8$ (Yield) ^a	
	3-Ar	Pyr ^b	3-Ar	Pyr ^b
10	76%	69%	68%	55%
7	69%	64%	69%	56%
5	63%	58%	64%	52%
3	51%	47%	51%	46%
1	27%	26%	30%	22%

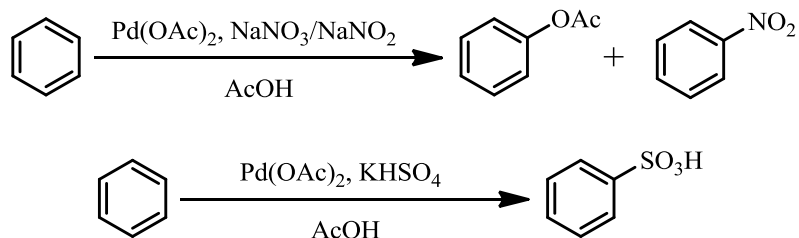
^a-Yields are based upon 1.0 equivalents of oxidant. ^b-1.8 mol %.

In comparing the two ligands, **3-Ar** outperforms pyridine under all reaction conditions. For the two ligands, the yields at each arene equivalent decrease in a similar

manner. In each column (Table 2.6), the yields did not show large reductions when the benzene equivalents were reduced from ten to five. However, further reduction to three or one equivalent resulted in significant diminishment in yield. In the case of $\text{PhI}(\text{OAc})_2$, the reduction in yield was accompanied by increases in the formation of acetoxyated iodobenzene (Scheme 2.17, **7a-7c**). With $\text{K}_2\text{S}_2\text{O}_8$, less than two percent of each diacetoxybenzene isomer (Scheme 2.17, **6a-6c**) was observed along with less than two percent of biphenyl (Scheme 2.17, **8**). Thus, for $\text{K}_2\text{S}_2\text{O}_8$, low reaction yield is not a function of secondary oxidation but low conversion and/or catalyst decomposition.

In previous studies with nitrate-based oxidations, competing C–OAc and C–NO₂ bond formation was observed (Scheme 2.20).^{16,17}

Scheme 2.20 Pd-catalyzed Acetoxylation versus Nitration.

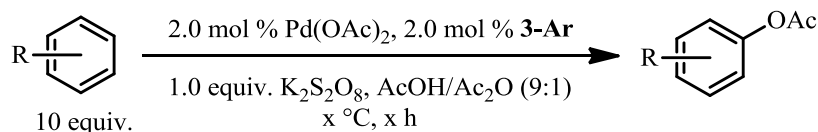


This was attributed to the thermal instability of nitrate, forming NO₂ in the reaction, which is responsible for nitration products. A similar decomposition of the bisulfate ion formed from the persulfate ions in these reactions to generate sulfur trioxide is possible, which could result in the formation of benzene sulfonic acid (Scheme 2.20). Given that these reactions are analyzed by gas chromatography of organic extractions following basic quenches of the reaction medium, one would not expect to observe benzenesulfonic acid by this method. To assay for its formation, a reaction with one equivalent of benzene, $\text{K}_2\text{S}_2\text{O}_8$, $\text{Pd}(\text{OAc})_2$, and **3-Ar** was repeated. Instead of quenching the reaction, the reaction was cooled, and the reaction mixture was filtered through celite.

The volatiles of the filtrate were removed under vacuum, and the residue was analyzed by ^1H NMR spectroscopy (in acetone- d_6) and compared against a commercial sample of benzenesulfonic acid. No peaks corresponding to benzenesulfonic acid were observed. To confirm this result, the reaction was repeated with the addition of 1 equivalent of KHSO_4 to the standard reaction conditions and analyzed by gas chromatography. The reaction yield was 29% compared with 30% under normal conditions (Table 2.6), indicating that the oxidant byproduct KHSO_4 does not inhibit the reaction. These results indicate that benzenesulfonic acid is not a side product in these reactions, and the excess of benzene is most likely required to trap a reactive intermediate.

2.2.6 Arene Substrate Scope

With the improved catalytic activity using $\text{K}_2\text{S}_2\text{O}_8$ and **3-Ar**, we wanted to investigate the substrate scope using a series of electron deficient aromatic substrates that have been historically difficult to functionalize. Standard reaction conditions were employed with 10 equivalents of substrate at both 80 and 100 °C. Reaction yields, completion times, and selectivity are illustrated below in Table 2.7.

Table 2.7 Arene Substrate Scope with $K_2S_2O_8$.

Substrate	Yield (Time)	
	<i>(o : m : p)</i> or $(\alpha : \beta)$	
	80 °C	100 °C
	60 % (45 h) (36 : 35 : 29)	52 % (19 h) (32 : 37 : 31)
	56 % (66 h) (26 : 38 : 36)	49 % (19 h) (17 : 45 : 38)
	39 % (97 h) (2 : 76 : 22)	41 % (29 h) (2 : 73 : 25)
	58 % (66 h) (10 : 70 : 20)	56 % (22 h) (13 : 61 : 26)
	52 % (93 h) (36 : 64)	52 % (25 h) (28 : 72)
	11 % (264 h) (0 : 100)	11 % (53 h) (0 : 100)

With arenes containing moderately electron withdrawing groups such as bromobenzene and chlorobenzene, modest yields were obtained at both 80 °C and 100 °C. Ethyl benzoate and 1,2-dichlorobenzene also showed moderate yields at both temperatures. Interestingly, temperature has a significant effect on the selectivity of chlorobenzene, ethyl benzoate, and 1,2-dichlorobenzene acetoxylation. Trifluorotoluene showed slightly poorer yields (~40%) with predominant functionalization occurring at the

meta position. Only when the strongly electron deficient 1,3-bis-trifluoromethylbenzene was used as a substrate were the reaction times prohibitively long and yields very poor (11%). Thus, the newly developed catalytic system using **3-Ar** and $K_2S_2O_8$ is effective for electron deficient substrates, providing much higher yields and turnover numbers than previously reported Pd-catalyzed arene functionalization reactions with $K_2S_2O_8$.²¹⁻²⁴

2.3 Conclusions

This chapter described the design of a new class of isolable cationic pyridinium-based bipyridine and pyridine ligands.³⁸ Using these ligands with Pt and Pd, we have demonstrated enhanced activity for C–H activation in both H/D exchange studies and in the oxidative functionalization of aromatic C–H bonds. Through the use of high-throughput ligand screening, we have identified two cationic monodentate pyridine ligands (**3-Ar** and **4-Ar**) that are more active than commercial pyridine in non-directed C–H oxidative functionalization to form C–O bonds. After initial studies with $PhI(OAc)_2$ as an oxidant, we have developed conditions using $K_2S_2O_8$ as a more environmentally friendly and cost effective alternative. With the use of this oxidant, we have determined that **3-Ar** produces a catalytic system approximately five times as active as pyridine and shows significant selectivity for the formation of C–O bonds in comparison to biphenyl. Through high-throughput screening and NMR analysis, we have shown that the higher activity results from a combination of equilibrium shift to form a higher fraction of $Pd(L)(OAc)_2$ as well as lowered reaction barriers for C–H functionalization. Using this system, we have also examined the substrate scope with electron deficient aromatic substrates. Moderate yields can be obtained even with these substrates and only the highly electron poor 1,3-bis-trifluoromethylbenzene is unreactive.

These reaction yields and turnover numbers are the highest reported for C–O bond formation using the cost-effective and environmentally benign $\text{K}_2\text{S}_2\text{O}_8$ oxidant.

2.4 Experimental Procedures

2.4.1 Instrumentation

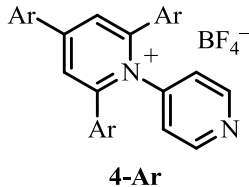
NMR spectra were recorded on Varian Inova 500 or Varian vnmrs 500 MHz NMR spectrometers with the residual solvent peak (acetone- d_6 : ^1H : $\delta=2.04$ ppm, ^{13}C : $\delta=206.0, 29.8$ ppm; AcOH- d_4 : ^1H : $\delta=11.53, 2.03$ ppm, ^{13}C : $\delta=178.4, 20.0$ ppm; acetonitrile- d_3 : ^1H : $\delta=1.94$ ppm, ^{13}C : $\delta=118.2, 1.3$ ppm; benzene- d_6 : ^1H : $\delta=7.15$ ppm, ^{13}C : $\delta=128.0$ ppm; chloroform- d_1 : ^1H : $\delta=7.24$ ppm, ^{13}C : $\delta=77.0$ ppm) as the internal reference unless otherwise noted. ^{19}F NMR is referenced to the residual solvent signal in the ^1H NMR. Chemical shifts are reported in parts per million (ppm) (δ). Multiplicities are reported as follows: br (broad resonance), s (singlet), d (doublet), t (triplet), q (quartet), m (multiplet). Coupling constants (J) are reported in Hz. Elemental analyses were performed by Atlantic Microlab, Inc., Norcross, Georgia.

2.4.2 Materials and Methods

All reactions were conducted without rigorous exclusion of air and moisture unless noted otherwise. AcOH- D_4 was purchased from Cambridge Isotopes Lab and stored in a Schlenk tubes under N_2 . Acetone- D_6 , acetonitrile- D_3 , C_6D_6 and CDCl_3 were purchased from Cambridge Isotopes Lab and used as received. Dichloromethane, diethylether, methanol, pentane, acetonitrile, toluene, acetone, and ethyl acetate were obtained from Fisher Scientific or Aldrich and used as purchased. Benzene for H/D exchange and acetoxylation was obtained from Aldrich and stored over 4 Å molecular

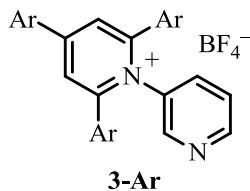
sieves. Ethanol, 200 proof, was obtained from Deacon Labs, Inc., and used as received. Celite and acetic anhydride were purchased from EM Science. Sodium acetate (anhydrous), bromobenzene, phosphorous oxychloride, potassium persulfate, and pyridine were purchased from Acros Organics. Chlorobenzene, glacial acetic acid, MgSO₄, and K₂CO₃ were purchased from Fisher Scientific. 1,2-Dichlorobenzene and α,α,α -trifluorotoluene were purchased from TCI America. Pd(OAc)₂ was purchased from Pressure Chemical Company. Iodosobenzene diacetate (PhI(OAc)₂) was obtained from Alfa Aesar. AgBF₄, ethyl benzoate, 2,2'-bipyridine (bpy), 4-aminopyridine, 3-aminopyridine, 2-aminopyridine, 1,3-bis-trifluoromethylbenzene, 1,1,2-trichloroethane, 4-*t*-butylbenzaldehyde, 2,4,6-triphenylpyrylium tetrafluoroborate, 4,4'-di-*t*-butyl-2,2'-bipyridine, Oxone®, NBu₄-Oxone, tetrafluoroboric acid, and copper(II) acetate hydrate were purchased from Aldrich. (bpym)PtCl₂ **1**,³⁶ (4,4'-di-*t*-butylbipyridine)PtCl₂,⁶⁵ (DMSO)₂PtCl₂,⁶⁶ 2,4,6-tris(4-*t*-butylphenyl)pyrylium tetrafluoroborate,⁵⁷ 4,4'-diaminobipyridine,⁶⁷⁻⁷⁰ (4,4'-di-*t*-butylbipyridine)PdCl₂,⁷¹ (COD)PdCl₂,⁷² ligand **2a**,⁵⁵ ligand **2b**,⁵⁸ complex **3a**,⁵⁸ complex **3b**,⁵⁸ complex **3c**,⁵⁸ and H₄PMo₁₁VO₄₀⁷³ were prepared according to literature procedures. All functionalized products in the substrate scope were compared to literature characterization.⁶⁰ Stock solutions of silver salts, bpy and pyridine were prepared using volumetric glassware and all liquid reagents were dispensed by difference using gas-tight Hamilton syringes.

2.4.3 Synthesis



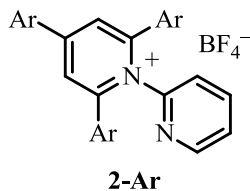
4-(2,4,6-tris-(4-*t*-butylphenyl)pyridinium)pyridine tetrafluoroborate (4-Ar)

9.00 g 2,4,6-tris-(4-*t*-butylphenyl)pyrylium tetrafluoroborate (15.9 mmol, 1.50 eq.), 1.00 g 4-aminopyridine (10.6 mmol, 1.00 eq.), and 12.55 g sodium acetate (153 mmol, 14.4 eq.) were added to a 1 L round bottom flask. 400 mL absolute ethanol was added and the reaction was heated to reflux under nitrogen for 20 hours. After the reaction was cooled, all volatiles were removed by rotary evaporation and the residue was suspended in 200 mL water. The suspension was filtered and the resulting solid was washed with 3x20 mL water. The solid was then dissolved in methylene chloride and dried with MgSO₄. The solid was filtered away and volatiles were removed by rotary evaporation. The residue was stirred with Et₂O resulting in a white precipitate which was collected by vacuum filtration resulting in 5.63 g product (83% yield). ¹H NMR (CD₃CN, 500.099 MHz): δ 8.39 (d, J = 5.9 Hz, 2H), 8.35 (s, 2H), 8.06 (d, J = 8.3 Hz, 2H), 7.69 (d, J = 8.8 Hz, 2H), 7.40 (d, J = 8.3 Hz, 4H), 7.31 (d, J = 8.3 Hz, 4H), 7.23 (d, J = 5.8 Hz, 2H), 1.38 (s, 9H), 1.25 (s, 18H). ¹³C NMR (CDCl₃, 125.762 MHz): δ 157.6, 156.2, 156.0, 154.0, 150.7, 146.5, 131.5, 129.6, 129.5, 128.2, 126.7, 125.7, 125.5, 123.4, 35.1, 34.8, 31.1, 31.0. ¹⁹F NMR (CD₃CN, 470.520 MHz): δ -152.9 (¹⁰B), -153.0 (¹¹B). HRMS electrospray (m/z) : [M-BF₄]⁺ calcd. for [C₄₀H₄₅N₂]⁺ 553.3577; found 553.3581. Anal. calcd. for C₄₀H₄₅N₂BF₄: C, 75.00; H, 7.08; N, 4.37. Found: C, 74.55; H, 7.16; N, 4.37.



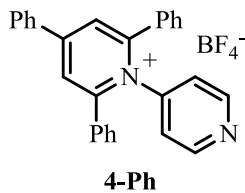
3-(2,4,6-tris-(4-*t*-butylphenyl)-pyridinium)pyridine tetrafluoroborate (3-Ar)

4.50 g 2,4,6-tris-(4-*t*-butylphenyl)pyrylium tetrafluoroborate (7.97 mmol, 1.50 eq.), 0.50 g 4-aminopyridine (5.3 mmol, 1.00 eq.), and 6.27 g sodium acetate (76.4 mmol, 14.4 eq.) were added to a 500 mL round bottom flask. 200 mL absolute ethanol was added and the reaction was heated to reflux under nitrogen for 20 hours. After the reaction was cooled, all volatiles were removed by rotary evaporation and the residue was suspended in 200 mL water. The suspension was filtered and the resulting solid was washed with 3x20 mL water. The solid was then dissolved in methylene chloride and dried with MgSO₄. The solid was filtered away and volatiles were removed by rotary evaporation. The residue was stirred with Et₂O resulting in a white precipitate which was collected by vacuum filtration resulting in 2.96 g product (87% yield). ¹H NMR (CD₃Cl, 500.099 MHz): δ 8.35 (dd, J = 4.8 Hz, J = 2.1 Hz, 1H), 8.24 (d, J = 2.1 Hz, 1H), 8.08 (s, 2H), 8.02 (m, 1H), 7.81 (d, J = 8.3 Hz, 2H), 7.55 (d, J = 8.5 Hz, 2H), 7.31 (m, 8H), 7.13 (dd, J = 8.0 Hz, J = 4.8 Hz, 1H), 1.35 (s, 9H), 1.22 (s, 18H). ¹³C NMR (CDCl₃, 125.762 MHz): 157.5, 156.8, 156.3, 153.8, 150.2, 147.8, 137.2, 136.6, 131.4, 129.7, 129.5, 128.2, 126.7, 125.6, 125.5, 123.7, 35.0, 34.8, 31.0, 31.0. ¹⁹F NMR (CDCl₃, 470.520 MHz): -153.0 (¹⁰B), -153.1 (¹¹B). HRMS electrospray (m/z) : [M-BF₄]⁺ calcd. for [C₄₀H₄₅N₂]⁺ 553.3577; found 553.3574. Anal. calcd. for C₄₀H₄₅N₂BF₄: C, 75.00; H, 7.08; N, 4.37. Found: C, 74.45; H, 7.09; N, 4.38.



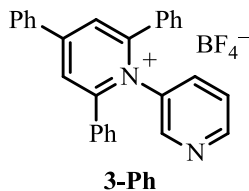
4-(2,4,6-tris-(4-*t*-butylphenyl)-pyridinium)pyridine tetrafluoroborate (2-Ar)

2.69 g 2,4,6-tris-(4-*t*-butylphenyl)pyrylium tetrafluoroborate (4.77 mmol, 0.90 eq.), 0.50 g 4-aminopyridine (5.3 mmol, 1.00 eq.), and 6.27 g sodium acetate (76.4 mmol, 14.4 eq.) were added to a 500 mL round bottom flask. 200 mL absolute ethanol was added and the reaction was heated to reflux under nitrogen for 20 hours. After the reaction was cooled, all volatiles were removed by rotary evaporation and the residue was suspended in 200 mL water. The suspension was filtered and the resulting solid was washed with 3x20 mL water. The solid was then dissolved in methylene chloride and dried with MgSO₄. The solid was filtered away and volatiles were removed by rotary evaporation. The residue was stirred with Et₂O resulting in a white precipitate which was collected by vacuum filtration resulting in 1.85 g product (54% yield). ¹H NMR (CD₃CN, 500.099 MHz): δ 8.35 (s, 2H), 8.27 (m, 1H), 8.06 (m, 2H), 7.70 (m, 2H), 7.62 (td, J = 7.8 Hz, J = 1.7 Hz, 1H), 7.38 (m, 4H), 7.27 (m, 6H), 1.38 (s, 9H), 1.24 (s, 18H). ¹³C NMR (CDCl₃, 125.762 MHz): δ 157.5, 156.2, 156.1, 153.6, 151.8, 148.0, 139.0, 131.6, 129.7, 129.6, 128.2, 126.7, 125.4, 125.3, 125.1, 35.1, 34.7, 31.1, 31.0. ¹⁹F NMR (CD₃CN, 470.520 MHz): δ -151.8 (¹⁰B), -151.9 (¹¹B). HRMS electrospray (m/z) : [M-BF₄]⁺ calcd for [C₄₀H₄₅N₂]⁺ 553.3577; found 553.3578. Anal. Calcd for C₄₀H₄₅N₂BF₄: C, 75.00; H, 7.08; N, 4.37. Found: C, 74.64; H, 7.07; N, 4.38.



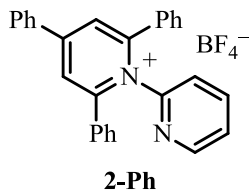
4-(2,4,6-triphenylpyridinium)pyridine tetrafluoroborate (4-Ph)

2.56 g 2,4,6-triphenylpyrylium tetrafluoroborate (6.46 mmol, 1.60 eq.), 0.380 g 4-aminopyridine (4.04 mmol, 1.00 eq.), and 3.57 g sodium acetate (43.5 mmol, 10.8 eq.) were added to a 40 mL Teflon screw cap vial. 35 mL absolute ethanol was added and the reaction was heated to 80 °C for 20 hours. After the reaction was cooled, all volatiles were removed by rotary evaporation and the residue was suspended in 100 mL water. The suspension was filtered and the resulting solid was washed with 3x20 mL water. The solid was then dissolved in methylene chloride and dried with MgSO₄. The solid was filtered away and volatiles were removed by rotary evaporation. The residue was dissolved in 5 mL acetonitrile and 5 mL acetone. The product was precipitated by the addition of 150 mL Et₂O to yield 1.74 g product (91%) ¹H NMR (CD₃CN, 500.099 MHz): δ 8.42 (s, 2H), 8.40 (m, 2H), 8.10 (m, 2H), 7.67 (m, 1H) 7.66 (m, 2H), 7.42 (m, 2H), 7.38 (m, 8H), 7.24 (m, 2H). ¹³C NMR (CDCl₃, 125.762 MHz): δ 158.3, 156.0, 150.8, 146.3, 134.5, 132.3, 132.2, 130.6, 129.7, 129.6, 128.6, 128.5, 126.4, 123.2. ¹⁹F NMR (CD₃CN, 470.520 MHz): δ -151.7 (¹⁰B), -151.8 (¹¹B). HRMS electrospray (m/z) : [M-BF₄]⁺ calcd. for [C₄₀H₄₅N₂]⁺ 385.1699; found 385.1697. Anal. calcd. for C₄₀H₄₅N₂BF₄: C, 71.21; H, 4.48; N, 4.593. Found: C, 71.16; H, 4.47; N, 5.92.



3-(2,4,6-triphenylpyridinium)pyridine tetrafluoroborate (3-Ph)

3.37 g 2,4,6-triphenylpyrylium tetrafluoroborate (8.51 mmol, 1.60 eq.), 0.500 g 3-aminopyridine (5.31 mmol, 1.00 eq.) , and 3.57 g sodium acetate (43.5 mmol, 8.19 eq.) were added to a 40 mL Teflon screw cap vial. 35 mL absolute ethanol was added and the reaction was heated to 80 °C for 20 hours. After the reaction was cooled, all volatiles were removed by rotary evaporation and the residue was suspended in 100 mL water. The suspension was filtered and the resulting solid was washed with 3x20 mL water. The solid was then dissolved in methylene chloride and dried with MgSO₄. The solid was filtered away and volatiles were removed by rotary evaporation. The residue was dissolved in 5 mL acetonitrile and 5 mL acetone. The product was precipitated by the addition of 150 mL Et₂O to yield 1.94 g product (57%) ¹H NMR (CD₃CN, 500.099 MHz): δ 8.44 (s, 2H), 8.42 (d, J = 2.4 Hz, 1H), 8.36 (dd, J = 4.9 Hz, J = 1.4 Hz, 1H), 8.11 (m, 2H), 7.1 (m, 1H), 7.67 (m, 3H), 7.40 (m, H), 7.18 (dd, J = 8.3Hz, J = 4.9 Hz, 1H). ¹³C NMR (CDCl₃, 125.762 MHz): δ 154.3, 152.2, 147.6, 144.3, 135.0, 130.6, 128.5, 128.3, 126.4, 125.8 (2 signals), 124.5 (2 signals), 122.1, 121.4, 121.0. ¹⁹F NMR (CD₃CN, 470.520 MHz): δ -152.9 (¹⁰B), -153.0 (¹¹B). HRMS electrospray (m/z) : [M-BF₄]⁺ calcd. for [C₄₀H₄₅N₂]⁺ 385.1699; found 385.1696. Anal. calcd. for C₄₀H₄₅N₂BF₄: C, 71.21; H, 4.48; N, 4.593. Found: C, 71.37; H, 4.40; N, 5.98.



2-(2,4,6-triphenylpyridinium)pyridine tetrafluoroborate (2-Ph)

6.02 g 2,4,6-triphenylpyrylium tetrafluoroborate (15.2 mmol, 1.43 eq.), 1.00 g 2-aminopyridine (10.6 mmol, 1.00 eq.), and 12.55 g sodium acetate (153 mmol, 14.4 eq.) were added to a 500 mL round bottom flask. 200 mL absolute ethanol was added and the reaction was heated to reflux under nitrogen for 20 hours. After the reaction was cooled, all volatiles were removed by rotary evaporation and the residue was suspended in 200 mL water. The suspension was filtered and the resulting solid was washed with 3x20 mL water. The solid was then dissolved in methylene chloride and dried with MgSO₄. The solid was filtered away and volatiles were removed by rotary evaporation. The residue was dissolved in 5 mL acetonitrile and 5 mL acetone. The product was precipitated by the addition of 150 mL Et₂O in 4.60 g product (92% yield). ¹H NMR (CD₃CN, 500.099 MHz): δ 8.40 (s, 2H), 8.28 (m, 1H), 8.11 (m, 2H), 7.67 (m, 4H), 7.38 (m, 11H), 7.26 (m, 1H). ¹³C NMR (CDCl₃, 125.762 MHz): δ 154.3, 152.2, 147.6, 144.3, 135.0, 130.6, 128.5, 128.3, 126.4, 125.8 (2 signals), 124.5 (2 signals), 122.1, 121.4, 121.0. ¹⁹F NMR (CD₃CN, 470.520 MHz): δ -153.1 (¹⁰B), -153.2 (¹¹B). HRMS electrospray (m/z) : [M-BF₄]⁺ calcd. for [C₄₀H₄₅N₂]⁺ 385.1699; found 385.1699. Anal. calcd. for C₄₀H₄₅N₂BF₄: C, 71.21; H, 4.48; N, 4.5.93. Found: C, 71.33; H, 4.41; N, 5.95.

2.4.4 Reaction Details

General Procedure For H/D Exchange Reactions Between C₆H₆ and AcOH-D₄.

To a 4 mL resealable Schlenk tube was added catalyst (5.0 μ mol, 2.0 mol %) and 0.10 mL (10 μ mol, 4.0 mol %) of a stock solution of AgBF₄ (19.5 mg, 100 μ mol) in 1.0 mL AcOH-D₄, which had been prepared immediately prior to use. An additional 0.27 mL of AcOH-D₄ was added, and the mixture was stirred for 1 min. Benzene (22.3 μ L, 19.5 mg, 0.250 mmol, 1.00 equiv) was added to the reaction vessel, which was subsequently sealed. The vessel was completely submerged in a preheated oil bath. At the end of the reaction, the vessel was cooled to room temperature. The reaction mixture was then filtered over a plug of Celite to remove any particulates and rinsed with EtOAc (1x2 mL) into a 20 mL scintillation vial. A saturated aqueous solution of K₂CO₃ (9 M in deionized H₂O, 2x1 mL) was added to the vial to quench and separate the acid. The organic layer was carefully separated and diluted with additional EtOAc to give a 12.8 mM solution of benzene (~1 mg/mL) for analysis by GC-MS.

The % deuterium incorporation was defined as the percent of C–H bonds converted to C–D bonds. The background reaction (in the absence of the Pt catalyst) at 150 °C is minimal with AcOH-d₄ and is described in detail in previous publications.⁵⁹ Turnover numbers (TONs) are calculated as mol deuterium incorporated per mol of catalyst. Reported values have been corrected for the background reaction in the presence of AgCl, which is formed in situ. The reported error is the standard deviation of at least two replicate trials.

Pd(OAc)₂ Benzene Acetoxylation Reactions

To a mixture of PhI(OAc)₂ (361 mg, 1.12 mmol, 1.00 equiv), and Pd(OAc)₂ (5.0 mg, 22.4 μ mol, 2.0 mol %) in a pressure resistant vial with a screw cap, glacial acetic acid

(0.90 mL) and acetic anhydride (0.10 mL) were added. The suspension was stirred at room temperature for 1 min, before benzene (1.00 mL, 875 mg, 11.2 mmol, 10.0 equiv) was added. The vial was sealed and heated to 100 °C using a preheated hotplate. At the end of the reaction, the vessel was cooled to room temperature and phenyl chloride (50 µL) was added as an internal standard for quantitative GC analysis. The mixture was diluted with EtOAc (2 mL) and filtered through a plug of celite. The filtrate was extracted with a saturated aqueous solution of K₂CO₃ (9 M in deionized H₂O, 2 x 2 mL) to quench and separate the acid. The organic layer was carefully separated and diluted with additional EtOAc to a total volume of 20 mL. The resulting solution was analyzed by GC.

Pd(OAc)₂ Catalyzed Acetoxylation of Benzene – Addition of Bipyridine

By analogy to the general procedure for acetoxylation of benzene (see above), PhI(OAc)₂ (361 mg, 1.12 mmol, 1.00 equiv), Pd(OAc)₂ (5.0 mg, 22.4 µmol, 2.0 mol %), 0.50 mL (11.2 µmol, 1.0 mol %) of a stock solution of bipyridine (35.0 mg, 224 µmol) in 10 mL AcOH, AcOH (0.40 mL), acetic anhydride (0.10 mL) and benzene (1.00 mL, 875 mg, 11.2 mmol, 10.0 equiv) were reacted at 100 °C. Workup and analysis were performed as described above.

Pd(OAc)₂ Catalyzed Acetoxylation of Benzene – Addition of Dicationic Ligand **2a**

By analogy to the general procedure for acetoxylation of benzene (see above), PhI(OAc)₂ (361 mg, 1.12 mmol, 1.00 equiv), Pd(OAc)₂ (5.0 mg, 22.4 µmol, 2.0 mol %), **2a** (10.6 mg, 11.2 µmol, 1.0 mol %), AcOH (0.90 mL), acetic anhydride (0.10 mL) and benzene (1.00 mL, 875 mg, 11.2 mmol, 10.0 equiv) were reacted at 100 °C. Workup and analysis were performed as described above.

High-Throughput Screening

Reaction plates were prepared with an automated sample processor (Symyx (now FreeSlate) core module). Reactions used 40 mm glass shell vials (1.5 mL), equipped with PTFE-coated stir bars. Ligand standard solutions were prepared by dissolving 178.3 mg (**4-Ar**, **3-Ar**, or **2-Ar**) (0.278 mmol) or 131.5 mg (**4-Ph**, **3-Ph**, or **2-Ph**) (0.278 mmol) in 10 mL volumetric flask in methylene chloride. A Pd(OAc)₂ standard solution was prepared by dissolving 416.7 mg Pd(OAc)₂ (1.86 mmol) in a 25 mL volumetric flask with benzene (gentle heating is required to dissolve). The oxidant PhI(OAc)₂ standard solution was prepared by dissolving 5.64 g PhI(OAc)₂ (17.5 mmol) in a 25 mL volumetric flask with a solvent mixture containing 65.6 mL benzene and 84.4 mL acetic acid (Note oxidant is poorly soluble and must be made at 50°C and maintained at this temperature prior to dispensing). A topping solvent to maintain constant volumes in all reactions was made with a mixture containing 20 mL benzene, 18 mL acetic acid, and 2 mL acetic anhydride. Pyridine standard solutions of 0.0278 M (22.4 μL), 0.167 M (134 μL), 0.306 M (246 μL), 0.445 M (358 μL), and 0.584 M (470 μL) were prepared by dissolving the appropriate amount of pyridine in a 10 mL volumetric flask using the topping solvent mixture above.

To prepare reactions containing cationic ligands, addition of the ligand standard solutions (40-440 μL in 40 μL increments—0.4 to 4.4 mol %) were added to reaction vials and volatiles were removed with an evaporator. 75 μL of the Pd(OAc)₂ standard solution, 25 μL of acetic anhydride, and 100 μL of topping solvent mixture was added using the FreeSlate core module. 400 μL of the PhI(OAc)₂ solution was added to each reaction with an electronic Ovation multi-pipette. Pyridine reactions were prepared

analogously with the addition of pyridine stock solutions to achieve (0.4-4.4 mol% loadings) along with an appropriate amount of topping solvent to achieve a total of 100 μL dispensed. As in above, Pd, acetic anhydride, and oxidant were added. Reaction plates were sealed with a teflon sheet and silicone gaskets and heated to 100 $^{\circ}\text{C}$, while stirring on a tumble stirrer.

After the indicated reaction time (1 or 2 hours), the reaction plates were cooled down to at least 30 $^{\circ}\text{C}$ before processing. 20 μL of neat internal standard (phenyl chloride) was added to each vial and the reactions were stirred at maximum speed for an additional 15-20 minutes. 50 μL aliquots were taken out of the vials and placed into a second set of vials equipped with sandwich-style stir elements (tuning forks) from VP Scientific. While gently stirring the plate, 225 μL of a 10 g/100 mL of a Na_2CO_3 solution was manually added with an electronic Ovation multi-pipette in increments of 25 μL (so 9 times 25 μL in each vial). The reactions were stirred an additional 3-4 minutes until evolution of carbon dioxide had ceased to be visually observed. 375 μL of EtOAc was added and the plate was stirred on a standard stirring plate to effect the full mixing of the 2 phases and establish equilibrium of the components. The plate was centrifuged to fully separate/settle the two phases and 100 μL was taken off the top phase into a third set off vials, which was diluted to 500 μL with EtOAc.

Analysis was performed with an Agilent 6850 GC-FID, equipped with a CTC-PAL (Leap Technologies) auto-sampler, on a HP-1 column (30 m, 0.32 mm, 0.25 μm , equipped with a guard column).

Pd(OAc)₂ Catalyzed Acetoxylation of Benzene – Addition of pyridine

By analogy to the general procedure for acetoxylation of benzene (see above), PhI(OAc)₂ (361 mg, 1.12 mmol, 1.00 equiv), Pd(OAc)₂ (5.0 mg, 22.4 μmol, 2.0 mol %), 0.40 mL (20.3 μmol, 1.8 mol %) of a stock solution of pyridine (40.8 μL, 506 μmol) in 10 mL AcOH, AcOH (0.50 mL), acetic anhydride (0.10 mL) and benzene (1.00 mL, 875 mg, 11.2 mmol, 10.0 equiv) were reacted at 80 or 100 °C. Workup and analysis were performed as described above.

Pd(OAc)₂ Catalyzed Acetoxylation of Benzene – Addition of cationic ligands

By analogy to the general procedure for acetoxylation of benzene (see above), PhI(OAc)₂ (361 mg, 1.12 mmol, 1.00 equiv), Pd(OAc)₂ (5.0 mg, 22.4 μmol, 2.0 mol %), cationic ligand (**4-Ar**, **3-Ar**, or **2-Ar** (14.3 mg, 22.4 μmol, 2.0 mol %); **4-Ph**, **3-Ph**, or **2-Ph** (14.3 mg, 22.4 μmol, 2.0 mol %)), AcOH (0.90 mL), acetic anhydride (0.10 mL) and benzene (1.00 mL, 875 mg, 11.2 mmol, 10.0 equiv) were reacted at 80 or 100 °C. Workup and analysis were performed as described above.

Pd(OAc)₂ Catalyzed Acetoxylation of Benzene – Oxidant Screening

By analogy to the general procedure for acetoxylation of benzene (see above), oxidant (see Table 2.8), Pd(OAc)₂ (5.0 mg, 22.4 μmol, 2.0 mol %), cationic ligand (**4-Ar**, **3-Ar**, or **2-Ar** (14.3 mg, 22.4 μmol, 2.0 mol %); **4-Ph**, **3-Ph**, or **2-Ph** (10.5 mg, 22.4 μmol, 2.0 mol %)), AcOH (0.90 mL), acetic anhydride (0.10 mL) and benzene (1.00 mL, 875 mg, 11.2 mmol, 10.0 equiv) were reacted at 80 or 100 °C. Workup and analysis were performed as described above.

Table 2.8 Oxidant Screening.

Oxidant	Amount	mmol	Equivalents
PhI(OAc) ₂	361.0 mg	1.12	1.00
Oxone	344.3 mg	1.12	1.00
NBu ₄ -Oxone	913.7 mg	1.12	1.00
Cu(OAc) ₂ ·H ₂ O	447.2 mg	2.24	2.00
H ₄ PMo ₁₁ VO ₄₀	96.9 mg	0.0560	0.05
K ₂ S ₂ O ₈	302.8 mg	1.12	1.00
Na ₂ S ₂ O ₈	266.7 mg	1.12	1.00
(NH ₄) ₂ S ₂ O ₈	255.6 mg	1.12	1.00

Equilibrium Analysis by ¹H NMR

¹H NMR at room temperature were recorded at room temperature with locking and referencing to CD₃COOD. 1,1,2-trichloroethane was used as an internal standard.

(1:1 ratio-pyridine) Pd(OAc)₂ (10.0 mg, 44.8 μmol, 1.00 eq.), pyridine (3.6 μL, 44.7 μmol, 1.00 eq.), and 1,1,2-trichloroethane (8.3 μL, 89.2 μmol, 2.00 eq.) were dissolved in 0.5 mL CD₃COOD and 0.5 mL C₆D₆ and sonicated for 1 h.

(1:2 ratio-pyridine) Pd(OAc)₂ (10.0 mg, 44.8 μmol, 1.00 eq.), pyridine (3.6 μL, 44.7 μmol, 1.00 eq.), and 1,1,2-trichloroethane (8.3 μL, 89.2 μmol, 2.00 eq.) were dissolved in 0.5 mL CD₃COOD and 0.5 mL C₆D₆ and sonicated for 1 h.

(1:1 ratio-**3-Ar**) Pd(OAc)₂ (5.0 mg, 22.4 μmol, 1.00 eq.), **3-Ar** (14.3 mg, 22.4 μmol, 1.00 eq.), and 1,1,2-trichloroethane (8.3 μL, 89.2 μmol, 2.00 eq.) were dissolved in 0.5 mL CD₃COOD and 0.5 mL C₆D₆ and sonicated for 1 h.

Pd(OAc)₂ Catalyzed Acetoxylation of Benzene – Varying Benzene Equivalents

By analogy to the general procedure for acetoxylation of benzene (see above), $\text{PhI}(\text{OAc})_2$ (361 mg, 1.12 mmol, 1.00 equiv) or $\text{K}_2\text{S}_2\text{O}_8$ (302.8 mg, 1.12 mmol, 1.00 equiv), and $\text{Pd}(\text{OAc})_2$ (5.0 mg, 22.4 μmol , 2.0 mol %) was added to the reaction vessel. *For pyridine:* 0.40 mL (20.3 μmol , 1.8 mol %) of a stock solution of pyridine (40.8 μL , 506 μmol) in 10 mL AcOH, AcOH (0.50 mL), acetic anhydride (0.10 mL) was added. *For 3-Ar:* **3-Ar** (14.3 mg, 22.4 μmol , 2.0 mol %), AcOH (0.90 mL), acetic anhydride (0.10 mL) was added. Benzene (1.00 mL - 10 eq.; 0.7 mL - 7 eq.; 0.5 mL - 5 eq.; 0.3 mL - 3 eq.; 0.1 mL - 0.1 eq.) was added and reacted at 80 or 100 °C. Workup and analysis were performed as described above.

Arene Substrate Scope

By analogy to the general procedure for acetoxylation of benzene (see above), $\text{K}_2\text{S}_2\text{O}_8$ (302.8 mg, 1.12 mmol, 1.00 equiv), $\text{Pd}(\text{OAc})_2$ (5.0 mg, 22.4 μmol , 2.0 mol %), **3-Ar** (14.3 mg, 22.4 μmol , 2.0 mol %), AcOH (0.90 mL), and acetic anhydride (0.10 mL) was added. Arenes were added according to the Table 2.9 and reacted at 80 or 100 °C. Workup (internal standard is listed below) and analysis were performed as described above.

Table 2.9 Substrate Scope Quantities.

Arene	Amount	mmol	Equivalents	Internal Standard
bromobenzene	1.76 g, 1.18 mL	11.2	10.0	PhCH ₂ C(CH ₃) ₃
Chorobenzene	1.26 g, 1.14 mL	11.2	10.0	PhCH ₂ C(CH ₃) ₃
1,2-dichlorobenzene	1.65 g, 1.26 mL	11.2	10.0	PhCH ₂ C(CH ₃) ₃
Ethyl benzoate	1.68 g, 1.60 mL	11.2	10.0	PhCH ₂ C(CH ₃) ₃
Trifluorotoluene	1.64 g, 1.38 mL	11.2	10.0	PhCl
1,3-bis-trifluoromethylebenzene	2.40 g, 1.74 mL	11.2	10.0	PhCl

2.5 References

- (1) Arndtsen, B. A.; Bergman, R. G.; Mobley, T. A.; Peterson, T. H. *Acc. Chem. Res.* **1995**, *28*, 154.
- (2) Sehnal, P.; Taylor, R. J. K.; Fairlamb, I. J. S. *Chem. Rev.* **2010**, *110*, 824.
- (3) Muñiz, K. *Angew. Chem. Int. Ed.* **2009**, *48*, 9412.
- (4) Lyons, T. W.; Sanford, M. S. *Chemical Reviews* **2010**, *110*, 1147.
- (5) Alonso, D. A.; Nájera, C.; Pastor, I. M.; Yus, M. *Chem. Eur. J.* **2010**, *16*, 5274.
- (6) Tsuji, J. *Synthesis* **1990**, 739.
- (7) Choy, P. Y.; Lau, C. P.; Kwong, F. Y. *J. Org. Chem.* **2010**, *76*, 80.
- (8) Mutule, I.; Suna, E.; Olofsson, K.; Pelcman, B. *J. Org. Chem.* **2009**, *74*, 7195.
- (9) Wang, G.-W.; Yuan, T.-T.; Wu, X.-L. *J. Org. Chem.* **2008**, *73*, 4717.
- (10) Yoneyama, T.; Crabtree, R. H. *J. Mol. Catal. A* **1996**, *108*, 35.
- (11) Shibahara, F.; Kinoshita, S.; Nozaki, K. *Org. Lett.* **2004**, *6*, 2437.
- (12) Muehlhofer, M.; Strassner, T.; Herrmann, W. A. *Angew. Chem. Int. Ed.* **2002**, *41*, 1745.
- (13) Jintoku, T.; Taniguchi, H.; Fujiwara, Y. *Chem. Lett.* **1987**, 1865.

- (14) Jintoku, T.; Takaki, K.; Fujiwara, Y.; Fuchita, Y.; Hiraki, K. *Bull. Chem. Soc. Jpn.* **1990**, *63*, 438.
- (15) Stock, L. M.; Tse, K.-t.; Vorvick, L. J.; Walstrum, S. A. *J. Org. Chem.* **1981**, *46*, 1757.
- (16) Henry, P. M. *J. Org. Chem.* **1971**, *36*, 1886.
- (17) Tissue, T.; Downs, W. J. *J. Chem. Soc. D* **1969**, 410a.
- (18) Davidson, J. M.; Triggs, C. *Chem. Ind.* **1966**, 457.
- (19) Liu, Y.; Murata, K.; Inaba, M. *J. Mol. Catal. A* **2006**, *256*, 247.
- (20) Burton, H. A.; Kozhevnikov, I. V. *J. Mol. Catal. A* **2002**, *185*, 285.
- (21) Ebersson, L.; Jonsson, E. *Acta Chem. Scand. B* **1974**, *B 28*, 771.
- (22) Ebersson, L.; Jonsson, L. *J. Chem. Soc.-Chem. Commun.* **1974**, 885.
- (23) Ebersson, L.; Jonsson, L. *Acta Chem. Scand. B* **1976**, *30*, 361.
- (24) Ebersson, L.; Jonsson, L. *Justus Liebigs Annalen Der Chemie* **1977**, 233.
- (25) Lyons, T. W.; Hull, K. L.; Sanford, M. S. *J. Am. Chem. Soc.* **2011**, *133*, 4455.
- (26) Hickman, A. J.; Sanford, M. S. *ACS Catalysis* **2011**, *1*, 170.
- (27) Deprez, N. R.; Kalyani, D.; Krause, A.; Sanford, M. S. *J. Am. Chem. Soc.* **2006**, *128*, 4972.
- (28) Goldshleger, N. F.; Eskova, V. V.; Shilov, A. E.; Shteinman, A. A. *Russ. J. Phys. Chem.* **1972**, *46*, 785.
- (29) Goldshleger, N. F.; Tyabin, M. B.; Shilov, A. E.; Shteinman, A. A. *Russ. J. Phys. Chem.* **1969**, *43*, 1222.
- (30) Shilov, A. E. *Activation of Saturated Hydrocarbons by Transition Metal Complexes*; D. Reidel Publishing Company: Dordrecht, Holland, 1984.
- (31) Shilov, A. E.; Shteinman, A. A. *Coord. Chem. Rev.* **1977**, *24*, 97.
- (32) Shilov, A. E.; Shul'pin, G. B. *Uspekhi Khimii* **1987**, *56*, 754.
- (33) Shilov, A. E.; Shul'pin, G. B. *Chem. Rev.* **1997**, *97*, 2879.
- (34) Shilov, A. E.; Shul'pin, G. B. *Activation and Catalytic Reactions of Saturated Hydrocarbons in the Presence of Metal Complexes*; Springer: Verlag, 2000.

- (35) Heyduk Alan, F.; Zhong, H. A.; Labinger Jay, A.; Bercaw John, E. In *Activation and Functionalization of C-H Bonds*; American Chemical Society: 2004; Vol. 885, p 250.
- (36) Bar-Nahum, I.; Khenkin, A. M.; Neumann, R. *J. Am. Chem. Soc.* **2004**, *126*, 10236.
- (37) Chen, G. S.; Labinger, J. A.; Bercaw, J. E. *Organometallics* **2009**, *28*, 4899.
- (38) Periana, R. A.; Taube, D. J.; Gamble, S.; Taube, H.; Satoh, T.; Fujii, H. *Science* **1998**, *280*, 560.
- (39) Ahlquist, M.; Nielsen, R. J.; Periana, R. A.; Goddard Iii, W. A. *J. Am. Chem. Soc.* **2009**, *131*, 17110.
- (40) Ahlquist, M.; Periana, R. A.; Goddard Iii, W. A. *Chem. Commun.* **2009**, 2373.
- (41) Ess, D. H.; Goddard, W. A.; Periana, R. A. *Organometallics* **2010**, *29*, 6459.
- (42) Ess, D. H.; Nielsen, R. J.; Goddard Iii, W. A.; Periana, R. A. *J. Am. Chem. Soc.* **2009**, *131*, 11686.
- (43) Kua, J.; Xu, X.; Periana, R. A.; Goddard, W. A. *Organometallics* **2001**, *21*, 511.
- (44) Xu, X.; Kua, J.; Periana, R. A.; Goddard, W. A. *Organometallics* **2003**, *22*, 2057.
- (45) Anslyn, E. V.; Dougherty, D. A. *Modern Physical Organic Chemistry*; University Science Books: Sausalito, California, 2006.
- (46) Black, M. L. *J. Phys. Chem.* **1955**, *59*, 670.
- (47) Wishart, J. F.; Bino, A.; Taube, H. *Inorg. Chem.* **1986**, *25*, 3318.
- (48) Johnson, C. R.; Shepherd, R. E. *Inorg. Chem.* **1983**, *22*, 2439.
- (49) Kaim, W.; Matheis, W. *Chem. Ber.* **1990**, *123*, 1323.
- (50) Matheis, W.; Kaim, W. *J. Chem. Soc., Faraday Trans.* **1990**, *86*, 3337.
- (51) Matheis, W.; Poppe, J.; Kaim, W.; Zalis, S. *J. Chem. Soc., Perkin Trans. 2* **1994**, 1923.
- (52) Waldhör, E.; Kaim, W.; Olabe, J. A.; Slep, L. D.; Fiedler, J. *Inorg. Chem.* **1997**, *36*, 2969.
- (53) Coe, B. J.; Chamberlain, M. C.; Essex-Lopresti, J. P.; Gaines, S.; Jeffery, J. C.; Houbrechts, S.; Persoons, A. *Inorg. Chem.* **1997**, *36*, 3284.
- (54) Fujihara, T.; Wada, T.; Tanaka, K. *Inorg. Chim. Acta* **2004**, *357*, 1205.

- (55) Laine, P. P.; Ciofini, I.; Ochsenein, P.; Amouyal, E.; Adamo, C.; Bedioui, F. *Chem. Eur. J.* **2005**, *11*, 3711.
- (56) Villalobos, J. M.; Hickman, A. J.; Sanford, M. S. *Organometallics* **2009**, *29*, 257.
- (57) Dimroth, K.; Tüncher, W.; Kaletsch, H. *Chem. Ber.* **1978**, *111*, 264.
- (58) Reprinted (adapted) with permission from (Emmert, M. H.; Gary, J. B.; Villalobos, J. M.; Sanford, M. S. *Angew. Chem. Int. Ed.* **2010**, *49*, 5884.) Copyright (2010) John Wiley and Sons.
- (59) Hickman, A. J.; Villalobos, J. M.; Sanford, M. S. *Organometallics* **2009**, *28*, 5316.
- (60) Emmert, M. H.; Cook, A. K.; Xie, Y. J.; Sanford, M. S. *Angew. Chem. Int. Ed.* **2011**, *50*, 9409.
- (61) Zhang, Y.-H.; Shi, B.-F.; Yu, J.-Q. *J. Am. Chem. Soc.* **2009**, *131*, 5072.
- (62) Desai, L. V.; Stowers, K. J.; Sanford, M. S. *J. Am. Chem. Soc.* **2008**, *130*, 13285.
- (63) Li, R.; Jiang, L.; Lu, W. *Organometallics* **2006**, *25*, 5973.
- (64) Ettetdgui, J.; Neumann, R. *J. Am. Chem. Soc.* **2008**, *131*, 4.
- (65) Vicente, J.; González-Herrero, P.; Pérez-Cadenas, M.; Jones, P. G.; Bautista, D. *Inorg. Chem.* **2007**, *46*, 4718.
- (66) Price, J. H.; Williamson, A. N.; Schramm, R. F.; Wayland, B. B. *Inorg. Chem.* **1972**, *11*, 1280.
- (67) Black, D. S.; Rothnie, N. E. *Aust. J. Chem.* **1983**, *36*, 1141.
- (68) Maerker, G.; Case, F. H. *J. Am. Chem. Soc.* **1958**, *80*, 2745.
- (69) Fallahpour, R. A.; Neuburger, M.; Zehnder, M. *New J. Chem.* **1999**, *23*, 53.
- (70) Fallahpour, R. A. *Eur. J. Inorg. Chem.* **1998**, 1205.
- (71) Foley, S. R.; Shen, H.; Qadeer, U. A.; Jordan, R. F. *Organometallics* **2003**, *23*, 600.
- (72) Drew, D.; Doyle, J. R. *Inorg. Synth.* **1990**, *28*, 346.
- (73) Villabrilie, P.; Romanelli, G.; Vazquez, P.; Caceres, C. *App. Cat. A; Gen.* **2004**, *270*, 101.

Chapter 3

Ir and Rh Cp* Complexes with Cationic Pyridine Ancillary Ligands for C–H

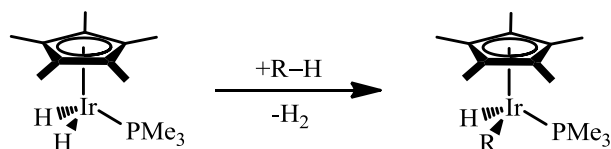
Activation

3.1 Background and Significance

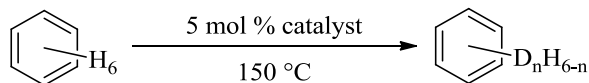
A major focus of organometallic research involves the activation and functionalization of C–H bonds.¹⁻¹⁸ Given the original success of the Shilov system in functionalizing C–H bonds, Pt^{II} and Pd^{II} have been a major focus for catalysis in the field.¹⁹⁻²⁸ These methods are often use electrophilic metal centers to form C–X bonds (X=OR, Cl, Br, F, and C). A consequence of having an electrophilic metal center is that these systems frequently require acidic conditions, are inhibited by coordinating solvents, and suffer from inhibition by products such as H₂O and CH₃OH.^{20,24} Since these systems require acid conditions and non-coordinating functionalities, strongly Lewis basic or acid sensitive functionalities cannot be tolerated. In order to circumvent these issues, it would be beneficial to turn to metal centers that are less electrophilic in nature.²⁹⁻³¹

A seminal example of the stoichiometric activation of C–H bonds using Ir was demonstrated with IrCp*(PMe₃)(H)₂ (Cp* = pentamethylcyclopentadienyl) activating both alkyl and aromatic C–H bonds.²⁹ Under photochemical conditions, H₂ was released followed by the oxidative addition of the C–H bond to generate species of the form IrCp*(PMe₃)RH (R= alkyl or aryl) (Scheme 3.1).

Scheme 3.1 Stoichiometric C–H Activation at IrCp* Complexes.



Analogous stoichiometric reactions have been reported utilizing other Rh^I and Ir^I Cp* complexes.^{3,32-35} While unsuccessful in the functionalization of C–H bonds, tremendous work for the activation of C–H bonds has been illustrated using Ir^{III}Cp* complexes.³⁶ These complexes are often of the form [IrCp*(PMe₃)X₂] (X=Cl, Me) and used as catalysts for C–H activation through H/D exchange. These complexes have also been heavily studied in both stoichiometric and catalytic applications for the activation of C–H bonds.^{37,38} Importantly, these complexes have been used to effectively incorporate deuterium into organic molecules with methanol-D₄, acetone-D₆, D₂O, and D₂ as deuterium sources, most of which are highly coordinating solvents.³⁹ The activity of the two most studied phosphine based catalyst systems (IrCp*(PMe₃)Cl₂ (**1**) and IrCp*(PMe₃)H₃(OTf) (**2**)) by Bergman and coworkers are summarized below (Table 3.1).³⁹

Table 3.1 IrCp* Catalyzed H/D Exchange of Benzene.³⁹

Solvent	IrCp*(PMe ₃)Cl ₂ (1)		IrCp*(PMe ₃)H ₃ (OTf) (2)	
	% D _{inc}	time	% D _{inc}	time
D ₂ O	90	5 d	66	17 h
D ₂ O/CD ₃ OD (1:1)	97	2 d	75	3 d
CD ₃ OD	58	2 d	95	3 d
CH ₃ OD	0	2 d	0	2 d
Acetone-D ₆	21	2 d	99	20 h

Interestingly, while CD₃OD was an effective deuterium source, CH₃OD showed no deuterium incorporation into organic substrates with the Cp*Ir catalysts. This result implicates the methyl-D as the source of deuterium in these transformations. Organic molecules possessing aromatic, benzylic, allylic, and alkyl C–H bonds have all been shown to undergo deuterium incorporation with these catalyst systems.³⁹ Earlier work with these complexes also showed that alcohols, ethers, and carboxylates are viable substrates in these transformations.³¹

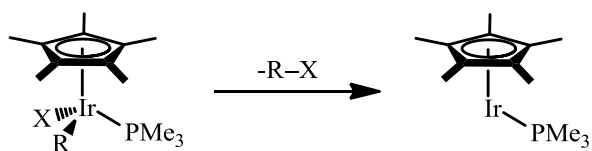
While tremendous strides have been made using electron rich phosphines, functionalization schemes often require strong oxidants that are incompatible with these ligands. While initial efforts involved PMe₃ derivatives, recent reports in the field have focused upon the use of N-heterocyclic carbene (NHC) ligands due to their increased stability in oxidizing environments and their strong electron donor abilities.⁴⁰⁻⁴⁵ The first example of using [IrCp*(NHC)] complexes for H/D exchange was reported by Peris, using the NHC was derived from 1,3-di-*n*-butylimidazolium.⁴⁰ In this system, CD₃OD

and acetone-D₆ were shown to be viable deuterium sources for the exchange. Importantly, the catalytic activity for aromatic, vinyl, and alkyl C–H bonds was reported to be enhanced in comparison to IrCp*(PMe₃)Cl₂.⁴⁰ Subsequent work in the Peris group has focused on stoichiometric studies comparing the reactivity of these complexes towards intramolecular alkyl and aromatic C–H bonds in cyclometallation reactions.⁴¹⁻⁴³ Other studies by the Ison group have focused on examining C–H activation at IrCp*(NHC)(X)₂ complexes containing different X ligands (X = sulfate, triflate, trifluoroacetate, chloride, and nitrate).⁴⁵

The mechanism of this C–H activation has been proposed to involve oxidative addition of a C–H bond to an Ir^{III} center generating an Ir^V–H intermediate.² While no observations of this intermediate exist, stable Ir^V analogs have been isolated (such as IrCp*(H)₄) and the oxidative additions of Si–H bonds has been demonstrated, both providing experimental evidence for this proposal.⁴⁶⁻⁴⁹ Significant computational studies have provided additional support for this mechanism.⁵⁰⁻⁵² Additionally, evidence for the oxidative addition mechanism of C–H bonds and Ir^V intermediates is seen in the observed ligand effects in IrCp*(L)Cl₂ complexes.³⁰ Given this mechanistic proposal, one would assume that L should be an electron rich ligand. Consistent with this hypothesis, PMe₃ has been shown to have enhanced reactivity toward benzene C–H bonds in comparison to P(OMe)₃, with approximately an approximately 30-fold rate enhancement.³⁰ Furthermore, the less electron rich rhodium analog RhCp*(PMe₃)Cl₂ is approximately 1000 times less reactive towards benzene C–H bonds.⁵³ Thus, the metal and ligand effects are consistent with the proposed oxidative addition mechanism.

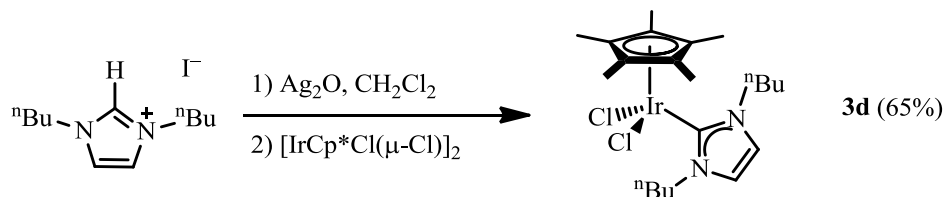
Recently, proposals for alternate mechanisms for C–H activation at Ir^{III}Cp* complexes have emerged. Davies and Macgregor recently suggested that acetate ions can serve as an intramolecular base and promote electrophilic C–H activation via a concerted metalation/deprotonation sequence (without a change in oxidation state at the Ir center). Importantly, this mechanism is analogous to that proposed for C–H activation at Pd centers.^{50,54-57} This was an especially noteworthy idea, given that the addition of acetate ions has been reported to promote Ir and Rh cyclometallation reactions.⁵⁸ With this proposal in reference and our recent work with electron withdrawing pyridine ligands (see Chapter 2), we hypothesized that the addition of pyridine and electron withdrawing pyridine ligands along with acetate ligands could promote the alternative electrophilic reaction mechanism in place of oxidative addition and show significantly different solvent effects and activities with deuterium sources. Also, given the lack of functionalization reactions to form C–X (X = O, N, Cl, Br, I, F) bonds at Ir centers, electron withdrawing ligands could generate complexes capable of undergoing reductive elimination reactions (Scheme 3.2). The ligand properties believed to promote C–H activation are in complete contrast with the ligand trends one would expect to promote reductive elimination. Thus, studying less electron donating ligands in C–H activation reactions could provide a broad advancement in the field of Ir- and Rh-based C–H functionalization chemistry.

Scheme 3.2 IrCp* C–X Bond Formation.



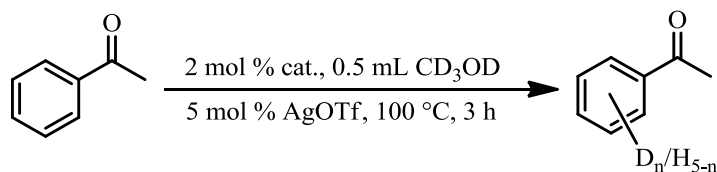
For comparison, we also synthesized $[\text{IrCp}^*(\text{NHC})\text{Cl}_2]$ (**3d**), which was previously reported and studied by Peris (Scheme 3.4).⁴⁰

Scheme 3.4 Peris Synthesis of $[\text{IrCp}^*(\text{NHC})\text{Cl}_2]$.⁴⁰



3.2.2 Initial H/D Exchange Investigations

With **3a-3d** in hand, we next wanted to evaluate the activity of these complexes for C–H activation by using an H/D exchange assay. We began by analyzing catalytic activity using an electron deficient aromatic substrate, acetophenone, with CD_3OD as the deuterium source as reported by Peris (Table 3.2).⁴⁰ The methyl group of the acetophenone shows a background reaction and is deuterated in the absence of Ir. Thus, this deuteration was not monitored or included in tabulated results. The addition of AgOTf was used to generate a metal complex with labile ligands (analogous to Peris's procedure).⁴⁰ Notably, silver salts are commonly added to generate open coordination sites during H/D exchange assays.⁵⁹

Table 3.2 H/D Exchange of Acetophenone with [IrCp*(L)Cl₂] Complexes.

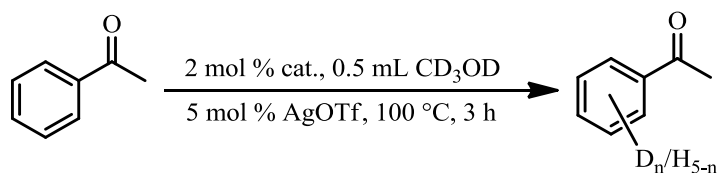
Catalyst	TON (<i>o</i> : <i>m</i> : <i>p</i>)	Catalyst	TON (<i>o</i> : <i>m</i> : <i>p</i>)
 3d	45 (2.4 : 2.0 : 1)	 3b	19 (3.4 : 1.1 : 1)
 3c	15 (5.0 : 1.5 : 1)	 3a	35 (2.1 : 0.9 : 1)

TON-turnover numbers; (*o* : *m* : *p*)-*ortho*, *meta*, and *para* ratio; TON and selectivities were determined by ¹H NMR spectroscopy.

Consistent with literature reports, complex **3d** showed high turnover numbers (TON = 45). Gratifyingly, both the py-*t*Bu (**3c**) and 4-**Ar** complexes (**3a** and **3b**) showed comparably high activity for H/D exchange. Thus, strongly donating N-heterocyclic carbenes or phosphines are not required for activity in [IrCp*(L)Cl₂] complexes. Furthermore, we found that the site selectivity is significantly different between the catalysts. The Ir complexes (**3b** and **3c**) show a higher amount of *ortho*-deuteration while the Rh complex (**3a**) shows diminished *meta*-deuteration when compared to **3d**. This indicates that the ligand and metal can affect the selectivity in these systems. With this

initial success in hand, we hypothesized that the deuterium source (solvent) might affect the reactivity and selectivity observed in the system given that the acidity of deuterium source could affect the rate of protonation of an Ir-Aryl intermediate. To test this hypothesis, we compared the activity of **3a** and **3d** (the most active complexes above) in both CD₃OD and CD₃CO₂D with acetophenone (Table 3.3).

Table 3.3 Solvent Affect in H/D Exchange of Acetophenone.



Catalyst	TON (<i>o</i> : <i>m</i> : <i>p</i>)	
	CD ₃ OD	CH ₃ COOD
<p>3d</p>	45 (2.4 : 2.0 : 1)	64 (47 : 1 : 1)
<p>3a</p>	35 (2.1 : 0.9 : 1)	32 (1 : 0 : 0)

TON-turnover numbers; (*o* : *m* : *p*)- *ortho*, *meta*, and *para* ratio; TON and selectivities are determined by ¹H NMR.

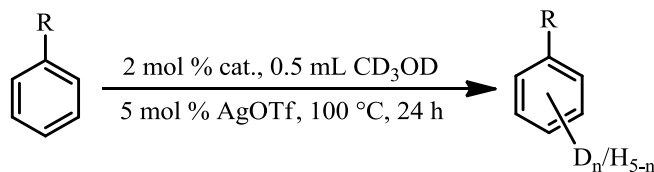
Using **3d**, the activity for H/D exchange is increased in acetic acid compared to methanol, and the selectivity is dramatically changed. Only *ortho*-deuteration is observed with acetic acid in contrast to a statistical ratio of products based upon the number of *ortho*, *meta*, and *para* hydrogens present in the substrate in methanol. When

using **3a** as the catalyst, the activity is comparable in both solvents although the selectivity shows a similar trend. Given the high *ortho* selectivity, this indicates that the acetophenone carbonyl is likely serving as a directing group in the C–H activation.

3.2.3 Expanding the Substrate Scope in H/D Exchange

With the initial success in H/D exchange of acetophenone using **3a-3c**, we next wanted to expand the substrate scope to other mono-substituted aromatic substrates in order to gain additional insight into the electronic effects of this reaction. In Table 3.4, we evaluated catalyst activity with a variety of mono-substituted aromatic substrates.

Table 3.4 Mono-substituted Aromatic Substrates for H/D Exchange.



Substrate	3b (TON)	3d (TON)	Substrate	3b (TON)	3d (TON)
	35±2 ^a	45±3 ^a		10±8	6±2
	5±2	16±2		15±2	15±5
	1±1 8±6 ^b	8±2 16±5 ^b			

^a-3 hour reaction; ^b-150 °C; 3b-[IrCp*(**4-Ar**)Cl₂]; 3d--[IrCp*(NHC)Cl₂]

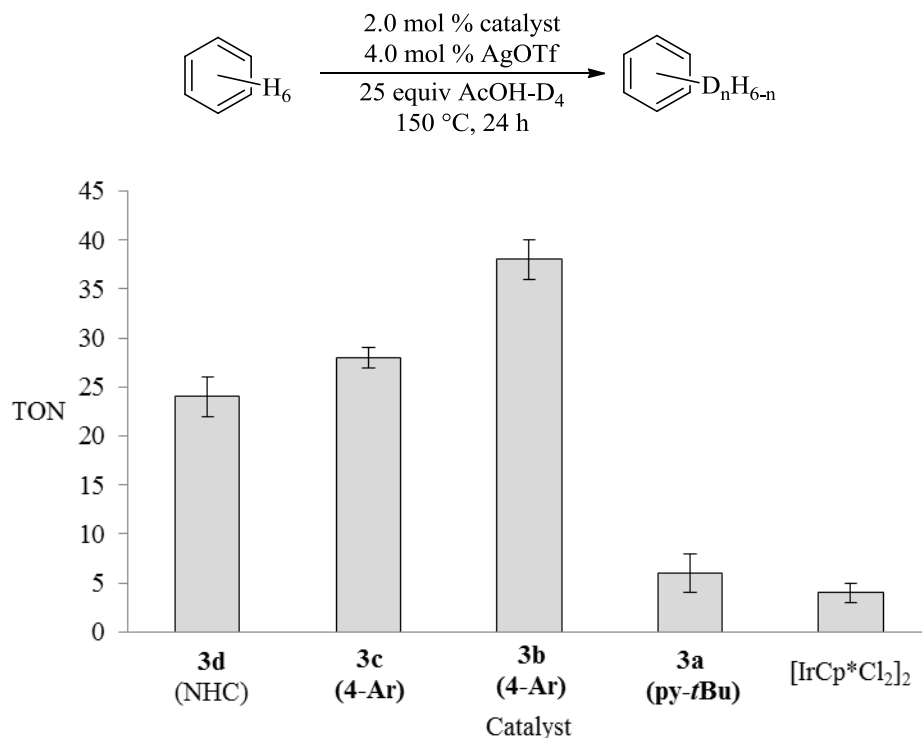
We surveyed alkyl benzenes, bromobenzene, as well as nitrobenzene, an electron deficient aromatic substrate. We found that with all of these substances, significantly lower reactivity is observed compared to acetophenone. This result is highlighted by the

low turnovers obtained even after 24 hours (Table 3.4). Given the low reactivity in these reactions, the selectivity is difficult to determine by ^1H NMR spectroscopy and is not reported. Even when bromobenzene is heated at 150 °C for 24 hours, considerably lower turnovers are observed when compared with acetophenone (Table 3.4). In order to explain this limited reactivity, we considered the structure of the substrates that we tested. All substrates subjected to the reaction conditions in Table 3.4 contain varying electron donating and electron withdrawing substituents. Thus, substrate electronics appear to have little effect on activity. Alternatively, Peris *et al.* found that substrates containing Lewis basic functionalities (e.g. diethyl ether, tetrahydrofuran, acetophenone) were especially active for H/D exchange in methanol with IrCp*(NHC) catalysts.⁴⁰ Thus, the apparent requirement for a directing group may complicate catalyst activity comparisons. This complication arises because the observed activities would be a combination of substrate binding and C–H activation. These steps could be conflicting and cause incorrect interpretations concerning the ligand effects on C–H activation activity.

3.2.4 H/D Exchange of Benzene

With the limited reactivity in mono-substituted aromatic substrates, we next chose to analyze reaction conditions for H/D exchange of benzene using a variety of solvents and catalysts. An additional benefit to using benzene is selectivity is not a factor, so the data can be analyzed more conveniently by mass spectrometry (relative isotope concentrations can be deconvoluted from the $\text{C}_6\text{H}_{6-n}\text{D}_n$ isotope fragment peaks) instead of signal loss relative to internal standard in ^1H NMR spectroscopy. We first chose to analyze the catalytic activity of **3a-3d** for the H/D exchange of benzene in the more acidic deuterium source acetic acid- D_4 (Figure 3.1).

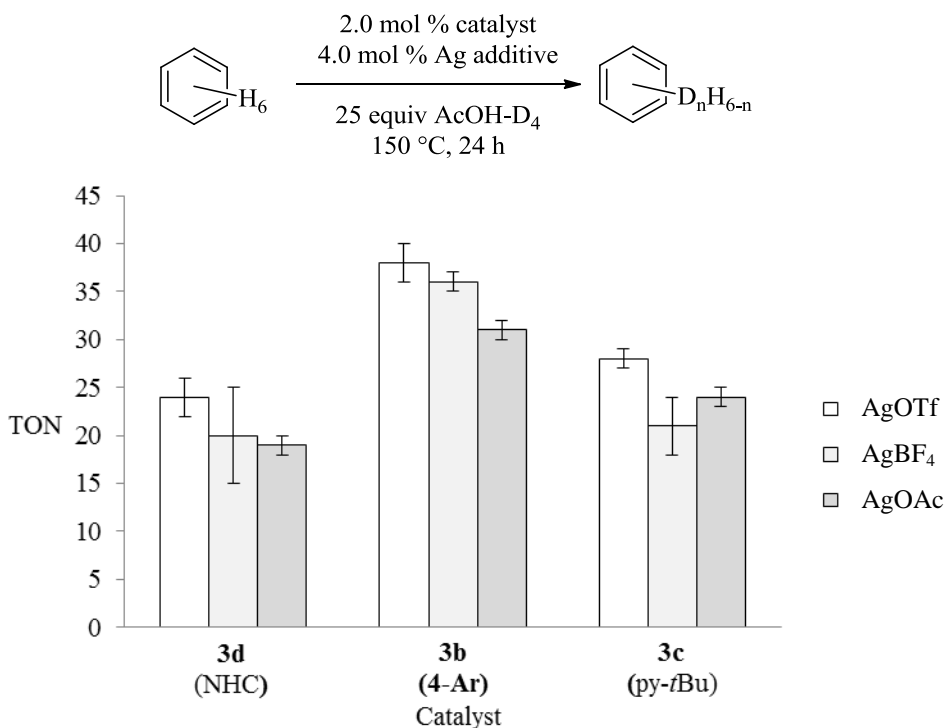
Figure 3.1 Benzene H/D Exchange with CD₃COOD.



The benchmark NHC catalyst **3d** showed intermediate activity for the H/D exchange of benzene. Catalyst **3c** (py-*t*Bu) shows slightly enhanced turnover numbers and catalyst **3b** (4-Ar) shows significantly higher activity when compared to **3d**. Catalyst **3a** gave particularly poor turnover numbers for C-H activation of benzene (in contrast to being very active in the H/D exchange studies with acetophenone, Table 3.2). We reasoned that the pyridine based ligands are more weakly coordinating than NHC ligands and labile, so ligand loss in **3b** and **3c** could play a role in the enhanced reactivity. In order to discount this possibility, we examined [IrCp*Cl₂]₂ as a catalyst and observed little catalytic activity. Thus, when benzene is the substrate with acetic acid-D₄, Rh-based **3a** appears to be an ineffective catalyst and the pyridine-based catalysts **3b** and **3c** are more active than the NHC-based **3d**.

Previous reports with catalyst **3d** used AgOTf to generate a labile coordination site.⁴⁰ Since the Ison group has previously shown anion identity can affect catalytic activity in these types of reactions,⁴⁵ we chose to test multiple silver salts (silver trifluoromethylsulfonate, AgOTf; silver tetrafluoroborate, AgBF₄; silver acetate, AgOAc), and the results are shown below in Figure 3.2.

Figure 3.2 Silver Additive Effect on Catalytic Activity.



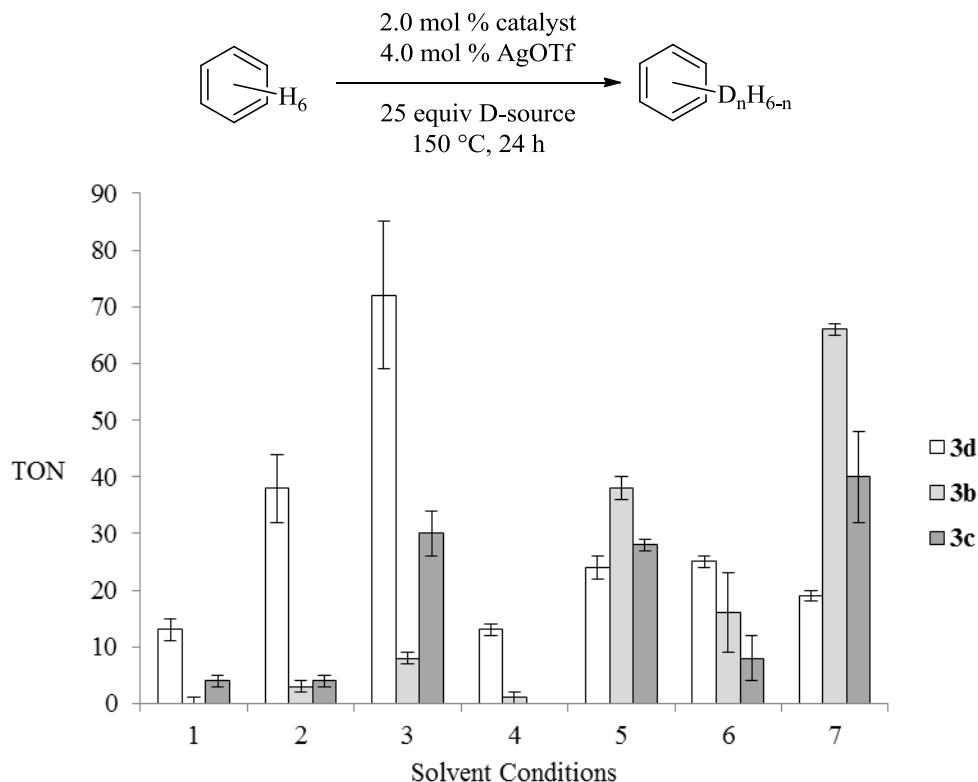
From this data, the less coordinating triflate anion proves to be a more effective counterion than acetate. Silver tetrafluoroborate possesses greater standard deviation between experiments (likely due to the highly hydroscopic nature of the compound, which limits accuracy) although it appears to be less effective than triflate as an additive.

3.2.5 Solvent Effects in H/D Exchange of Benzene

With the success of silver triflate as an additive and the varying solvent effects highlighted above in Table 3.3, we wanted to gain added insight into the solvent effects

of this system. We examined the catalytic activity of **3b-3d** in mixtures of methanol-D₄, D₂O, and acetic acid-D₄ with and without added silver triflate (Figure 3.3).

Figure 3.3 Solvent Effects in H/D Exchange.



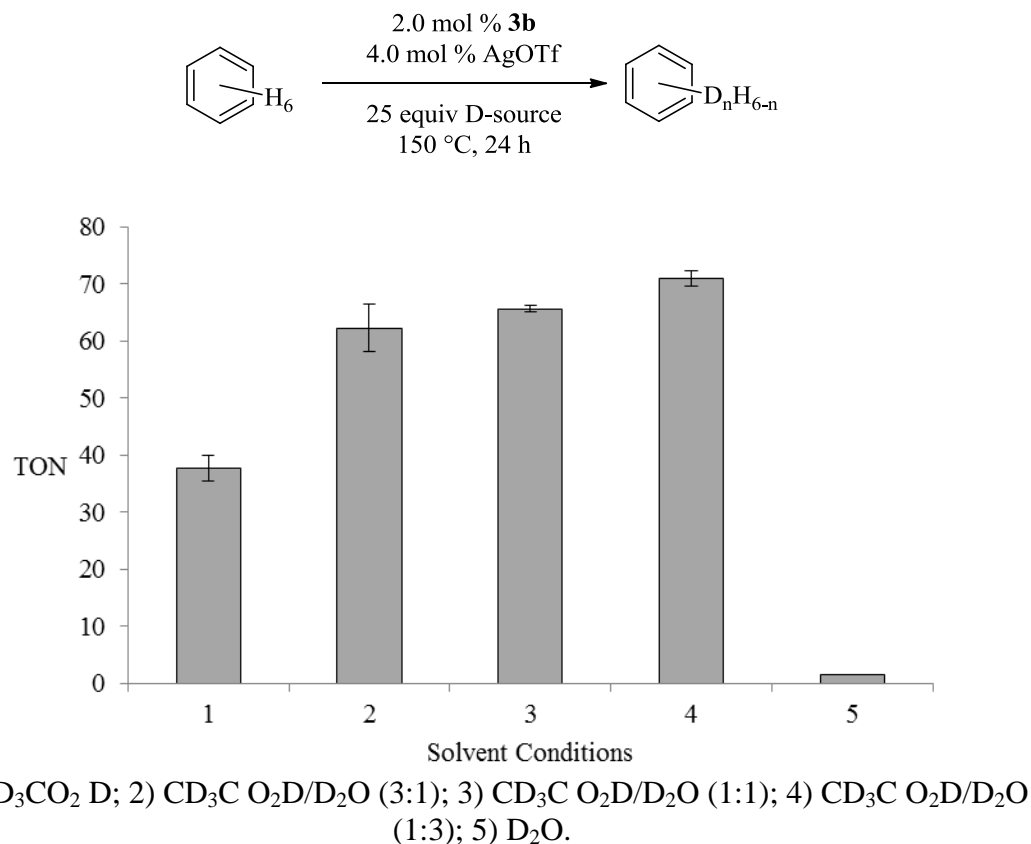
- 1) CD₃OD, no additive; 2) CD₃OD, AgOTf; 3) CD₃OD/D₂O (1:1), no additive; 4) CD₃COOD, no additive; 5) CD₃COOD, AgOTf; 6) CD₃COOD/D₂O (1:1), no additive; 7) CD₃COOD/D₂O (1:1), AgOTf

Complex **3d** shows significantly higher activity in methanol-D₄ in comparison to complexes **3b** and **3c** (conditions 1-3, Figure 3.3). Low reactivity with all three complexes is observed in acetic acid-D₄ with no additive (conditions 4, Figure 3.3). However, the opposite trend is observed in acetic acid-D₄ with silver triflate, where the pyridine-based systems (**3b** and **3c**) show enhanced reactivity compared to **3d** (conditions 5, Figure 3.3). Interestingly, the addition of silver triflate has a dramatic effect on catalysis with complexes **3b** and **3c** (conditions 4 versus 5 and 6 versus 7, Figure 3.3).

Silver triflate has much less significant effect when using catalyst **3d**. This trend suggests that with less electron rich ligands, such as pyridine-based systems, loss of an X-type ligand is likely a key to high reactivity, and thus, chloride abstraction has a dramatic effect on catalytic activity. However, in **3d**, the NHC is a much more electron donating ligand, which facilitates chloride loss. The high activity of **3d** in methanol/water mixtures is consistent with this hypothesis, as increasing the polarity of the solvent should aid in ligand loss. Notably, a similar proposal was previously made by the Ison group.⁴⁵

We also tested an acetic acid/water mixture with the addition of silver triflate for catalytic activity (Condition 7, Figure 3.3). Consistent with our hypothesis, these conditions generated the most active catalyst system for **3b** and **3c**. With the high activity of **3b** under these conditions, we wondered how the acetic acid and water ratio would affect catalytic activity. To gain insight into this effect, we performed H/D exchange reactions in pure acetic acid-D₄, 3:1, 1:1, and 1:3 ratios of acetic acid-D₄ and water (D₂O) along with pure water (D₂O) with silver triflate (Figure 3.4).

Figure 3.4 Acetic Acid-D₄ and D₂O Ratios in H/D Exchange.

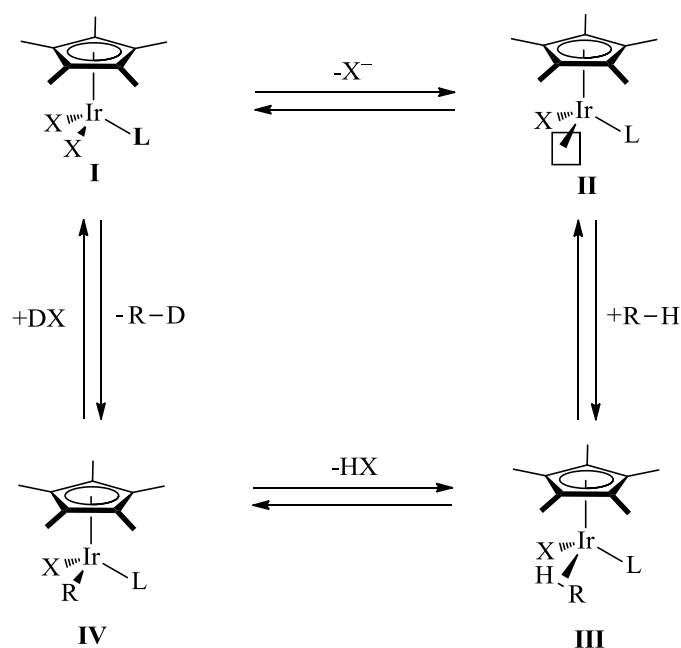


As can be inferred from Figure 3.4, the addition of D₂O to the reaction mixture causes a significant increase in catalytic activity, although the ratio has a much smaller effect on the activity. Interestingly, **3b** in D₂O shows no catalytic activity. This could be due to the low solubility of the catalyst in solvent, as the reaction appears to be heterogeneous.

In comparing the solvent effects in totality, it appears that acetic acid is a key solvent component in achieving high catalytic activity with pyridine-based catalysts. The role of acetic acid could be due to the acidic nature of the D-source. For example, protonation of the Ir-aryl bond of intermediate **III** could require a relatively acidic deuterium source (Figure 3.5). Alternatively, the acidic environment could aid the ligand

loss through the protonation of X-type ligands, making them less coordinating. Finally, the acetate may assist in C–H activation via a CMD mechanism as was proposed by Macgregor and Davies (*vide supra*).^{50,54-57}

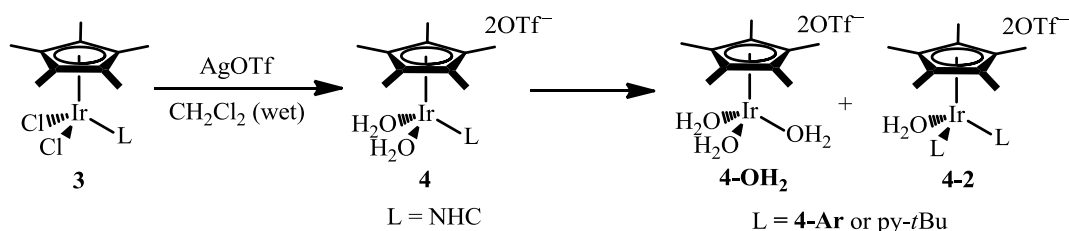
Figure 3.5 Potential H/D Exchange Catalytic Cycle.



3.2.6 Active Catalyst System

We next attempted to isolate the active catalyst produced *in situ* in our H/D exchange studies through halide abstraction analogous to the isolated structures (**4**-Scheme 3.5).⁴⁵ When attempting to isolate the complexes of the form **4** when using **3b** and **3c** with the published procedure, we observed ¹H NMR spectra consistent with the formation of **4-2** indicating ligand disproportionation. This result is in contrast to the use of **3d**, where **4** can be isolated.⁴⁵

Scheme 3.5 Active Catalyst Isolation Attempts.

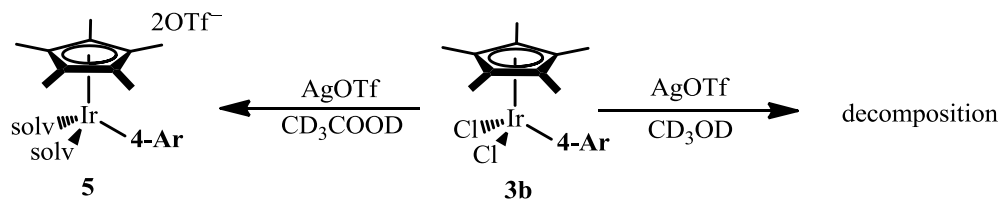


This disproportionation is likely a result of the low solubility of **4-OH₂**, which drives the reaction. In an effort to understand this reaction, we performed the analogous halide abstraction of **3b** in CDCl_3 and monitored the reaction by ^1H NMR. Under these conditions, the ^1H NMR spectra were complicated but indicated the formation of **4-2** along with other complex products. These results indicate that isolation is difficult due to the decomposition of **4** which is likely due to disproportionation.

Although we were unable to isolate halide abstraction products, we wanted to observe the active catalyst by ^1H NMR spectroscopy. When **3b** or **3c** and 2 equivalents of AgOTf are dissolved in acetic acid- D_4 at room temperature, two products are observed by ^1H NMR spectroscopy. These are likely mixtures of acetate or coordinated acetic acid complexes; but importantly, the complexes all show a 1:1 Cp^* to ligand ratio. Heating these reactions at $100\text{ }^\circ\text{C}$ for 20 hours shows no signs of decomposition. The ratio of the two complexes changes with complex **3c**, but still these species are stable. With **3b**, a third product is observed in the mixture, but all three species are of the form IrCp^*LX_2 where X is derived from the solvent (Scheme 3.6). However, when the analogous reactions are performed in methanol- D_4 with **3b** and **3c** at room temperature, at least three products are observed. The form of these complexes is unclear and significant precipitation of the complexes occurs upon heating at $100\text{ }^\circ\text{C}$ for 20 hours, accompanied by loss of ^1H NMR signals. Analogous reactions of complexes with NHC ligands by the

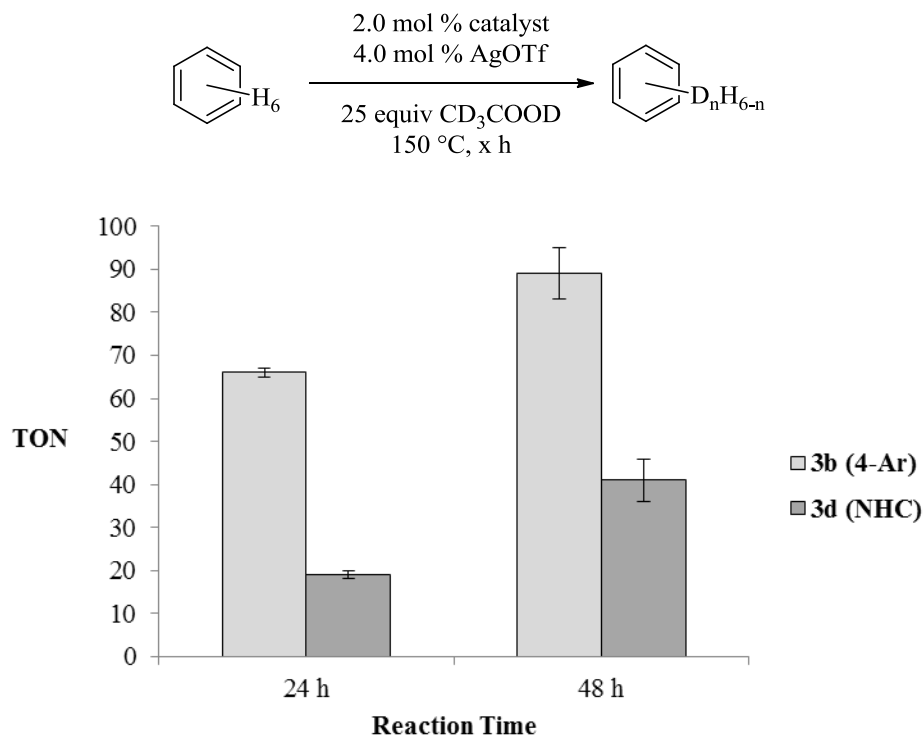
Ison Group at North Carolina State University indicate that Ir-hydride species are produced with methanol as a solvent. For complexes **3b** and **3c**, hydride formation is possible but the products are likely not stable. Attempts at isolation and characterization have not been explored given their low activities for H/D exchange reactions in methanol.

Scheme 3.6 Observation of Putative Active Catalyst by ^1H NMR Spectroscopy.



With the stability observed for halide abstraction products of **3b** and **3c** under the reaction conditions in acetic acid, we hypothesized that catalytic activity should be maintained after 24 hours. To test this hypothesis, we performed 24 and 48 hour reactions of H/D exchange with complexes **3b** and **3d** in acetic acid- D_4 (Figure 3.6).

Figure 3.6 Catalyst Activity at Longer Reaction Times.



With complexes **3b** and **3d**, catalytic activity is maintained after 24 hours, as evident by the additional turnovers observed in 48 hour reactions. This result corroborates the ¹H NMR spectroscopic studies above indicating that mono-ligated Ir species are present after halide abstractions and that these species are stable to prolonged heating.

3.3 Conclusions

We have successfully developed complexes that efficiently catalyze H/D exchange that do not contain strongly donating supporting ligands. Ir complexes with Cp* ligands have been heavily studied for C–H activation.^{29,36} Specifically, these systems usually have the formula IrCp*(L)Cl₂, where L is a strongly donating phosphine or N-heterocyclic carbene ligand.^{30,32,37,39,40} The highly electron donating ligand has been

proposed in the literature to be required for catalytic activity.^{30,46-53} Given the lack of examples of carbon-heteroatom bond forming reductive elimination reactions in these systems, we hypothesized that our success with pyridine-based ligands could allow for C–H activation in these systems and in the future could allow for more facile reductive elimination reactions. Towards this goal, we studied and compared the reactivity of Ir and Rh-based Cp* systems using N-heterocyclic carbenes, 4-*t*-butylpyridine, and **4-Ar** (see Chapter 2) for activation of C–H bonds. Using these complexes, we identified **3b** and **3c** as pyridine-based catalyst systems that show high activity for C–H activation through H/D exchange assays. Acetic acid and a silver triflate additive were found to be critical to achieve high activity, while limited reactivity is observed in methanol. Thus, strongly electron donating phosphine or NHC ligands are not required for C–H activation in these systems depending on solvent conditions. Overall, our extensive studies of solvent effects provide a cautionary tale in employing narrow reaction conditions to assay catalytic activity. With these results in H/D exchange, complexes **3a-3c** can provide a starting point for fundamental studies in C-X bond formations (X=Cl, Br, I, O, N).

3.4 Experimental Procedures

3.4.1 Instrumentation

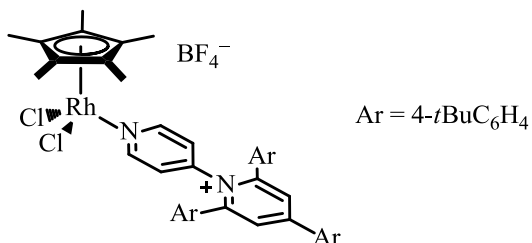
NMR spectra were recorded on Varian Inova 500, Varian vnmrs 500 MHz, Varian MR400 400 MHz, or Varian vnmrs 700 MHz NMR spectrometers with the residual solvent peak (methanol-d₄: ¹H: δ=4.78, 3.30 ppm, ¹³C: δ=49.0 ppm; AcOH-d₄: ¹H: δ=11.53, 2.03 ppm, ¹³C: δ=178.4, 20.0 ppm; acetonitrile-d₃: ¹H: δ=1.94 ppm, ¹³C: δ=118.2, 1.3 ppm; benzene-d₆: ¹H: δ=7.15 ppm, ¹³C: δ=128.0 ppm; chloroform-d₁: ¹H:

$\delta=7.24$ ppm, ^{13}C : $\delta=77.0$ ppm) as the internal reference unless otherwise noted. ^{19}F NMR is referenced to the residual solvent signal in the ^1H NMR. Chemical shifts are reported in parts per million (ppm) (δ). Multiplicities are reported as follows: br (broad resonance), s (singlet), d (doublet), t (triplet), q (quartet), m (multiplet). Coupling constants (J) are reported in Hz. Elemental analyses were performed by Atlantic Microlab, Inc., Norcross, Georgia.

3.4.2 Materials and Methods

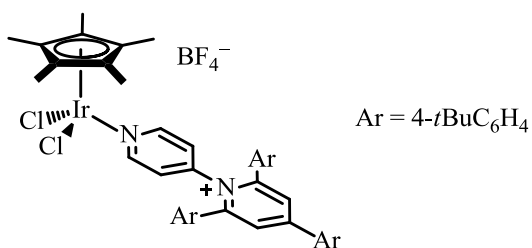
All reactions were conducted without rigorous exclusion of air and moisture unless noted otherwise. AcOH- d_4 were purchased from Cambridge Isotopes Lab and stored in Schlenk tubes under N_2 . Acetonitrile- d_3 , CD_3COOD , CD_3OD , CDCl_3 , and D_2O were purchased from Cambridge Isotopes Lab and used as received. Dichloromethane and pentane were obtained from Fisher Scientific or Aldrich and used as purchased. Benzene for H/D exchange was obtained from Aldrich and stored over 4 Å molecular sieves. Bromobenzene, nitrobenzene, silver triflate, and 1,2,3,4,5-pentamethylcyclopentadiene were purchased from Acros Organics. K_2CO_3 was purchased from Fisher Scientific. 4-*t*-butylpyridine was purchased from TCI America. RhCl_3 hydrate and IrCl_3 hydrate were purchased from Pressure Chemical Company. Neopentylbenzene and silver acetate were obtained from Alfa Aesar. AgBF_4 , 4-*t*-butylpyridine, acetophenone, and 1,1,2-trichloroethane were purchased from Aldrich. $[\text{IrCp}^*\text{Cl}_2]_2$,⁶⁰ $[\text{RhCp}^*\text{Cl}_2]_2$,⁶⁰ 1,3-di-*n*-butylimidazolium iodide,⁶¹ **3d**,⁴⁰ and **4-Ar** (Chapter 2) were prepared according to literature procedures. All liquid reagents were dispensed by difference using gas-tight Hamilton syringes.

3.4.3 Synthesis



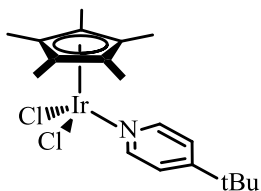
RhCp*Cl₂(4-Ar) (3a)

4-Ar (829 mg, 1.29 mmol, 2.00 eq.) and [RhCp*Cl₂]₂ (400 mg, 647 μmol, 1.00 eq.) were dissolved in 10 mL CH₂Cl₂ separately and mixed in a round bottom flask. After 1 hour of stirring at room temperature the volatiles were removed by rotary evaporation. Pentanes (10 mL) was added to the resulting waxy solid and the mixture was sonicated for 5 minutes. The pentane was removed by rotary evaporation resulting in a yellow powder. The desired product was collected and dried *in vacuo* to give 1.12 g (97% yield). ¹H NMR (CD₃CN, 699.765 MHz): δ 8.76 (d, J = 4.6 Hz, 2H), 8.34 (s, 2H), 8.06 (d, J = 8.6 Hz, 2H), 7.69 (d, J = 8.6 Hz, 2H), 7.43 (d, J = 8.4 Hz, 4H), 7.39 (d, J = 6.1 Hz, 2H), 7.34 (d, J = 8.4 Hz, 4H), 1.37 (s, 9H), 1.36 (br, 15H), 1.26 (s, 18H). ¹³C NMR (CD₃CN, 175.974 MHz, 40 °C): δ 1158.1, 157.9, 157.0, 155.3, 148.7, 131.5, 130.6, 130.3, 129.5, 127.9, 126.6, 126.5, 125.5, 95.1 (d, J = 12.2 Hz), 35.8, 35.5, 31.2, 31.1, 9.0 (1 overlapping aryl carbon). ¹⁹F NMR (CD₃CN, 376.836 MHz): δ -151.8 (¹⁰B), -151.9 (¹¹B). Anal. calcd. for RhC₅₀H₆₀N₂Cl₂BF₄: C, 63.24; H, 6.37; N, 2.95. Found: C, 62.71; H, 6.44; N, 2.94.



IrCp*Cl₂(4-Ar) (3b)

4-Ar (322 mg, 503 μ mol, 2.00 eq.) and [IrCp*Cl₂]₂ (200 mg, 251 μ mol, 1.00 eq.) were dissolved in CH₂Cl₂ (10 mL) separately and mixed in a round bottom flask. After 1 hour of stirring at room temperature the volatiles were removed by rotary evaporation. Pentane (10 mL) was added to the resulting waxy solid and the mixture was sonicated for 5 minutes. The pentane was removed by rotary evaporation resulting in a yellow powder. The desired product was collected and dried *in vacuo* to give 474 mg (91% yield). ¹H NMR (CDCl₃, 500.096 MHz): δ 8.77 (d, J = 5.8 Hz, 2H), 7.89 (s, 2H), 7.64 (d, J = 8.3 Hz, 2H), 7.46 (d, J = 8.6 Hz, 2H), 7.40 (d, J = 5.9 Hz, 2H), 7.34 (m, 8H), 1.35 (br, 15H), 1.32 (s, 9H), 1.23 (s, 18H). ¹³C NMR (CDCl₃, 125.762 MHz): δ 157.9, 156.7, 156.0, 154.5, 154.4, 147.7, 131.1, 129.6, 129.2, 128.3, 126.8, 126.0, 125.9, 125.1, 85.9, 35.1, 34.9, 31.0 (2 signals), 8.5. ¹⁹F NMR (CD₃CN, 470.520 MHz): δ -152.5 (¹⁰B), -152.6 (¹¹B). Anal. calcd. for IrC₅₀H₆₀N₂Cl₂BF₄: C, 57.80; H, 5.82; N, 2.70. Found: C, 57.51; H, 5.90; N, 2.65.



IrCp*Cl₂(py-*t*Bu) (3c)

[IrCp*Cl₂]₂ (250 mg, 314 μmol, 1.00 eq.) was dissolved in CH₂Cl₂ (10 mL) in a round bottom flask and 4-*t*-butylpyridine (92.7 μL, 627 μmol, 2.00 eq.) was added by syringe. After 1 hour of stirring at room temperature the volatiles were removed by rotary evaporation. Pentane (10 mL) was added to the resulting waxy solid and the mixture was sonicated for 5 minutes. The pentane was removed by rotary evaporation resulting in a yellow powder. The desired product was collected and dried *in vacuo* to give 291 mg (78% yield). ¹H NMR (CDCl₃, 500.096 MHz): δ 8.80 (d, J = 6.4 Hz, 2H), 7.28 (d, J = 6.6 Hz, 2H), 1.52 (s, 15H), 1.28 (br, 9H). ¹³C NMR (CDCl₃, 125.762 MHz): δ 162.5, 152.7, 122.6, 85.5, 34.9, 30.3, 8.53. Anal. calcd. for IrC₁₉H₂₈NCl₂: C, 42.77; H, 5.29; N, 2.63. Found: C, 42.64; H, 5.31; N, 2.59.

3.4.4 Reaction Details

General Procedure For H/D Exchange Reactions Between Acetophenone and CD₃COOD/CD₃OD.

To a 4 mL resealable Schlenk tube was added catalyst (9.0 mg **3a**, 9.8 mg **3b**, 5.6 mg **3c**, or 5.5 mg **3d**) (9.4 μmol, 2.0 mol %), AgOTf (4.9 mg, 19.1 μmol, 4.0 mol %), deuterium source (0.680 mL CD₃COOD (11.8 mmol, 25.2 equiv.) or 0.480 mL CD₃OD (11.8 mmol, 25.1 equiv.)), and a Teflon stirbar was added. Acetophenone (55.1 μL, 0.472 mmol, 1.00 equiv), was added to the reaction vessel, which was subsequently sealed. The vessel was completely submerged in a preheated oil bath at the indicated reaction

temperature. At the end of the reaction, the vessel was cooled to room temperature. 1,1,2-trichloroethane (43.8 μL , 0.472 mmol, 1.00 equiv) was added to the tube. The contents were mixed by pipet and added to an NMR tube. The percent deuterium incorporation was defined as the percent of C–H bonds converted to C–D bonds and was determined by the loss of signal integration by ^1H NMR and compared to an independent sample of a 1:1 ratio of acetophenone and 1,1,2-trichloroethane. ^1H NMR spectra were recorded as one scan spectrum with gain set to zero to minimize relaxation delay errors. Turnover numbers (TON) is determined by total percent deuterium incorporation divided by catalyst loading.

General Procedure For H/D Exchange Reactions Between Mono-Substituted Arenes and CD_3OD .

To a 4 mL resealable Schlenk tube was added catalyst (9.8 mg **3b** or 5.5 mg **3d**) (9.4 μmol , 2.0 mol %), AgOTf (4.9 mg, 19.1 μmol , 4.0 mol %), 0.480 mL CD_3OD (11.8 mmol, 25.1 equiv.), and a Teflon stirbar was added. Substrate (0.472 mmol, 1.00 equiv, see Table 3.5 for amounts), was added to the reaction vessel, which was subsequently sealed. The vessel was completely submerged in a preheated oil bath at the indicated reaction temperature. At the end of the reaction, the vessel was cooled to room temperature. 1,1,2-trichloroethane (43.8 μL , 0.472 mmol, 1.00 equiv) was added to the tube. The contents were mixed by pipet and added to an NMR tube. The percent deuterium incorporation was defined as the percent of C–H bonds converted to C–D bonds and was determined by the loss of signal integration by ^1H NMR and compared to an independent sample of a 1:1 ratio of acetophenone and 1,1,2-trichloroethane. ^1H NMR spectra were recorded as one scan spectrum with gain set to zero to minimize

relaxation delay errors. Turnover numbers (TON) is determined by total percent deuterium incorporation divided by catalyst loading.

Table 3.5 Substrate Volumes for H/D Exchange.

Substrate	Amount (μL)
acetophenone	55.1
nitrobenzene	48.4
bromobenzene	49.5
<i>t</i> -butylbenzene	73.0
neopentylbenzene	82.3

**General Procedure For H/D Exchange Reactions Between Benzene and CD_3COOD
– Silver Additives.**

To a 4 mL resealable Schlenk tube was added catalyst (9.8 mg **3b**, 5.6 mg **3c**, or 5.5 mg **3d**) (9.4 μmol , 2.0 mol %), silver additive (19.1 μmol , 4.0 mol % : 4.9 mg AgOTf; 3.7 mg AgBF₄; or 1.6 mg AgOAc), 0.680 mL CD₃COOD (11.8 mmol, 25.2 equiv.), and a Teflon stirbar was added. Benzene (42.0 μL , 0.472 mmol, 1.00 equiv) was added to the reaction vessel, which was subsequently sealed. The vessel was completely submerged in a preheated oil bath at the indicated reaction temperature. At the end of the reaction, the vessel was cooled to room temperature. The reaction mixture was then filtered over a plug of Celite to remove any particulates and rinsed with EtOAc (1 x 2 mL) into a 20 mL scintillation vial. A saturated aqueous solution of K₂CO₃ (9 M in deionized H₂O, 2 x 1 mL) was added to the vial to quench and separate the acid. The organic layer was carefully separated and diluted with additional EtOAc to give a 12.8 mM solution of benzene (~1 mg/mL) for analysis by GC-MS.

The percent deuterium incorporation was defined as the percent of C–H bonds converted to C–D bonds. The background reaction (in the absence of the Ir/Rh catalyst) at 150 °C is minimal with AcOH-d₄ and is described in detail in previous publications.⁵⁹ Turnover numbers (TONs) are calculated as mole deuterium incorporated per mole of catalyst. Reported values have been corrected for the background reaction in the presence of AgCl, which is formed in situ. The reported error is the standard deviation of at least two replicate trials.

General Procedure For H/D Exchange Reactions Benzene – Solvent Screen.

To a 4 mL resealable Schlenk tube was added catalyst (9.8 mg **3b**, 5.6 mg **3c**, or 5.5 mg **3d**) (9.4 μmol, 2.0 mol %), AgOTf (4.9 mg, 19.1 μmol, 4.0 mol %), solvent (see below), and a Teflon stirbar was added. Benzene (42.0 μL, 0.472 mmol, 1.00 equiv) was added to the reaction vessel, which was subsequently sealed. The vessel was completely submerged in a preheated oil bath at the indicated reaction temperature. At the end of the reaction, the vessel was cooled to room temperature. The reaction mixture was then filtered over a plug of Celite to remove any particulates and rinsed with EtOAc (1 x 2 mL) into a 20 mL scintillation vial. A saturated aqueous solution of K₂CO₃ (9 M in deionized H₂O, 2 x 1 mL) was added to the vial to quench and separate the acid. The organic layer was carefully separated and diluted with additional EtOAc to give a 12.8 mM solution of benzene (~1 mg/mL) for analysis by GC-MS.

The percent deuterium incorporation was defined as the percent of C–H bonds converted to C–D bonds. The background reaction (in the absence of the Ir catalyst) at 150 °C is minimal with AcOH-d₄ and is described in detail in previous publications.⁵⁹ Turnover numbers (TONs) are calculated as mole deuterium incorporated per mole of

catalyst. Reported values have been corrected for the background reaction in the presence of AgCl, which is formed in situ. The reported error is the standard deviation of at least two replicate trials.

Table 3.6 Solvent Volumes for H/D Exchange.

Solvent	Solvent 1		Solvent 2	
	Amount (μL)	mmol (equiv.)	Amount (μL)	mmol (equiv.)
CD ₃ OD	480	11.8 (25.1)	-	-
CD ₃ OD/D ₂ O	240	5.9 (12.6)	107	5.9 (12.6)
CD ₃ COOD	680	11.8 (25.2)	-	-
CD ₃ COOD/D ₂ O (1:1)	340	5.9 (12.6)	107	5.9 (12.6)
CD ₃ COOD/D ₂ O (3:1)	510	8.9 (18.9)	60	3.3 (7.1)
CD ₃ COOD/D ₂ O (1:3)	170	3.0 (6.3)	180	10.0 (21.2)
D ₂ O	214	11.8 (25.1)	-	-

General Procedure For Active Catalyst Species – CD₃COOD/CD₃OD.

To a 5 mL resealable Teflon capped vial was added catalyst (9.8 mg **3b**, 5.6 mg **3c**) (9.4 μmol, 2.0 mol %), AgOTf (4.9 mg, 19.1 μmol, 4.0 mol %), 0.5 mL CD₃COOD or CD₃OD. The reaction was mixed by pipet at room temperature and ¹H NMR spectra were recorded. Samples were placed back in the vial and heated to 100 °C for 20 hours. Reactions were cooled to room temperature and ¹H NMR spectra were recorded.

3.5 References

- (1) Labinger, J. A.; Bercaw, J. E. *Nature* **2002**, *417*, 507.
- (2) Arndtsen, B. A.; Bergman, R. G.; Mobley, T. A.; Peterson, T. H. *Acc. Chem. Res.* **1995**, *28*, 154.

- (3) Jones, W. D.; Feher, F. J. *Acc. Chem. Res.* **1989**, *22*, 91.
- (4) Crabtree, R. H. *Chem. Rev.* **1985**, *85*, 245.
- (5) Crabtree, R. H. *Chem. Rev.* **1995**, *95*, 987.
- (6) Goldberg, K. I.; Goldman, A. S. *Activation and Functionalization of C-H Bonds*; Oxford University Press: Washington, DC, 2004.
- (7) Crabtree, R. H. *J. Chem. Soc.-Dalton Trans.* **2001**, 2437.
- (8) Periana, R. A.; Bhalla, G.; Tenn, W. J.; Young, K. J. H.; Liu, X. Y.; Mironov, O.; Jones, C. J.; Ziatdinov, V. R. *J. Mol. Catal. A-Chem.* **2004**, *220*, 7.
- (9) Labinger, J. A. *J. Mol. Catal. A-Chem.* **2004**, *220*, 27.
- (10) Tenaglia, A.; Heumann, A. *Angew. Chem. Int. Ed.* **1999**, *38*, 2180.
- (11) Dyker, G. *Handbook of C-H Transformations*; Wiley-VCH: Weinheim, Germany, 2005.
- (12) Ritleng, V.; Sirlin, C.; Pfeffer, M. *Chem. Rev.* **2002**, *102*, 1731.
- (13) Feng, Y.; Lail, M.; Barakat, K. A.; Cundari, T. R.; Gunnoe, T. B.; Petersen, J. L. *J. Am. Chem. Soc.* **2005**, *127*, 14174.
- (14) Tenn, W. J.; Young, K. J. H.; Bhalla, G.; Oxgaard, J.; Goddard, W. A.; Periana, R. A. *J. Am. Chem. Soc.* **2005**, *127*, 14172.
- (15) Feng, Y.; Lail, M.; Foley, N. A.; Gunnoe, T. B.; Barakat, K. A.; Cundari, T. R.; Petersen, J. L. *J. Am. Chem. Soc.* **2006**, *128*, 7982.
- (16) Meier, S. K.; Young, K. J. H.; Ess, D. H.; Tenn, W. J.; Oxgaard, J.; Goddard, W. A.; Periana, R. A. *Organometallics* **2009**, *28*, 5293.
- (17) Young, K. J. H.; Oxgaard, J.; Ess, D. H.; Meier, S. K.; Stewart, T.; Goddard, I. I. W. A.; Periana, R. A. *Chemical Communications* **2009**, 3270.
- (18) Ahlquist, M.; Periana, R. A.; Goddard, W. A. *Chem. Commun.* **2009**, 2373.
- (19) Goldshleger, N. F.; Eskova, V. V.; Shilov, A. E.; Shteinman, A. A. *Russ. J. Phys. Chem.* **1972**, *46*, 785.
- (20) Goldshleger, N. F.; Tyabin, M. B.; Shilov, A. E.; Shteinman, A. A. *Russ. J. Phys. Chem.* **1969**, *43*, 1222.
- (21) Labinger, J. A.; Bercaw, J. E. In *Higher Oxidation State Organopalladium and Platinum Chemistry*; Canty, A. J., Ed.; Springer-Verlag Berlin: Berlin, 2011; Vol. 35, p 29.

- (22) Lin, M.; Shen, C.; Garcia-Zayas, E. A.; Sen, A. *J. Am. Chem. Soc.* **2001**, *123*, 1000.
- (23) Shilov, A. E. *Activation of Saturated Hydrocarbons by Transition Metal Complexes*; D. Reidel Publishing Company: Dordrecht, Holland, 1984.
- (24) Shilov, A. E.; Shteinman, A. A. *Coord. Chem. Rev.* **1977**, *24*, 97.
- (25) Shilov, A. E.; Shulpin, G. B. *Uspekhi Khimii* **1987**, *56*, 754.
- (26) Shilov, A. E.; Shul'pin, G. B. *Chem. Rev.* **1997**, *97*, 2879.
- (27) Shilov, A. E.; Shul'pin, G. B. *Activation and Catalytic Reactions of Saturated Hydrocarbons in the Presence of Metal Complexes*; Springer: Verlag, 2000.
- (28) Zamashchikov, V. V.; Kitaigorodskii, A. N.; Litvinenko, S. L.; Rudakov, E. S.; Uzhik, O. N.; Shilov, A. E. *Bulletin of the Academy of Sciences of the Ussr Division of Chemical Science* **1985**, *34*, 1582.
- (29) Janowicz, A. H.; Bergman, R. G. *J. Am. Chem. Soc.* **1982**, *104*, 352.
- (30) Tellers, D. M.; Yung, C. M.; Arndtsen, B. A.; Adamson, D. R.; Bergman, R. G. *J. Am. Chem. Soc.* **2002**, *124*, 1400.
- (31) Klei, S. R.; Golden, J. T.; Tilley, T. D.; Bergman, R. G. *J. Am. Chem. Soc.* **2002**, *124*, 2092.
- (32) Bengali, A. A.; Arndtsen, B. A.; Burger, P. M.; Schultz, R. H.; Weiller, B. H.; Kyle, K. R.; Moore, C. B.; Bergman, R. G. *Pure & Appl. Chem.* **1995**, *67*, 281.
- (33) Vetter, A. J.; Rieth, R. D.; Brennessel, W. W.; Jones, W. D. *J. Am. Chem. Soc.* **2009**, *131*, 10742.
- (34) Bergman, R. G. *Science* **1984**, *223*, 902.
- (35) Janowicz, A. H.; Bergman, R. G. *J. Am. Chem. Soc.* **1983**, *105*, 3929.
- (36) Arndtsen, B. A.; Bergman, R. G. *Science* **1995**, *270*, 1970.
- (37) Klei, S. R.; Golden, J. T.; Burger, P.; Bergman, R. G. *J. Mol. Catal. A* **2002**, *189*, 79.
- (38) Klei, S. R.; Tilley, T. D.; Bergman, R. G. *Organometallics* **2002**, *21*, 4905.
- (39) Yung, C. M.; Skaddan, M. B.; Bergman, R. G. *J. Am. Chem. Soc.* **2004**, *126*, 13033.
- (40) Corberán, R.; Sanaú, M.; Peris, E. *J. Am. Chem. Soc.* **2006**, *128*, 3974.
- (41) Tanabe, Y.; Hanasaka, F.; Fujita, K.-i.; Yamaguchi, R. *Organometallics* **2007**, *26*, 4618.

- (42) Viciano, M.; Feliz, M.; Corberán, R.; Mata, J. A.; Clot, E.; Peris, E. *Organometallics* **2007**, *26*, 5304.
- (43) Corberán, R.; Sanaú, M.; Peris, E. *Organometallics* **2006**, *25*, 4002.
- (44) Costa, A. P. d.; Viciano, M.; Sanaú, M.; Merino, S.; Tejada, J.; Peris, E.; Royo, B. *Organometallics* **2008**, *27*, 1305.
- (45) Feng, Y.; Jiang, B.; Boyle, P. A.; Ison, E. A. *Organometallics* **2010**, *29*, 2857.
- (46) Burger, P.; Bergman, R. G. *J. Am. Chem. Soc.* **1993**, *115*, 10462.
- (47) Klei, S. R.; Tilley, T. D.; Bergman, R. G. *J. Am. Chem. Soc.* **2000**, *122*, 1816.
- (48) Gilbert, T. M.; Bergman, R. G. *Organometallics* **1983**, *2*, 1458.
- (49) Alaimo, P. J.; Bergman, R. G. *Organometallics* **1999**, *18*, 2707.
- (50) Boutadla, Y.; Davies, D. L.; Macgregor, S. A.; Poblador-Bahamonde, A. I. *Dalton Transactions* **2009**, 5820.
- (51) Su, M.-D.; Chu, S.-Y. *J. Am. Chem. Soc.* **1997**, *119*, 5373.
- (52) Niu, S.; Hall, M. B. *J. Am. Chem. Soc.* **1998**, *120*, 6169.
- (53) Corkey, B. K.; Taw, F. L.; Bergman, R. G.; Brookhart, M. *Polyhedron* **2004**, *23*, 2943.
- (54) Boutadla, Y.; Davies, D. L.; Macgregor, S. A.; Poblador-Bahamonde, A. I. *Dalton Transactions* **2009**, 5887.
- (55) Davies, D. L.; Donald, S. M. A.; Al-Duaij, O.; Macgregor, S. A.; Pölleth, M. *Journal of the American Chemical Society* **2006**, *128*, 4210.
- (56) Davies, D. L.; Donald, S. M. A.; Macgregor, S. A. *Journal of the American Chemical Society* **2005**, *127*, 13754.
- (57) Lapointe, D.; Fagnou, K. *Chemistry Letters* **2010**, *39*, 1119.
- (58) Li, L.; Brennessel, W. W.; Jones, W. D. *J. Am. Chem. Soc.* **2008**, *130*, 12414.
- (59) Hickman, A. J.; Villalobos, J. M.; Sanford, M. S. *Organometallics* **2009**, *28*, 5316.
- (60) White, C.; Yates, A.; Maitlis, P. M.; Heinekey, D. M. In *Inorganic Syntheses*; John Wiley & Sons, Inc.: 2007, p 228.
- (61) Sala, A.; Ferrario, F.; Rizzi, E.; Catinella, S.; Traldi, P. *Rapid Commun. Mass Spectrom.* **1992**, *6*, 388.

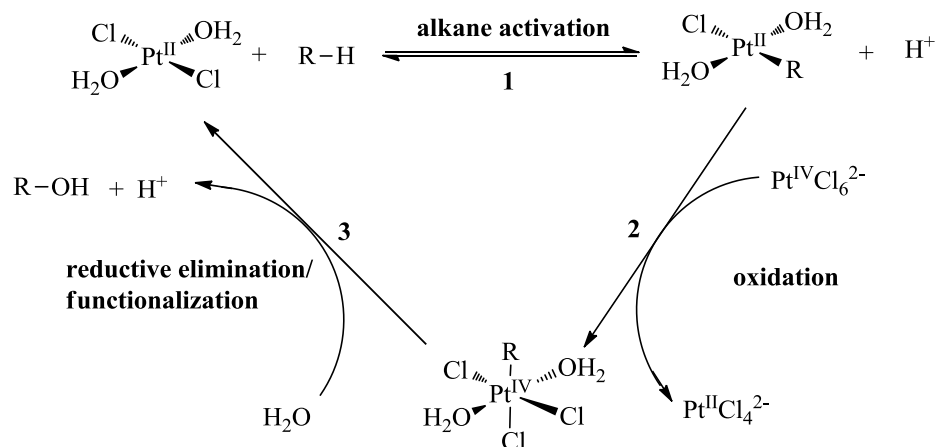
Chapter 4

Rh^I and Rh^{III} Complexes with Pyridinium Substituted Bipyridine Ligands

4.1 Background and Significance

A major focus of organometallic research involves the activation and functionalization of C–H bonds.¹⁻¹⁸ Given the original success of the Shilov system in C–H oxidation, catalysts based upon Pt and Pd has been a major focus (Scheme 4.1).¹⁹⁻²⁸ While tremendous strides have been made in this arena, these transformations typically require the use of strong, sometimes costly, or toxic oxidants (K₂Cr₂O₇, iodine(III)-based systems, K₂S₂O₈, *N*-halosuccinimides, oxygen, copper(II), or Oxone®).²⁹⁻³¹ Although Pt has been more effective in C–H activation, Pd has seen more extensive use in catalysis for functionalizing aromatic C–H bonds.^{30,32-35} The requirement for thermodynamically strong oxidants is related in the large potential required for Pd^{II}/Pd^{IV} redox couple while Pt is complicated by the low activity of Pt^{IV} complexes towards sp³ C–H bonds.⁷

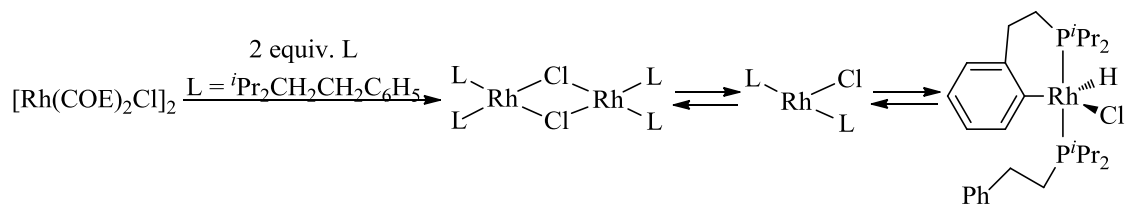
Scheme 4.1 Shilov Catalytic Cycle.



Catalysis via $\text{Rh}^{\text{I}}/\text{Rh}^{\text{III}}$ redox couples would be an interesting complement to the group 10 systems. Unlike most $\text{Pd}^{\text{II}}/\text{Pt}^{\text{II}}$ complexes, Rh^{I} complexes are kinetically reactive towards oxygen and other mild oxidants to generate high oxidation state species.³⁶ With the Shilov system, the use of a Pt^{IV} oxidant provides a significant drawback because of the expense of the oxidant. Substitution with other strong oxidants have proven to be very challenging due to the formation of Pt^{IV} which is not competent for alkane C–H activation.⁷

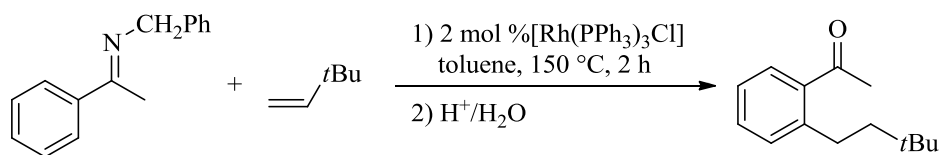
Simple modification of the catalytic cycle by substituting Rh^{I} for Pt^{II} would provide an isoelectronic catalyst system with the possibility to utilize air as an oxidant. In considering the possibilities of performing “Shilov” type chemistry at Rh centers, Rh complexes have been heavily studied in stoichiometric C–H activation reactions.³⁷⁻⁶¹ These studies have mainly focused on the activation of tethered C–H bonds of phosphine based ligands. The C–H activation results in the formation of cyclometallated complexes.³⁷⁻⁵² One representative example,³⁸ shown below in Scheme 4.2, illustrates this strategy in which the phosphine ligand contains a tethered aromatic ring, which results in the formation of a Rh^{III} -hydride species (Scheme 4.2).

Scheme 4.2 C–H Activation of Pendant Carbon Fragments.³⁸



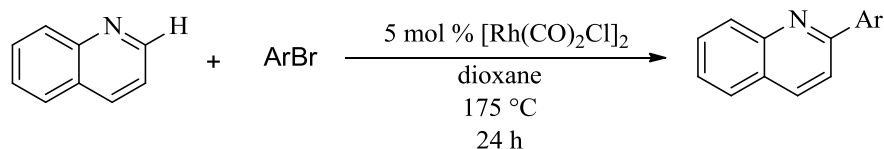
While C–H activation of pendant ligand groups in a directed fashion is well preceded, extensive studies have also provided significant evidence for the activation of C–H bonds in undirected substrates.⁵³⁻⁶¹ Rh complexes have also been shown to be active in H/D exchange reactions.⁶² Rh-catalyzed C–H functionalization has mainly focused on C–H activation of arenes followed by olefin or alkyne insertion steps to generate alkylated products.^{12,63-96} A representative example of this type of transformation is shown below in Scheme 4.3. These alkylation reactions use Rh^{I} -phosphine complexes as catalysts.

Scheme 4.3 Catalytic C–H Functionalization Through Olefin Insertion.⁷³



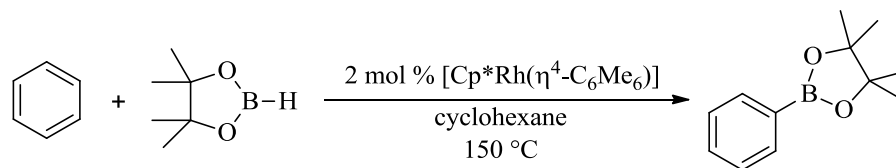
Similar activity has also been observed for biaryl coupling reactions. These reactions have also been observed to be catalyzed by low valent Rh complexes (Scheme 4.4).^{90,97-99}

Scheme 4.4 Rh Catalyzed Arylation Reactions.^{90,97-99}



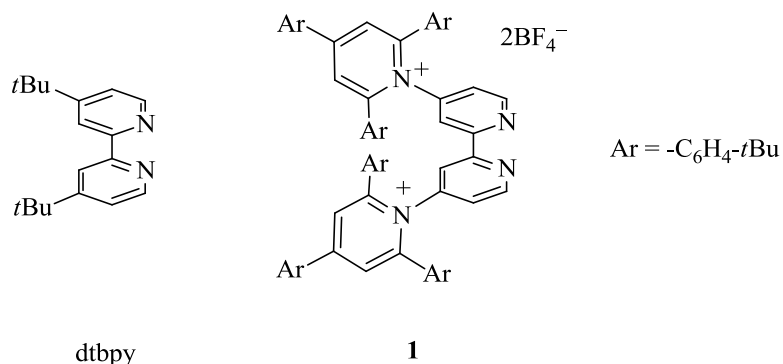
While C–C and C–H bond-forming reductive eliminations from Rh are well established, reductive eliminations to form C–X bonds (X = Cl, Br, I, F, O, B, and N) are much less common.¹⁰⁰⁻¹⁰⁶ The most successful example of this type of reaction is Rh-catalyzed C–H borylation reactions, in which Rh-promoted C–B coupling is a key step (Scheme 4.5).

Scheme 4.5 Rh-Catalyzed C–H Borylation.^{90,97-99}



While phosphines have been well established as ligands for Rh-based catalyst systems, phosphine ligands are often susceptible to oxidation in the presence of O₂ or other oxidants. Thus, we wanted to turn to ligands which are more stable towards oxidizing environments. Although reports with bipyridine systems have been scarce for catalysis, multiple Rh complexes of bipyridine-type ligands are known.¹⁰⁷⁻¹¹⁰ Herein, we describe our efforts to study these ligands for reactions relevant to C–H functionalization chemistry with *t*-butyl-bipyridine and our cationic bipyridine system described in Chapter 2 (Scheme 4.6).

Scheme 4.6 Bipyridine Ligands Studied.



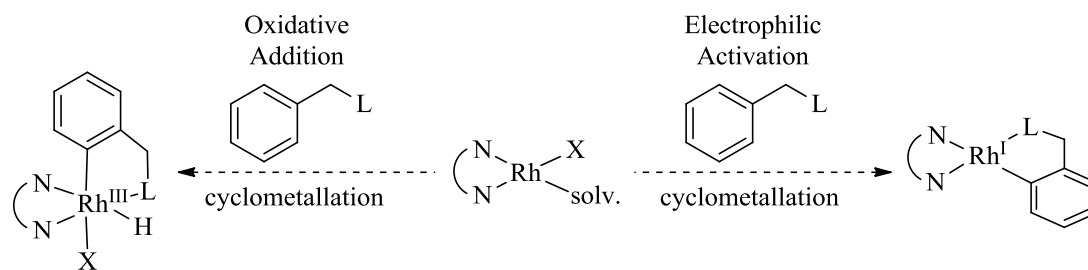
4.2 Results and Discussions

4.2.1 Computational Analysis – Competing Oxidative versus Electrophilic C–H

Activation

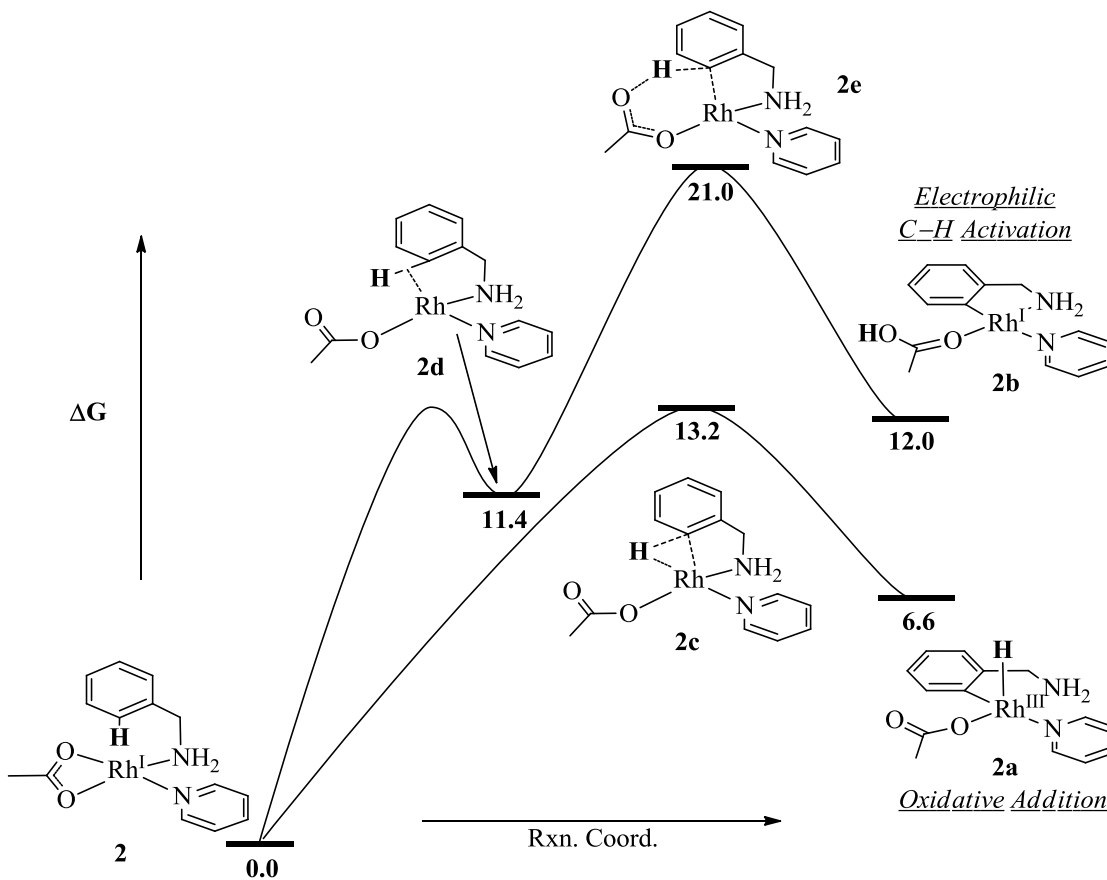
Traditional Rh^{I} complexes are known to activate C–H bonds through oxidative addition. Previously known systems to activate C–H bonds typically use phosphine based ligands. Given our success with cationic bipyridine ligands (Scheme 4.6), we first turned to computational studies to understand how nitrogen ligands affect C–H activation, especially electrophilic versus oxidative addition mechanisms for C–H activation. In order to maintain a two electron Shilov type catalytic system, electrophilic C–H activation would be key in the substitution of Rh^{I} for Pt^{II} as a catalyst. In an effort to substitute Rh complexes with the Shilov cycle (Scheme 4.1), we wanted to test the activity of our cationic ligands to activate C–H bonds and compare these results to a simple bipyridine ligand. We hypothesized that bipyridine ligands could promote C–H activation through the typical oxidative additional manifold, while our cationic based ligands might promote electrophilic C–H activation, which would be key in the substitution of Rh^{I} for Pt^{II} as a catalyst (Scheme 4.7).

Scheme 4.7 Oxidative versus Electrophilic C-H Activation.



To test this hypothesis, we turned to computational analysis to compare the relative activation energies and thermodynamics of electrophilic versus oxidative addition mechanisms for C-H activation. Using the model of acetate assisted C-H activation from Davies and Macgregor,¹¹¹⁻¹¹⁴ we modeled both pathways using density functional theory (DFT) for the cyclometallation of the model complex [Rh(py)(OAc)(L)] (L = benzylamine) (**2**). For these calculations, we used the B3LYP/CEP121-G(d,p) level of theory with gas phase calculations (see section 4.4.1 for complete details). The two pathways are outlined in Figure 4.1.

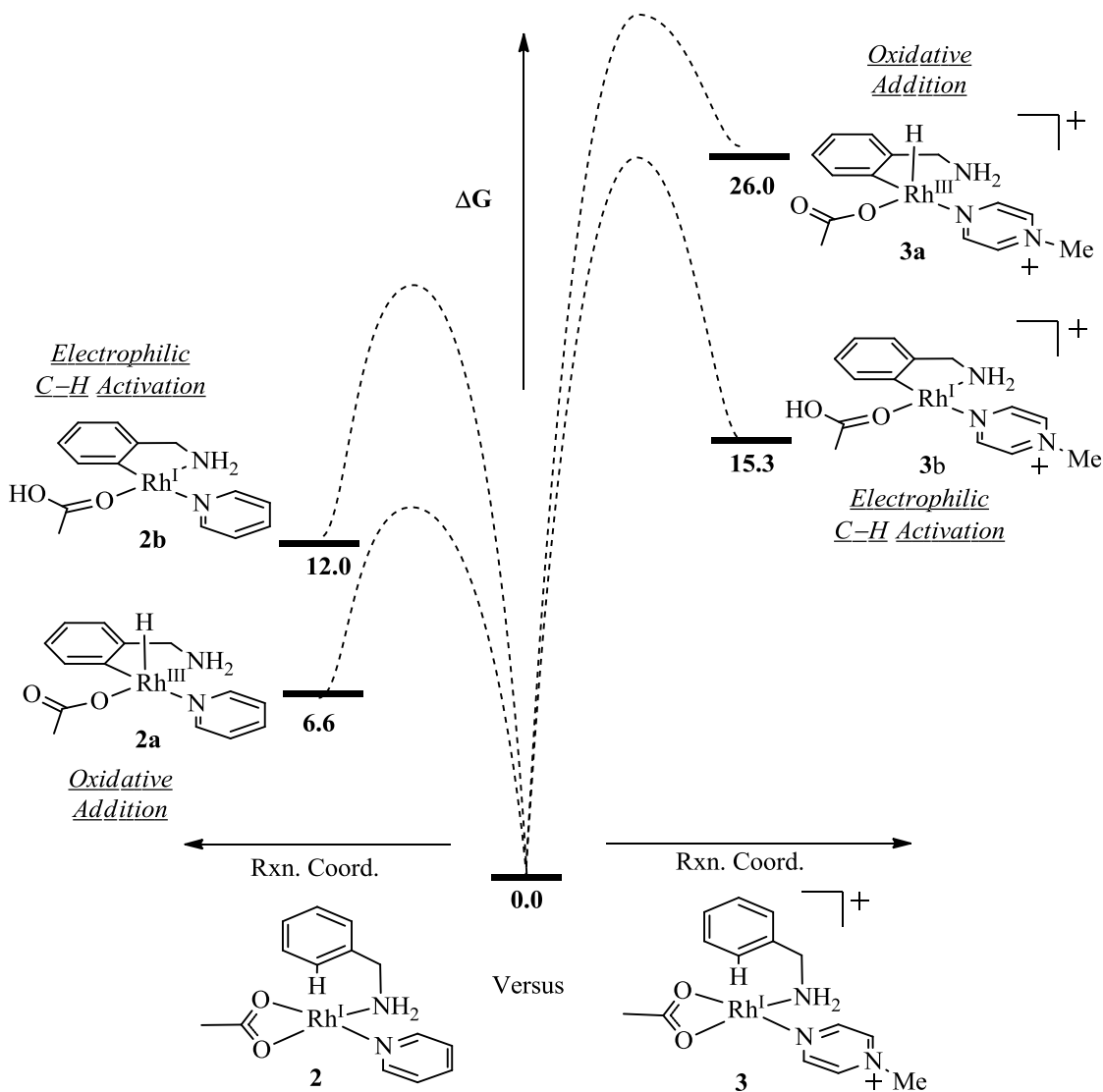
Figure 4.1 Oxidative versus Electrophilic C–H Activation.



Consistent with experimental observations with phosphine ligands, using a neutral ligand (pyridine), C–H activation is calculated to favor oxidative addition. The oxidative addition transition state has a gas phase Gibbs energy of 13.2 kcal/mol (Figure 4.1) and the overall reaction pathway to form a 5-coordinate Rh^{III} -hydride complex is thermodynamically uphill by 6.6 kcal/mol. In comparison, the electrophilic mechanistic pathway is calculated to have a reaction barrier of 21.0 kcal/mol and is thermodynamically uphill by 12.0 kcal/mol. Thus, the oxidative addition pathway is calculated to be kinetically favored by 7.8 kcal/mol and thermodynamically favored by 5.4 kcal/mol. With these results, we questioned how the addition of a cationic substituent would affect these relative energies. Given that the kinetics and thermodynamic

preference was very similar with pyridine, we modified the pyridine ligand by substituting it with an *N*-methylpyrazine ligand. With this model complex, we calculated the thermodynamics of C–H activation for an electrophilic and oxidative addition mechanism (Figure 4.2)

Figure 4.2 Oxidative versus Electrophilic C–H Activation.



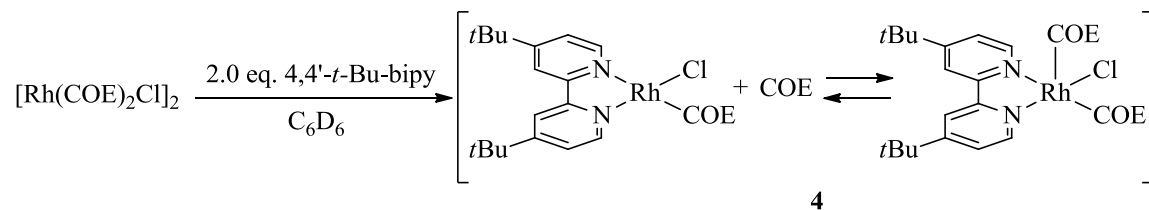
Comparing these model complexes (pyridine versus *N*-methylpyrazine), the calculated thermodynamics for C–H activation through an electrophilic pathway changes very little (~ 3 kcal/mol), while the oxidative addition pathway is destabilized by 19

kcal/mol with the substitution of *N*-methylpyrazine. Thus, these calculations suggest that the addition of electron withdrawing ligands preferentially affects the energy of an oxidative addition. These results indicate that ligands with cationic substituents could allow for a switch in C–H activation mechanisms, which would be key in using Rh^I as a catalyst. Also, the electrophilic C–H activation product is calculated to be a thermodynamically accessible intermediate.

4.2.2 Rh^I Complexes for C–H Activation Studies.

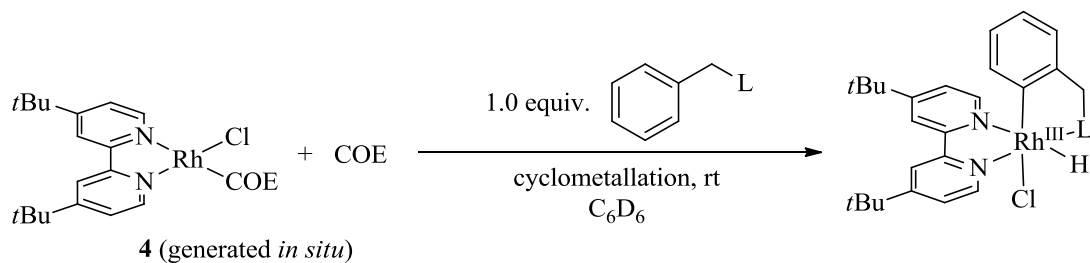
To test the computational results, we turned to synthesizing Rh^I complexes containing bipyridine and cationic bipyridine ligand (**1**) for experimental studies of C–H activation. While significant studies of stoichiometric C–H activation have been performed with Rh^I-phosphine complexes, relatively little study of bipyridine based ligands for C–H activation has been disclosed.¹¹⁰ First, we studied the reaction of a simple Rh^I olefin complex [Rh(COE)₂Cl]₂ (COE = cyclooctene) with 4,4'-*t*-butyl-2,2'-bipyridine (dtbpy). The addition of two equivalents of dtbpy to the Rh dimer in benzene result in an immediate color change from red/orange to a dark blue/black solution (Scheme 4.8).

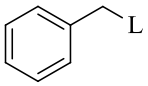
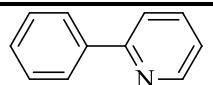
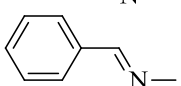
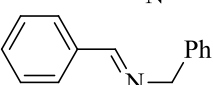
Scheme 4.8 Bipyridine Addition to [Rh(COE)₂Cl]₂.



The ¹H NMR spectra of this reaction showed quantitative conversion to one unsymmetrical bipyridine complex (**4**). While the bipyridine aromatic signals were quite

sharp, only one broad set of cyclooctene resonances was observed. This observation indicates that either the free and bound cyclooctene are undergoing exchange, or the complex exists as a 5-coordinate species in which both COE olefins are bound which could undergo fast geometric rearrangements. Related 5-coordinate species have been observed by Schrock previously in a Rh^I tricarbonyl complex with phosphine supporting ligands.¹¹⁵ Attempts at isolation of this Rh complex by solvent evaporation or precipitation resulted in decomposition to unidentified products. However, the complex was stable in solution and the addition of one equivalent of a ligand that can form a metallacycle cycle via directed C–H activation resulted in the formation of free cyclooctene and one new Rh containing product in good yields as determined by ¹H NMR spectroscopic analysis of the crude mixture (>90% yield in all cases) (Table 4.1). The formation of Rh^{III} hydride products are quite distinct by ¹H NMR given that Rh is an NMR active nuclei (I = ½, 100 % abundance) and this causes the metal hydride peak to have a characteristic chemical shift and appear as doublet. Chemical shifts of the hydride in the Rh-cyclometallated complexes are tabulated below in Table 4.1.

Table 4.1 C–H Activation with Cyclometallating Reagents.

	Hydride ^1H NMR Signal
	-14.95 ($^1J_{\text{Rh-H}}$ 24.5 Hz)
	-15.51 ($^1J_{\text{Rh-H}}$ 24.5 Hz)
	-15.71 ($^1J_{\text{Rh-H}}$ 24.5 Hz)

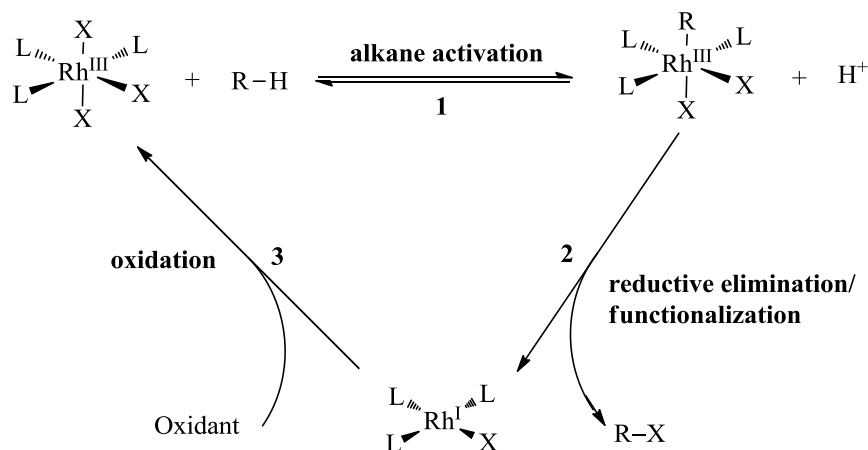
With this success in hand, we turned to analogous studies with our cationic bipyridine ligand **1**. Surprisingly, **1** did not react with the $[\text{Rh}(\text{COE})_2\text{Cl}]_2$ dimer in benzene. Changing the solvent to CDCl_3 resulted in the formation of a variety of Rh-containing products, which were not isolated. Thus, we were unable to form comparable Rh^{I} complexes for C–H activation studies with **1**. Analogous reactions were performed using the more soluble $[\text{Rh}(\text{COD})\text{Cl}]_2$ but did not prove successful in achieving complexes which were viable for comparative C–H activation studies.

4.2.3 Rh^{III} Complexes for C–H Activation Studies.

With generation of Rh^{I} complexes of our cationic ligand proving problematic, we next turned to the synthesis of Rh^{III} complexes for ligand comparisons, given that an alternative catalytic cycle could be proposed with slight modifications (Scheme 4.9). We envisioned that a simple rearrangement of the mechanistic steps would still allow for a

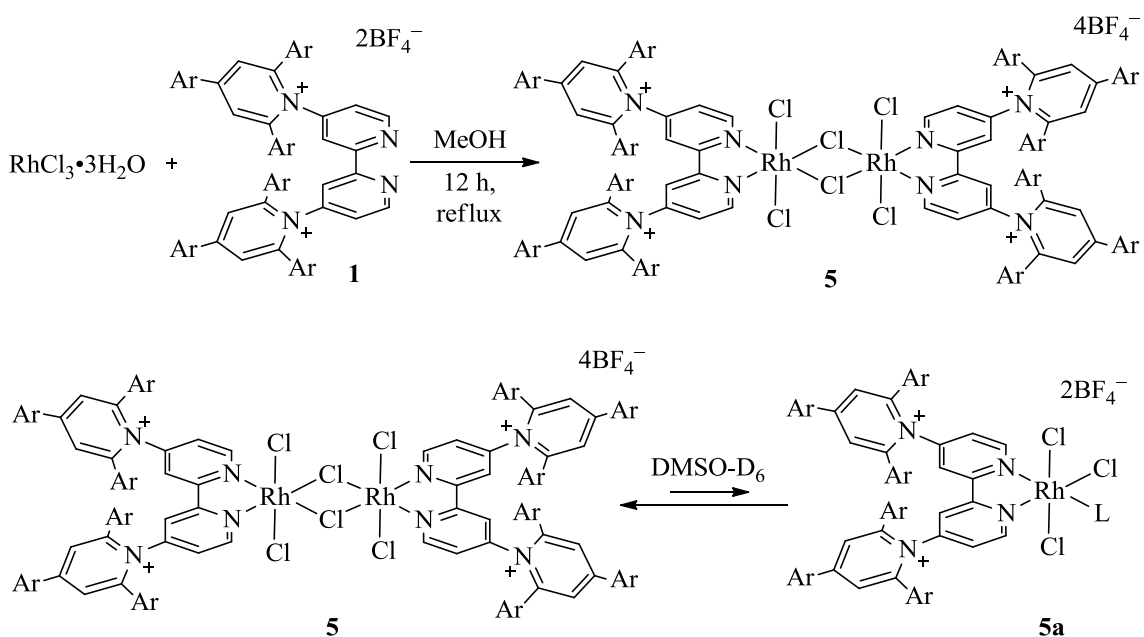
potential catalytic cycle. The only change involves a Rh^{III} complex performing electrophilic C–H activation versus a Rh^{I} complex (rearranging steps **1** and **2**-Scheme 4.1). This C–H activation step has precedent, as a Rh^{III} pincer complex has been reported to activate aromatic C–H bonds to form stable Rh^{III} -aryl species.¹¹⁶

Scheme 4.9 Rh^{III} -based Shilov Catalytic Cycle.



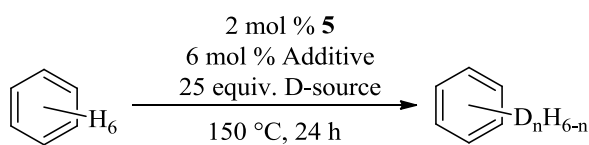
With the goal of synthesizing Rh^{III} complexes containing **1**, we refluxed a methanol solution of rhodium trichloride hydrate with **1** for 12 hours, which resulted in the formation of a precipitate. The product (**5**) was collected by filtration of the cooled reaction mixture (Scheme 4.10). Analysis of this complex is complicated by the fact that it is only soluble in highly polar solvents such as dimethyl sulfoxide (DMSO). The complex was observed to be primarily in the dimeric state in solution **5** but also shows an associated unsymmetrical ligand monomer (**5a**) in the ^1H NMR spectrum in $\text{DMSO-}D_6$ (Scheme 4.11). The monomer **5** versus dimer **5a** was assigned based upon the asymmetry observed in the ^1H NMR of the dimer **5a**.

Scheme 4.10 Rh^{III} Complex Synthesis.



With this Rh^{III} complex in hand, we wanted to test the activity of this complex for C–H activation by an H/D exchange assay. Using standard conditions, we examined **5**-catalyzed H/D exchange of benzene with a variety of deuterium sources (Table 4.2).

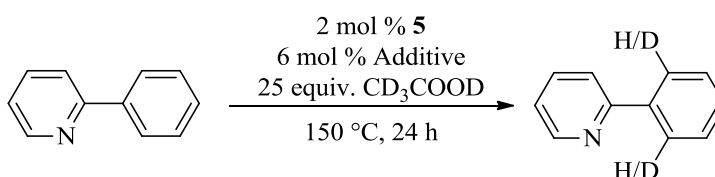
Table 4.2 Benzene H/D Exchange in Various Solvents.



D-Source	Additive	TON
CD ₃ COOD	None	1
CD ₃ COOD	AgOAc	41
CD ₃ OD	None	0
CD ₃ OD	AgOAc	0
D ₂ O	AgOAc	0

Similar to our results in Chapter 3, acetic acid is an effective deuterium source for H/D exchange. Silver acetate is required to achieve significant turnovers. Methanol-D₄ or D₂O does not serve as an effective deuterium source for catalytic activity. We also evaluated complex **5** for the C–H activation of a directed substrate (2-phenylpyridine) through H/D exchange (Table 4.3).

Table 4.3 H/D Exchange of 2-Phenylpyridine.



D-Source	Additive	TON
CD ₃ COOD	None	14
CD ₃ COOD	AgOAc	38
CD ₃ OD	None	0
CD ₃ OD	AgOAc	0
D ₂ O	AgOAc	0

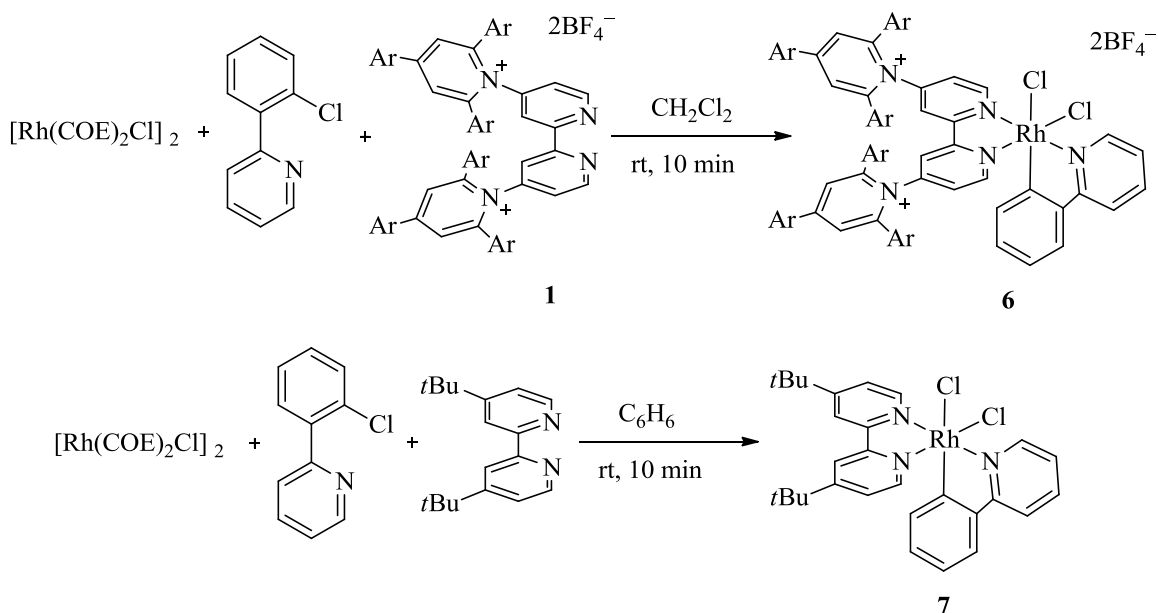
With a directed substrate, the addition of silver acetate as an additive is less important when compared to using benzene as a substrate. This result is evident by the 14 versus 1 turnover observed for H/D exchange with the two substrates. Analogous synthesis to Scheme 4.11 was attempted using dtbpy. A similar chloride bridge dimer was not obtained although a complex of the form [Rh(bpy)₂Cl₂]Cl¹⁰⁸ was observed, but given this complex possesses two bipyridine ligands per rhodium and has a coordination

environment different from **5**, these complexes were not pursued for H/D exchange studies for comparisons to **5**.

4.2.4 Rh^{III} Cyclometallated Complexes with **1** and dtbpy.

With our success in directed C–H activation with 2-phenylpyridine, we wanted to synthesize potential Rh^{III} cyclometallated complexes with both **1** and dtbpy ligands containing 2-phenylpyridine for comparison. The addition of 2 equivalents of **1** to $[Rh(COE)_2Cl]_2$ followed by addition of 2-(2-chlorophenyl)pyridine in methylene chloride resulted in the formation of **6** in 82% yield (Scheme 4.11). Importantly, a side reaction is observed if the aryl chloride is not added within a few minutes. This side reaction appears to involve the halogenated solvent, but the products were not determined. Analogous reactions can be performed with dtbpy with the addition of 2 equivalents of dtbpy to $[Rh(COE)_2Cl]_2$ in benzene followed by the addition 2-(2-chlorophenyl)pyridine to afford **7** in 89% yield. Interestingly, these complexes were found to be highly stable in acetic acid- D_4 for prolonged heating up to 130 °C.

Scheme 4.11 Rh^{III} Cyclometallated Complex Synthesis.

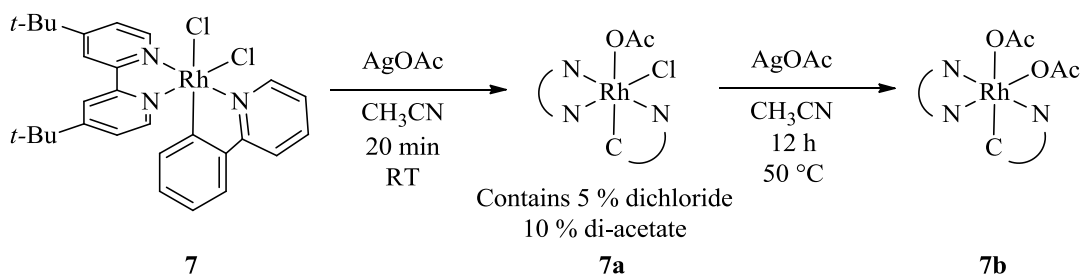


We first tested simple halide abstraction reactions. Upon the addition of 3 equivalents of AgOAc to **7** in acetonitrile at 50 °C overnight, we observed the formation of $[\text{Rh}(\text{dtbpy})(\text{phpy})(\text{OAc})_2]$ (**7b**) which was isolated by filtration of the silver chloride by-product (Scheme 4.13). Interestingly, one of the acetate resonances is very broad in the ^1H NMR spectrum, suggesting that the acetate trans to the aryl substituent is labile and fluxional on the NMR time scale. Consistent with this interpretation, ^{13}C NMR spectroscopic analysis at room temperature shows only one acetate resonance. ^{13}C NMR spectroscopic analysis at 50 °C showed a second broad acetate signal.

Lowering the temperature of the reaction to room temperature, shortening the reaction time to 20 minutes, and the use of 1.1 equivalents of silver acetate allowed for the observation of a mono-acetate species (**7a**), although the second halide abstraction reaction is competitive. Thus, **7**, **7a**, and **7b** are all observed in the isolated product

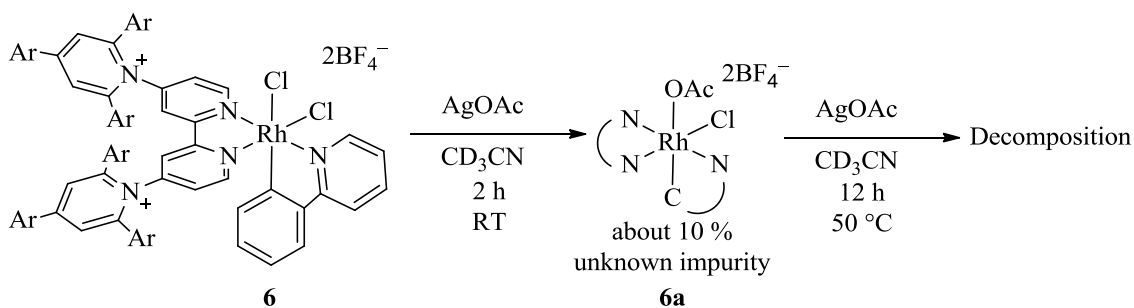
mixture although the mono-acetate complex can clearly be identified by ^1H NMR, and is formed in ~85% purity (Scheme 4.12).

Scheme 4.12 Halide Abstraction Reactions with **7**.



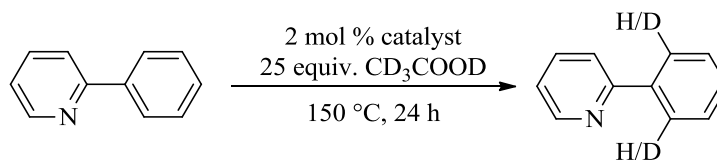
When analogous reactions were performed using **6**, the addition of 3 equivalents of silver acetate at 50 °C resulted in decomposition of the Rh complex. However, the addition of 1.1 equivalents of silver acetate at room temperature allowed for the observation of a mono-acetate complex by ^1H NMR spectroscopy (Scheme 4.13).

Scheme 4.13. Halide Abstraction Reactions with **6**.



With a comparative series of cyclometallated complexes, we evaluated these complexes for C–H activation of 2-phenylpyridine through H/D exchange in acetic acid- D_4 . Data for these reactions are displayed below in Table 4.4.

Table 4.4 Cyclometallated Complexes for 2-Phenylpyridine H/D Exchange.



Catalyst	TON
6	16
7	8
7b	33

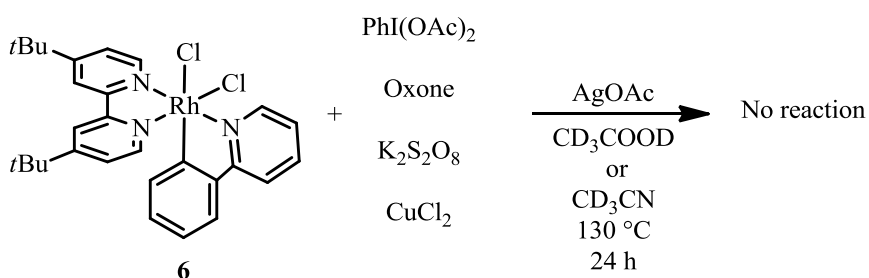
Interestingly, the isolated cyclometallated complex **6** compares quite nicely in H/D exchange activity in acetic acid-D₄ with **5** (16 versus 14 turnovers). This result indicates that this cyclometallated species (**6**) is a likely an intermediate in the catalytic H/D exchange reaction. This is an important observation given that we were not able to isolate a simple chloride bridged Rh^{III} complex with dtbpy for comparison to **5**. Since the cyclometallation complex **6** appears to be a viable intermediate in H/D exchange, one can compare the activity of **6** and **7**. The comparison indicates that the cationic ligand **1** provides a beneficial effect in C–H activation and results in a complex twice as active for C–H activation in comparison to dtbpy.

4.2.5 Attempts at Functionalization of Rh^{III}-Alkyl Bonds Through Reductive Elimination or Olefin/Alkyne Insertion.

With the synthesis of the cyclometallated complex **6** and **7** and halide abstraction reaction activity known, we wanted to analyze the complexes for both reductive elimination and reactivity towards insertion of alkenes or alkynes. First, we examined the thermal stability of these complexes and observed that **6** and **7** are stable for days

upon prolonged heating at 130 °C in acetic acid-D₄. No evidence for reductive elimination was detected under thermal conditions in the absence of oxidant or additives (Scheme 4.14). We also examined these complexes for oxidatively induced reductive elimination. We added a variety of oxidants (PhI(OAc)₂, Oxone®, K₂S₂O₈, and CuCl₂) to solutions of complexes **5** and **6** in acetic acid-D₄ (Scheme 4.14). With or without the addition of silver acetate, no organic reductive elimination products (aryl chlorides or acetates) were observed by ¹H NMR or GCMS analysis even after prolonged heating up to 130 °C.

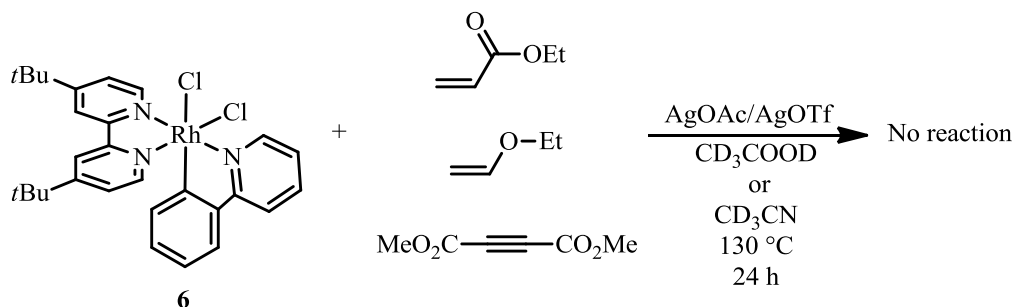
Scheme 4.14 Attempts at Oxidatively-Induced Reductive Elimination Studies with **7**.



Additionally, reactions of **6** and **7** with olefins (ethyl acrylate and ethyl vinyl ether) and with an electron deficient alkyne (dimethyl acetylenedicarboxylate) were heated to 130 °C in acetic acid-D₄ and acetonitrile-D₃ and monitored by ¹H NMR spectroscopy (Scheme 4.15). None of these reactions indicated the formation of an insertion product into the Rh-aryl bond. The reactions were repeated with the addition of two equivalent of either AgOAc or AgOTf. Again in these reactions, no evidence for insertion products was observed. The lack of reactivity towards olefin or alkyne insertion is likely a function of the low ligand lability in these systems. In both **6** and **7**, the chloride trans to the aryl moiety is much more labile and would likely be the site of olefin

or alkyne binding. From this geometry, insertion is not possible due to the requirement for the ligands to adopt a cis-orientation for reactivity.

Scheme 4.15 Attempts at Olefin or Alkyne into Rh–Aryl Bonds.



4.3 Conclusions

Rh complexes have been heavily studied for C–H activation using phosphine ligands. The use of nitrogen-based ligands has been much less explored. Computational studies indicated that Rh complexes containing cationic pyridinium substituents on bipyridine ligands could change the C–H activation mechanism to favor an electrophilic pathway, opposite to the oxidative addition process typically observed at Rh^I. We have shown that Rh^I-bipyridine species provide viable complexes for C–H activation. Analogous complexes of the cationic bipyridine ligand **1** could not be synthesized. Alternatively, we have explored the use of these bipyridine ligands for Rh^{III} complexes. These studies have shown that ligand **1** has a beneficial effect on C–H activation, as complex **6** is twice as active for H/D exchange when compared to **7** using 2-phenylpyridine as a substrate. Complexes **6** and **7** show that ligand **1** has a dramatic effect on the lability of X-type ligands in these complexes. Limited reactivity towards reductive elimination and olefin insertion is likely a function of multiple bidentate ligands stabilizing the Rh^{III} center. Moving forward, the use of the monodentate pyridinium

ligands highlighted in Chapter 2 could provide a viable alternative to expand functionalization reactions while maintaining increased activity for C–H activation.

4.4 Experimental Procedures

4.4.1 Computational Methods

Using the Gaussian 03 suite of programs,¹¹⁷ all density functional theory (DFT) calculations were performed with the B3LYP functional¹¹⁸⁻¹²⁰ along with the Stevens (CEP-121G)^{121,122} valence basis sets with effective core potentials. The CEP-121G basis sets are triple- ξ for Rh and triple- ξ for all main group elements. A polarization function (see 6-311G**++)^{123,124} was added to all elements: $\xi_d = 0.8$ for oxygen, $\xi_d = 0.913$ for nitrogen, $\xi_d = 0.626$ for carbon, $\xi_p = 0.8$ for hydrogen, and $\xi_f = 1.350$ for rhodium¹²⁵ along with a diffuse function for all atoms except Rh: $\xi_{sp} = 0.1.292$ for oxygen, $\xi_d = 0.0639$ for nitrogen, $\xi_d = 0.0438$ for carbon, and $\xi_s = 0.036$ for hydrogen (referred to as CEP-121G(d,p)++ level of theory). All geometries were optimized using B3LYP/CEP-121G(d,p)++ without symmetry constraints using the restricted Kohn-Sham formalism for all complexes. All minima were confirmed by the absence of imaginary frequencies and all transition states were verified by visual inspection of the single imaginary frequency vibration along with optimization along the potential energy surface to confirm associated minimum structures. Thermochemical data was calculated using unscaled vibrational frequencies and default parameters at 298.15 K and 1 atm.

4.4.2 Instrumentation

NMR spectra were recorded on Varian Inova 500, Varian vnmrs 500 MHz, Varian MR400 400 MHz, or Varian vnmrs 700 MHz NMR spectrometers with the

residual solvent peak (methanol-D₄: ¹H: δ=4.78, 3.30 ppm, ¹³C: δ=49.0 ppm; AcOH-D₄: ¹H: δ=11.53, 2.03 ppm, ¹³C: δ=178.4, 20.0 ppm; acetonitrile-D₃: ¹H: δ=1.94 ppm, ¹³C: δ=118.2, 1.3 ppm; benzene-D₆: ¹H: δ=7.15 ppm, ¹³C: δ=128.0 ppm; chloroform-D₁; DMSO-D₆: ¹H: δ=2.49 ppm) as the internal reference unless otherwise noted. ¹⁹F NMR is referenced to the residual solvent signal in the ¹H NMR. Chemical shifts are reported in parts per million (ppm) (δ). Multiplicities are reported as follows: br (broad resonance), s (singlet), d (doublet), t (triplet), q (quartet), m (multiplet). Coupling constants (*J*) are reported in Hz. Elemental analyses were performed by Atlantic Microlab, Inc., Norcross, Georgia. High-res mass spectrometry was performed on an Agilent Q-TOF HPLC-MS.

4.4.3 Materials and Methods

All reactions were conducted without rigorous exclusion of air and moisture unless noted otherwise. AcOH-d₄ was purchased from Cambridge Isotopes Lab and stored in Schlenk tubes under N₂. Acetonitrile-d₃, CD₃COOD, CD₃OD, CDCl₃, DMSO-D₆, and D₂O were purchased from Cambridge Isotopes Lab and used as received. Dichloromethane, acetonitrile, methanol, and pentane were obtained from Fisher Scientific or Aldrich and used as received. Benzene for H/D exchange was obtained from Aldrich and stored over 4 Å molecular sieves. Bromobenzene, nitrobenzene, silver triflate, copper(II) chloride, cyclooctene, potassium persulfate, and 1,5-cyclooctadiene were purchased from Acros Organics. K₂CO₃ was purchased from Fisher Scientific. 4-*t*-butylpyridine was purchased from TCI America. RhCl₃ hydrate and IrCl₃ hydrate were purchased from Pressure Chemical Company. Iodosobenzene diacetate (PhI(OAc)₂), silver acetate, *N*-benzylidenemethylamine, and 2-phenylpyridine were obtained from Alfa Aesar. 4,4'-di-*t*-butyl-2,2'-bipyridine, ethyl acrylate, ethyl vinyl ether, dimethyl

acetylenedicarboxylate, *N*-benzylidenebenzylamine, Oxone®, and 1,1,2-trichloroethane were purchased from Aldrich. **1**,¹²⁶ 2-(2-chlorophenyl)-pyridine,¹²⁷ $[\text{Rh}(\text{COE})_2\text{Cl}]_2$,¹²⁸ and $[\text{Rh}(\text{COD})\text{Cl}]_2$ ¹²⁹ were prepared according to literature procedures. All liquid reagents were dispensed by difference using gas-tight Hamilton syringes.

4.4.4 Synthesis

$[\text{Rh}(\text{dtbpy})(\text{COE})_2\text{Cl}]$ (**4**)

dtbpy (7.4 mg, 0.0279 mmol, 2.00 equiv.) was dissolved in C_6D_6 (0.75 mL) and added to $[\text{Rh}((\text{COE})_2\text{Cl})_2]$ (10.0 mg, 0.0139 mmol, 1.00 equiv.). After 5 minutes at room temperature, ^1H NMR indicated the formation $[\text{Rh}(\text{dtbpy})(\text{COE})_2\text{Cl}]$ quantitatively. Product decomposes upon isolation but is stable for days in solution. ^1H NMR (C_6D_6 , 499.90 MHz): δ 9.97 (d, $J = 6.0$ Hz, 1H), 7.53 (d, $J = 1.7$ Hz, 1H), 7.34 (d, $J = 2.0$ Hz, 1H), 7.10 (d, $J = 5.9$ Hz, 1H), 6.80 (dd, $J = 5.9$ Hz, $J = 1.6$ Hz, 1H), 6.30 (dd, $J = 6.0$ Hz, 1.7 Hz, 1H), 4.93 (br, 4H), 2.50 (br, 8 H), 1.00 (s, 9H), 0.98 (s, 9H).

$[\text{Rh}(\mathbf{1})\text{Cl}_3]_2$ (**5**)

$\text{RhCl}_3 \cdot 3\text{H}_2\text{O}$ (25.0 mg, 94.9 μmol , 1.00 equiv) and **1** (121.5 mg, 94.9 μmol , 1.00 equiv) were added to a 20 mL screw cap Teflon sealed vial. Methanol (4 mL) was added and the reaction was heated to 80 °C for 2 hours. The resulting yellow precipitate was collected by vacuum filtration and washed with diethyl ether (2 x 5 mL) to yield 90.1 mg of product (64% yield). ^1H NMR ($\text{DMSO}-\text{D}_6$, 499.90 MHz): δ 9.47 (d, $J = 6.4$ Hz, 4H), 8.37 (s, 8H), 8.49 (d, $J = 1.9$ Hz, 4H), 8.38 (d, $J = 8.6$ Hz, 8H), 7.77 (dd, $J = 6.1$ Hz, 1.9 Hz, 4H), 7.69 (d, $J = 8.6$ Hz, 8H), 7.40 (d, $J = 8.8$ Hz, 16H), 7.35 (d, $J = 8.8$ Hz, 16H), 1.36 (s, 36H), 1.20 (s, 72H). ^{19}F NMR ($\text{DMSO}-\text{D}_6$, 376.836 MHz): δ -148.2 (^{10}B), -148.3

(¹¹B). ¹H NMR contains solvent broken up dimer [Rh(**1**)LCI₃] with water or solvent. This monomer/dimer mixture precludes ¹³C NMR analysis. HRMS electrospray (m/z): [M-BF₄]⁺ calcd. for [RhCl₃C₈₀H₉₀ON₄BF₄]⁺ 1417.5259; found 1417.5255.

[Rh(**1**)(Phpy)Cl₂] (**6**)

In a nitrogen filled glove box, **1** (356.6 mg, 0.279 mmol, 1.96 equiv.) was dissolved in of dry methylene chloride (10 mL) and added to [Rh(COE)₂Cl]₂ (102.0 mg, 0.142 mmol, 1.00 equiv.). The solution was stirred for 1 minute resulting in a dark orange solution. 2-(2-chlorophenyl)-pyridine (59.2 mg, 0.310 mmol, 2.18 equiv.) was added by syringe and stirred for 1 hour. In air, pentane (40 mL) was added and the resulting yellow precipitate was collected by filtration and washed with pentane (2 x 10 mL). The product was dried in vacuo to yield 341.2 mg (82% yield). ¹H NMR (CD₃CN, 499.904 MHz): δ 9.69 (d, J = 5.9 Hz, 1H), 9.50 (d, J = 6.2 Hz, 1H), 8.53 (d, J = 2.3 Hz, 1H), 8.50 (d, J = 2.0 Hz, 1H), 8.47 (d, J = 2.0 Hz, 1H), 8.39 (d, J = 2.1 Hz, 1H), 8.15 (m, 2H), 8.08 (m, 2H), 7.99 (m, 2H), 7.94 (d, J = 2.1 Hz, 1H), 7.81 (d, J = 2.3 Hz, 1H), 7.74 (m, 3H), 7.69 (m, 2H), 7.57 (dd, J = 6.2 Hz, 2.1 Hz, 1H), 7.52 (m, 2H), 7.45 (m, 2H), 7.41 (m, 4H), 7.35 (m, 1H), 7.31 (m, 2H), 7.08 (m, 8H), 6.90 (td, J = 6.0 Hz, 2.3 Hz, 1H), 6.85 (dd, J = 6.2 Hz, 2.3 Hz, 1H), 5.90 (d, J = 7.8 Hz, 1H), 1.39 (s, 9H), 1.37 (s, 9H), 1.32 (s, 9H), 1.31 (s, 9H), 1.29 (s, 9H), 1.15 (s, 9H). ¹³C NMR (CD₃CN, 175.974 MHz): δ 165.55, 164.36 (d, J = 28 Hz), 159.15, 159.13, 158.67, 158.66, 157.68, 157.47, 157.22, 157.20, 156.99, 156.97, 156.21, 155.97, 155.93, 155.89, 154.40, 153.63, 152.05, 150.10, 149.67, 145.25, 140.64, 132.58, 132.11, 132.02, 131.50, 131.37, 131.16, 131.06, 131.04, 130.66, 130.22, 130.18, 130.13, 130.08, 129.95, 128.55, 128.38, 128.35, 127.92, 127.54, 127.11, 126.93, 126.84,

126.76, 126.64, 126.46, 126.34, 125.42, 124.58, 124.52, 124.10, 121.27, 36.31, 36.28, 36.14, 36.12, 36.09, 35.93, 31.98, 31.92 (2 carbons), 31.82, 31.64, 31.61 (1 aryl carbon overlapping). ^{19}F NMR (CD_3CN , 376.836 MHz): δ -151.6 (^{10}B), -151.7 (^{11}B). HRMS electrospray (m/z): $[\text{M}-\text{BF}_4]^+$ calcd. for $[\text{RhCl}_2\text{C}_{91}\text{H}_{96}\text{N}_5\text{BF}_4]^+$ 1518.6127; found 1518.6158.

$[\text{Rh}(\text{dtbpy})(\text{phpy})\text{Cl}_2]$ (**7**)

In a nitrogen filled glove box, 4,4'-di-*t*-butyl-2,2'-bipyridine (190.0 mg, 0.708 mmol, 2.03 equiv.) was dissolved in of dry benzene (10 mL) and added to $[\text{Rh}(\text{COE})_2\text{Cl}]_2$ (250.0 mg, 0.348 mmol, 1.00 equiv.). The solution was stirred for 5 minutes resulting in a dark blue solution. 2-(2-chlorophenyl)-pyridine (146.1 mg, 0.766 mmol, 2.20 equiv.) was added by syringe and stirred for 1 hour to yield a cloudy pale yellow precipitate. In air, pentane (40 mL) was added and the resulting yellow precipitate was collecting by filtration and washed with pentane (2 x 10 mL). The product was dried in vacuo to yield 370.9 mg (89% yield). ^1H NMR (CD_3CN , 699.765 MHz): δ 9.97 (m, 1H), 9.59 (m, 1H), 8.41 (d, $J = 2.0$ Hz, 1H), 8.28 (d, $J = 2.1$, 1H), 8.09 (m, 1H), 8.05 (td, $J = 8.2$ Hz, 1.7 Hz, 1H), 8.84 (dd, $J = 6.2$ Hz, 2.1 Hz, 1H), 7.78 (dd, $J = 7.5$ Hz, 1.4 Hz, 1H), 7.49 (m, 1H), 7.29 (m, 1H), 7.24 (dd, $J = 6.2$ Hz, 2.0 Hz), 6.99 (td, $J = 7.3$ Hz, 1.0 Hz, 1H), 6.87 (td, $J = 7.5$ Hz, 1.4 Hz, 1H), 6.26 (d, $J = 7.9$ Hz, 1H), 1.52 (s, 9H), 1.31 (s, 9H). ^{13}C NMR (CD_3CN , 175.974 MHz): δ 165.32, 165.95 (d, $J = 21.1$ Hz), 164.66, 164.27, 156.67, 156.60, 153.06, 151.73, 149.72, 145.06, 139.69, 133.50, 130.66, 125.37, 125.33, 124.95, 124.39, 124.05, 121.84, 121.74, 120.56, 36.42, 36.19, 30.43, 30.14. HRMS electrospray

(m/z): [M-Cl]⁺ calcd. for [RhClC₂₉H₃₂N₃]⁺ 560.1334; found 560.1335. Anal. calcd. for C₄₀H₄₅N₂BF₄: C, 58.40; H, 5.41; N, 7.05. Found: C, 58.21; H, 5.56; N, 6.97.

[Rh(dtbpv)(phpy)(OAc)₂] (**7b**)

In air, [Rh(bpy)(Phpy)Cl₂] (75.0 mg, 0.126 mmol, 1.00 eq.) was dissolved in acetonitrile (8 mL) and added to AgOAc (63.0 mg, 0.377 mmol, 3.00 eq.). After stirring for 12 hours at 50 °C, the suspension was passed through a pad of celite and washed with acetonitrile (5 mL). Solvent was removed by vacuum resulting in pale yellow powder, 65.0 mg (80.3 % yield). ¹H NMR (CD₃CN, 699.765 MHz): δ 9.51 (d, J = 5.5 Hz, 1H), 9.22 (d, J = 5.9 Hz, 1H), 8.36 (d, J = 1.5 Hz, 1H), 8.19 (d, J = 1.6 Hz, 1H), 8.01 (m, 2H), 7.85 (dd, J = 6.0 Hz, 2.1 Hz, 1H), 7.70 (dd, J = 6.0 Hz, 2.1 Hz, 1H), 7.44 (td, J = 6.7 Hz, 2.3 Hz, 1H), 7.14 (m, 2H), 6.94 (m, 1H), 6.80 (td, J = 7.7 Hz, 1.3 Hz, 1H), 6.13 (d, J = 7.7 Hz, 1H), 1.69 (br, 3H), 1.65 (s, 3H), 1.52 (s, 9H), 1.29 (s, 9H). ¹³C NMR (CD₃CN, 50 °C, 175.974 MHz): δ 176.78, 176.52 (br), 166.40, 165.12, 164.49 (d, J = 29.9 Hz), 164.24, 158.18, 157.55, 152.76, 152.72, 150.36, 150.21, 146.62, 139.61, 134.14, 130.12, 124.82, 124.74, 124.41, 124.37, 123.26, 121.08, 119.90, 36.64, 36.30, 30.80, 30.47, 24.96, 24.60 (br). HRMS electrospray (m/z): [M-OAc]⁺ calcd. for [RhC₃₁H₃₅N₃O₂]⁺ 584.1779; found 584.1785.

[Rh(dtbpv)(Phpy)(OAc)Cl] (**7a**)

In air, [Rh(bpy)(Phpy)Cl₂] (75.0 mg, 0.126 mmol, 1.00 equiv.) was dissolved in acetonitrile (8 mL) and added to AgOAc (23.1 mg, 0.138 mmol, 1.10 equiv.). After stirring for 15 minutes at room temperature, the suspension was passed through a pad of

celite and washed with acetonitrile (5 mL). Solvent was removed by vacuum resulting in a pale yellow solid, 58.2 mg (74 % yield). Product is impure containing **6** (~5%) and **6b** (~10%). ^1H NMR (CD_3CN , 699.765 MHz): δ 9.60 (d, $J = 6.0$ Hz, 1H), 9.51 (d, $J = 5.5$ Hz, 1H), 8.34 (d, $J = 1.7$ Hz, 1H), 8.19 (d, $J = 1.7$ Hz, 1H), 8.06 (m, 2H), 7.79 (dd, $J = 6.1$ Hz, 1.9 Hz, 1H), 7.75 (d, $J = 8.8$ Hz, 1H), 7.51 (m, 1H), 7.30 (d, $J = 6.1$ Hz, 1H), 7.17 (dd, $J = 6.2$ Hz, 1.9 Hz, 1H), 6.95 (m, 1H), 6.83 (m, 1H), 6.13 (d, $J = 7.7$ Hz, 1H), 1.66 (s, 3H), 1.51 (s, 9H), 1.30 (s, 9H). ^{13}C NMR (CD_3CN , 175.974 MHz): δ 176.91, 165.52, 164.40, 164.14 (d, $J = 28.6$ Hz), 163.97, 158.00, 157.86, 151.85, 151.78, 150.07, 145.36, 139.72, 134.01, 130.35, 125.12, 124.63, 124.21, 124.12, 123.85, 120.92, 120.76, 120.35, 36.37, 36.13, 30.54, 30.25, 25.76. HRMS electrospray (m/z): $[\text{M-OAc}]^+$ calcd. for $[\text{RhClC}_{29}\text{H}_{32}\text{N}_3]^+$ 560.1335; found 560.1335; $[\text{M-Cl}]^+$ calcd. for $[\text{RhC}_{31}\text{H}_{35}\text{N}_3\text{O}_2]^+$ 584.1779; found 584.1779.

$[\text{Rh}(\mathbf{1})(\text{Phpy})(\text{OAc})\text{Cl}]$ (**6a**)

In air, $[\text{Rh}(\mathbf{1})(\text{Phpy})\text{Cl}_2]$ (30.0 mg, 0.0187 mmol, 1.00 equiv.) was dissolved in acetonitrile (5 mL) and added to AgOAc (12.5 mg, 0.0749 mmol, 4.00 equiv.). The solution was stirred for 40 minutes and the suspension was filtered through a pad of celite and washed with acetonitrile (5 mL). The volatiles were removed by vacuum to yield 22.0 mg (72 % yield). ^1H NMR (CD_3CN , 699.765 MHz): Due to impurities only signature peaks are reported δ 9.56 (d, $J = 2.2$ Hz, 1H), 9.27 (d, $J = 5.5$ Hz, 1H), 8.47 (d, $J = 2.1$ Hz, 1H), 8.42 (d, $J = 2.0$ Hz, 1H), 8.37 (d, $J = 10$ Hz, 1H), 8.31 (d, $J = 2.1$ Hz, 1H), 5.81 (d, $J = 7.5$ Hz, 1H), 1.78 (s, 3H), 1.39 (s, 9H), 1.36 (s, 9H), 1.29 (s, 18H), 1.28 (s, 9H), 1.15 (s, 9H). ^{19}F NMR (CD_3CN , 376.836 MHz): δ -151.6 (^{10}B), -151.7 (^{11}B).

HRMS electrospray (m/z): [M-BF₄]⁺ calcd. for [RhClC₉₃H₉₉N₅O₂BF₄]⁺ 1542.6572; found 1542.6632.

4.4.5 Reaction Details

General Procedure For Cyclometallation Studies.

dtbpy (7.4 mg, 0.0279 mmol, 2.00 equiv.) was dissolved in 0.75 mL C₆D₆ and added to [Rh((COE)₂Cl)₂] (10.0 mg, 0.0139 mmol, 1.00 equiv.). After 5 minutes at room temperature cyclometallating reagent (Table 4.1) (0.0279 mmol, 2.00equiv.) was added. ¹H NMR were acquired with 10 minutes indicating the formation of a Rh^{III}-hydride.

General Procedure For H/D Exchange Reactions With C₆H₆.

To a 4 mL resealable Schlenk tube was added catalyst (5.0 μmol, 2.0 mol %), AgOAc (if applicable) (2.5 mg, 15 μmol, 6.0 mol %), and a Teflon stirbar. Deuterium source (6.25 mmol, 25 equiv.: CD₃COOD 357.9 μL; CD₃OD 253.5 μL; D₂O 112.9 μL) was added. Benzene (22.3 μL, 19.5 mg, 0.250 mmol, 1.00 equiv) was added to the reaction vessel, which was subsequently sealed. The vessel was completely submerged in a preheated oil bath. At the end of the reaction, the vessel was cooled to room temperature. The reaction mixture was then filtered over a plug of Celite to remove any particulates and rinsed with EtOAc (1x2 mL) into a 20 mL scintillation vial. A saturated aqueous solution of K₂CO₃ (9 M in deionized H₂O, 2x1 mL) was added to the vial to quench and separate the acid. The organic layer was carefully separated and diluted with additional EtOAc to give a 12.8 mM solution of benzene (~1 mg/mL) for analysis by GC-MS. The percent deuterium incorporation was defined as the percent of C–H bonds converted to C–D bonds. The background reaction (in the absence of the catalyst) at 150 °C is minimal with deuterium source and is described in detail in previous publications.¹³⁰ Turnover

numbers (TONs) are calculated as mole deuterium incorporated per mole of catalyst. Reported values have been corrected for the background reaction in the presence of AgCl, which is formed in situ.

General Procedure for H/D Exchange Reactions with 2-phenylpyridine.

To a 4 mL resealable Schlenk tube was added catalyst (5.0 μmol , 2.0 mol %) and AgOAc (if applicable) (2.5 mg, 15 μmol , 6.0 mol %), and a Teflon stirbar. Deuterium source (6.25 mmol, 25 equiv.: CD_3COOD 357.9 μL ; CD_3OD 253.5 μL ; D_2O 112.9 μL) was added. 2-phenylpyridine (35.8 μL , 38.8 mg, 0.250 mmol, 1.00 equiv) was added to the reaction vessel, which was subsequently sealed. The vessel was completely submerged in a preheated oil bath at the indicated reaction temperature. At the indicated reaction time, the vessel was cooled to room temperature. 1,1,2-trichloroethane (23.2 μL , 0.250 mmol, 1.00 equiv) was added to the tube. The contents were mixed by pipet and added to an NMR tube. The percent deuterium incorporation was defined as the percent of C–H bonds converted to C–D bonds and was determined by the loss of signal integration by ^1H NMR and compared to an independent sample of a 1:1 ratio of 2-phenylpyridine and 1,1,2-trichloroethane. ^1H NMR spectra were recorded as one scan spectrum with gain set to zero to minimize relaxation delay errors. Turnover numbers (TON) is determined by total percent deuterium incorporation divided by catalyst loading.

General Procedure for Thermolysis of 6 and 7.

6 or **7** (6 μmol) was dissolved in acetic acid- D_4 (0.75 mL) and placed in a Teflon screw cap sealed NMR tube. The tube was heating in an oil bath at 130 $^\circ\text{C}$ and found to be stable by ^1H NMR monitoring periodically after days of heating.

General Procedure for Oxidatively Induced Reductive Elimination of **6** and **7**.

6 or **7** (6.0 μmol , 1.00 equiv.) was dissolved in acetic acid- D_4 (0.75 mL) or acetonitrile- D_3 (0.75 mL). Oxidant (12.0 μmol , 2.00 equiv.; see Scheme 4.15) was added to the solution. Reactions were prepared with and without silver acetate or silver triflate (6.0 or 12.0 μmol , 1.00 or 2.00 equiv.). The reaction mixture was placed in a Teflon screw cap sealed NMR tube. The tube was heating in an oil bath at 130 $^\circ\text{C}$ and monitored periodically by ^1H NMR.

General Procedure for Olefin or Alkyne Insertion of **6** and **7**.

6 or **7** (6.0 μmol , 1.00 equiv.) was dissolved in acetic acid- D_4 (0.75 mL) or acetonitrile- D_3 (0.75 mL). Olefin or alkyne (6.0 μmol , 1.00 equiv.-see Scheme 4.16) was added to the solution. Reactions were prepared with and without silver acetate or silver triflate (6.0 or 12.0 μmol , 1.00 or 2.00 equiv.). The reaction mixture was placed in a Teflon screw cap sealed NMR tube. The tube was heating in an oil bath and heated to 130 $^\circ\text{C}$ and monitoring periodically ^1H NMR.

4.4.6 XYZ coordinates – Calculated Structures

	Rh(pyridine)($\text{NH}_2\text{CH}_2\text{Ph}$)(κ^2 -OAc) (2)		
Rh	-1.01017400	0.51730400	-0.02591400
N	-1.95490100	-1.26495700	-0.02095600
C	-3.31670200	-1.21153900	0.10988700
C	-1.40336900	-2.50574000	-0.14579100
C	-4.12771200	-2.34906300	0.12354300
H	-3.73043100	-0.21295100	0.19830600
C	-2.14995600	-3.68919200	-0.14202500
H	-0.32516300	-2.54522100	-0.25652800
C	-3.54544900	-3.62289500	-0.00354700
H	-5.20138900	-2.22678400	0.23169700
H	-1.63529800	-4.63979500	-0.24872400
H	-4.15303700	-4.52305400	0.00278900
N	0.93827400	-0.29210800	-0.03198500
H	1.11038400	-0.80674100	-0.89863700

H	1.06397600	-0.95945100	0.73198600
O	-0.58282800	2.60132000	-0.02811400
C	-1.84525800	2.85366600	-0.00430300
O	-2.66771700	1.86546500	-0.00342900
C	-2.34967400	4.28483900	0.05392200
H	-1.65244700	4.95072600	-0.46220100
H	-3.34890900	4.35055700	-0.38485200
H	-2.40920700	4.59473400	1.10525700
C	2.00293200	0.76934800	0.09685600
H	1.80488900	1.29595200	1.03376500
H	1.83453700	1.47877100	-0.71679600
C	3.41368900	0.19887000	0.06168700
C	4.10290800	0.06036200	-1.16150200
C	4.04560900	-0.23164900	1.24737300
C	5.38953500	-0.50427200	-1.20200800
H	3.63520600	0.40523200	-2.08205700
C	5.33185800	-0.79707900	1.21220600
H	3.53398900	-0.11348700	2.20111800
C	6.00667900	-0.93541100	-0.01412100
H	5.90976600	-0.59798900	-2.15196700
H	5.80750000	-1.11814900	2.13553200
H	7.00368900	-1.36732700	-0.04265900

Rh(pyridine)(NH₂CH₂Ph)(OAc) Agostic (**2d**)

Rh	-0.12779900	-0.11534400	-0.15573500
N	0.36182800	-2.14684100	-0.59143700
H	-0.33583900	-2.58567200	-1.19425200
H	0.39964200	-2.68610900	0.27651300
C	1.71866900	-2.21415600	-1.24477600
H	2.09487100	-3.24491600	-1.28471500
H	1.58794000	-1.84665200	-2.26909600
C	2.63785100	-1.30638500	-0.45692100
C	3.83989500	-1.75268500	0.11210000
C	2.18777000	0.01760100	-0.21614200
C	4.61398900	-0.87838500	0.90122600
H	4.17312500	-2.77560200	-0.05311000
C	2.97095700	0.89124700	0.56293600
H	1.42660800	0.51272600	-0.91350700
C	4.17587100	0.43787200	1.12912600
H	5.54877100	-1.22601200	1.33403400
H	2.63639400	1.91493500	0.68570700
H	4.77589800	1.11254500	1.73471400
N	-2.12399000	-0.54395300	0.11811900
C	-2.56507500	-1.67009900	0.73914300
C	-3.06305200	0.33612500	-0.32619000
C	-3.92134400	-1.96723700	0.91884300

H	-1.79832500	-2.33926500	1.11539900
C	-4.43767100	0.10523700	-0.19318200
H	-2.66957900	1.24028500	-0.77212600
C	-4.88501300	-1.06646700	0.43778100
H	-4.20414600	-2.88143700	1.43194200
H	-5.13678900	0.84119000	-0.57856700
H	-5.94597900	-1.26812100	0.55616000
O	-0.67304600	1.82449500	0.24826500
C	-0.02345900	2.87954900	-0.18526400
O	1.02571700	2.86838300	-0.85827400
C	-0.69525900	4.20976700	0.20135100
H	-1.57541200	4.36477100	-0.43666100
H	-1.03865100	4.18076400	1.24066600
H	0.00140000	5.03766200	0.04810700

Rh(pyridine)(NH₂CH₂Ph)(OAc) Electrophilic TS (**2e**)

Rh	0.13912000	-0.12196300	0.01548500
N	-0.25617100	-2.09571600	0.66930700
H	0.46786000	-2.46349500	1.28778500
H	-0.32395300	-2.72397500	-0.13501700
C	-1.59249300	-2.08651400	1.37639000
H	-1.95751700	-3.10744000	1.55604000
H	-1.42154900	-1.59738700	2.34264300
C	-2.52606300	-1.28022200	0.49993600
C	-3.83737200	-1.69360600	0.21622300
C	-1.94485900	-0.12265800	-0.10607000
C	-4.63151100	-0.95144800	-0.67870900
H	-4.23932900	-2.59326400	0.68108400
C	-2.77022600	0.59187600	-1.01437200
H	-1.24944400	0.94810200	0.70778900
C	-4.08626600	0.18705800	-1.29958000
H	-5.65022900	-1.26371800	-0.89471400
H	-2.37802000	1.48396600	-1.49778200
H	-4.68678400	0.75927000	-2.00411400
N	2.22940800	-0.43238000	-0.12205400
C	2.76660800	-1.58055500	-0.61101100
C	3.09445300	0.55171100	0.24221100
C	4.14500700	-1.79379500	-0.74018800
H	2.05812200	-2.34340500	-0.91955300
C	4.48528200	0.41817500	0.14900200
H	2.63300000	1.46382300	0.60103300
C	5.03024500	-0.77663600	-0.34918700
H	4.50534400	-2.73536000	-1.14373700
H	5.12063700	1.24135100	0.46183700
H	6.10534000	-0.90890400	-0.43333800
O	0.47890800	1.91484000	-0.40496000

C	-0.27145800	2.68734600	0.29080900
O	-1.20221100	2.24508000	1.05538300
C	-0.06058000	4.19322800	0.20383800
H	0.15135200	4.58642700	1.20446700
H	0.75974400	4.42993900	-0.47711400
H	-0.98579300	4.66593700	-0.14403000

Rh(pyridine)(NH₂CH₂Ph)(HOAc) Electrophilic Product (**2b**)

Rh	0.03994600	-0.24063600	-0.14548100
N	-0.37286700	-2.21218300	0.44783100
H	0.34221600	-2.63335300	1.04110600
H	-0.42395000	-2.77209200	-0.40657500
C	-1.71873500	-2.26252400	1.13670600
H	-2.11695100	-3.28801400	1.15089100
H	-1.53992000	-1.95034800	2.17325200
C	-2.62917800	-1.28365000	0.42037900
C	-4.02489800	-1.44564000	0.38596400
C	-1.96610800	-0.18159000	-0.20455600
C	-4.82569400	-0.48994000	-0.26831600
H	-4.49213900	-2.30714500	0.86403100
C	-2.80616800	0.75330100	-0.86525700
H	-0.26253000	1.19658000	1.36418000
C	-4.20733000	0.60895200	-0.89355600
H	-5.90646400	-0.60681200	-0.29684500
H	-2.35904900	1.60356800	-1.37860000
H	-4.81707700	1.34770300	-1.41219800
N	2.21608700	-0.45747700	-0.11145000
C	2.84573200	-1.25275300	-1.01360700
C	2.99781400	0.20858600	0.77610500
C	4.23701100	-1.41740200	-1.05975600
H	2.19773800	-1.75865400	-1.72423600
C	4.39592300	0.10614900	0.80008500
H	2.46991200	0.83689700	1.48724600
C	5.03503800	-0.72510600	-0.13410000
H	4.67582300	-2.06958300	-1.80913200
H	4.96182500	0.66658200	1.53848400
H	6.11668300	-0.82870400	-0.14167200
O	0.27342000	1.81173400	-0.70822900
C	0.08555900	2.63100900	0.21709500
O	-0.19728700	2.23029700	1.45462300
C	0.14753500	4.12830900	0.01196500
H	0.77801800	4.58705700	0.78041200
H	0.53035500	4.34961700	-0.98555700
H	-0.86266000	4.54049100	0.12111400

Rh₂(pyridine)(NH₂CH₂Ph)(OAc) Oxidative Addition TS (**2c**)

Rh	0.08661900	-0.11326000	-0.18937900
N	0.63032900	-2.10540800	-0.73242800
H	0.02774700	-2.50323300	-1.45308500
H	0.54035500	-2.70068700	0.09309200
C	2.07138700	-2.13119300	-1.18854700
H	2.49670700	-3.14002200	-1.10645400
H	2.06163000	-1.85091900	-2.24953000
C	2.83456300	-1.10750100	-0.37209400
C	4.18654800	-1.25044300	-0.02217600
C	2.09126900	0.03998200	0.02851600
C	4.83618800	-0.23028800	0.69882500
H	4.73424300	-2.14694500	-0.30983500
C	2.76346100	1.06835500	0.72754700
H	1.16491100	0.47426400	-1.15251000
C	4.12121900	0.92505500	1.06686800
H	5.88404900	-0.33644500	0.96747500
H	2.20857000	1.95555400	1.01645600
H	4.62135600	1.71562400	1.62250400
N	-2.00692600	-0.66646300	0.17427100
C	-2.34425100	-1.58391000	1.11314400
C	-3.00296500	-0.09036900	-0.54702200
C	-3.66668800	-1.96984900	1.36534500
H	-1.52410600	-2.00851000	1.68668000
C	-4.35155000	-0.43301700	-0.36383100
H	-2.68254700	0.67492000	-1.24947400
C	-4.69471400	-1.38634700	0.60617300
H	-3.87632400	-2.70335700	2.13785400
H	-5.10881100	0.05544800	-0.96925900
H	-5.73236200	-1.66403700	0.77177100
O	-0.26270800	1.80694400	0.44693400
C	-0.92778000	2.66451600	-0.28928500
O	-1.49040900	2.41708600	-1.37684600
C	-0.95428200	4.08430100	0.30155400
H	-1.77080000	4.65874000	-0.14327600
H	-1.05146900	4.05049900	1.39129500
H	-0.00434600	4.58092500	0.06463100

Rh(H)(pyridine)(NH₂CH₂Ph)(OAc) Oxidative Addition Product (**2a**)

Rh	-0.07794600	-0.21728800	-0.09199400
N	-0.57066300	-2.26273100	0.24380900
H	0.13142500	-2.76484400	0.78794800
H	-0.65248900	-2.74789800	-0.65213000
C	-1.91351100	-2.32283500	0.94291700
H	-2.36743200	-3.31733100	0.83639300
H	-1.70809500	-2.15214400	2.00680200
C	-2.77428700	-1.21253400	0.37236200

C	-4.17684800	-1.29512100	0.31488700
C	-2.07318900	-0.05987500	-0.08376700
C	-4.91852400	-0.20992100	-0.18729500
H	-4.69129400	-2.19176800	0.65962000
C	-2.84035000	1.01687500	-0.58394700
H	-0.10337000	0.01259400	1.40168100
C	-4.24579500	0.94244700	-0.63502700
H	-6.00341900	-0.26574100	-0.23201900
H	-2.33053200	1.90965000	-0.93552400
H	-4.81658300	1.78298300	-1.02547400
N	2.13533300	-0.56667500	-0.14083200
C	2.69715800	-1.48395500	-0.96328400
C	2.95587000	0.13825900	0.67898000
C	4.07312900	-1.74420400	-1.00361300
H	2.01532900	-2.02185600	-1.61916700
C	4.34512300	-0.06333100	0.70479800
H	2.46383100	0.88524300	1.29734800
C	4.91828200	-1.01859900	-0.14741900
H	4.46330500	-2.48935700	-1.69029400
H	4.95446000	0.52935100	1.38026800
H	5.99123300	-1.19196300	-0.14934000
O	0.17775600	1.74327500	-0.56151100
C	0.63769900	2.66390200	0.25548800
O	1.07012200	2.47267100	1.40919000
C	0.57985600	4.08187800	-0.33580700
H	1.33058500	4.71527000	0.14388200
H	0.71983000	4.06368700	-1.42065500
H	-0.41260700	4.50243300	-0.12751200

Rh(*N*-Me-pyrazine)(NH₂CH₂Ph)(κ²-OAc) (**3**)

Rh	-0.65073200	0.87128900	0.00247500
N	-1.86546000	-0.64230700	-0.00769000
C	-3.22321000	-0.33993200	0.01021600
C	-1.58391100	-1.99728400	-0.03367500
C	-4.20478500	-1.30247900	0.00533500
H	-3.47859800	0.71291700	0.02787800
C	-2.55928000	-2.97306400	-0.03881200
H	-0.54389800	-2.29419500	-0.05199700
H	-5.25712200	-1.04296700	0.02031400
H	-2.30782600	-4.02713700	-0.05905300
N	1.13683700	-0.25925400	-0.00246700
H	1.21738700	-0.83099600	-0.84685700
H	1.18278300	-0.91210400	0.78333100
O	0.14275500	2.77751700	0.00856400
C	-1.05038500	3.29363500	0.01027900
O	-2.03577700	2.46364300	0.00974500

C	-1.25307600	4.78673000	0.00589400
H	-0.84335500	5.19811500	-0.92393700
H	-2.31472400	5.02761800	0.08527200
H	-0.69506100	5.22961300	0.83769800
C	2.39074600	0.60290900	0.06822900
H	2.31241800	1.18797000	0.98773400
H	2.33924000	1.29599000	-0.77440100
C	3.65469500	-0.23748800	0.03427800
C	4.27657800	-0.54291600	-1.19473700
C	4.20625500	-0.74958900	1.22787800
C	5.42318400	-1.35456700	-1.23178700
H	3.87691200	-0.13199900	-2.12036400
C	5.35206500	-1.56211200	1.19328200
H	3.75321300	-0.49780800	2.18553500
C	5.96113500	-1.86643900	-0.03748900
H	5.90033900	-1.57413200	-2.18293300
H	5.77461100	-1.94199500	2.11942000
H	6.85195000	-2.48773800	-0.06447600
C	-4.95638900	-3.67035100	-0.02127400
H	-5.58569900	-3.54023700	-0.90645300
H	-4.49573300	-4.65890300	-0.04500600
H	-5.56050200	-3.57143700	0.88528900
N	-3.88579600	-2.64132300	-0.01848800

Rh(H)(*N*-Me-pyrazine)(NH₂CH₂Ph)(OAc) Oxidative Product (**3a**)

Rh	-0.34587700	-0.24797100	-0.13838600
N	-0.77687000	-2.31762400	0.16851800
H	-0.06751400	-2.83526100	0.68921700
H	-0.86699100	-2.77655500	-0.74125700
C	-2.11232300	-2.44421700	0.88343400
H	-2.53269900	-3.44649800	0.73832300
H	-1.90158200	-2.31068000	1.95100400
C	-3.00300500	-1.34086200	0.35904000
C	-4.40310900	-1.44406000	0.32599500
C	-2.34120000	-0.15600800	-0.07166600
C	-5.16989200	-0.35292700	-0.12235700
H	-4.89630000	-2.35831800	0.65050200
C	-3.12886300	0.93350300	-0.50940100
H	-0.38460500	0.01590900	1.35208200
C	-4.53094800	0.82941200	-0.54014400
H	-6.25348600	-0.42655000	-0.14722500
H	-2.64442900	1.84415300	-0.84499500
H	-5.12480900	1.66961500	-0.89138300
N	1.82448300	-0.43260000	-0.16230000
C	2.53133100	-1.42091200	-0.77560100
C	2.55358900	0.49629000	0.52775500

C	3.91961100	-1.49970400	-0.72945400
H	1.97630100	-2.16461300	-1.33797500
C	3.94239200	0.43753600	0.59460900
H	1.97999700	1.28950700	1.02573900
H	4.47770900	-2.27982100	-1.23377000
H	4.52408000	1.17171300	1.14077400
O	-0.21141800	1.72290700	-0.59733300
C	0.11484900	2.69350000	0.23533200
O	0.64403300	2.52401600	1.35419000
C	-0.21626300	4.09281400	-0.28426900
H	0.44257600	4.82931100	0.18105000
H	-0.14919100	4.13624300	-1.37445800
H	-1.24960200	4.32649700	0.00296900
C	6.11781200	-0.58394300	-0.01439800
H	6.46084700	-1.58084500	-0.29392600
H	6.49895600	0.15634800	-0.72382700
H	6.45722500	-0.34694700	0.99594600
N	4.62569700	-0.56012000	-0.04043500

Rh(*N*-Me-pyrazine)(NH₂CH₂Ph)(HOAc) Electrophilic Product (**3b**)

Rh	0.17556100	-0.16248000	-0.19976300
N	0.45239100	-2.21500500	-0.62477600
H	-0.12897600	-2.60514500	-1.36682000
H	0.21597900	-2.72432900	0.22991600
C	1.90704600	-2.48975100	-0.95424600
H	2.14389000	-3.54964000	-0.79728000
H	2.03347700	-2.26755700	-2.02051200
C	2.74355600	-1.56431200	-0.09653300
C	4.07484100	-1.84871100	0.24383300
C	2.09598700	-0.36699200	0.33786900
C	4.79700200	-0.94118300	1.04193300
H	4.55089700	-2.76600300	-0.09764500
C	2.84420200	0.51333900	1.16470500
H	1.34036900	1.36683600	-1.66907100
C	4.17868200	0.23662200	1.50495300
H	5.82692000	-1.15861100	1.31142000
H	2.37793700	1.41552100	1.55425600
H	4.73454800	0.92666500	2.13502500
N	-1.87818500	-0.15633800	-0.23841900
C	-2.67910700	-1.19200100	-0.69006000
C	-2.55638200	0.76907500	0.54241700
C	-4.00808700	-1.33968500	-0.35609400
H	-2.22956200	-1.90880600	-1.36571600
C	-3.88209600	0.64616200	0.89123300
H	-1.98107800	1.61674400	0.89170700
H	-4.60727100	-2.16048400	-0.73348300

H	-4.38324600	1.38073600	1.51083800
O	0.13470600	1.94143100	0.20127400
C	0.71627800	2.75183800	-0.55756900
O	1.38328400	2.35912400	-1.63991300
C	0.72115100	4.24165600	-0.32051600
H	0.31065000	4.75129700	-1.19891200
H	0.14005800	4.48165800	0.57010600
H	1.75645700	4.57947600	-0.19958300
C	-6.04449800	-0.58878400	0.87020300
H	-6.56204200	-1.21496700	0.14061500
H	-6.08941900	-1.06103600	1.85755600
H	-6.52655400	0.39114500	0.90773000
N	-4.63401500	-0.42151100	0.44969900

4.5 References

- (1) Labinger, J. A.; Bercaw, J. E. *Nature* **2002**, *417*, 507.
- (2) Arndtsen, B. A.; Bergman, R. G.; Mobley, T. A.; Peterson, T. H. *Acc. Chem. Res.* **1995**, *28*, 154.
- (3) Jones, W. D.; Feher, F. J. *Acc. Chem. Res.* **1989**, *22*, 91.
- (4) Crabtree, R. H. *Chem. Rev.* **1985**, *85*, 245.
- (5) Crabtree, R. H. *Chem. Rev.* **1995**, *95*, 987.
- (6) Goldberg, K. I.; Goldman, A. S. *Activation and Functionalization of C-H Bonds*; Oxford University Press: Washington, DC, 2004.
- (7) Crabtree, R. H. *J. Chem. Soc.-Dalton Trans.* **2001**, 2437.
- (8) Periana, R. A.; Bhalla, G.; Tenn, W. J.; Young, K. J. H.; Liu, X. Y.; Mironov, O.; Jones, C. J.; Ziatdinov, V. R. *J. Mol. Catal. A-Chem.* **2004**, *220*, 7.
- (9) Labinger, J. A. *J. Mol. Catal. A-Chem.* **2004**, *220*, 27.
- (10) Tenaglia, A.; Heumann, A. *Angew. Chem. Int. Ed.* **1999**, *38*, 2180.
- (11) Dyker, G. *Handbook of C-H Transformations*; Wiley-VCH: Weinheim, Germany, 2005.
- (12) Ritleng, V.; Sirlin, C.; Pfeffer, M. *Chem. Rev.* **2002**, *102*, 1731.
- (13) Feng, Y.; Lail, M.; Barakat, K. A.; Cundari, T. R.; Gunnoe, T. B.; Petersen, J. L. *J. Am. Chem. Soc.* **2005**, *127*, 14174.
- (14) Tenn, W. J.; Young, K. J. H.; Bhalla, G.; Oxgaard, J.; Goddard, W. A.; Periana, R. A. *J. Am. Chem. Soc.* **2005**, *127*, 14172.

- (15) Feng, Y.; Lail, M.; Foley, N. A.; Gunnoe, T. B.; Barakat, K. A.; Cundari, T. R.; Petersen, J. L. *J. Am. Chem. Soc.* **2006**, *128*, 7982.
- (16) Meier, S. K.; Young, K. J. H.; Ess, D. H.; Tenn, W. J.; Oxgaard, J.; Goddard, W. A.; Periana, R. A. *Organometallics* **2009**, *28*, 5293.
- (17) Young, K. J. H.; Oxgaard, J.; Ess, D. H.; Meier, S. K.; Stewart, T.; Goddard, I. I. W. A.; Periana, R. A. *Chemical Communications* **2009**, 3270.
- (18) Ahlquist, M.; Periana, R. A.; Goddard, W. A. *Chem. Commun.* **2009**, 2373.
- (19) Goldshleger, N. F.; Eskova, V. V.; Shilov, A. E.; Shteinman, A. A. *Russ. J. Phys. Chem.* **1972**, *46*, 785.
- (20) Goldshleger, N. F.; Tyabin, M. B.; Shilov, A. E.; Shteinman, A. A. *Russ. J. Phys. Chem.* **1969**, *43*, 1222.
- (21) Labinger, J. A.; Bercaw, J. E. In *Higher Oxidation State Organopalladium and Platinum Chemistry*; Canty, A. J., Ed.; Springer-Verlag Berlin: Berlin, 2011; Vol. 35, p 29.
- (22) Lin, M.; Shen, C.; Garcia-Zayas, E. A.; Sen, A. *J. Am. Chem. Soc.* **2001**, *123*, 1000.
- (23) Shilov, A. E. *Activation of Saturated Hydrocarbons by Transition Metal Complexes*; D. Reidel Publishing Company: Dordrecht, Holland, 1984.
- (24) Shilov, A. E.; Shteinman, A. A. *Coord. Chem. Rev.* **1977**, *24*, 97.
- (25) Shilov, A. E.; Shul'pin, G. B. *Uspekhi Khimii* **1987**, *56*, 754.
- (26) Shilov, A. E.; Shul'pin, G. B. *Chem. Rev.* **1997**, *97*, 2879.
- (27) Shilov, A. E.; Shul'pin, G. B. *Activation and Catalytic Reactions of Saturated Hydrocarbons in the Presence of Metal Complexes*; Springer: Verlag, 2000.
- (28) Zamashchikov, V. V.; Kitaigorodskii, A. N.; Litvinenko, S. L.; Rudakov, E. S.; Uzhik, O. N.; Shilov, A. E. *Bulletin of the Academy of Sciences of the USSR Division of Chemical Science* **1985**, *34*, 1582.
- (29) Ebersson, L.; Jonsson, E. *Acta Chem. Scand. B* **1974**, *B 28*, 771.
- (30) Lyons, T. W.; Sanford, M. S. *Chem. Rev.* **2010**, *110*, 1147.
- (31) Yoneyama, T.; Crabtree, R. H. *J. Mol. Catal. A* **1996**, *108*, 35.
- (32) Dick, A. R.; Kampf, J. W.; Sanford, M. S. *Organometallics* **2005**, *24*, 482.
- (33) Canty, A. J.; Denney, M. C.; van Koten, G.; Skelton, B. W.; White, A. H. *Organometallics* **2004**, *23*, 5432.

- (34) Huang, T. M.; Chen, J. T.; Lee, G. H.; Wang, Y. *Organometallics* **1991**, *10*, 175.
- (35) Wolowska, J.; Eastham, G. R.; Heaton, B. T.; Iggo, J. A.; Jacob, C.; Whyman, R. *Chem. Commun.* **2002**, 2784.
- (36) Dorta, R.; Shimon, Linda J. W.; Rozenberg, H.; Milstein, D. *Eur. J. Inorg. Chem.* **2002**, *2002*, 1827.
- (37) Lorenzini, F.; Marcazzan, P.; Patrick, B. O.; James, B. R. *Can. J. Chem.* **2008**, *86*, 253.
- (38) Canepa, G.; Brandt, C. D.; Ilg, K.; Wolf, J.; Werner, H. *Chem. Eur. J.* **2003**, *9*, 2502.
- (39) Rybtchinski, B.; Cohen, R.; Ben-David, Y.; Martin, J. M. L.; Milstein, D. *J. Am. Chem. Soc.* **2003**, *125*, 11041.
- (40) Vigalok, A.; Uzan, O.; Shimon, L. J. W.; Ben-David, Y.; Martin, J. M. L.; Milstein, D. *J. Am. Chem. Soc.* **1998**, *120*, 12539.
- (41) Whitmore, B. C.; Eisenberg, R. *J. Am. Chem. Soc.* **1984**, *106*, 3225.
- (42) Boaretto, R.; Paolucci, G.; Sostero, S.; Traverso, O. *J. Mol. Catal. A* **2003**, *204-205*, 253.
- (43) Nonoyama, M. *J. Organomet. Chem.* **1974**, *74*, 115.
- (44) Nonoyama, M. *J. Organomet. Chem.* **1975**, *92*, 89.
- (45) Santa María*, M. D.; Claramunt, R. M.; Campo, J. A.; Cano*, M.; Criado, R.; Heras, J. V.; Ovejero, P.; Pinilla, E.; Torres, M. R. *J. Organomet. Chem.* **2000**, *605*, 117.
- (46) van Baar, J. F.; Vrieze, K.; Stufkens, D. J. *J. Organomet. Chem.* **1975**, *97*, 461.
- (47) Ezhova, M. B.; Patrick, B. O.; James, B. R. *Organometallics* **2005**, *24*, 3753.
- (48) Keyes, M. C.; Young, V. G.; Tolman, W. B. *Organometallics* **1996**, *15*, 4133.
- (49) Marcazzan, P.; Patrick, B. O.; James, B. R. *Organometallics* **2005**, *24*, 1445.
- (50) Sjövall, S.; Andersson, C.; Wendt, O. F. *Organometallics* **2001**, *20*, 4919.
- (51) Van der Zeijden, A. A. H.; Van Koten, G.; Nordemann, R. A.; Kojic-Prodic, B.; Spek, A. L. *Organometallics* **1988**, *7*, 1957.
- (52) Marcazzan, P.; Patrick, B. O.; James, B. R. *Russ. Chem. Bull., Int. Ed.* **2003**, *52*, 2715.

- (53) Bromberg, S. E.; Yang, H.; Asplund, M. C.; Lian, T.; McNamara, B. K.; Kotz, K. T.; Yeston, J. S.; Wilkens, M.; Frei, H.; Bergman, R. G.; Harris, C. B. *Science* **1997**, *278*, 260.
- (54) Hanson, S. K.; Heinekey, D. M.; Goldberg, K. I. *Organometallics* **2008**, *27*, 1454.
- (55) Jones, W. D. *Acc. Chem. Res.* **2002**, *36*, 140.
- (56) Jones, W. D.; Feher, F. J. *Organometallics* **1983**, *2*, 562.
- (57) Jones, W. D.; Feher, F. J. *J. Am. Chem. Soc.* **1986**, *108*, 4814.
- (58) Kohl, G.; Rudolph, R.; Pritzkow, H.; Enders, M. *Organometallics* **2005**, *24*, 4774.
- (59) Kovács, G.; Schubert, G.; Joó, F.; Pápai, I. *Organometallics* **2005**, *24*, 3059.
- (60) van der Boom, M. E.; Milstein, D. *Chem. Rev.* **2003**, *103*, 1759.
- (61) Verat, A. Y.; Pink, M.; Fan, H.; Tomaszewski, J.; Caulton, K. G. *Organometallics* **2007**, *27*, 166.
- (62) Atzrodt, J.; Derau, V.; Fey, T.; Zimmermann, J. *Angew. Chem. Int. Ed.* **2007**, *46*, 7744.
- (63) Ackermann, L. In *Topics in Organometallic Chemistry*; Chatani, N., Ed.; Springer Berlin / Heidelberg: 2007; Vol. 24, p 35.
- (64) Aulwurm, U. R.; Melchinger, J. U.; Kisch, H. *Organometallics* **1995**, *14*, 3385.
- (65) Colby, D. A.; Bergman, R. G.; Ellman, J. A. *Chem. Rev.* **2009**, *110*, 624.
- (66) Fagnou, K.; Lautens, M. *Chem. Rev.* **2002**, *103*, 169.
- (67) Fukutani, T.; Umeda, N.; Hirano, K.; Satoh, T.; Miura, M. *Chem. Commun.* **2009**, 5141.
- (68) Guimond, N.; Fagnou, K. *J. Am. Chem. Soc.* **2009**, *131*, 12050.
- (69) Guimond, N.; Gouliaras, C.; Fagnou, K. *J. Am. Chem. Soc.* **2010**, *132*, 6908.
- (70) Hawkes, K. J.; Cavell, K. J.; Yates, B. F. *Organometallics* **2008**, *27*, 4758.
- (71) Huang, L.-Y.; Aulwurm, U. R.; Heinemann, F. W.; Kisch, H. *Eur. J. Inorg. Chem.* **1998**, *1998*, 1951.
- (72) Hyster, T. K.; Rovis, T. *J. Am. Chem. Soc.* **2010**, *132*, 10565.
- (73) Jun, C.-H.; Moon, C. W.; Hong, J.-B.; Lim, S.-G.; Chung, K.-Y.; Kim, Y.-H. *Chem. Eur. J.* **2002**, *8*, 485.

- (74) Kakiuchi, F. In *Topics in Organometallic Chemistry*; Chatani, N., Ed.; Springer Berlin / Heidelberg: 2007; Vol. 24, p 1.
- (75) Lewis, J. C.; Bergman, R. G.; Ellman, J. A. *Acc. Chem. Res.* **2008**, *41*, 1013.
- (76) Li, L.; Brennessel, W. W.; Jones, W. D. *J. Am. Chem. Soc.* **2008**, *130*, 12414.
- (77) Li, L.; Brennessel, W. W.; Jones, W. D. *Organometallics* **2009**, *28*, 3492.
- (78) Li, L.; Jiao, Y.; Brennessel, W. W.; Jones, W. D. *Organometallics* **2010**, *29*, 4593.
- (79) Lim, Y.-G.; Lee, K.-H.; Koo, B. T.; Kang, J.-B. *Tetrahedron Lett.* **2001**, *42*, 7609.
- (80) Mochida, S.; Hirano, K.; Satoh, T.; Miura, M. *J. Org. Chem.* **2009**, *74*, 6295.
- (81) Mochida, S.; Umeda, N.; Hirano, K.; Satoh, T.; Miura, M. *Chem. Lett.* **2010**, *39*, 744.
- (82) Parthasarathy, K.; Cheng, C.-H. *J. Org. Chem.* **2009**, *74*, 9359.
- (83) Patureau, F. W.; Glorius, F. *J. Am. Chem. Soc.* **2010**, *132*, 9982.
- (84) Rakshit, S.; Patureau, F. W.; Glorius, F. *J. Am. Chem. Soc.* **2010**, *132*, 9585.
- (85) Satoh, T.; Miura, M. *Chem. Eur. J.* **2010**, *16*, 11212.
- (86) Schipper, D. J.; Hutchinson, M.; Fagnou, K. *J. Am. Chem. Soc.* **2010**, *132*, 6910.
- (87) Stuart, D. R.; Bertrand-Laperle, M. g.; Burgess, K. M. N.; Fagnou, K. *J. Am. Chem. Soc.* **2008**, *130*, 16474.
- (88) Ueura, K.; Satoh, T.; Miura, M. *J. Org. Chem.* **2007**, *72*, 5362.
- (89) Umeda, N.; Tsurugi, H.; Satoh, T.; Miura, M. *Angew. Chem. Int. Ed.* **2008**, *47*, 4019.
- (90) Berman, A. M.; Lewis, J. C.; Bergman, R. G.; Ellman, J. A. *J. Am. Chem. Soc.* **2008**, *130*, 14926.
- (91) Colby, D. A.; Bergman, R. G.; Ellman, J. A. *J. Am. Chem. Soc.* **2006**, *128*, 5604.
- (92) Colby, D. A.; Bergman, R. G.; Ellman, J. A. *J. Am. Chem. Soc.* **2008**, *130*, 3645.
- (93) Lewis, J. C.; Bergman, R. G.; Ellman, J. A. *J. Am. Chem. Soc.* **2007**, *129*, 5332.
- (94) Tan, K. L.; Bergman, R. G.; Ellman, J. A. *J. Am. Chem. Soc.* **2001**, *123*, 2685.
- (95) Tsai, A. S.; Bergman, R. G.; Ellman, J. A. *J. Am. Chem. Soc.* **2008**, *130*, 6316.
- (96) Yotphan, S.; Bergman, R. G.; Ellman, J. A. *J. Am. Chem. Soc.* **2008**, *130*, 2452.

- (97) Kim, M.; Kwak, J.; Chang, S. *Angew. Chem. Int. Ed.* **2009**, *48*, 8935.
- (98) Oi, S.; Fukita, S.; Inoue, Y. *Chem. Commun.* **1998**, 2439.
- (99) Zhao, X.; Yu, Z. *J. Am. Chem. Soc.* **2008**, *130*, 8136.
- (100) Hartwig, J. F. *Acc. of Chem. Res.* **2011**.
- (101) Mkhallid, I. A. I.; Barnard, J. H.; Marder, T. B.; Murphy, J. M.; Hartwig, J. F. *Chem. Rev.* **2009**, *110*, 890.
- (102) Tse, M. K.; Cho, J.-Y.; Smith, M. R. *Org. Lett.* **2001**, *3*, 2831.
- (103) Guan, Z.-H.; Ren, Z.-H.; Spinella, S. M.; Yu, S.; Liang, Y.-M.; Zhang, X. *J. Am. Chem. Soc.* **2008**, *131*, 729.
- (104) Young, K. J. H.; Mironov, O. A.; Periana, R. A. *Organometallics* **2007**, *26*, 2137.
- (105) Feller, M.; Iron, M. A.; Shimon, L. J. W.; Diskin-Posner, Y.; Leitun, G.; Milstein, D. *J. Am. Chem. Soc.* **2008**, *130*, 14374.
- (106) Ye, Z.; Wang, W.; Luo, F.; Zhang, S.; Cheng, J. *Org. Lett.* **2009**, *11*, 3974.
- (107) Garcia, M. P.; Millan, J. L.; Esteruelas, M. A.; Oro, L. A. *Polyhedron* **1987**, *6*, 1427.
- (108) McKenzie, E. D.; Plowman, R. A. *J. Inorg. Nucl. Chem.* **1970**, *32*, 199.
- (109) Śliwińska, U.; Pruchnik, F. P.; Pelińska, I.; Ułaszewski, S.; Wilczok, A.; Zajdel, A. *J. Inorg. Biochem.* **2008**, *102*, 1947.
- (110) Zuber, M.; Pruchnik, F. P. *Polyhedron* **2006**, *25*, 2773.
- (111) Boutadla, Y.; Davies, D. L.; Macgregor, S. A.; Poblador-Bahamonde, A. I. *Dalton Transactions* **2009**, 5820.
- (112) Boutadla, Y.; Davies, D. L.; Macgregor, S. A.; Poblador-Bahamonde, A. I. *Dalton Transactions* **2009**, 5887.
- (113) Davies, D. L.; Donald, S. M. A.; Al-Duaij, O.; Macgregor, S. A.; Pölleth, M. *Journal of the American Chemical Society* **2006**, *128*, 4210.
- (114) Davies, D. L.; Donald, S. M. A.; Macgregor, S. A. *Journal of the American Chemical Society* **2005**, *127*, 13754.
- (115) Osborn, J. A.; Schrock, R. R. *J. Am. Chem. Soc.* **1971**, *93*, 2397.
- (116) Ito, J.-i.; Nishiyama, H. *Eur. J. Inorg. Chem.* **2007**, *2007*, 1114.

- (117) Gaussian 03, Revision C.02, Frisch, M. J.; Trucks, G. W.; Schlegel, H. B.; Scuseria, G. E.; Robb, M. A.; Cheeseman, J. R.; Montgomery, Jr., J. A.; Vreven, T.; Kudin, K. N.; Burant, J. C.; Millam, J. M.; Iyengar, S. S.; Tomasi, J.; Barone, V.; Mennucci, B.; Cossi, M.; Scalmani, G.; Rega, N.; Petersson, G. A.; Nakatsuji, H.; Hada, M.; Ehara, M.; Toyota, K.; Fukuda, R.; Hasegawa, J.; Ishida, M.; Nakajima, T.; Honda, Y.; Kitao, O.; Nakai, H.; Klene, M.; Li, X.; Knox, J. E.; Hratchian, H. P.; Cross, J. B.; Bakken, V.; Adamo, C.; Jaramillo, J.; Gomperts, R.; Stratmann, R. E.; Yazyev, O.; Austin, A. J.; Cammi, R.; Pomelli, C.; Ochterski, J. W.; Ayala, P. Y.; Morokuma, K.; Voth, G. A.; Salvador, P.; Dannenberg, J. J.; Zakrzewski, V. G.; Dapprich, S.; Daniels, A. D.; Strain, M. C.; Farkas, O.; Malick, D. K.; Rabuck, A. D.; Raghavachari, K.; Foresman, J. B.; Ortiz, J. V.; Cui, Q.; Baboul, A. G.; Clifford, S.; Cioslowski, J.; Stefanov, B. B.; Liu, G.; Liashenko, A.; Piskorz, P.; Komaromi, I.; Martin, R. L.; Fox, D. J.; Keith, T.; Al-Laham, M. A.; Peng, C. Y.; Nanayakkara, A.; Challacombe, M.; Gill, P. M. W.; Johnson, B.; Chen, W.; Wong, M. W.; Gonzalez, C.; and Pople, J. A.; Gaussian, Inc., Wallingford CT, 2004.
- (118) Becke, A. D. *J Chem Phys.* **1993**, *98*, 5648.
- (119) Vosko, S. H.; Wilk, L.; Nusair, M. *Can. J. Phys.* **1980**, *58*, 1200.
- (120) Lee, C.; Yang, W.; Parr, R. G. *Physical Review B* **1988**, *37*, 785.
- (121) Stevens, W. J.; Basch, H.; Krauss, M. *J. Chem. Phys.* **1984**, *81*, 6026.
- (122) Stevens, W. J.; Krauss, M.; Basch, H.; Jasien, P. G. *Can. J. Chem.* **1992**, *70*, 612.
- (123) Feller, D. *J. Comp. Chem.* **1996**, *17*, 1571.
- (124) Schuchardt, K. L.; Didier, B. T.; Elsethagen, T.; Sun, L.; Gurumoorthi, V.; Chase, J.; Li, J.; Windus, T. L. *J. Chem. Inf. Model.* **2007**, *47*, 1045.
- (125) Ehlers, A. W.; Böhme, M.; Dapprich, S.; Gobbi, A.; Höllwarth, A.; Jonas, V.; Köhler, K. F.; Stegmann, R.; Veldkamp, A.; Frenking, G. *Chem. Phys. Lett.* **1993**, *208*, 111.
- (126) Emmert, M. H.; Gary, J. B.; Villalobos, J. M.; Sanford, M. S. *Angew. Chem. Int. Ed.* **2010**, *49*, 5884.
- (127) Kalyani, D.; Dick, A. R.; Anani, W. Q.; Sanford, M. S. *Tetrahedron* **2006**, *62*, 11483.
- (128) Van Der Ent, A.; Onderdelinden, A. L.; Schunn, R. A. In *Inorganic Syntheses*; John Wiley & Sons, Inc.: 2007, p 90.
- (129) Giordano, G.; Crabtree, R. H.; Heintz, R. M.; Forster, D.; Morris, D. E. In *Inorganic Syntheses*; John Wiley & Sons, Inc.: 2007, p 88.
- (130) Hickman, A. J.; Villalobos, J. M.; Sanford, M. S. *Organometallics* **2009**, *28*, 5316.

Chapter 5

Computational Analysis on the Mechanism of Aryl–CF₃ and Aryl–O₂CR Reductive Elimination

5.1 Background and Significance

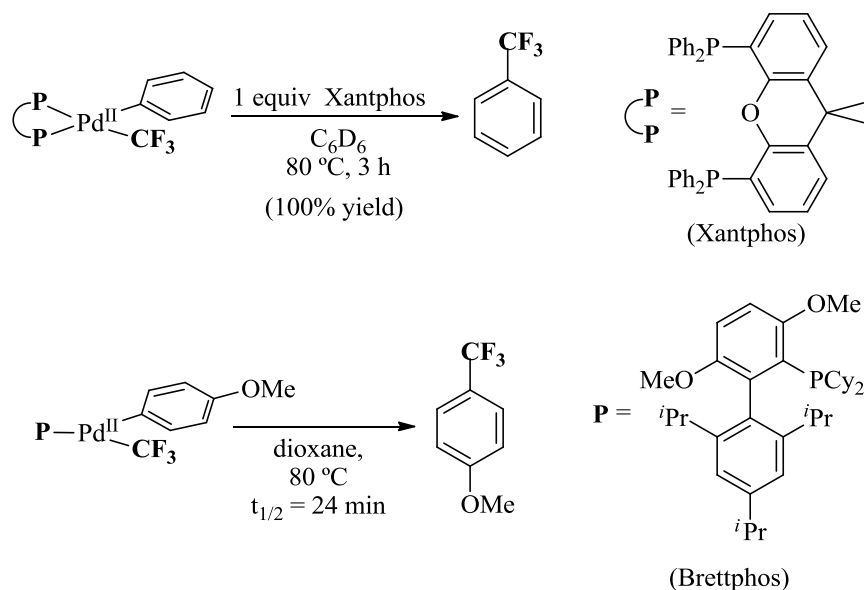
5.1.1 Aryl–CF₃ Bond Formation

The C–CF₃ bond functionality is a key functional group in pharmaceutical and agrochemicals.¹ The substitution of fluorine atoms for hydrogens has a dramatic effect on the physical and biological properties of a molecule by modifying polarity and susceptibility towards oxidative degradation.² Given the importance of this functionality, the design of reliable methods to form C–CF₃ bonds has received a tremendous amount of attention.³⁻⁶ Relatively few methods exist for Aryl–CF₃ bond constructions⁷⁻¹¹ while many more methods are available for the formation of C–CF₃ bonds at sp³-C centers.³⁻⁶

Palladium mediated cross coupling between Aryl–X and CF₃–Y could serve as a viable method to form molecules with Aryl–CF₃ functionalities, given the success with copper-based catalysis.¹²⁻²³ The strategy of Pd-based catalysis for this transformation is of particular interest given the success in other Pd-catalyzed carbon–carbon bond-forming reactions.²⁴⁻²⁸ Development of this methodology has been plagued by the inherent stability of Pd^{II}(Aryl)(CF₃) species towards reductive elimination, the key bond forming step in a typical cross-coupling catalytic cycle.^{7,29-34}

Given this limited reactivity, two methods have been pursued to promote the desired reactivity: (1) ligand modification of Pd^{II} species or (2) modulating the oxidation state of the metal. The first strategy has been used to induce reductive elimination of Aryl–CF₃ species by modifying the steric and electronic properties of ancillary ligands (L) at (L)_nPd^{II}(Aryl)(CF₃). For example, Grushin demonstrated that the Xantphos ligand (Xantphos = 4,5-bis(diphenylphosphino)-9,9-dimethylxanthene) promotes reductive elimination to form trifluorotoluene from (Xantphos)Pd^{II}(Ph)(CF₃) at 80 °C (Scheme 5.1).³³ Also using the ligand modification strategy, Buchwald recently reported stoichiometric reductive elimination (Scheme 5.1) and catalytic cross coupling of aryl chlorides and Et₃SiCF₃ at 130–140 °C to form trifluoromethylated arenes using the sterically bulky phosphine ligand Brettphos (Brettphos = 2-(dicyclohexylphosphino)-3,6-dimethoxy-2',4',6'-triisopropyl-1,1'-biphenyl).^{35,36}

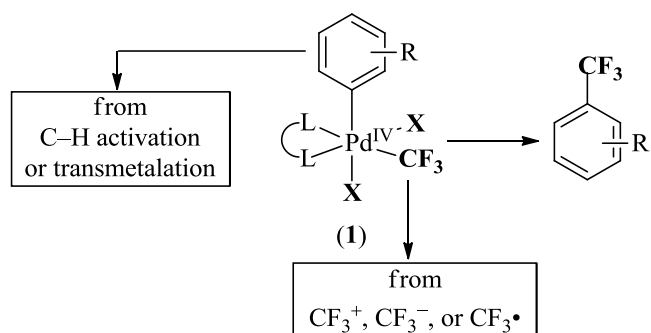
Scheme 5.1 Stoichiometric Aryl–CF₃ Reductive Elimination.^{33,35}



While the approach of ligand modification has provided significant advances, Pd^{II}-mediated Aryl–CF₃ bond-forming reactions still suffer from the requirement for

unique and costly phosphine ligands,^{37,38} high reaction temperatures (80-140 °C), and expensive Et_3SiCF_3 ³⁹ in catalytic processes. Given these limitations, a divergent strategy to improve reactivity involves the modification of the metal oxidation state to promote reductive elimination.^{31,40,41} As shown in Scheme 5.2, it was hypothesized that palladium(IV) complexes of the general structure $(\text{L})_2(\text{X})_2\text{Pd}^{\text{IV}}(\text{Aryl})(\text{CF}_3)$ (**1**) would be highly kinetically and thermodynamically reactive towards Aryl- CF_3 coupling. This hypothesis is predicated based upon literature reports showing that Pd^{IV} complexes participate in numerous carbon-heteroatom bond-forming reductive elimination reactions that remain challenging at Pd^{II} centers.⁴²⁻⁵⁸ A key advantage of this approach would be that Pd^{IV} intermediate **1** could potentially be accessed using nucleophilic (CF_3^-) ,³²⁻³⁴ electrophilic (CF_3^+) ,⁵⁹⁻⁶¹ or free-radical (CF_3^\bullet) ⁶² based trifluoromethylating reagents. However, given multiple carbon fragments (Aryl and CF_3) along with two different X-type ligands, multiple coupling pairs are possible which could lead to a mixture or predominantly undesired products.

Scheme 5.2 General CF_3 Bond Forming Strategy.



Using this approach, Yu and coworkers demonstrated $\text{Pd}^{\text{II/IV}}$ -catalyzed ligand-directed C-H trifluoromethylation with electrophilic trifluoromethylating reagents (CF_3^+ reagents).⁴⁰ Subsequent stoichiometric studies were disclosed by our group which

implicate a mechanism initiated by Pd^{II} C–H activation, oxidation with CF₃⁺ to generate Pd^{IV}(Aryl)(CF₃), and Aryl–CF₃ bond-forming reductive elimination from Pd^{IV} to form the product.⁴¹ In a second example, our group has shown the viability of stoichiometric Aryl–CF₃ bond-forming reductive elimination from Pd^{IV} centers with simple Aryl ligands.³¹ In this system, the key Pd^{IV} intermediate was generated via oxidation of a pre-assembled Pd^{II}(Aryl)(CF₃) species with an *N*-fluoropyridinium reagent. This thesis chapter describes DFT studies of the Aryl–CF₃ coupling reactions that have enabled the identification of new ligands that accelerate this transformation.

5.1.2 Aryl–O₂CR Bond Formation

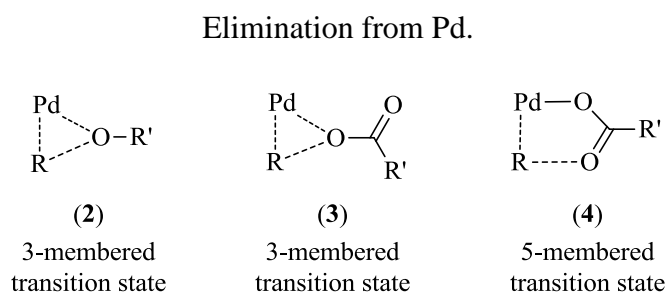
The formation of carbon-oxygen bonds through reductive elimination is an important fundamental reaction in organometallic chemistry.^{25,63-66} This transformation is the key product-forming step in a variety of Pd-catalyzed transformations, including C–H bond oxygenation,⁶⁷⁻⁸⁷ alkene difunctionalization,⁸⁸⁻⁹⁶ aryl halide etherification,⁹⁷⁻¹¹² and allylic C–H acetoxylation.¹¹³⁻¹¹⁸ Due to the importance of this reaction, stoichiometric studies of C–O bond-forming reductive elimination have been conducted with a variety of different Pd complexes, including Pd^{IV} and Pd^{II} aryl species,^{46,119,120} cyclometalated Pd^{III} dimers,^{121,122} and Pd^{II}-allyl adducts.¹²³⁻¹²⁶

Over the past 15 years, reductive elimination from Pd^{II}(Aryl)(alkoxide) complexes has been particularly well studied both experimentally and computationally.^{97,101,107,109,110,120,127} These transformations are believed to proceed via three-membered transition states involving attack of the nucleophilic alkoxide oxygen atom on the ipso-carbon of the aryl ring (**2** in Figure 5.1).^{97,127,128} More recently, a number of groups have become interested in the mechanism of C–O reductive

elimination reactions in which the oxygen coupling partner is a carboxylate.^{46,68,122-126,129}

The bond-forming step of such transformations has typically been assumed to involve a three-membered transition state (**3** in Figure 5.1), analogous to that proposed for aryl-alkoxide coupling. For example, such a transition state was invoked in a computational study of aryl-acetate bond-formation from the Pd^{IV} complex [(phpy)₂Pd^{IV}(OAc)₂] (phpy = 2-phenylpyridine).¹²⁹

Figure 5.1 Proposed Transition States for C–OR and C–O₂CR Bond-Forming Reductive



We hypothesized that carbon–carboxylate coupling might proceed by an alternative five-membered transition state (**4** in Figure 5.1), in which the pendant carbonyl oxygen acts as the nucleophilic coupling partner for C–O bond formation. This hypothesis was inspired by recent computational studies showing that the carbonyl oxygen of κ^1 -carboxylate ligands can serve as an intramolecular nucleophile and/or base in several other transition metal-mediated reactions. In a first example, Musashi and Sakaki have investigated O–H bond-forming reductive elimination from M(O₂CH)(H) complexes (M = Ru and Rh, Figure 5.2).^{130,131} Both five-membered transition state **5** and three-membered transition state **6** were considered for this transformation (which is formally a deprotonation of the acidic M–H bond by the basic formate ligand). In the Ru complexes examined, transition state **5** was favored by 18-23 kcal/mol, depending on the

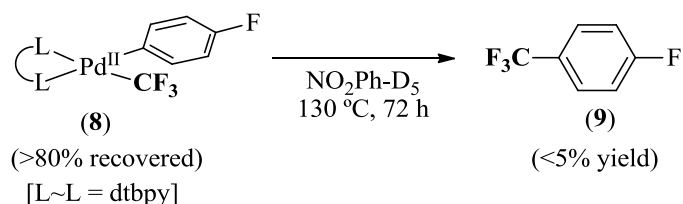
Herein, we report a density functional theory (DFT) study of C–OAc bond-forming reductive elimination from a series of different Pd^{IV}, Pd^{III}, and Pd^{II} complexes. Both the three-membered transition state **3** and the five-membered transition state **4** have been evaluated for each of these reactions. In all cases, we calculate a large energetic preference for carbonyl participation in reductive elimination via the five-membered transition state **4**.

5.2 Results and Discussions

5.2.1 Experimental Rational for Computational Studies

All experimental results were obtained by Dr. Nicholas Ball and Yingda Ye in our lab.^{31,139} A brief overview of the key results will be highlighted to provide context to computational analysis below.^{31,139} Initial studies began by the synthesis of complexes with the general form [(dtbpy)Pd^{II}(aryl)(CF₃)]. These complexes were found to be quite thermally stable and resistant to reductive elimination (<5% aryl–CF₃ coupling) as expected based on the known stability of Pd^{II}–CF₃ complexes (Scheme 5.3).

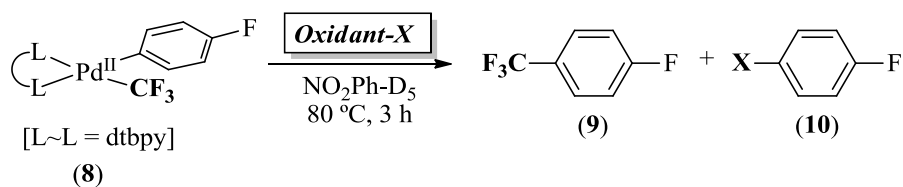
Scheme 5.3 Oxidative Aryl–X versus Aryl–CF₃ Bond Formation.



My coworkers reasoned that modifying the metal oxidation state to Pd^{IV} might facilitate the desired reactivity given our group's success in promoting Aryl–X coupling (X = Cl, Br, I, F, OR) through high oxidation state Pd intermediates.^{42-52,54-58,71} Treatment with common oxidants (*N*-bromosuccinimide (NBS), *N*-chlorosuccinimide

(NCS), and $\text{PhI}(\text{OAc})_2$) resulted in the formation of Aryl–X products (**10**) (Table 5.1). In an effort to eliminate the undesired Aryl–X bond formation, electrophilic fluorinating reagents (F^+) were employed due to the known difficulty in achieving Aryl–F reductive elimination (Table 5.1).⁴⁵

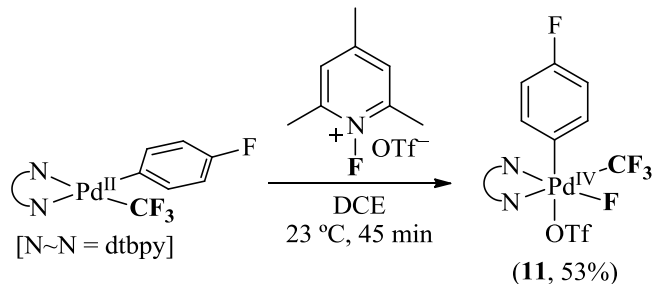
Table 5.1 Oxidative Aryl–X versus Aryl– CF_3 Bond Formation.



Oxidant–X	Yield 9	Yield 10 (X)
	<5%	75% (Br)
	<5%	70% (Cl)
	<5%	20% (OAc)
	70%	<5%

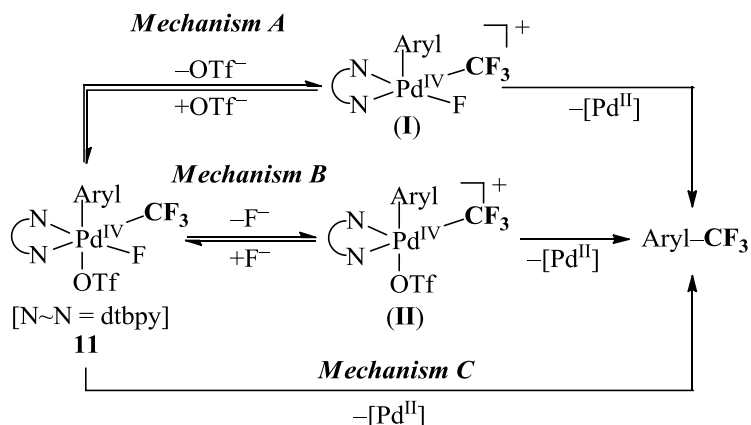
With an electrophilic fluorinating reagent (N-fluoro-1,3,5-trimethylpyridinium triflate (NFTPT)), the desired Aryl– CF_3 coupling product (**9**) was formed in good yield. Other F^+ sources were also effective in promoting this transformation. Interestingly, lowering the temperature to room temperature allowed for the isolation of a Pd^{IV} intermediate (**11**, Scheme 5.4).

Scheme 5.4 Pd^{IV} Intermediate Isolation.



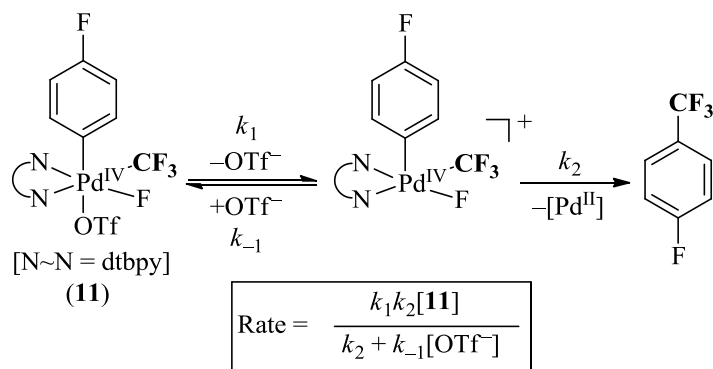
Three mechanisms were envisioned for formation of an Aryl-CF₃ product from the Pd^{IV} intermediate (Scheme 5.5). Mechanism A involves the pre-equilibrium loss of triflate to generate a five-coordinate intermediate, which could then undergo bond forming reductive elimination. Mechanism B is a similar proposal with pre-equilibrium loss of a fluoride ion followed by reductive elimination. Mechanism C involves the direct reductive elimination from the six-coordinate intermediate.

Scheme 5.5 Proposed Mechanisms for Aryl-CF₃ Reductive Elimination.



With the inverse first order kinetics in triflate and the addition of NBu₄PF₆ enhancing the rate of Aryl-CF₃ bond formation, Mechanism A was proposed as the most likely pathway responsible for product formation. The mechanism and kinetic equation (derived using the steady state approximation for the cationic intermediate) is shown below in Scheme 5.6.

Scheme 5.6 Proposed Mechanism for Aryl–CF₃ Reductive Elimination.



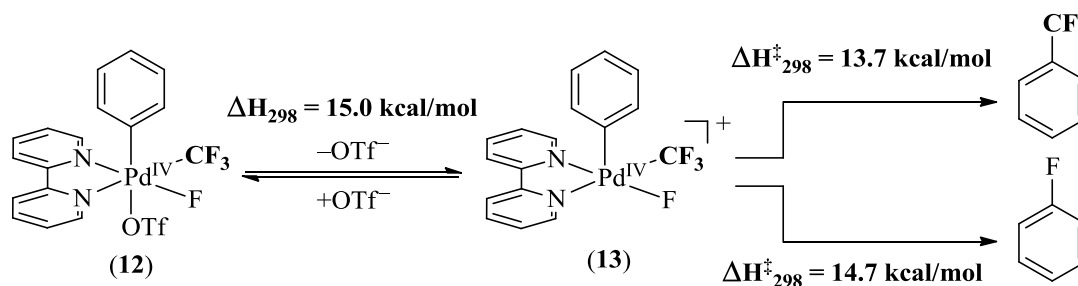
Using initial rate studies as a function of temperature, an Eyring plot showed that ΔH^\ddagger was 29.1 ± 0.2 kcal/mol and the ΔS^\ddagger was $+9.48 \pm 0.8$ eu. Also, electron rich aromatic groups were found to undergo faster reductive elimination.

5.2.2 DFT calculations – Aryl–CF₃ Coupling.

While the experimental data was consistent with Mechanism A (Scheme 5.5), the nature of the fundamental reductive elimination step was elusive. Given the multistep reaction sequence, the observation of enhanced reaction rates from isolated Pd^{IV} complexes with electron rich aromatic systems could be the result of the changing the kinetics or thermodynamics of the loss of triflate or an electronic effect in the fundamental Aryl–CF₃ bond forming step. In order to deconvolute these effects, we turned to density functional theory (DFT) calculations to more fully explore the mechanism of Aryl–CF₃ bond formation. The complex [(bpy)Pd^{IV}(Ph)(CF₃)(F)(OTf)] (**12**) (bpy = 2,2'-bipyridyl, Scheme 5.6) was employed as a model for **11** (Scheme 5.4), and the CEP-31G(d) basis set^{140,141} and M06¹⁴² functional (chosen due to the functional success in related late transition metal organometallic complexes)¹⁴³⁻¹⁴⁷ were used along with a single point solvent correction in nitrobenzene (SMD solvation model).¹⁴⁸ As

shown in Scheme 5.7, the calculated ΔH_{298} for loss of OTf^- from **12** in nitrobenzene to form cationic intermediate ($[(\text{bpy})\text{Pd}^{\text{IV}}(\text{Ph})(\text{CF}_3)(\text{F})]^+$ (**13**)) is 15.0 kcal/mol. Furthermore, the activation enthalpy (ΔH_{298}^\ddagger) for $\text{Ph}-\text{CF}_3$ bond-forming reductive elimination from **13** is 13.7 kcal/mol. Thus, we calculate that mechanism **A** has an overall ΔH_{298}^\ddagger of 28.7 kcal/mol, which is in excellent agreement with the experimental value ($+29.1 \pm 0.2$ kcal/mol, *vide supra*).

Scheme 5.7 Calculated Reductive Elimination Pathway Calculated Energies.

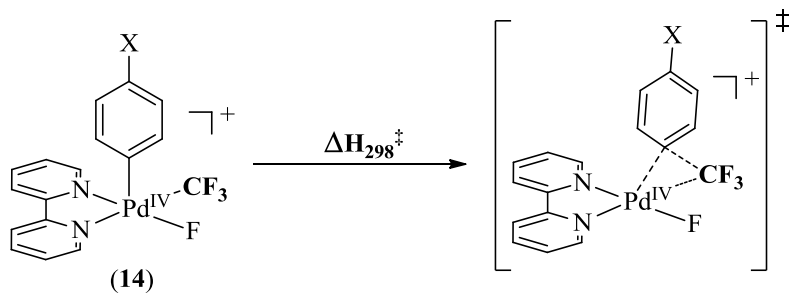


As discussed above, we observe experimentally that trifluoromethylated products are formed selectively over the corresponding fluorinated compounds. To gain further insights into this selectivity, we used DFT to examine the transition state for $\text{Ph}-\text{F}$ bond-forming reductive elimination from intermediate **13**. As shown in Scheme 5.7, ΔH_{298}^\ddagger for $\text{Ph}-\text{F}$ coupling is 14.7 kcal/mol. As such, this is a higher energy pathway than $\text{Ph}-\text{CF}_3$ bond-formation ($\Delta\Delta H_{298}^\ddagger = 1$ kcal/mol), consistent with the experimental results.

The calculated charge distribution of intermediate **13** using Natural Bond Order (NBO)¹⁴⁹⁻¹⁵³ analysis indicates that the CF_3 carbon carries a significant positive charge (+1.18), while the α -carbon of the phenyl ligand bears a charge of +0.07. The ground state structure of the analogous CH_3 complex ($[(\text{bpy})\text{Pd}^{\text{IV}}(\text{Ph})(\text{CH}_3)(\text{F})]^+$) has calculated charges of -0.58 and +0.06 on the CH_3 and Ph carbons, respectively. This charge difference is amplified in the transition state for $\text{C}-\text{CF}_3$ bond-forming reductive

elimination, where the CF₃ carbon carries an enhanced positive charge of +1.24, and the charge on the Ph carbon decreases to -0.11. These data imply that the Ph group is acting as the nucleophile during the bond-forming event. This is in sharp contrast to other reports of reductive elimination from Pd^{IV} in which the aryl or alkyl ligand typically serves as the electrophilic coupling partner.^{42-52,54-58,71}

We next used DFT to determine the transition state enthalpies (ΔH_{298}^\ddagger) for Aryl-CF₃ coupling from complexes of general structure [(bpy)Pd^{IV}(*p*-XC₆H₄)(CF₃)(F)]⁺. As expected based on the NBO analysis, ΔH_{298}^\ddagger was smallest with electron donating *para* substituents (X) on the aromatic ring, consistent with a transition state involving electrophilic attack by the CF₃ moiety on the arene (Table 5.2). Furthermore, the ΔH_{298}^\ddagger values showed better correlation with Hammett σ^+ values for X than the corresponding σ or σ^- parameters ($\rho^+ = -0.79$; $R^2 = 0.84$). This implicates significant resonance effects in the transition state for Aryl-CF₃ coupling since much poorer correlation were observed with σ and σ^- ($\rho = -1.17$; $R^2 = 0.57$; $\rho^- = -0.86$ and $R^2 = 0.52$).

Table 5.2 Gas Phase Values of $\Delta H_{298}^{\ddagger}$ for C–CF₃ Bond-Formation from

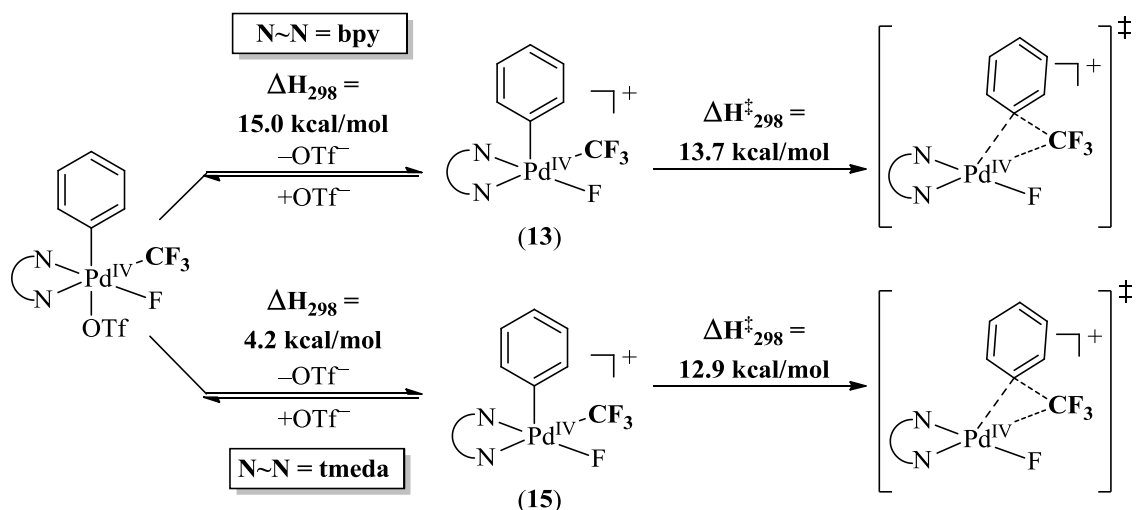
X	$\Delta H_{298}^{\ddagger}$ (kcal/mol)	σ^+
NMe ₂	6.89	-1.70
NH ₂	7.10	-1.30
OH	7.71	-0.92
OMe	7.86	-0.78
SMe	7.79	-0.60
Me	9.19	-0.30
F	8.41	-0.07
H	9.41	0
CF ₃	9.43	0.53
CN	9.23	0.71
NO ₂	9.23	0.78

^a Complexes are calculated using CEP-31G(d)/M06 level of theory.

Finally, we sought to identify supporting ligands that would lower the energy barrier for Ph–CF₃ bond-forming reductive elimination in this system. Literature studies have shown that (tmeda)Pd^{IV}(CH₃)₂(Ph)(I) (tmeda = tetramethylethylenediamine) is significantly more reactive towards C–C bond-forming reductive elimination than its bipyridine analogue (bpy)Pd^{IV}(CH₃)₂(Ph)(I).¹⁵⁴ Thus, we hypothesized that using tmeda in place of dtbpy in our system might impart a similar effect. Consistent with this hypothesis, DFT calculations show that the nitrobenzene solvent-corrected transition state

enthalpy (ΔH_{298}^\ddagger) for formation of trifluorotoluene from $[(\text{tmeda})\text{Pd}^{\text{IV}}(\text{Ph})(\text{CF}_3)(\text{F})]^+$ is 0.8 kcal/mol lower than that for the analogous bpy complex (12.9 versus 13.7 kcal/mol) (eq. 9). Furthermore, ΔH_{298} for the loss of OTf^- from $[(\text{tmeda})\text{Pd}^{\text{IV}}(\text{Ph})(\text{CF}_3)(\text{F})(\text{OTf})]$ is >10 kcal/mol lower than that from **12** (4.2 versus 15 kcal/mol). Thus, the calculated overall ΔH_{298}^\ddagger for reductive elimination from the tmeda complex is 17.1 kcal/mol, suggesting that Aryl- CF_3 coupling should proceed at significantly lower temperatures than from **12**.

Scheme 5.8 Calculated Reductive Elimination Pathway for bpy versus tmeda.



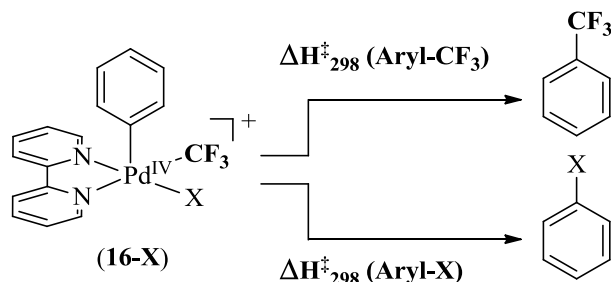
Consistent with calculations, replacing bpy with tmeda in the experimental system resulted in efficient bond formation at room temperature.

5.2.3 Comparison of CF_3 versus Cl and OAc Reductive Elimination

We next wanted to expand our study of Aryl- CF_3 coupling in **16** with other X ligands (Table 5.3). When comparing Cl versus CF_3 , the Aryl- Cl reductive elimination was found to be the kinetically preferred pathway by 7.8 kcal/mol, consistent with experimental observations (Table 5.1). When comparing OAc versus CF_3 , the Aryl- CF_3

reductive elimination was found to be the kinetically preferred pathway by 3.4 kcal/mol, which was inconsistent with experimental observations (Table 5.1).

Table 5.3 Competing Aryl–CF₃ versus Aryl–X Reductive Elimination.



X	ΔH^\ddagger_{298} (Aryl-CF ₃)	ΔH^\ddagger_{298} (Aryl-X)	Difference (Preferred)
Cl	13.9	6.1	7.8 (Aryl-X)
OAc	7.5	10.9	3.4 (Aryl-CF ₃)

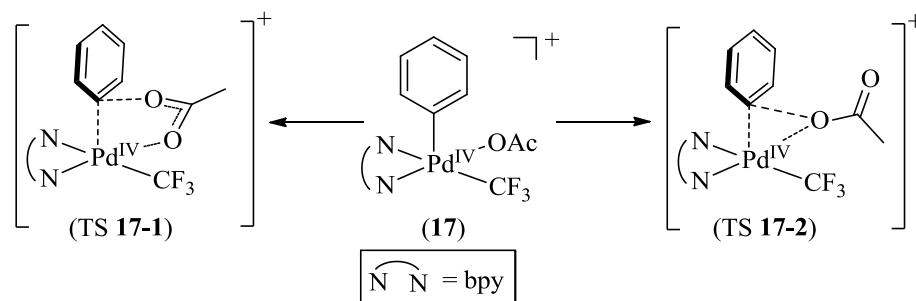
^a Complexes are calculated using CEP-31G(d)/M06 level of theory. Energy in kcal/mol.

Given the incorrect chemoselectivity predicted by our calculations for acetate (Table 5.3), we wanted to analyze this system in greater detail.

5.2.4 Aryl–O₂CR bond-forming reductive elimination with [(bpy)Pd(Ph)(CF₃)(O₂CR)]⁺.

We first compared three- and five-membered transition states **3** and **4** for Ph–OAc coupling from [(bpy)Pd(Ph)(CF₃)(OAc)]⁺ (bpy = 2,2'-bipyridine) **17** (Figure 4).¹⁵⁵ Again, these calculations were performed in Gaussian09 using density functional theory (DFT) in the gas phase with the CEP-31G(d) basis set^{140,141} and M06 functional.¹⁴² Solvent corrections (SMD solvation model)¹⁴⁸ were conducted with both non-polar (dichloromethane) and polar (acetonitrile) solvents¹⁴⁷ using default parameters.

Scheme 5.9 Five-membered (**17-1**) and three-membered (**17-2**) transition states for reductive elimination from [(bpy)Pd(Ph)(CF₃)(OAc)]⁺ (**17**).



The optimized geometries of the two transition states for Ph–OAc coupling from **17** are shown in Scheme 5.9 (**17-1** and **17-2**, respectively). The activation energy (ΔG_{298}^\ddagger) for converting complex **17** to transition state **17-1** in the gas phase is 3.8 kcal/mol, while the corresponding value to form **17-2** is 12.3 kcal/mol. This corresponds to a gas phase energy difference ($\Delta\Delta G_{298}^\ddagger$) of approximately 8 kcal/mol favoring the five-membered transition state. The observed transition state energy for Aryl–CF₃ coupling (Table 5.3) was 7.5 kcal/mol. Thus, the consideration of the 5-membered transition state now predicts the correct product distribution observed in the experimental system (Table 5.1) in which Aryl–acetate coupling is observed over Aryl–CF₃ coupling.

Given this newly observed transition state responsible for Aryl–acetate coupling (**17-1**), we wanted to investigate these two transition states (3-membered versus 5-membered) for carboxylate coupling to understand the generality of this mechanism. As shown in Table 5.4, solvent corrections in dichloromethane and acetonitrile changed the transition state energies but maintained a large preference (9–13 kcal/mol) for the carbonyl-participation transition state **17-1**. Notably, $\Delta\Delta G_{298}^\ddagger$ was calculated to be largest in the polar medium of acetonitrile.

Table 5.4 Calculated energies for C–O bond-forming reductive elimination from complexes **17** and **18** via three-membered and five-membered transition states.

TS	$\Delta H_{298}^{\ddagger}$	$\Delta G_{298}^{\ddagger}$	$\Delta G_{298}^{\ddagger}(\text{CH}_2\text{Cl}_2)$	$\Delta G_{298}^{\ddagger}(\text{CH}_3\text{CN})$
[(bpy)Pd(Ph)(CF ₃)(OAc)] ⁺ (17)				
5-mem 17-1	3.1	3.8	3.1	2.3
5-mem 17-2	10.9	12.3	12.5	15.0
Difference	7.8	8.5	9.4	12.7
[(bpy)Pd(Ph)(CF ₃)(tfa)] ⁺ (18)				
5-mem 18-1	4.1	4.9	5.6	6.6
5-mem 18-2	12.6	12.7	14.7	16.3
Difference	8.5	7.8	9.1	9.7

$\Delta H_{298}^{\ddagger}$ and $\Delta G_{298}^{\ddagger}$ are zero point energy corrected gas phase enthalpies and Gibbs free energies. $\Delta G_{298}^{\ddagger}(\text{CH}_2\text{Cl}_2)$ and $\Delta G_{298}^{\ddagger}(\text{CH}_3\text{CN})$ are solvent corrected values at the gas phase geometries (in kcal/mol).

In an effort to explain the kinetic preference for **17-1**, we conducted a geometric analysis of the two transition states (Table 2). The most striking difference between **17-1** and **17-2** is the length of the aryl-oxygen bond (C–O_A) that is being formed (2.33 Å versus 2.11 Å, respectively). The significantly shorter C–O bond in **17-2** indicates that this is a much later transition state with more C–O bonding character. Transition state **17-2** also has slightly longer Pd–O and Pd–C_{Aryl} bonds than **17-1** (Table 2), further consistent with **A-2** as the more product-like transition structure.

Table 5.5 Selected bond distances (Å) for structures **17**, **17-1**, **17-2** and **18**, **18-1**, **18-2**.

TS **17-1**; R=CH₃
TS **18-1**; R=CF₃

TS **17-2**; R=CH₃
TS **18-2**; R=CF₃

Structure	Pd-C	Pd-O _B /O _A	C-O _A
17	2.06	2.00	2.92
17-1	2.17	2.04	2.33
17-2	2.21	2.06	2.11
18	2.07	2.01	2.90
18-1	2.19	2.05	2.35
18-2	2.25	2.08	2.08

The movement of the atoms in transition states **17-1** and **17-2** is also quite different. In the three-membered transition state **17-2**, the plane of the aryl ring effectively slides down the Pd–OAc bond causing a large distortion of the C–Pd–O bond angle from 91.9° in **17** to 59.1° in **17-2**. In contrast, in **17-1** the aryl ring tilts away from the incoming oxygen atom as the carbonyl oxygen attacks the aromatic π -system, resulting in widening of the C–Pd–O bond angle from 91.9° to 94.5°. This wider angle appears to facilitate nucleophilic attack of the pendant carbonyl ligand on the aromatic π -system in this five-membered transition state. All of these factors likely contribute to a lower energy process for C–O bond formation.

Related transition states were also calculated for [(bpy)Pd(Ph)(CF₃)(tfa)]⁺ (**18**) where the acetate has been substituted for a less nucleophilic trifluoroacetate ligand (tfa). From **18**, the gas phase activation energy to form the three-membered transition state (**18-**

2) is 12.7 kcal/mol, while that for the five-membered transition state (**18-1**) is 4.9 kcal/mol (Table 5.4). Thus, the gas phase preference for the five-membered transition state in this system (~8 kcal/mol) is nearly identical to that for acetate complex **17**. This data suggests that the electronic nature of the carboxylate has an influence on the overall activation energies for C–O bond-forming reductive elimination but maintains a significant preference for the 5-membered transition structure.

Similar to the results with **17-2/17-1**, transition state **18-2** has a significantly shorter C_{Aryl}–O bond than in **18-1** (2.08 versus 2.35 Å, Table 5.5). Furthermore, the Pd–C_{Aryl} and Pd–O bonds are longer in the three-membered versus five-membered transition state by 0.06 and 0.03 Å, respectively. These results suggest that the three-membered transition state is later and more product-like in the trifluoroacetate system as well.

5.2.5 Examination of known C–OAc bond-forming reactions from Pd^{IV}, Pd^{III}, and Pd^{II}.

We next conducted DFT studies to probe the preferred pathway for C–OAc bond-forming reductive elimination from three different Pd complexes with varied oxidation states and structures. These systems – Pd^{IV} cyclometallated species,^{68,46} Pd^{III}-dimers,^{121,122} and Pd^{II} π-allyl complexes¹²³⁻¹²⁶ – were all selected based on experimental reports of C–OAc coupling under mild conditions.

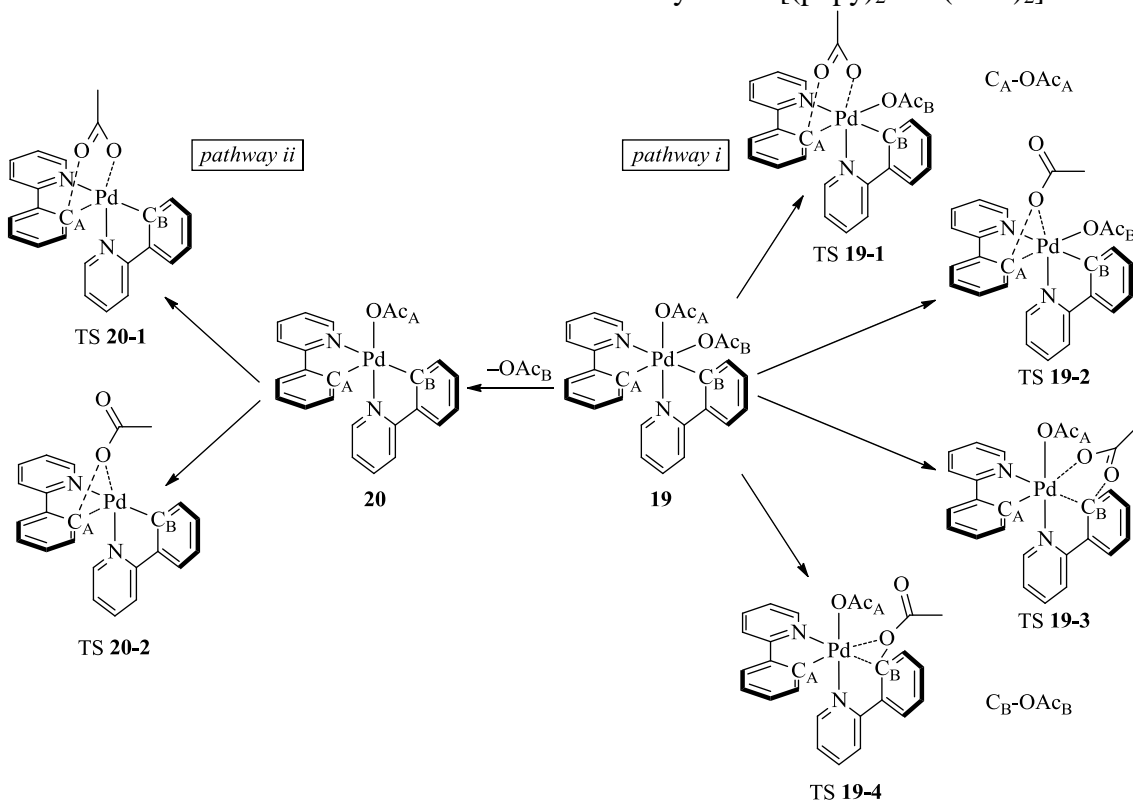
Table 5.6. Calculated Energies for C–O Reductive Elimination from **19–23**.

TS	ΔH_{298}^\ddagger	ΔG_{298}^\ddagger	$\Delta G_{298}^\ddagger(\text{CH}_2\text{Cl}_2)$	$\Delta G_{298}^\ddagger(\text{CH}_3\text{CN})$
[(phpy) ₂ Pd ^{IV} (OAc) ₂] (19)				
5-mem 19-1	14.9	15.8	16.2	15.8
3-mem 19-2	26.0	26.8	25.7	25.4
Difference	11.1	11.0	9.5	9.6
[(phpy) ₂ Pd ^{IV} (OAc) ₂] (19)				
5-mem 19-3	13.2	15.2	16.5	16.5
3-mem 19-4	25.5	25.2	25.3	25.0
Difference	12.3	10.0	8.8	8.5
[(phpy) ₂ Pd ^{IV} (OAc)] ⁺ (20)				
5-mem 20-1	2.1	4.5	3.7	4.5
3-mem 20-2	16.0	17.7	19.3	20.2
Difference	13.9	13.2	15.6	15.7
[{(phpy)Pd(OAc)} ₂ (μ-OAc) ₂] (21)				
5-mem 21-1	6.5	5.3	11.1	8.5
3-mem 21-2	11.2	11.8	16.5	14.8
Difference	4.7	6.5	5.4	6.3
[{(phpy)Pd(OAc)}(μ-OAc) ₂ {(phpy)Pd}] ⁺ (22)				
5-mem 22-1	0.3	1.0	5.2	5.9
3-mem 22-2	9.4	9.4	12.4	11.3
Difference	9.1	8.4	7.2	5.4
[Pd(bq)(allyl)(OAc)] (23)				
5-mem 23-1	0.6	3.9	4.1	3.4
3-mem 23-2*	13.6	15.6	13.4	12.2
Difference	13.0	11.7	9.2	8.8

*-transition state is not an optimized structure and contains geometric constraints. ΔH_{298}^\ddagger and ΔG_{298}^\ddagger are zero point energy corrected gas phase enthalpies and Gibbs free energies. $\Delta G_{298}^\ddagger(\text{CH}_2\text{Cl}_2)$ and $\Delta G_{298}^\ddagger(\text{CH}_3\text{CN})$ are solvent corrected values at the gas phase geometries (in kcal/mol).

We first examined the bis-cyclometallated Pd^{IV} compound [(phpy)₂Pd^{IV}(OAc)₂] (phpy = 2-phenylpyridine), (**19**). As shown in Scheme 1, reductive elimination from **19** could proceed by at least two different pathways: (i) direct C–OAc bond-formation from the six-coordinate starting material (**19**) or (ii) pre-equilibrium dissociation of an acetate ligand to form cationic, five-coordinate complex **20**, followed by C–OAc coupling. Computational studies by Fu *et al*¹²⁹ proposed the direct pathway *i* for this transformation, while a recent experimental paper from our group provided data consistent with pathway *ii*.⁴⁶ Based on these two proposals, our calculations have probed the C–O bond-forming step from both six-coordinate complex **19** and 5-coordinate intermediate **20**.

Scheme 5.10 Reductive Elimination Pathways from [(phpy)₂Pd^{IV}(OAc)₂].

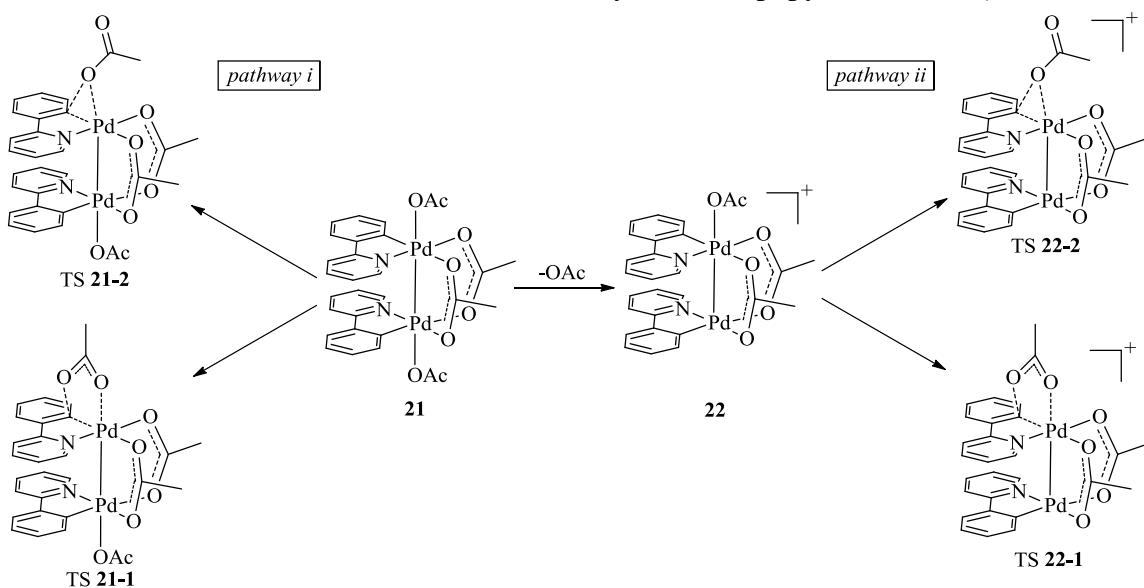


In considering pathway *i*, we noted that complex **19** contains two chemically different σ -aryl ligands and two chemically different acetates. This inequivalency means that reductive elimination could potentially proceed by coupling of C_A with OAc_A , C_B with OAc_B , or C_B with OAc_A . We were unable to locate a transition state for coupling between C_B and OAc_A , likely due to the requirement for reductive elimination to occur by attack of the acetate on the aromatic π -system, which is not geometrically possible for these coupling partners. For the other two possibilities, we identified both three- and five-membered transition states. As shown in Table 3, the five-membered transition state is favored in both cases by 8-11 kcal/mol in the gas phase and in CH_3CN and CH_2Cl_2 solutions. Notably, these calculations indicate that coupling of C_A with OAc_A (transition state **19-1**) versus C_B with OAc_B (transition state **19-3**) are virtually isoenergetic in this system.

Reductive elimination via pathway *ii* could proceed from **20** by coupling of C_A with OAc_A or of C_B with OAc_A . Similar to the reactions of **19** (*vide supra*), no transition state could be located for C_B - OAc_A bond-formation, again presumably due to geometric requirements of the Aryl-O coupling reaction. For bond-formation between C_A and OAc_A from **20** (Scheme 5.10), we optimized two distinct transition states. The gas phase activation energy for proceeding from **20** to the three-membered transition structure (**20-2**) is calculated to be 17.7 kcal/mol, while that to the analogous five-membered transition state (**20-1**) is 4.5 kcal/mol. Thus, these calculations show a large energetic preference for carbonyl participation in reductive elimination from Pd^{IV} complex $[(\text{phpy})_2Pd^{IV}(OAc)_2]$ for all viable C-O coupling partners in both pathways *i* and *ii*.

Recently, Ritter and coworkers demonstrated that the Pd^{III} dimer **21**¹²¹ (Scheme 5.11) undergoes clean and high yielding Aryl–OAc bond-forming reductive elimination at 40 °C. We next sought to computationally examine the C–O bond-forming step in this transformation. Based on literature precedent,^{122,147} two pathways were considered for this C–O coupling reaction: (i) direct C–O coupling from the neutral dimer **21** and (ii) pre-equilibrium acetate dissociation followed by reductive elimination from cationic intermediate **22** (Scheme 5.9).

Scheme 5.11 Reductive Elimination Pathways from $[\{(ph\acute{y})Pd(OAc)}_2(\mu-OAc)_2]$.

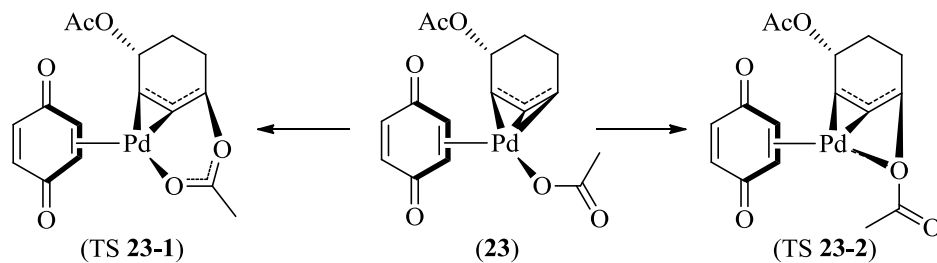


For pathway *i*, two transition states were optimized with the apical acetate serving to form the Aryl–OAc bond from the Pd^{III}-Pd^{III} starting material $[\{(ph\acute{y})Pd(OAc)}_2(\mu-OAc)_2]$ **21** (Scheme 5.11). The three-membered transition state (**21-2**) has a ΔG^\ddagger_{298} of 11.8 kcal/mol, while the analogous five-membered transition state is considerably lower in energy ($\Delta G^\ddagger_{298} = 5.3$ kcal/mol). Analogous results were found for reductive elimination from cationic dimer **22** [with ΔG^\ddagger_{298} for **22-2** of 9.4 kcal/mol and a substantially lower value of 1.0 kcal/mol for **22-1**]. Thus, while acetate dissociation has a

significant influence on the relative activation energies, our data show that the five-membered transition state (**21-1/22-1**) is favored by ~6 kcal/mol for all calculated reductive elimination pathways from these Pd^{III} dimers.

Finally, we examined C–OAc bond-forming reductive elimination from the Pd^{II} allyl complex [Pd(bq)(allyl)(OAc)] (**23**) (bq = benzoquinone; allyl = trans-4-acetoxycyclohexane, Scheme 5.12). This compound is a proposed intermediate in the Pd(OAc)₂-catalyzed reaction of 1,3-hexadiene with LiOAc and benzoquinone at room temperature.¹²⁵ Studies of the stereochemistry of reductive elimination under these conditions indicate that the acetate ligand reacts with the allyl moiety from the metal center (rather than via external attack). Indeed, in this paper the authors propose a five-membered transition state like **23-1** (Scheme 3) for the C–O bond-forming event.

Scheme 5.12 Reductive Elimination Transition states from [Pd(bq)(allyl)(OAc)].



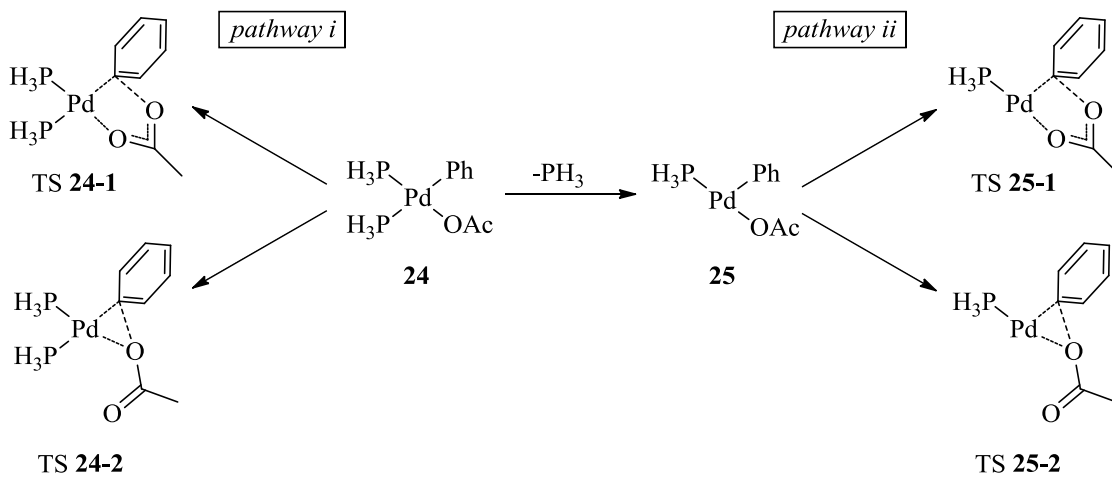
We are only able to locate a single transition state (five-membered structure **23-1**) for C–O coupling from **23**, with a gas phase ΔG_{298}^\ddagger of 3.9 kcal/mol. Optimization of the corresponding three-membered transition state (**23-2**) required constraints on both the Pd–OAc and C–O bond distances. One structure was identified that possessed a single imaginary frequency (-267 cm^{-1}) and had a ΔG_{298}^\ddagger of 15.6 kcal/mol. However, all attempts to release the constraints on this molecule resulted in conversion to **23-1** within ~5-10 geometric steps. On this basis, we can only estimate the energy difference between

these two structures to be approximately 10 kcal/mol. Interestingly, this reductive elimination energy (~16 kcal/mol) is strikingly similar to a previous study by Szabó,¹⁵⁶ in which the transition state energy for C–Cl reductive elimination from [Pd(bq)(allyl)(Cl)] was calculated to be 15 kcal/mol.

5.2.6 Comparison of C–OAc and C–OR bond-forming reductive elimination at Pd^{II}.

A final set of investigations focused on C–OAc coupling from the Pd^{II} complex (PH₃)₂Pd^{II}(Ph)(OAc) (**24**). To our knowledge, such phosphine Pd^{II} compounds are not experimentally known to undergo carbon–acetate bond-forming reductive elimination reactions; however, they do participate in well-studied carbon–alkoxide couplings.^{64,97,101,107,109,110,127} As such, this system provided an opportunity to directly compare these different C–O bond-forming reactions. There are two possible pathways for reductive elimination from **24**: (i) direct C–O bond-formation from the square planar starting material or (ii) dissociation of phosphine to form three-coordinate **I** followed by C–O coupling (Scheme 5.13).

Scheme 5.13 Reductive Elimination Pathways from (PH₃)₂Pd^{II}(Ph)(OAc) (**24**) and (PH₃)Pd^{II}(Ph)(OAc) (**25**)



Two transition states (**24-1** and **24-2**) were optimized for the direct reductive elimination pathway (*i*) from **24**. As summarized in Table 4, the gas phase activation energies for C–OAc bond-formation in this system (23.4 kcal/mol for **24-1** and 36.6 kcal/mol for **24-2**) are significantly higher than those for complexes **17–23**. Nonetheless, the five-membered transition state **24-1** was still favored (by approximately 13 kcal/mol in the gas phase). Nearly identical values were observed for C–OAc coupling from 3-coordinate complex **25** (Table 5.7).

For comparison, we examined $\Delta G_{298}^{\ddagger}$ for C–O bond-forming reductive elimination from the analogous alkoxide complexes $(\text{PH}_3)_2\text{Pd}^{\text{II}}(\text{Ph})(\text{OMe})$ (**26**) and $(\text{PH}_3)\text{Pd}^{\text{II}}(\text{Ph})(\text{OMe})$ (**27**). As discussed above, analogous $\text{Pd}^{\text{II}}(\text{Aryl})(\text{alkoxide})$ adducts are well-known to undergo C–O coupling via putative three-membered transition states.^{64,97,101,107,109,110 127} These studies revealed that $\Delta G_{298}^{\ddagger}$ for C–OMe coupling from **26** is 18.1 kcal/mol while the analogous value from **27** is 11.4 kcal/mol. Thus, the alkoxide reductive elimination is calculated to be significantly faster than acetate reductive elimination from Pd^{II} , consistent with experimental observations.

Table 5.7 Calculated Energies for C–O Reductive Elimination from **24** and **25**.

TS	ΔH_{298}^\ddagger	ΔG_{298}^\ddagger	$\Delta G_{298}^\ddagger(\text{CH}_2\text{Cl}_2)$	$\Delta G_{298}^\ddagger(\text{CH}_3\text{CN})$
[Pd(PH ₃) ₂ (Ph)(OAc)] (24)				
5-mem 24-1	23.5	23.4	27.8	28.1
3-mem 24-2	36.3	36.6	39.5	39.3
Difference	12.8	13.2	11.7	11.2
[Pd(PH ₃)(Ph)(OAc)] (25)				
5-mem 25-1	24.9	25.1	27.8	28.1
3-mem 25-2	38.0	38.1	39.1	39.2
Difference	13.1	13.0	11.3	11.1

ΔH_{298}^\ddagger and ΔG_{298}^\ddagger are zero point energy corrected gas phase enthalpy and Gibbs free energies. $\Delta G_{298}^\ddagger(\text{CH}_2\text{Cl}_2)$ and $\Delta G_{298}^\ddagger(\text{CH}_3\text{CN})$ are solvent corrected values at the gas phase geometries (in kcal/mol).

5.3 Conclusions

Using DFT calculations, we were able to determine that Mechanism A is most likely operable from an isolated [(dtbpy)Pd^{II}(aryl)(CF₃)(F)(OTf)] complex (pre-equilibrium loss of triflate followed by reductive elimination) to form Aryl–CF₃ reductive elimination products. Through these calculations, we have identified that the aryl group acts as the nucleophilic coupling partner during reductive elimination, in sharp contrast to other reports of reductive elimination from Pd^{IV} in which the aryl or alkyl ligand typically serves as the electrophilic coupling partner.^{42-52,54-58,71} Also, calculations show that tmeda substitutions for bpy lower overall reaction barriers for triflate loss, allowing for efficient room temperature reductive elimination.

In comparing OAc versus CF₃ reductive elimination from [(bpy)Pd^{IV}(aryl)(CF₃)(OAc)]⁺, calculations incorrectly predicted Aryl–CF₃ coupling to be preferred, which was inconsistent with experiment. Using a new reductive elimination

mechanism (a 5-membered transition state) for C–O bond formation, we were able to correctly predict the selectivity observed experimentally. With this result, we expanded our studies to computationally analyze Aryl–carboxylate reductive elimination from Pd^{IV}, Pd^{III}, and Pd^{II} complexes. Although these reactions are well-precedented experimentally in both catalytic and stoichiometric contexts, until now little was known about the intimate mechanism of the C–O bond-forming step. Analogous Pd-mediated Aryl–alkoxide bond-forming reductive elimination reactions proceed via 3-membered transition states involving direct attack of the Pd-bound oxygen atom on the ipso carbon of the Pd–Aryl bond.^{64,97,101,107,109,110,127} A similar mechanism was assumed in one prior computational study of Aryl–carboxylate coupling.¹²⁹ However, the investigations detailed here implicate an alternative, lower energy pathway for sp²-carbon–carboxylate bond-forming reductive elimination involving participation of the pendant carbonyl oxygen. For all of the reactions studied, the 5-membered transition state was significantly lower in energy (by 4.7-13.2 kcal/mol) than the analogous 3-membered transition structure. While the activation barrier for this reductive elimination process changed significantly as a function of the oxidation state and ligand environment at the Pd center, the overall preferred pathway remained constant across all of the complexes examined. On this basis, we hypothesize that carbonyl participation via a 5-membered transition state may be a general mechanism responsible for sp² C–acetate reductive elimination reactions from Pd. This work adds to a growing set of studies implicating a nucleophilic role for pendant carbonyl groups in metal mediated reactions, including metal hydride reduction, C–H activation, and now reductive elimination. We anticipate that this concept could ultimately prove more broadly useful for enabling new transition

metal mediated bond-formations to incorporate other tethered oxygen, nitrogen, phosphorus or sulfur based nucleophiles.

5.4 Experimental Procedures

5.4.1 Computational Methods

Using the Gaussian 09 suite of programs,¹⁵⁷ all density functional theory (DFT) calculations were performed with the M06 functional¹⁴² along with the Stevens (CEP-31G) valence basis sets with effective core potentials.^{140,141} The CEP-31G basis sets are triple- ξ for Pd and double- ξ for all main group elements. A d-polarization function (see 6-31G*)^{158,159} was added to all non-hydrogen main group elements: $\xi_d = 0.8$ for carbon, nitrogen, oxygen, and fluorine, $\xi_d = 0.55$ for phosphorus, and $\xi_d = 0.65$ for sulfur (referred to as CEP-31G(d) level of theory). All geometries were optimized using CEP-31G(d)/M06 without symmetry constraints using the restricted Kohn-Sham formalism for all complexes.. All minima were confirmed by the absence of imaginary frequencies and all transition states were verified by visual inspection of the single imaginary frequency vibration and optimized along the reaction coordinate. Thermochemical data was calculated using unscaled vibrational frequencies and default parameters at 298.15 K and 1 atm. Solvent corrections were performed as single point calculations using the SMD model¹⁴⁸ with default settings at the optimized geometries from gas phase calculations. NBO analysis¹⁴⁹⁻¹⁵³ was used to determine relevant charge distribution in transition states.

5.4.2 XYZ coordinates – Calculated Structures

	16-Cl cation		
Pd	-0.37661800	-0.09481500	-0.70221100
C	1.64593200	-2.52882400	-0.60565900
C	2.53115200	-0.43623900	-0.00298700

C	2.90522600	-3.15710300	-0.47563500
H	0.74683200	-3.08185300	-0.90830800
C	3.82648600	-0.98663400	0.13745900
C	4.01301600	-2.36611100	-0.10525100
H	3.00126400	-4.22891600	-0.66730400
H	4.67877300	-0.36533000	0.42628900
H	5.00810700	-2.81040600	-0.00248600
C	0.59044200	2.69560500	0.34690000
C	2.22363200	1.00342000	0.26165300
C	1.52802500	3.65561100	0.78249400
H	-0.45824200	2.96830500	0.20675600
C	3.21638900	1.91414000	0.69260500
C	2.86885400	3.25591100	0.95483700
H	1.19903000	4.67957300	0.97648000
H	4.24989800	1.58199200	0.82381200
H	3.62943700	3.96752300	1.29062900
C	-1.33606500	-0.54775200	1.08084300
C	-2.71481200	-0.80434100	1.08396900
C	-0.48653700	-0.58787700	2.19706800
C	-3.28987500	-1.09251400	2.35114900
H	-3.32790400	-0.80120500	0.17984200
C	-1.10532500	-0.88214300	3.44367300
H	0.58957500	-0.40094800	2.14663600
C	-2.49449200	-1.13032000	3.51921000
H	-4.36488900	-1.29840100	2.39769200
H	-0.48046000	-0.90896800	4.34352800
H	-2.95507200	-1.35764200	4.48610600
C	-1.90851900	1.18366300	-1.24412400
F	-3.01928500	0.64773900	-1.72488400
F	-2.26769100	2.01444700	-0.24489100
F	-1.33712100	1.92800700	-2.21247500
N	0.92423600	1.41033100	0.08721500
N	1.47514600	-1.21110300	-0.37988100
Cl	-1.37952300	-1.84820800	-1.77754700

16-Cl Aryl-CF₃ ts

Pd	-0.10950100	-0.45367500	-0.26882500
C	2.20037700	-2.46923600	0.18845900
C	2.76586100	-0.19328300	0.38640600
C	3.49731200	-2.87436500	0.57358200
H	1.41555800	-3.19409500	-0.05944600
C	4.08059000	-0.52452500	0.78516100
C	4.45125000	-1.88345000	0.88247200
H	3.73322900	-3.94018300	0.62733600
H	4.80495400	0.25818900	1.02671900
H	5.46450100	-2.15672300	1.19300500

C	0.49187000	2.63517100	-0.22708400
C	2.29676400	1.21027300	0.23144000
C	1.30907800	3.78285400	-0.17361400
H	-0.57521200	2.73039300	-0.45240600
C	3.17864600	2.31455600	0.31011800
C	2.68178100	3.61770800	0.10895100
H	0.86860400	4.76687100	-0.35361300
H	4.24345000	2.15897200	0.50410300
H	3.35327200	4.48028400	0.15805900
C	-2.03429900	-0.00585400	0.54184000
C	-3.07597700	-0.95879500	0.58376000
C	-1.90540200	1.01958000	1.51068200
C	-3.99083200	-0.89757700	1.66327000
H	-3.18723800	-1.72526500	-0.18568100
C	-2.82511200	1.04962800	2.58568300
H	-1.11321700	1.77186000	1.47314900
C	-3.86878900	0.09643100	2.66146900
H	-4.79837200	-1.63579800	1.70958000
H	-2.71958800	1.82534200	3.35181500
H	-4.58465800	0.13459000	3.48906700
C	-1.78032600	0.50467600	-1.51608800
F	-2.68567500	-0.30755900	-2.01580900
F	-2.32548500	1.70666700	-1.29100100
F	-0.84936200	0.70817700	-2.47557100
N	0.96226400	1.38306400	-0.01974700
N	1.84931000	-1.16768100	0.09920800
Cl	-0.80243000	-2.56596400	-0.89468100

16-Cl Aryl-Cl ts

Pd	-0.32076700	-0.00034100	-0.71738400
C	1.75009000	-2.40852700	-0.88483600
C	2.56045000	-0.41769500	0.05942200
C	3.01537100	-3.03001300	-0.80098200
H	0.87914000	-2.92911800	-1.30393800
C	3.85895200	-0.96884100	0.18122200
C	4.08700000	-2.29211700	-0.25340700
H	3.14437000	-4.05430000	-1.16033500
H	4.68624600	-0.38073700	0.58802600
H	5.08581500	-2.73220200	-0.17087500
C	0.65835700	2.72196600	0.50012300
C	2.23504000	0.98255000	0.46992800
C	1.54783500	3.59459000	1.16165100
H	-0.34855900	3.05571700	0.24009200
C	3.17714100	1.79828700	1.13958800
C	2.83354900	3.12028100	1.49096900
H	1.22469200	4.60962600	1.40600000

H	4.16544400	1.40680800	1.39485900
H	3.55456500	3.75941000	2.00982000
C	-1.61384400	-0.96669500	0.79855600
C	-2.93127600	-0.53136500	0.99210100
C	-0.80849100	-1.63595200	1.73151800
C	-3.43073300	-0.66376400	2.31423400
H	-3.54899300	-0.12423800	0.18866300
C	-1.35111500	-1.74737100	3.04103900
H	0.17869400	-2.03794400	1.48967200
C	-2.64768500	-1.26220300	3.33061000
H	-4.44804500	-0.31529300	2.52346200
H	-0.74880900	-2.23331500	3.81668800
H	-3.05846400	-1.37426400	4.33909300
C	-1.74280800	1.35492900	-1.29551400
F	-2.81008200	0.86979200	-1.92401000
F	-2.19475100	2.11843900	-0.27581200
F	-1.09318500	2.17006400	-2.15098600
N	0.98492200	1.45381200	0.15962800
N	1.53291500	-1.14504300	-0.46227900
Cl	-1.52591200	-1.82993200	-1.46723900

16-CF₃ ts

Pd	0.11637800	0.25578800	-0.08843500
C	-1.95982800	2.17358800	1.09066300
C	-2.74697900	0.01585900	0.56569500
C	-3.22413200	2.56937800	1.57848400
H	-1.09107800	2.84246400	1.09762500
C	-4.04149500	0.33937800	1.03181900
C	-4.28084500	1.63429200	1.54186100
H	-3.36308700	3.57964300	1.97175100
H	-4.84697700	-0.40021100	1.00766200
H	-5.27647700	1.90396400	1.90762200
C	-0.66130100	-2.65013400	-0.88125800
C	-2.37594000	-1.31241400	0.00398600
C	-1.54818500	-3.71509600	-1.13960400
H	0.39600500	-2.73279500	-1.15644300
C	-3.32349200	-2.33893800	-0.21648400
C	-2.90651500	-3.55760300	-0.78961900
H	-1.17191500	-4.63094800	-1.60243200
H	-4.37531700	-2.18242900	0.03955800
H	-3.62986200	-4.35889400	-0.96912000
C	1.94895200	-0.49456800	0.70052200
C	2.87784300	0.46418100	1.15562200
C	1.83792700	-1.78184400	1.27805800
C	3.70412500	0.12103500	2.25453800
H	2.95688600	1.44844000	0.68919400

C	2.66502200	-2.09544300	2.38135400
H	1.13803600	-2.53572900	0.90639100
C	3.59986800	-1.14866500	2.86725900
H	4.42710800	0.85713600	2.62204300
H	2.57650200	-3.08232500	2.84837200
H	4.24476100	-1.40360900	3.71467200
C	1.87494400	-0.43717400	-1.39103100
F	2.73045200	0.54143500	-1.63164600
F	2.50930800	-1.61514600	-1.45407400
F	0.99694800	-0.46973400	-2.42173900
N	-1.05377500	-1.48884300	-0.31037800
N	-1.74409300	0.93882400	0.59789300
O	0.91033400	2.11404100	-0.03234800
C	0.45974800	2.76485600	-1.10982600
O	-0.37844700	2.28271100	-1.87579500
C	1.10521000	4.13559900	-1.28416500
H	2.08396200	3.99790700	-1.77562200
H	0.46772700	4.75838200	-1.92956500
H	1.28039500	4.62214700	-0.31126100

5.5 References

- (1) Kirk, K. L. *Org. Process Res. Dev.* **2008**, *12*, 305.
- (2) Purser, S.; Moore, P. R.; Swallow, S.; Gouverneur, V. *Chem. Soc. Rev.* **2008**, *37*, 320.
- (3) Ma, J. A.; Cahard, D. *Chem. Rev.* **2004**, *104*, 6119.
- (4) Ma, J.-A.; Cahard, D. *Chem. Rev.* **2008**, *108*, PR1.
- (5) Prakash, G. K. S.; Chacko, S. *Curr. Opin. Drug Discov. Dev.* **2008**, *11*, 793.
- (6) Shibata, N.; Mizuta, S.; Kawai, H. *Tetrahedron-Asymmetry* **2008**, *19*, 2633.
- (7) Grushin, V. V. *Accounts Chem. Res.* **2010**, *43*, 160.
- (8) Swartzs, F. *Bull. Acad. R. Belg.* **1892**, *24*, 415.
- (9) Henne, A. L.; Whaley, A. M.; Stevenson, J. K. *J. Am. Chem. Soc.* **1941**, *63*, 3478.
- (10) Furuta, S.; Kuroboshi, M.; Hiyama, T. *Bull. Chem. Soc. Jpn.* **1999**, *72*, 805.
- (11) Yang, J. J.; Kirchmeier, R. L.; Shreeve, J. M. *J. Org. Chem.* **1998**, *63*, 2656.
- (12) Kobayash, Y.; Kumadaki, I. *Tetrahedron Lett.* **1969**, 4095.
- (13) Kondratenko, N. V.; Vechirko, E. P.; Yagupolskii, L. M. *Synthesis* **1980**, 932.

- (14) Matsui, K.; Tobita, E.; Ando, M.; Kondo, K. *Chem. Lett.* **1981**, 1719.
- (15) Suzuki, H.; Yoshida, Y.; Osuka, A. *Chem. Lett.* **1982**, 135.
- (16) Urata, H.; Fuchikami, T. *Tetrahedron Lett.* **1991**, 32, 91.
- (17) Dubinina, G. G.; Furutachi, H.; Vicic, D. A. *J. Am. Chem. Soc.* **2008**, 130, 8600.
- (18) Dubinina, G. G.; Ogikubo, J.; Vicic, D. A. *Organometallics* **2008**, 27, 6233.
- (19) Chu, L. L.; Qing, F. L. *Org. Lett.* **2010**, 12, 5060.
- (20) Senecal, T. D.; Parsons, A. T.; Buchwald, S. L. *J. Org. Chem.* **2011**, 76, 1174.
- (21) Zhang, C. P.; Wang, Z. L.; Chen, Q. Y.; Zhang, C. T.; Gu, Y. C.; Xiao, J. C. *Angew. Chem., Int. Ed.* **2011**, 50, 1896.
- (22) Oishi, M.; Kondo, H.; Amii, H. *Chem. Commun.* **2009**, 1909.
- (23) Knauber, T.; Arikan, F.; Roschenthaler, G. V.; Goossen, L. J. *Chem. Eur. J.* **2011**, 17, 2689.
- (24) Hassan, J.; Sevignon, M.; Gozzi, C.; Schulz, E.; Lemaire, M. *Chem. Rev.* **2002**, 102, 1359.
- (25) Beccalli, E. M.; Brogini, G.; Martinelli, M.; Sottocornola, S. *Chem. Rev.* **2007**, 107, 5318.
- (26) Chen, X.; Engle, K. M.; Wang, D.-H.; Yu, J.-Q. *Angew. Chem., Int. Ed.* **2009**, 48, 5094.
- (27) McGlacken, G. P.; Bateman, L. M. *Chem. Soc. Rev.* **2009**, 38, 2447.
- (28) Daugulis, O.; Do, H.-Q.; Shabashov, D. *Accounts Chem. Res.* **2009**, 42, 1074.
- (29) Morrison, J. A. *Adv. Organomet. Chem.* **1993**, 35, 211.
- (30) Hughes, R. P. In *Adv. Organomet. Chem.*; Stone, F. G. A., Robert, W., Eds.; Academic Press: 1990; Vol. Volume 31, p 183.
- (31) Ball, N. D.; Kampf, J. W.; Sanford, M. S. *J. Am. Chem. Soc.* **2010**, 132, 2878.
- (32) Culkin, D. A.; Hartwig, J. F. *Organometallics* **2004**, 23, 3398.
- (33) Grushin, V. V.; Marshall, W. J. *J. Am. Chem. Soc.* **2006**, 128, 4632.
- (34) McReynolds, K. A.; Lewis, R. S.; Ackerman, L. K. G.; Dubinina, G. G.; Brennessel, W. W.; Vicic, D. A. *J. Fluor. Chem.* **2010**, 131, 1108.

- (35) Cho, E. J.; Senecal, T. D.; Kinzel, T.; Zhang, Y.; Watson, D. A.; Buchwald, S. L. *Science* **2010**, *328*, 1679.
- (36) Kitazume, T.; Ishikawa, N. *Chem. Lett.* **1982**, 137.
- (37) Current price for Xantphos = \$18,122/mol. Determined based on the largest quantity of Xantphos available from Sigma-Aldrich on March 17, 2011 (25 g/\$783.00).
- (38) Current price for Brettphos = \$99,195/mol. Determined based on the largest quantity of Brettphos available from Strem Chemicals on March 17, 2011 (5 g/\$924.00).
- (39) Price for the largest quantity of TESC₃ available from Sigma-Aldrich on March 17, 2011: 1 g/\$72.90, \$13,433/mol. Price for the largest quantity of TMSCF₃ available from Sigma-Aldrich on March 17, 2011: 25 mL/\$397.00, \$2,347/mol.
- (40) Wang, X. S.; Truesdale, L.; Yu, J. Q. *J. Am. Chem. Soc.* **2010**, *132*, 3648.
- (41) Ye, Y. D.; Ball, N. D.; Kampf, J. W.; Sanford, M. S. *J. Am. Chem. Soc.* **2010**, *132*, 14682.
- (42) Dick, A. R.; Kampf, J. W.; Sanford, M. S. *J. Am. Chem. Soc.* **2005**, *127*, 12790.
- (43) Whitfield, S. R.; Sanford, M. S. *J. Am. Chem. Soc.* **2007**, *129*, 15142.
- (44) Dick, A. R.; Remy, M. S.; Kampf, J. W.; Sanford, M. S. *Organometallics* **2007**, *26*, 1365.
- (45) Ball, N. D.; Sanford, M. S. *J. Am. Chem. Soc.* **2009**, *131*, 3796.
- (46) Racowski, J. M.; Dick, A. R.; Sanford, M. S. *J. Am. Chem. Soc.* **2009**, *131*, 10974.
- (47) Arnold, P. L.; Sanford, M. S.; Pearson, S. M. *J. Am. Chem. Soc.* **2009**, *131*, 13912.
- (48) Alsters, P. L.; Engel, P. F.; Hogerheide, M. P.; Copijn, M.; Spek, A. L.; Vankoten, G. *Organometallics* **1993**, *12*, 1831.
- (49) Lagunas, M. C.; Gossage, R. A.; Spek, A. L.; van Koten, G. *Organometallics* **1998**, *17*, 731.
- (50) van Belzen, R.; Elsevier, C. J.; Dedieu, A.; Veldman, N.; Spek, A. L. *Organometallics* **2003**, *22*, 722.
- (51) Canty, A. J.; Denney, M. C.; Patel, J.; Sun, H. L.; Skelton, B. W.; White, A. H. *J. Organomet. Chem.* **2004**, *689*, 672.
- (52) Canty, A. J.; Denney, M. C.; Skelton, B. W.; White, A. H. *Organometallics* **2004**, *23*, 1122.

- (53) Yamamoto, Y.; Kuwabara, S.; Matsuo, S.; Ohno, T.; Nishiyama, H.; Itoh, K. *Organometallics* **2004**, *23*, 3898.
- (54) Kaspi, A. W.; Yahav-Levi, A.; Goldberg, I.; Vigalok, A. *Inorg. Chem.* **2008**, *47*, 5.
- (55) Furuya, T.; Benitez, D.; Tkatchouk, E.; Strom, A. E.; Tang, P. P.; Goddard, W. A.; Ritter, T. *J. Am. Chem. Soc.* **2010**, *132*, 3793.
- (56) Vicente, J.; Arcas, A.; Julia-Hernandez, F.; Bautista, D. *Chem. Commun.* **2010**, *46*, 7253.
- (57) Oloo, W.; Zavalij, P. Y.; Zhang, J.; Khaskin, E.; Vedernikov, A. N. *J. Am. Chem. Soc.* **2010**, *132*, 14400.
- (58) Zhao, X. D.; Dong, V. M. *Angew. Chem., Int. Ed.* **2011**, *50*, 932.
- (59) Umemoto, T. *Chem. Rev.* **1996**, *96*, 1757.
- (60) Eisenberger, P.; Gischig, S.; Togni, A. *Chem. Eur. J.* **2006**, *12*, 2579.
- (61) Kieltsch, I.; Eisenberger, P.; Stanek, K.; Togni, A. *Chimia* **2008**, *62*, 260.
- (62) Stanek, K.; Koller, R.; Togni, A. *J. Org. Chem.* **2008**, *73*, 7678.
- (63) Muci, A. R.; Buchwald, S. L. *Top. Curr. Chem.* **2002**, *219*, 131.
- (64) Hartwig, J. F. *Accounts Chem. Res.* **1998**, *31*, 852.
- (65) Stahl, S. S.; Labinger, J. A.; Bercaw, J. E. *Angew. Chem., Int. Ed.* **1998**, *37*, 2180.
- (66) Han, R. Y.; Hillhouse, G. L. *J. Am. Chem. Soc.* **1997**, *119*, 8135.
- (67) Lyons, T. W.; Sanford, M. S. *Chem. Rev.* **2010**, *110*, 1147.
- (68) Kalyani, D.; Sanford, M.; Chatani, N., Ed.; Springer Berlin / Heidelberg: 2007; Vol. 24, p 85.
- (69) Henry, P. M. *J. Org. Chem.* **1971**, *36*, 1886.
- (70) Eberson, L.; Jonsson, L. *J. Chem. Soc., Chem. Commun.* **1974**, 885.
- (71) Yoneyama, T.; Crabtree, R. H. *J. Mol. Catal. A* **1996**, *108*, 35.
- (72) Dick, A. R.; Hull, K. L.; Sanford, M. S. *J. Am. Chem. Soc.* **2004**, *126*, 2300.
- (73) Desai, L. V.; Hull, K. L.; Sanford, M. S. *J. Am. Chem. Soc.* **2004**, *126*, 9542.
- (74) Desai, L. V.; Malik, H. A.; Sanford, M. S. *Org. Lett.* **2006**, *8*, 1141.

- (75) Reddy, B. V. S.; Reddy, L. R.; Corey, E. J. *Org. Lett.* **2006**, *8*, 3391.
- (76) Wang, D. H.; Hao, X. S.; Wu, D. F.; Yu, J. Q. *Org. Lett.* **2006**, *8*, 3387.
- (77) Giri, R.; Liang, J.; Lei, J. G.; Li, J. J.; Wang, D. H.; Chen, X.; Naggar, I. C.; Guo, C. Y.; Foxman, B. M.; Yu, J. Q. *Angew. Chem., Int. Ed.* **2005**, *44*, 7420.
- (78) Zhang, J.; Khaskin, E.; Anderson, N. P.; Zavalij, P. Y.; Vedernikov, A. N. *Chem. Commun.* **2008**, 3625.
- (79) Crabtree, R. H. *J. Chem. Soc.-Dalton Trans.* **2001**, 2437.
- (80) Zerella, M.; Mukhopadhyay, S.; Bell, A. T. *Chem. Commun.* **2004**, 1948.
- (81) Muehlhofer, M.; Strassner, T.; Herrmann, W. A. *Angew. Chem., Int. Ed.* **2002**, *41*, 1745.
- (82) Crabtree, R. H. *J. Organomet. Chem.* **2004**, *689*, 4083.
- (83) Periana, R. A.; Bhalla, G.; Tenn, W. J.; Young, K. J. H.; Liu, X. Y.; Mironov, O.; Jones, C. J.; Ziatdinov, V. R. *J. Mol. Catal. A* **2004**, *220*, 7.
- (84) Burton, H. A.; Kozhevnikov, I. V. *J. Mol. Catal. A* **2002**, *185*, 285.
- (85) Passoni, L. C.; Cruz, A. T.; Buffon, R.; Schuchardt, U. *J. Mol. Catal. A* **1997**, *120*, 117.
- (86) Desai, L. V.; Stowers, K. J.; Sanford, M. S. *J. Am. Chem. Soc.* **2008**, *130*, 13285.
- (87) Vickers, C. J.; Mei, T.-S.; Yu, J.-Q. *Org. Lett.* **2010**, *12*, 2511.
- (88) Satterfield, A. D.; Kubota, A.; Sanford, M. S. *Org. Lett.* **2011**, *13*, 1076.
- (89) Rodriguez, A.; Moran, W. J. *Eur. J. Org. Chem.* **2009**, 1313.
- (90) Li, Y.; Song, D.; Dong, V. M. *J. Am. Chem. Soc.* **2008**, *130*, 2962.
- (91) Wang, W.; Wang, F.; Shi, M. *Organometallics* **2010**, *29*, 928.
- (92) Zhu, M. K.; Zhao, J. F.; Loh, T. P. *J. Am. Chem. Soc.* **2010**, *132*, 6284.
- (93) Wang, A. Z.; Jiang, H. F.; Chen, H. J. *J. Am. Chem. Soc.* **2009**, *131*, 3846.
- (94) Park, C. P.; Lee, J. H.; Yoo, K. S.; Jung, K. W. *Org. Lett.* **2010**, *12*, 2450.
- (95) Alexanian, E. J.; Lee, C.; Sorensen, E. J. *J. Am. Chem. Soc.* **2005**, *127*, 7690.
- (96) Liu, G.; Stahl, S. S. *J. Am. Chem. Soc.* **2006**, *128*, 7179.

- (97) Widenhoefer, R. A.; Zhong, H. A.; Buchwald, S. L. *J. Am. Chem. Soc.* **1997**, *119*, 6787.
- (98) Harkal, S.; Kumar, K.; Michalik, D.; Zapf, A.; Jackstell, R.; Rataboul, F.; Riermeier, T.; Monsees, A.; Beller, M. *Tetrahedron Lett.* **2005**, *46*, 3237.
- (99) Palucki, M.; Wolfe, J. P.; Buchwald, S. L. *J. Am. Chem. Soc.* **1996**, *118*, 10333.
- (100) Palucki, M.; Wolfe, J. P.; Buchwald, S. L. *J. Am. Chem. Soc.* **1997**, *119*, 3395.
- (101) Widenhoefer, R. A.; Buchwald, S. L. *J. Am. Chem. Soc.* **1998**, *120*, 6504.
- (102) Aranyos, A.; Old, D. W.; Kiyomori, A.; Wolfe, J. P.; Sadighi, J. P.; Buchwald, S. L. *J. Am. Chem. Soc.* **1999**, *121*, 4369.
- (103) Torraca, K. E.; Kuwabe, S.-I.; Buchwald, S. L. *J. Am. Chem. Soc.* **2000**, *122*, 12907.
- (104) Parrish, C. A.; Buchwald, S. L. *J. Org. Chem.* **2001**, *66*, 2498.
- (105) Torraca, K. E.; Huang, X.; Parrish, C. A.; Buchwald, S. L. *J. Am. Chem. Soc.* **2001**, *123*, 10770.
- (106) Kuwabe, S.-i.; Torraca, K. E.; Buchwald, S. L. *J. Am. Chem. Soc.* **2001**, *123*, 12202.
- (107) Mann, G.; Hartwig, J. F. *J. Am. Chem. Soc.* **1996**, *118*, 13109.
- (108) Mann, G.; Hartwig, J. F. *Tetrahedron Lett.* **1997**, *38*, 8005.
- (109) Mann, G.; Incarvito, C.; Rheingold, A. L.; Hartwig, J. F. *J. Am. Chem. Soc.* **1999**, *121*, 3224.
- (110) Shelby, Q.; Kataoka, N.; Mann, G.; Hartwig, J. *J. Am. Chem. Soc.* **2000**, *122*, 10718.
- (111) Kataoka, N.; Shelby, Q.; Stambuli, J. P.; Hartwig, J. F. *J. Org. Chem.* **2002**, *67*, 5553.
- (112) Watanabe, M.; Nishiyama, M.; Koie, Y. *Tetrahedron Lett.* **1999**, *40*, 8837.
- (113) Hansson, S.; Heumann, A.; Rein, T.; Aakermark, B. *J. Org. Chem.* **1990**, *55*, 975.
- (114) McMurry, J. E.; Kocovsky, P. *Tetrahedron Lett.* **1984**, *25*, 4187.
- (115) Chen, M. S.; Prabakaran, N.; Labenz, N. A.; White, M. C. *J. Am. Chem. Soc.* **2005**, *127*, 6970.
- (116) Chen, M. S.; White, M. C. *J. Am. Chem. Soc.* **2004**, *126*, 1346.

- (117) Covell, D. J.; White, M. C. *Angew. Chem., Int. Ed.* **2008**, *47*, 6448.
- (118) Campbell, A. N.; White, P. B.; Guzei, I. A.; Stahl, S. S. *J. Am. Chem. Soc.* **2010**, *132*, 15116.
- (119) Racowski, J.; Sanford, M.; Canty, A. J., Ed.; Springer Berlin / Heidelberg: 2011; Vol. 503, p 61.
- (120) Hartwig, J. F. *Inorg. Chem.* **2007**, *46*, 1936.
- (121) Powers, D. C.; Geibel, M. A. L.; Klein, J. E. M. N.; Ritter, T. *J. Am. Chem. Soc.* **2009**, *131*, 17050.
- (122) Powers, D. C.; Benitez, D.; Tkatchouk, E.; Goddard, W. A.; Ritter, T. *J. Am. Chem. Soc.* **2010**, *132*, 14092.
- (123) Bäckvall, J. E.; Nordberg, R. E.; Björkman, E. E.; Moberg, C. *J. Chem. Soc., Chem. Commun.* **1980**, 943.
- (124) Bäckvall, J. E.; Byström, S. E.; Nordberg, R. E. *J. Org. Chem.* **1984**, *49*, 4619.
- (125) Bäckvall, J. E.; Nordberg, R. E. *J. Am. Chem. Soc.* **1981**, *103*, 4959.
- (126) Grennberg, H.; Gogoll, A.; Bäckvall, J. E. *J. Org. Chem.* **1991**, *56*, 5808.
- (127) Cundari, T. R.; Deng, J. *J. Phys. Org. Chem.* **2005**, *18*, 417.
- (128) Vedernikov, A. N.; Binfield, S. A.; Zavalij, P. Y.; Khusnutdinova, J. R. *J. Am. Chem. Soc.* **2006**, *128*, 82.
- (129) Fu, Y.; Li, Z.; Liang, S.; Guo, Q.-X.; Liu, L. *Organometallics* **2008**, *27*, 3736.
- (130) Musashi, Y.; Sakaki, S. *J. Am. Chem. Soc.* **2000**, *122*, 3867.
- (131) Musashi, Y.; Sakaki, S. *J. Am. Chem. Soc.* **2002**, *124*, 7588.
- (132) Biswas, B.; Sugimoto, M.; Sakaki, S. *Organometallics* **2000**, *19*, 3895.
- (133) Boutadla, Y.; Davies, D. L.; Macgregor, S. A.; Poblador-Bahamonde, A. I. *Dalton Trans.* **2009**, 5820.
- (134) Boutadla, Y.; Davies, D. L.; Macgregor, S. A.; Poblador-Bahamonde, A. I. *Dalton Trans.* **2009**, 5887.
- (135) Davies, D. L.; Donald, S. M. A.; Al-Duaij, O.; Macgregor, S. A.; Pölleth, M. *J. Am. Chem. Soc.* **2006**, *128*, 4210.
- (136) Davies, D. L.; Donald, S. M. A.; Macgregor, S. A. *J. Am. Chem. Soc.* **2005**, *127*, 13754.

- (137) Ackermann, L. *Chem. Rev.* **2011**, *111*, 1315.
- (138) Lapointe, D.; Fagnou, K. *Chem. Lett.* **2010**, *39*, 1119.
- (139) Reprinted (adapted) with permission from (Ball, N. D.; Gary, J. B.; Ye, Y.; Sanford, M. S. *J. Am. Chem. Soc.* **2011**, *133*, 7577.) Copyright (2011) American Chemical Society.
- (140) Stevens, W. J.; Basch, H.; Krauss, M. *J. Chem. Phys.* **1984**, *81*, 6026.
- (141) Stevens, W. J.; Krauss, M.; Basch, H.; Jasien, P. G. *Can. J. Chem.-Rev. Can. Chim.* **1992**, *70*, 612.
- (142) Zhao, Y.; Truhlar, D. G. *Theor. Chem. Acc.* **2008**, *120*, 215.
- (143) Sieffert, N.; Buhl, M. *Inorg. Chem.* **2009**, *48*, 4622.
- (144) Benitez, D.; Tkatchouk, E.; Goddard, W. A. *Organometallics* **2009**, *28*, 2643.
- (145) Benitez, D.; Shapiro, N. D.; Tkatchouk, E.; Wang, Y. M.; Goddard, W. A.; Toste, F. D. *Nat. Chem.* **2009**, *1*, 482.
- (146) Ariafard, A.; Hyland, C. J. T.; Canty, A. J.; Sharma, M.; Brookes, N. J.; Yates, B. F. *Inorg. Chem.* **2010**, *49*, 11249.
- (147) Ariafard, A.; Hyland, C. J. T.; Canty, A. J.; Sharma, M.; Yates, B. F. *Inorg. Chem.* **2011**, *50*, 6449.
- (148) Marenich, A. V.; Cramer, C. J.; Truhlar, D. G. *J. Phys. Chem. B* **2009**, *113*, 6378.
- (149) Glendening, E. D.; Reed, A. E.; Carpenter, J. E.; Weinhold, F. NBO, version 3.1. See http://www.gaussian.com/g_tech/g_ur/m_citation.htm.
- (150) Foster, J. P.; Weinhold, F. *J. Am. Chem. Soc.* **1980**, *102*, 7211.
- (151) Reed, A. E.; Weinhold, F. *J. Chem. Phys.* **1985**, *83*, 1736.
- (152) Reed, A. E.; Curtiss, L. A.; Weinhold, F. *Chem. Rev.* **1988**, *88*, 899.
- (153) Reed, A. E.; Weinhold, F. *The Journal of Chemical Physics* **1983**, *78*, 4066.
- (154) Markies, B. A.; Canty, A. J.; Boersma, J.; Vankoten, G. *Organometallics* **1994**, *13*, 2053.
- (155) Reprinted (adapted) with permission from (Gary, J. B.; Sanford, M. S. *Organometallics* **2011**, *30*, 6143.) Copyright (2011) America Chemical Society.

(156) Szabó, K. J. *Organometallics* **1998**, *17*, 1677.

(157) Gaussian 09, Revision **A.1**, Frisch, M. J.; Trucks, G. W.; Schlegel, H. B.; Scuseria, G. E.; Robb, M. A.; Cheeseman, J. R.; Scalmani, G.; Barone, V.; Mennucci, B.; Petersson, G. A.; Nakatsuji, H.; Caricato, M.; Li, X.; Hratchian, H. P.; Izmaylov, A. F.; Bloino, J.; Zheng, G.; Sonnenberg, J. L.; Hada, M.; Ehara, M.; Toyota, K.; Fukuda, R.; Hasegawa, J.; Ishida, M.; Nakajima, T.; Honda, Y.; Kitao, O.; Nakai, H.; Vreven, T.; Montgomery, Jr., J. A.; Peralta, J. E.; Ogliaro, F.; Bearpark, M.; Heyd, J. J.; Brothers, E.; Kudin, K. N.; Staroverov, V. N.; Kobayashi, R.; Normand, J.; Raghavachari, K.; Rendell, A.; Burant, J. C.; Iyengar, S. S.; Tomasi, J.; Cossi, M.; Rega, N.; Millam, N. J.; Klene, M.; Knox, J. E.; Cross, J. B.; Bakken, V.; Adamo, C.; Jaramillo, J.; Gomperts, R.; Stratmann, R. E.; Yazyev, O.; Austin, A. J.; Cammi, R.; Pomelli, C.; Ochterski, J. W.; Martin, R. L.; Morokuma, K.; Zakrzewski, V. G.; Voth, G. A.; Salvador, P.; Dannenberg, J. J.; Dapprich, S.; Daniels, A. D.; Farkas, Ö.; Foresman, J. B.; Ortiz, J. V.; Cioslowski, J.; Fox, D. J. Gaussian, Inc., Wallingford CT, 2009.

(158) Feller, D. *J. Comp. Chem.* **1996**, *17*, 1571.

(159) Schuchardt, K. L.; Didier, B. T.; Elsethagen, T.; Sun, L.; Gurumoorthi, V.; Chase, J.; Li, J.; Windus, T. L. *J. Chem. Inf. Model.* **2007**, *47*, 1045.

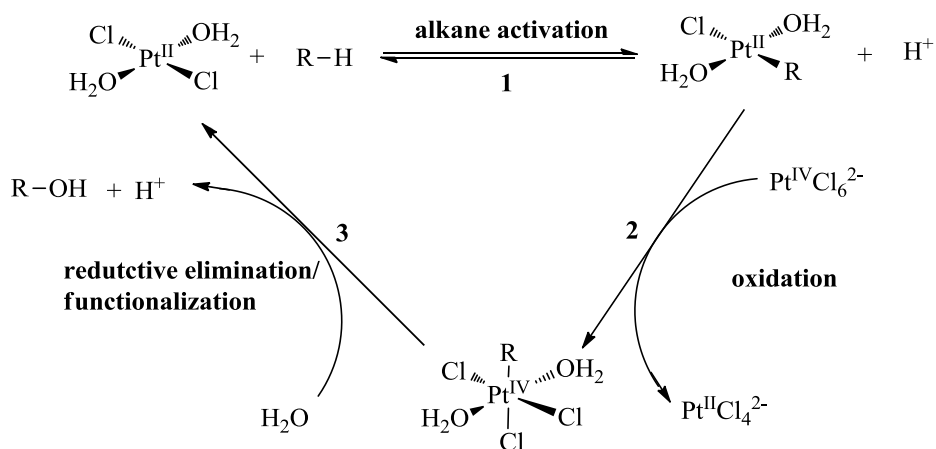
Chapter 6

Conclusions and Future Prospects

6.1 Conclusions

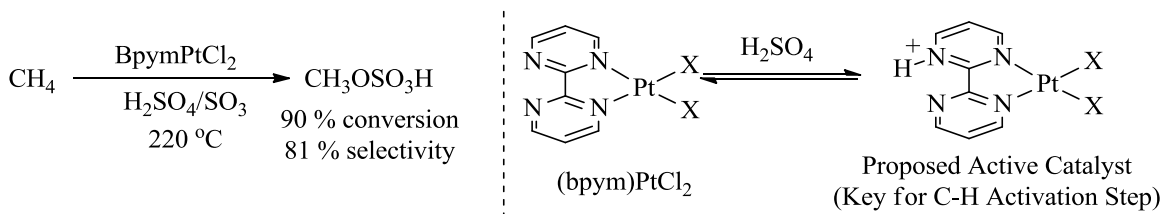
The activation and functionalization of C–H bonds has been a long standing goal in organometallic chemistry.¹ Since the original discovery of the oxidative functionalization of methane by Shilov,² tremendous efforts have been focused upon understanding and improving this system (Figure 6.1).³⁻¹¹

Figure 6.1. Shilov Catalytic Cycle.²



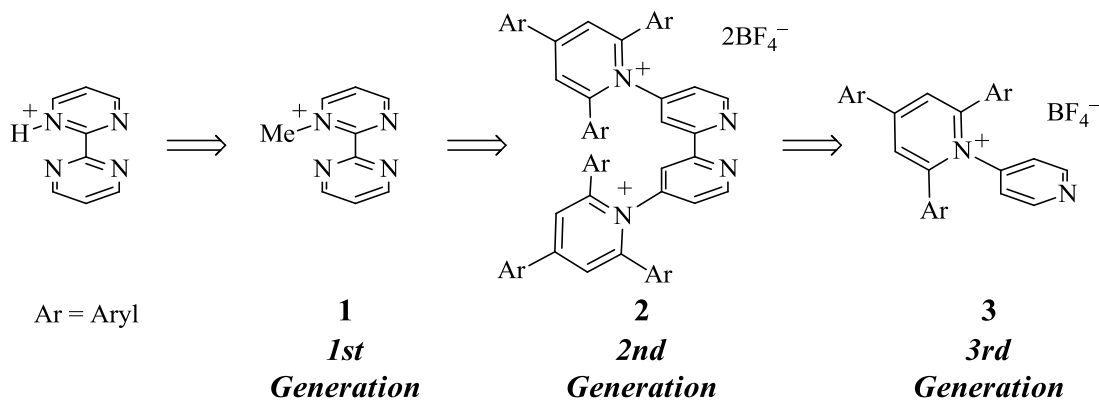
The Shilov system is plagued by low catalyst turnovers and the cost-prohibitive use of Pt^{IV} as a stoichiometric oxidant.⁷ Given these limitations, improving catalyst stability and modification of the system to utilize more cost-effective oxidants are the main challenges in this system.^{7,12} To address these issues, my Ph. D. studies have used computational analysis, ligand design, high-throughput screening, stoichiometric studies, and catalytic assays in an effort to achieve the rational design of new catalysts.

Figure 6.2. Catalytica Methane Oxidation System.¹³



Tremendous strides with the challenge of catalyst stability and oxidant substitution occurred with the discovery of the Catalytica system (Figure 6.2).¹³ In this system, the fuming sulfuric acid serves as solvent, catalyst activator, and oxidant. Our group generated a first generation isolable ligand system that serves as an analog of the Catalytica system (Figure 6.3).¹⁴ However, this catalyst was prone to decomposition through demethylation by solvent.

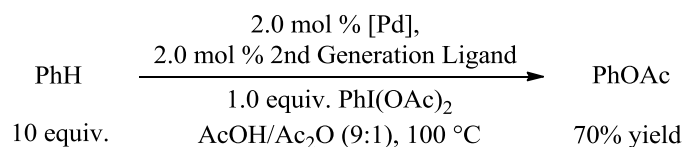
Figure 6.3 Cationic Ligand Design Strategy.



Through ligand design with 2nd and 3rd generation systems, Pt-analogs of the Catalytica system were synthesized and studied for C–H activation through an H/D exchange assay. The 2nd generation ligand system with Pt resulted in dramatic improvement in arene H/D exchange activity and allowed for efficient catalysis at 100°C in acetic acid- D_4 , a temperature at which traditional bipyridine and bipyrimidine

(Catalytica System) show no activity. With these second generation ligands, Pd-based catalysis was achieved for the acetoxylation of benzene (Scheme 6.1).¹⁵

Scheme 6.1 Benzene Acetoxylation Reaction.



Through the use of high-throughput ligand screening with 3rd generation ligands, two cationic monodentate pyridines (**3-Ar** and **4-Ar**, Chapter 2) were found to produce more active catalysts than commercial pyridine in Pd-catalyzed non-directed C–H oxidative functionalization to form C–O bonds. A Pd to ligand ratio of 1:1 was also found to be key in maximizing activity. After our initial studies with PhI(OAc)₂ as an oxidant, we developed K₂S₂O₈ conditions as a more environmentally friendly and cost effective alternative. Through the use of potassium persulfate, we have determined that **3-Ar** (Chapter 2) produces a catalytic system approximately five times as active as pyridine and shows significant selectivity for the formation of C–O bonds in comparison to biphenyl. Through the use of high-throughput screening and NMR analysis, we have shown that the higher activity results from a combination of equilibrium shift to form a higher fraction of Pd(L)(OAc)₂ as well as lowered reaction barriers for C–H functionalization. Acetoxylation of a variety of other electron deficient aromatic substrates was also demonstrated. The reaction yields and turnover numbers are the highest reported for C–O bond formation using the cost-effective and environmentally benign K₂S₂O₈ oxidant.

With the success of Pd-based catalysis with these 3rd generation ligands, we have applied these 3rd generation ligands to the IrCp*(L)Cl₂ catalyst systems popularized by

Bergman,¹⁶⁻²¹ Peris,²²⁻²⁶ and Ison (Chapter 3).²⁷ Given the proposed oxidative addition mechanism for C–H activation in these systems, strongly donating alkyl phosphines and *N*-heterocyclic carbenes have typically been employed. While IrCp*(L)Cl₂ complexes with L = 3rd generation cationic pyridine ligands were not as highly active for H/D exchange in methanol-D₄ or D₂O as the previously reported phosphine/carbene systems, we did observe high activity in acetic acid-D₄. This indicates that the reaction medium has a dramatic effect on catalytic activity. Furthermore, it shows that “conventional wisdom” on ligand effects in these systems is a function of the conditions employed in these studies and not necessarily of the inherent activity of the complexes.

Next, we employed 2nd generation ligands in fundamental investigations of C–H activation at Rh^{III} complexes. In these studies, we have been able to show that our 2nd generation ligands have a dramatic effect on the reactivity of resulting Rh^{III} complexes. Comparing these ligands to bipyridine in halide abstraction reactions illustrates the dramatic effect these ligands have on catalyst stability and reactivity. The isolation of cyclometallated complexes using 2-phenylpyridine has allowed for direct comparison of 2nd generation ligands and bipyridine for C–H activation. In these studies, the 2nd generation ligands again improve catalytic activity. Thus, our 2nd generation and 3rd generation ligands have shown enhanced activity for C–H activation in Pt, Pd, Rh, and Ir systems.

Finally, bond-forming reductive elimination has been a significant challenge in C–H functionalization catalysis.²⁸⁻³³ Pd-based systems have been most effective in a wide variety of bond formations. Pt, Rh, and Ir have shown much less versatility. In an effort to better understand this problematic step, we have used DFT computational

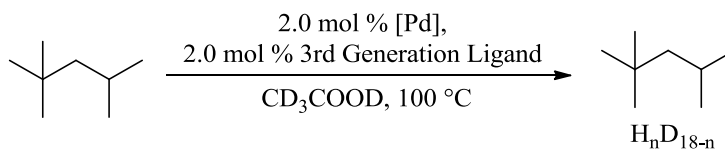
analysis to probe Aryl–X bond formation from Pd^{IV} centers (X = CF₃ and F) given the challenges associated in forming these functionalities. Through the studies, we have identified a nucleophilic role for the aromatic coupling partner in Aryl–CF₃ reductive elimination. Also, when comparing CF₃ and other competing X-type ligands (X = Cl, F, OAc) for reductive elimination, we discovered a novel mechanism for Aryl-carboxylate reductive elimination.³⁴

All of these results have highlighted the combined use of computational analysis, ligand design, high-throughput screening, stoichiometric studies, and catalytic assays in an effort to achieve rational catalyst design.

6.2 Future Prospects

While significant insights and catalytic activity enhancements have been discovered, many questions and research directions remain to be studied. First, the Pd-based catalysts containing 3rd generation ligands have shown high activity for the functionalization of aromatic C–H bonds. More detailed studies are required to understand the exact nature of the enhanced reactivity in these systems. Initial investigations indicate that the ligand charge has a significant role in catalyst improvement. Further mechanistic understanding in this system could allow for improved ligand designs in the future. Expanding this system to sp³ C–H bonds would provide a significant advance in the field. Initial experiments of H/D exchange activity between acetic acid-D₄ and isooctane showed very small deuterium incorporation activity by mass spectrometry.

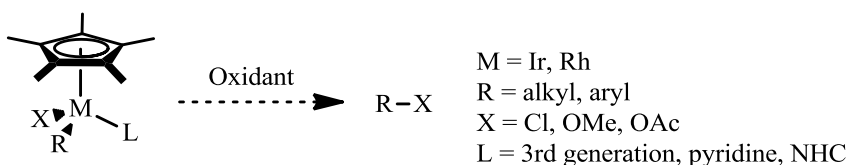
Scheme 6.2 sp^3 H/D Exchange.



Repeating these experiments and quantifying this activity in this substrate and other alkanes should be a first priority. The corresponding functionalization reactions will likely require higher reaction temperatures and more soluble oxidants to avoid β -hydride elimination pathways of alkyl intermediates to provide catalytic functionalization. The use of alkylammonium salts with $K_2S_2O_8$ could improve oxidant solubility to limit low reaction rates and undesired side reactions. Methane should be an obvious goal, but significant complications arise from the analytic requirements of analyzing gases.

In the $IrCp^*$ based systems described in Chapter 3, bond-forming reductive elimination should be a major goal. Related Rh systems have been shown to undergo oxidatively-induced reductive elimination to form ethane from dimethyl complexes.³⁵ Using the ideas in Scheme 6.3, the synthesis of a variety of Ir^{III} and Rh^{III} complexes would be beneficial to expand the thermal or oxidatively-induced reductive elimination scope in these systems. Understanding of this key step will be crucial to achieving catalytic C–H functionalization reactions in these systems.

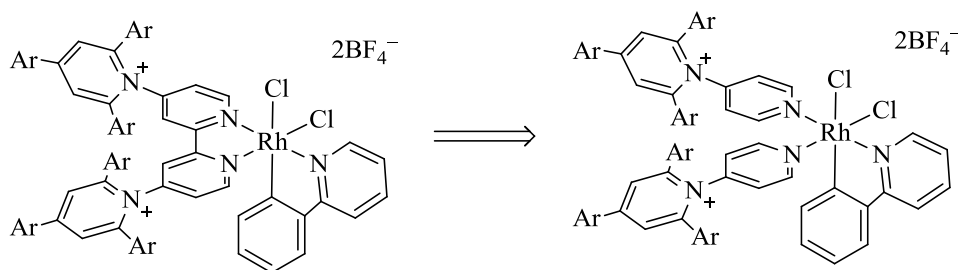
Scheme 6.3 Oxidatively Induced Reductive Elimination.



Finally, in the Rh^{III} cyclometallated complexes described in Chapter 4, increased catalytic activity for C–H activation was observed with 2nd generation ligands but

stoichiometric studies of the isolated cyclometallated complexes showed no reactivity towards olefins or alkynes. Moving to 3rd generation ligands in these systems could allow for more flexibility in the system (Scheme 6.4). This flexibility could allow for ligands to rearrange and allow for olefins or alkynes to bind cis to the aryl group and facilitate reactivity.

Scheme 6.4 3rd Generation Ligands for Rh^{III} Complexes.



All of these areas represent additional potential benefits for our cationic ligand designs. These benefits could allow for additional breakthroughs to expand the application of C–H functionalization for the synthesis of organic molecules.

6.3 References

- (1) Arndtsen, B. A.; Bergman, R. G.; Mobley, T. A.; Peterson, T. H. *Acc. Chem. Res.* **1995**, *28*, 154.
- (2) Goldshleger, N. F.; Eskova, V. V.; Shilov, A. E.; Shteinman, A. A. *Russ. J. Phys. Chem.* **1972**, *46*, 785.
- (3) Kakiuchi, F.; Chatani, N. *Adv. Synth. Catal.* **2003**, *345*, 1077.
- (4) Arakawa, H.; Aresta, M.; Armor, J. N.; Barteau, M. A.; Beckman, E. J.; Bell, A. T.; Bercaw, J. E.; Creutz, C.; Dinjus, E.; Dixon, D. A.; Domen, K.; DuBois, D. L.; Eckert, J.; Fujita, E.; Gibson, D. H.; Goddard, W. A.; Goodman, D. W.; Keller, J.; Kubas, G. J.; Kung, H. H.; Lyons, J. E.; Manzer, L. E.; Marks, T. J.; Morokuma, K.; Nicholas, K. M.; Periana, R.; Que, L.; Rostrup-Nielson, J.; Sachtler, W. M. H.; Schmidt, L. D.; Sen, A.; Somorjai, G. A.; Stair, P. C.; Stults, B. R.; Tumas, W. *Chem. Rev.* **2001**, *101*, 953.
- (5) Lyons, T. W.; Sanford, M. S. *Chem. Rev.* **2010**, *110*, 1147.
- (6) Labinger, J. A. *J. Mol. Catal. A-Chem.* **2004**, *220*, 27.

- (7) Crabtree, R. H. *J. Chem. Soc.-Dalton Trans.* **2001**, 2437.
- (8) Labinger, J. A.; Bercaw, J. E. *Nature* **2002**, 417, 507.
- (9) Periana, R. A.; Bhalla, G.; Tenn, W. J.; Young, K. J. H.; Liu, X. Y.; Mironov, O.; Jones, C. J.; Ziatdinov, V. R. *J. Mol. Catal. A-Chem.* **2004**, 220, 7.
- (10) Shilov, A. E.; Shulpin, G. B. *Uspekhi Khimii* **1987**, 56, 754.
- (11) Conley, B. L.; Tenn, W. J.; Young, K. J. H.; Ganesh, S. K.; Meier, S. K.; Ziatdinov, V. R.; Mironov, O.; Oxgaard, J.; Gonzales, J.; Goddard, W. A.; Periana, R. A. *J. Mol. Catal. A* **2006**, 251, 8.
- (12) Stahl, S. S.; Labinger, J. A.; Bercaw, J. E. *Angew. Chem. Int. Ed.* **1998**, 37, 2180.
- (13) Periana, R. A.; Taube, D. J.; Gamble, S.; Taube, H.; Satoh, T.; Fujii, H. *Science* **1998**, 280, 560.
- (14) Villalobos, J. M.; Hickman, A. J.; Sanford, M. S. *Organometallics* **2009**, 29, 257.
- (15) Reprinted (adapted) with permission from (Emmert, M. H.; Gary, J. B.; Villalobos, J. M.; Sanford, M. S. *Angew. Chem. Int. Ed.* **2010**, 49, 5884.) Copyright (2010) John Wiley and Sons.
- (16) Arndtsen, B. A.; Bergman, R. G. *Science* **1995**, 270, 1970.
- (17) Bengali, A. A.; Arndtsen, B. A.; Burger, P. M.; Schultz, R. H.; Weiller, B. H.; Kyle, K. R.; Moore, C. B.; Bergman, R. G. *Pure & Appl. Chem.* **1995**, 67, 281.
- (18) Yung, C. M.; Skaddan, M. B.; Bergman, R. G. *J. Am. Chem. Soc.* **2004**, 126, 13033.
- (19) Tellers, D. M.; Yung, C. M.; Arndtsen, B. A.; Adamson, D. R.; Bergman, R. G. *J. Am. Chem. Soc.* **2002**, 124, 1400.
- (20) Klei, S. R.; Golden, J. T.; Tilley, T. D.; Bergman, R. G. *J. Am. Chem. Soc.* **2002**, 124, 2092.
- (21) Golden, J. T.; Andersen, R. A.; Bergman, R. G. *J. Am. Chem. Soc.* **2001**, 123, 5837.
- (22) Viciano, M.; Feliz, M.; Corberán, R.; Mata, J. A.; Clot, E.; Peris, E. *Organometallics* **2007**, 26, 5304.
- (23) Pontes da Costa, A.; Viciano, M.; Sanaú, M.; Merino, S.; Tejada, J.; Peris, E.; Royo, B. *Organometallics* **2008**, 27, 1305.
- (24) Costa, A. P. d.; Viciano, M.; Sanaú, M.; Merino, S.; Tejada, J.; Peris, E.; Royo, B. *Organometallics* **2008**, 27, 1305.
- (25) Corberán, R.; Sanaú, M.; Peris, E. *Organometallics* **2006**, 25, 4002.

- (26) Corberán, R.; Sanaú, M.; Peris, E. *J. Am. Chem. Soc.* **2006**, *128*, 3974.
- (27) Feng, Y.; Jiang, B.; Boyle, P. A.; Ison, E. A. *Organometallics* **2010**, *29*, 2857.
- (28) Reprinted (adapted) with permission from (Ball, N. D.; Gary, J. B.; Ye, Y.; Sanford, M. S. *J. Am. Chem. Soc.* **2011**, *133*, 7577.) Copyright (2011) American Chemical Society.
- (29) Ball, N. D.; Kampf, J. W.; Sanford, M. S. *J. Am. Chem. Soc.* **2010**, *132*, 2878.
- (30) Ball, N. D.; Sanford, M. S. *J. Am. Chem. Soc.* **2009**, *131*, 3796.
- (31) Ye, Y. D.; Ball, N. D.; Kampf, J. W.; Sanford, M. S. *J. Am. Chem. Soc.* **2010**, *132*, 14682.
- (32) Grushin, V. V. *Accounts Chem. Res.* **2010**, *43*, 160.
- (33) Grushin, V. V.; Marshall, W. J. *J. Am. Chem. Soc.* **2006**, *128*, 12644.
- (34) Reprinted (adapted) with permission from (Gary, J. B.; Sanford, M. S. *Organometallics* **2011**, *30*, 6143.) Copyright (2011) American Chemical Society.
- (35) Pedersen, A.; Tilset, M. *Organometallics* **1993**, *12*, 56.